Adipose Tissue Engineering

Development of a 3-D Model System of Adipogenesis

Dissertation zur Erlangung des Doktorgrades der Naturwissenschaften
(Dr. rer. nat.)
der Fakultät für Chemie und Pharmazie
der Universität Regensburg

vorgelegt von
Claudia Fischbach
aus Ichenhausen
im Juli 2003

Diese Doktorarbeit entstand in der Zeit von Oktober 1998 bis Juni 2003 am Lehrstuhl für Pharmazeutische Technologie an der Universität Regensburg

Die Arbeit wurde angeleitet von Prof. Dr. Achim Göpferich.

Promotionsgesuch eingereicht am:	9. Juli 2003	
Datum der mündlichen Prüfung:	28. Juli 2003	
Prüfungsausschuß:	Vorsitzender:	Prof. Dr. S. Elz
	Erstgutachter:	Prof. Dr. A. Göpferich
	Zweitgutachter:	PD Dr. J. Seufert.
	Drittprüfer:	Prof. Dr. G. Franz

Meiner Familie in Liebe und Dankbarkeit gewidmet.

Wir sollen heiter Raum um Raum durchschreiten,
An keinem wie an einer Heimat hängen,
Der Weltgeist will nicht fesseln uns und engen,
Er will uns Stuf˝ um Stufe heben, weiten.

(Hermann Hesse, Stufen)

Table of Contents

Chapter 1

Introduction
and
Goals of the Thesis

Tissue engineering

Background:

The loss or failure of an organ or tissue represents one of the most devastating and costly problems in medicine [1-3]. Current strategies that have evolved to deal with these defects include organ transplantation, surgical reconstruction, and replacement with mechanical devices [3-5]. Despite incorporating significant advances, the applicability of these strategies is substantially limited, especially in the field of transplantation. The shortcomings associated with organ transplantation include a critical shortage of donor organs and permanent immunosuppressive medication with its increased risk of adverse side effects [5-7]. Surgical reconstruction equally suffers from scarcity of available donor tissue. Furthermore, it often matches the particular reconstructive need only imperfectly and may entail donor site morbidity [5,8]. Finally, infection, poor biocompatibility, and limited durability complicate the use of artificial prostheses [3-5]. In order to overcome these drawbacks, the interdisciplinary field of tissue engineering (TE) emerged. Motivated by the challenge to develop biological substitutes that restore, maintain, or improve tissue functions, TE combines the principles of engineering and the life sciences towards the production of tissue substitutes [1,2,9].

Concept:

The most common approach to guiding tissue regeneration is the use of cell-matrix constructs [5,7,10] (Fig. 1). This concept stemmed from biological observations reporting that A) every tissue undergoes constant remodeling, B) isolated cells can reorganize themselves into the desired tissue when placed in appropriate cell culture conditions, and C) appropriate histological reorganization only occurs when cells are delivered within a template guiding restructuring and allowing for diffusion of nutrients and oxygen to the cells [1]. Accordingly, autologous cells isolated and expanded from a small tissue biopsy are seeded onto scaffolds, which function to direct the development of the new tissue by providing structural support and an appropriate three-dimensional (3-D) environment [1,6,8]. Usually, the scaffolds are fashioned from either synthetic or natural biodegradable and biocompatible polymers that are gradually be replaced by regenerated tissue, minimizing the inflammatory response [6,8]. Once the cells are adhered onto matrices and proliferate, cellular reorganization is triggered by treatment with the appropriate tissue-inducing substances, e.g. hormones and growth

factors [1,7]. Subsequent to the formation of the desired tissue, the cell-matrix constructs can be used for transplantation purposes (Fig. 1). Furthermore, it has become increasingly recognized that the tissue-like constructs supply valuable 3-D model systems for both basic research *in vitro* and *in vivo* (Fig. 1). Compared to conventional two-dimensional (2-D) cell culture, the engineered tissue equivalents may better reflect *in vivo* conditions and are, therefore, thought to substantially contribute to the understanding of tissue-inherent functions and processes.

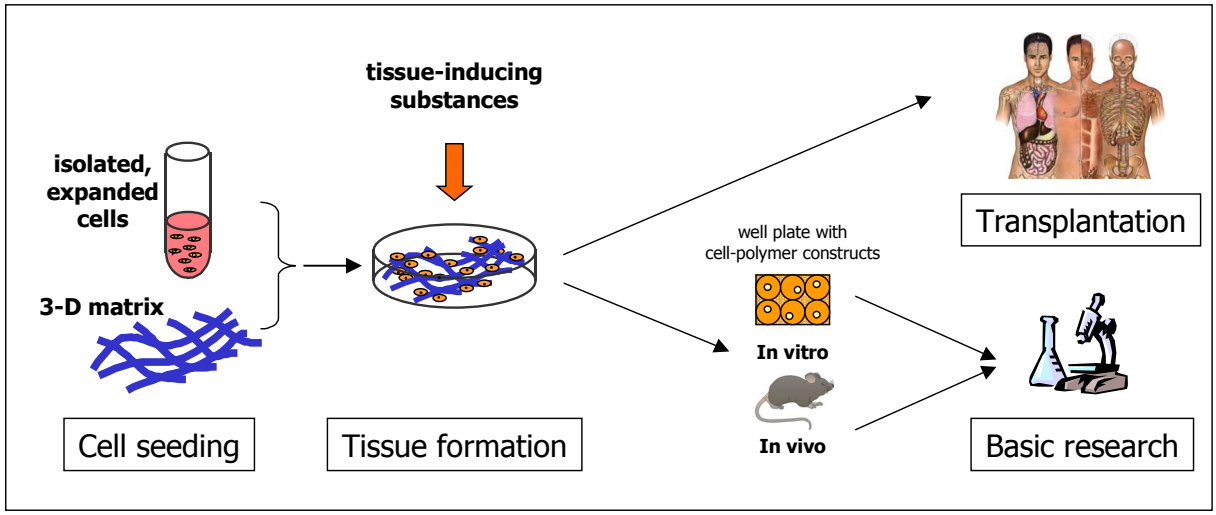

Fig. 1: Tissue engineering
Cell-matrix constructs for clinical application and basic research

Adipose tissue – Challenges for tissue engineering

The traditional role attributed to adipose tissue is the storage of triacylglycerol in times of nutrient excess and the mobilization of energy during periods of caloric deprivation [11,12]. However, over the past decades it has become increasingly acknowledged as a major secretory and endocrine organ involved in a range of functions beyond simple fat storage [13-15]. Due to its usefulness for plastic and reconstructive surgery and its impact on metabolically related disorders, adipose tissue has gained substantial clinical and research interest.

Plastic and reconstructive surgery:

In plastic and reconstructive surgery, autologous fat grafts serve as an appropriate filling material in the reconstruction of soft tissue defects [16,17]. In particular, adipose tissue offers the potential to act as a natural bulking material to treat congenital or acquired (traumatic and

degenerative) volume defects. Furthermore, it is transplanted for cosmetic, corrective, and orthotic-related indications [18,19]. Standard approaches currently used in the restoration of soft tissue volume and contour defects include the grafting of fat, as well as injection of single cell suspensions, which are harvested in prior procedures using direct excision and needle or cannula aspiration techniques [16,19,20]. However, autografting often entails donor site morbidity such as hypertrophic scarring [18,21] and is furthermore limited by the low and unpredictable survival rates of the transplants [16,18,22]. Due to the resorption of the graft over time, the procedures often need repeating [19,23] or require hypercorrection to offset [24]. Potential reasons for the poor results are attributed to inadequate neovascularization of the graft subsequent to transplantation leading to insufficient blood supply at the center and, thus, to reduced viability of the transplants. Injection of single cell suspensions of mature adipocytes was thought to circumvent these difficulties by being apter to be supported by diffusion processes alone until vascularization is initiated [25]. However, fat derived from liposuction techniques becomes highly traumatized during surgical aspiration, resulting in large foreign body reactions, inflammation, and, finally, resorption of the injected tissue mass [26,27]. Accordingly, aspirated fat is currently regarded as being less suitable for reconstructive purposes than free fat autografts [18,26,27,27].

In summary, adipose tissue represents the most natural filling material for reconstruction of soft tissue defects. Nevertheless, presently applied techniques remain minimally effective and are unsuitable for providing satisfying surgical solutions to treat large volume deficiencies such as oncologic defects after mastectomy. With the objective of developing alternative approaches capable of providing functional adipose tissue equivalents for transplantation, the application of TE strategies appears to be promising.

Basic research of obesity and related disorders:

Immoderately increased adipose tissue, a condition commonly called obesity, is generally accepted to cause or exacerbate many health problems. Specifically, it is associated with the development of type 2 diabetes mellitus, coronary heart disease, an enhanced incidence of certain forms of cancer, respiratory complications (obstructive sleep apnoea) and osteoarthritis of large and small joints [12,28-30]. Though the underlying basis for this linkage remains to be clarified, the health hazard of obesity is increasingly accepted to be due in part to bioactive factors secreted by adipocytes [15,31]. However, despite evidences from epidemiological studies and life-insurance data confirming that increasing degrees of overweight are important predictors of longevity, the prevalence of obesity is dramatically

escalating [12,28]. Accordingly, obesity has become to a considerable economic factor, as developed countries already spend 2-7% of their total health costs on obesity related health problems [28]. In order to establish novel and effective strategies for the prevention and treatment of obesity and related disorders, progress has to be made in understanding adipose tissue development, as well as adipocyte functions.

Generally, the enlargement of adipose tissue in obesity results from both increased fat cell number (hyperplasia) and increased fat cell size (hypertrophy) [30,32]. As the number of adipocytes is controlled primarily by the differentiation process, which generates mature adipocytes from fibroblast-like preadipocytes, a thorough comprehension of the adipogenic program has to be gained. Therefore, various cell models, including preadipose cell lines [11,33-35] and primary cultures of precursor cells either isolated from the stromal vascular fraction of adipose tissue [11,36,37] or from bone marrow [38-40], have been used to elaborately study adipocyte differentiation *in vitro*. Furthermore, transgenic animals were developed offering experimenters new and precise models to investigate functions of adipose genes *in vivo* [41-43]. By using the current approaches, the knowledge about the mechanisms that direct adipocyte differentiation and adipocyte specific gene expression rapidly advanced. In particular, they substantially contributed to defining the sequence of events in the adipose differentiation program and identifying key transcription factors that regulate the program [32,44,45]. However, the presently used cell culture systems are limited in that they lack the inherent 3-D cell-cell and cell-extracellular matrix (ECM) interactions present within real adipose tissue [44]. Though these interactions are increasingly accepted to most likely account for critical steps of adipogenesis, the currently employed *in vitro* systems do not allow for the particular investigations of cellular properties within a tissue-like context [11,34,46]. The importance of tissue-inherent interactions on adipose tissue properties was demonstrated for instance by MacDougald et al.. It was shown that adipocytes differentiated in conventional 2-D cell culture expressed the obese gene leptin at levels substantially diminished (~1%) relative to those found in mouse fat [47]. This failure was attributed to a tissue factor(s), e.g. ECM, or a condition, e.g. neighboring cell-cell contact, present *in vivo* but lacking *in vitro* [47,48].

In order to gain thorough insight into how 3-D cell-cell and cell-ECM interactions impact adipose tissue development, it would be desirable to perform the respective studies under culture conditions, which enable dissection of separate tissue-inherent effects and concomitantly provide a 3-D environment. A 3-D adipose tissue model developed by means of TE is suggested to ideally meet these requirements. Such a model would prove beneficial

to properly imitate the 3-D interactions present within native fat and would thereby enable researchers to comprehensively analyze adipogenesis within a tissue-like environment *in vitro*. In addition to performing the studies under well-defined conditions *in vitro*, the engineered constructs could be transplanted. This would allow for both verification of the results within a physiological surrounding and clarification of additional effects mediated, for instance, by other cell types.

Characteristics of adipose tissue

Anatomical and histological features:

Adipose tissue originates from the mesenchyme and belongs to the class of connective tissues [49,50]. Due to its color, which varies from white to yellowish depending on the carotinoid content, adipose tissue is also designated as white adipose tissue (WAT)[1]. In healthy humans, the percentage of adipose tissue per body weight depends on the gender as well as on the age of the individual; in males approx. 15% of the whole body weight are composed of adipose tissue, whereas it takes up about 25% in females [50,51]. Although adipose tissue is ubiquitously distributed throughout the body, the two major compartments are represented by the subcutaneous (~80%) and the visceral fat (~10%), which differ both in their distribution and metabolism [44,52-54]. Additional sites of fat pad localization accounting for the remainder are situated in retroperitoneal, perirenal, and orbital areas [12,55].

In terms of the cellular composition, lipid filled unilocular adipocytes form the main part of cells in WAT (Fig. 2), whereby the remaining fraction is composed of a complex array of various blood cells, endothelial cells, pericytes, adipose precursor cells, and fibroblasts [49]. According to the amount of stored triglycerides, fat cells can achieve sizes over 100 µm in diameter (compared to approx. 10 µm of undifferentiated cells) and typically exhibit the so called signet ring form, characterized by a large single lipid droplet, which is surrounded by a thin rim of cytoplasma, and a nucleus located peripherally [56].

[1] In addition to WAT, which is the major type, mammals have another sort of adipose tissue referred to as brown adipose tissue (BAT). It represents an activatable thermogenic organ, which furthermore differs from white adipose tissue with regard to cell morphology, vascularization, and depot localization [49-51]. This work was focused on WAT and, therefore, BAT will be disregarded below.

Fig. 2: White adipose tissue (excised from rat femora, magnification 200 fold)

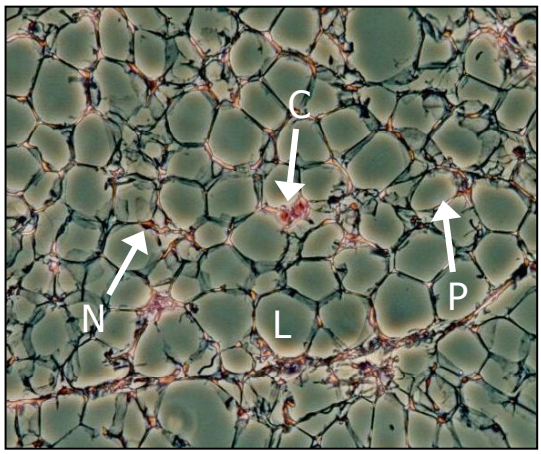

2A)
H&E stained. (N: nucleus, C: capillary, P: cytoplasma, L: former lipid inclusion)

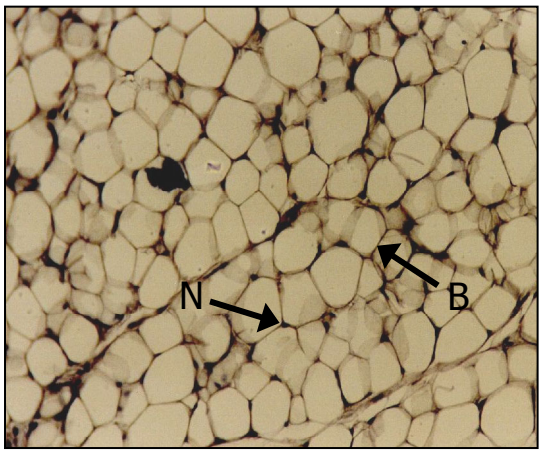

2B)
Immuno-stained for laminin, a major component of the basement membrane. (N: nucleus, B: basement membrane)

Due to their close arrangement within the tissue, the cells adopt a hexagonal configuration as shown in Fig. 2. In times of nutrient deprivation, mature adipocytes can equally adopt a multilocular appearance, which is caused by mobilization of triglycerides accompanied by disaggregation of the central lipid vacuole into smaller droplets. In conventional cross-sections prepared from paraffin embedded samples, organic solvents are used and, thereby, intacellular triglyceride inclusions are dissolved. Hence, the lipid droplets are only detectable in the form of blank spaces enveloped by the remaining cellular structures (Fig. 2A).

Another feature of adipose tissue is the ECM, which fills the space between the adipocytes. It is composed of a variety of versatile proteins and polysaccharides assembled into a meshwork closely associated with the cell surface. Adipocytes are primarily surrounded by a network of collagen fibers and a basement membrane typically containing collagen type IV and laminin (Fig. 2B) [11,51,56,57].

Functions of adipose tissue:

The functional tasks of adipose tissue can be grouped generally into three categories with potentially overlapping modalities. Traditionally, energy storage in the form of triglycerides in times of nutritional excess and the release of energy as free fatty acids (FFA) and glycerol during periods of caloric deprivation are considered to represent the central functions [11,15]. Furthermore, WAT is known to fulfill mechanical tasks such as cushioning

and thermal isolation and to serve the body as a padding to fill up cavities, e.g. to keep room free for later augmentation of organs such as the breast. However, over the past decades, it has become recognized that adipose tissue additionally operates as a multipotential endocrine and immune organ by releasing factors targeting a variety of physiological functions [30,45]. In particular, adipocytes secrete various cytokines, hormones, and other biochemically active molecules involved in the regulation of insulin sensitivity, glucose homeostasis, inflammation, energy balance, lipid metabolism, vascular haemostasis, and reproduction (Fig. 3) [12,13,15,58]. For instance, an increasing body of evidence now indicates that adipose tissue substantially contributes to the control over insulin secretion and ultimately glucose homeostasis by releasing a subset of metabolically active substances. Hence, it seems likely that the development of insulin resistance in type 2 diabetes mellitus is thereby linked to obesity. Specifically, adipocytes secrete leptin, a peptide hormone involved in regulation of energy intake and expenditure, that counteracts a subset of insulin actions [15,59], and the cytokine tumor necrosis factor α (TNFα), which has been reported to impair glucose homeostasis by interfering with insulin signaling [12,60]. TNFα is described as being up-regulated in obesity and to exert its impact by blocking phosphorylation of insulin receptor substrate IRS-1, a target of the insulin receptor, and additionally through reduction of gene expression of the glucose transporter GLUT-4 [61]. Furthermore, chronically elevated levels of circulating FFA caused by the diminished antilipolytic activity of insulin in type 2 diabetes mellitus are strongly implicated in the development of insulin resistance and β-cell dysfunction [12,55]. Though some of the adipose tissue dependent mechanisms begin to be clarified, novel adipocyte secreted factors involved in insulin sensitivity are permanently discovered. For instance, the adipocytokines adiponectin and resistin have recently been recognized as linkers between obesity and insulin resistance [13,15,62].

The vasoregulatory functions of adipose tissue are mediated in part by the secretion of angiotensinogen (Ang) and by the plasminogen activator inhibitor 1 (PAI-1). Ang represents a presursor of angiotensin I of the renin-angiotensin system, which is responsible for regulation of systemic blood pressure [15,63], whereas PAI-1 is a fibrinolytic protein up-regulated in obesity [64,65]. Though in obesity cardiovascular functions are mainly affected through expansion of tissue mass entailing increased stroke volume and cardiac output, which can finally result in heart failure [28], the above mentioned substances seemingly play a part as well.

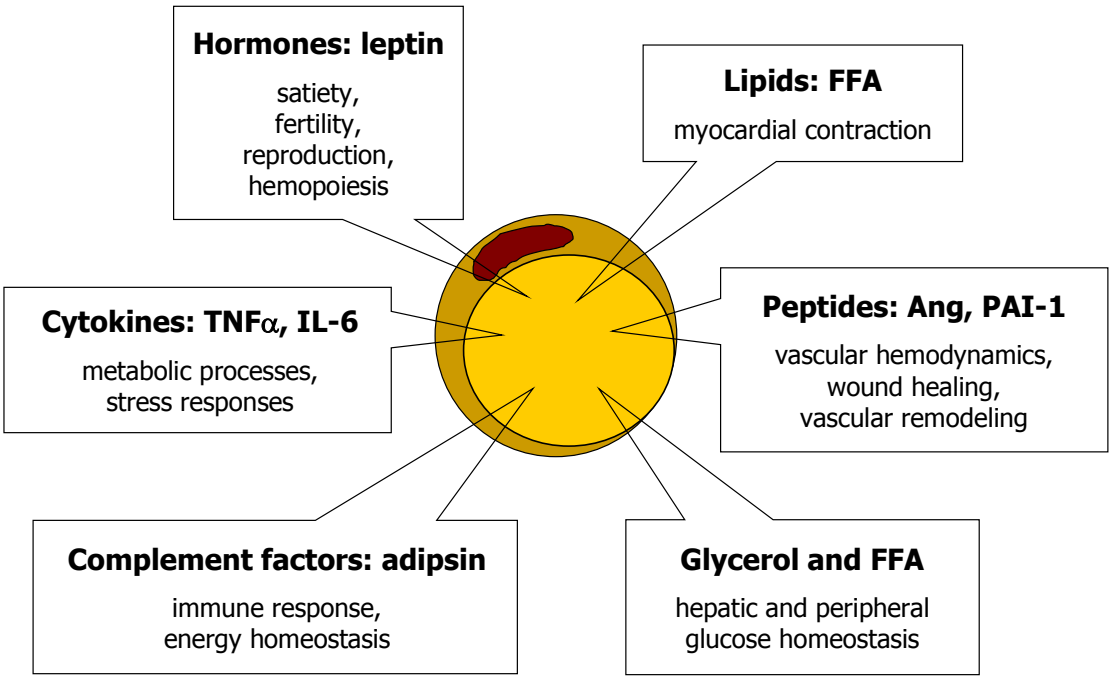

Fig. 3: Secretory functions of adipose tissue
Examples for signaling factors known to be produced by adipocytes.

In summary, the recent data demonstrate endocrine and paracrine/autocrine function of adipocytes, which facilitate adipose tissue to play a dynamic role in a wide range of physiological processes other than regulation of energy balance.

Adipocyte differentiation:

Though the developmental origin of adipocytes is still poorly understood, recent studies suggest that adipocyte precursor cells (preadipocytes) derive from multipotent mesodermal cells that originate from embryonic stem cells [31,32]. However, the molecular events that promote determination to the adipocyte lineage have yet to be identified [11,31]. In contrast, the molecular and cellular processes involved in conversion of fibroblast-like preadipocytes into mature adipocytes have become increasingly understood. Much of our knowledge has thereby evolved from the use of immortalized preadipocyte cell lines. For instance, 3T3-L1 cells, which were generated from 3T3 fibroblasts [33], have substantially contributed to reveal many factors that regulate adipogenesis and to identify a well concerted differentiation program controlled primarily by the transcription factors CCAAT/enhancer binding proteins (C/EBPα, β, and δ) and peroxisome proliferator-activated receptor γ (PPARγ) [31,58,66,67].

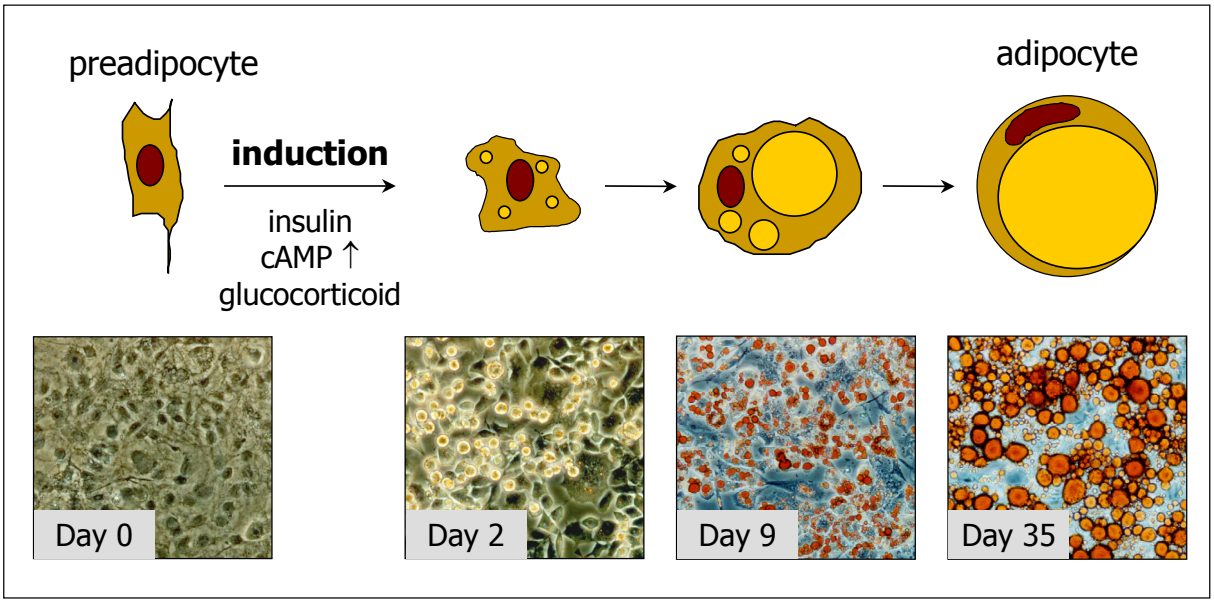

Fig. 4: Adipogenesis
Changes in cellular morphology and triglyceride storage (schematically and in 2-D cell culture of 3T3-L1 cells, which were stained with oil red O in order to visualize lipid droplets).

Usually, preadipocytes are induced to differentiate with the addition of mitogens (contained in serum) and hormonal agents (insulin, glucocorticoids, and cAMP elevating agents) over a period of 2 days (Fig. 4) [35,58]. During adipogenesis, the acquisition of the adipose phenotype is characterized through chronological changes in the expression of early, intermediate, and late mRNA/protein markers and massive triglyceride accumulation [11,32]. One of the first steps is the re-entry of growth arrested preadipocytes into the cell cycle and the completion of several rounds of clonal expansion (Fig. 4, day 0 to day 2) [68,69]. Simultaneously, early changes in gene expression have become evident and comprise the induction of the key transcription factors C/EBPs and PPARγ that act cooperatively to promote the adipocyte differentiation [35,70]. Specifically, C/EBPβ and C/EBPδ are transiently induced in response to hormonal stimulation [44,71]. This is followed by the stimulation of PPARγ and C/EBPα, which mutually induces the expression of the other by a positive feedback loop [11,44,67,71]. In turn, the cooperative action between PPARγ and C/EBPα drives the expression of genes typical for the adipose phenotype. Concomitantly, cells undergo a marked change in cell morphology from a fibroblastic form to a nearly spherical shape (Fig. 4), which is accompanied by decreased synthesis and assembly of the cytosleketal proteins actin and tubulin [46,72]. Furthermore, composition of the ECM is altered as well [73-75]. In particular, the relative concentrations of fibroblast-expressed type I and III collagen declines, whereas the secretion of type IV collagen, which is typically

contained in basement membranes, increases [76]. During the late phases of adipogenesis, markedly increased triglyceride biosynthesis due either to *de novo* or enhanced expression of most lipogenic genes can be observed, e.g. glycerol-3-phosphate dehydrogenase, fatty acid synthase, acetyl CoA carboxylase, GLUT-4, and the insulin receptor are up-regulated [11,32]. Thereby, cells adopt first a multilocular appearance and then, through coalescence of the small intracellular lipid droplets, the typical signet ring form, which is paralleled by a significant increase in cell size (Fig. 4). Concomitant with the expression of the mature adipose phenotype, the fat cells acquire the ability of exerting functionality with respect to the biosynthesis of endocrine factors (see p. 15).

Adipose tissue engineering

Since the first conceptual work in 1998 by Patrick et al. [21], major efforts pursuing the aim of guiding adipose tissue development for clinical use have been initiated. However, development of a 3-D model system for basic research has not yet been comprehensively addressed. To the successful generation of fat equivalents, the utilization of cell-matrix constructs emerged as the most promising concept [18,21,77,78]. Using this strategy, four integral components are required, i.e., cells, 3-D matrices, tissue-inducing substances, and suitable culture methodologies (Fig. 5).

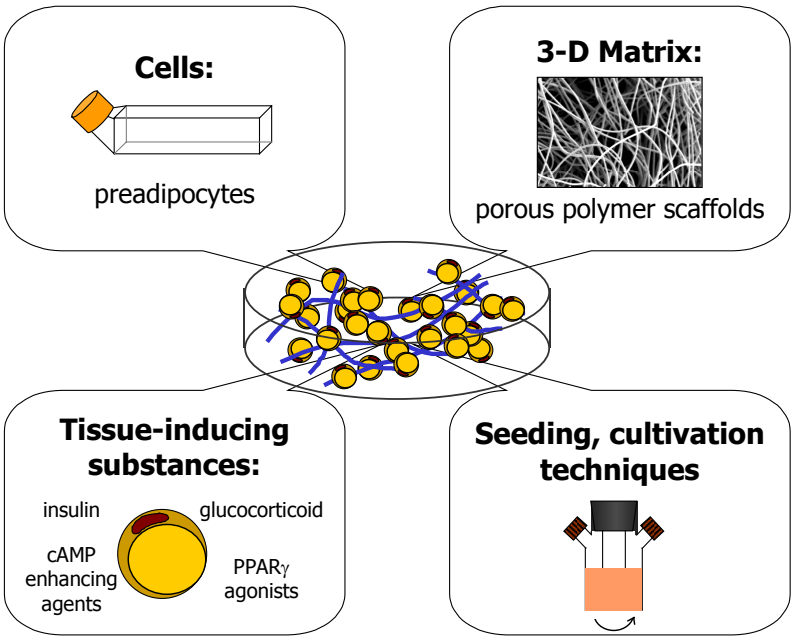

Fig. 5: Adipose tissue engineering
Components critical to the generation of coherent adipose tissue constructs in vitro.

Cells:

The starting point for any attempt is to choose an appropriate cell type capable of being expanded in cell culture and, furthermore, of expressing functional characteristics so as to achieve the desired behavior desired. Although adipose tissue consists of a distinct mix of cells, the recent approaches focus on exclusively utilizing fat cells. Thereby, the engineering process is simplified as manipulations are clearly attributable to this specific cell type. The biggest drawback of employing mature adipocytes, the major cell type present in adipose tissue, is their low mechanical resistance [21,77,79]. Although these cells are thought to feature a considerable proliferation capacity when cultured under appropriate conditions [80,81], their tremendous fragility and buoyancy precludes the use of common isolation and cell culture techniques [18,21]. Therefore, adipocyte precursor cells represent an attractive alternative. As they lack intracellular triglyceride, which causes decreased size and fragility, they tolerate the mechanical stress associated with cell harvest and cultivation technologies better than their mature counterparts (Fig. 5). Autologous precursor cells can be isolated from the stromal vascular fraction of removed fat pads or from bone marrow [21,37,39]. However, these cells often entail limitations with regard to cellular heterogeneity, sometimes low proliferation rates, and donor dependent differentiation capacity [11]. To circumvent these restrictions, preadipocyte cell lines, particularly the well-characterized 3T3-L1 cells, are proposed as an alternative cell source providing researchers with highly reproducible conditions. Though 3T3-L1 cells can not be applied in future cell-based therapies, they represent a powerful tool for basic research, which, in turn, may serve the development of adipose tissue transplants for clinical purposes.

Current approaches for adipose TE mainly use primary preadipocytes isolated from human or rat adipose tissue [82-85]. Cells from a cell line (3T3-F442A) until now were only employed *in vivo*, not *in vitro* [86].

3-D matrices:

The scaffolds used for adipose TE are processed from either natural or synthetic biodegradable polymers. Naturally occurring polymers are used in the form of collagen gels and sponges [82,87-89], Matrigel [86,90-92], alginate covalently linked to the cell adhesion peptide RGD [93], and scaffolds based on hyaluronic acid modified by esterification (Hyaff) [94,95]. Most of the current approaches were conducted *in vivo* and demonstrated development of adipose tissue at the implantation site. In contrast, only limited work has been

done pertaining the usage of these matrices in 3-D cell culture. Though the few studies performed *in vitro* showed adipogenesis of preadipocytes to lipid containing fat cells, reorganization to a coherent fat-like construct has not yet been achieved [87,95]. For instance, Halbleib et al. differentiated human preadipocytes on hyaluronic acid-based scaffolds; however, formation of a coherent construct imitating a physiological environment was completely lacking [95].

Alternatively, 3-D matrices processed from synthetic polymers are employed. As these carriers can be fabricated reproducibly in almost unlimited quantities with controlled chemical and physical properties, they facilitate investigations into adipose tissue formation under more reproducible conditions as compared to natural polymer scaffolds [96]. To date, adipose tissue engineering exclusively applies scaffolds, which were processed from poly(lactic-co-glycolic acid) (PLGA) by using a solvent casting - particulate leaching technique [85,96-98]. Although this approach has resulted in fat pad formation *in vivo*, it did not yield satisfying results with respect to long-term maintenance. Furthermore, constructs generated *in vitro* were lacking tissue coherence similar to the results achieved with matrices processed from natural polymers.

Tissue-inducing substances:

To reorganize into native histological structures of adipose tissue, the preadipocytes need to convert into their differentiated phenotype. For triggering the particular cellular differentiation cascade, the cell-seeded constructs can be either implanted into the physiological environment or they are subjected to appropriate cell culture media containing a hormonal cocktail typically composed of insulin, a glucocorticoid, and an agent enhancing intracellular levels of the second messenger cAMP (see p. 17). Sometimes, indomethacin or troglitazone is additionally supplemented. These substances have proven useful as they promote adipogenesis by activating the transcription factor PPARγ [99-101] (Fig. 5).

Present approaches for adipose tissue engineering achieve adipogenesis of 3-D cell-polymer constructs by both implantation *in vivo* and hormonal stimulation *in vitro*. However, as described above, neither of those studies resulted in fully satisfactory results with regard to long-term maintenance *in vivo* and tissue coherence *in vitro*.

Culture methodologies:

The culture techniques used for construct assembly must provide adequate conditions for cell attachment, proliferation, and differentiation [3]. Cell seeding for adipose TE

purposes is currently conducted statically, e.g. by injecting or soaking a preadipocyte suspension into the scaffolds [82,85]. However, for other cell types dynamic delivery in mixed flasks, so called bioreactors, has been reported to improve spatially uniform cell distribution [102]. As mixing conditions, generated for example in spinner flasks or rotating vessels [103], prevent sedimentation of the cells, advanced seeding efficiency can be achieved. Hence, it remains to be clarified if preadipocyte seeding under dynamic conditions may prove advantageous over static conditions.

Subsequent cultivation of the cell-polymer constructs must be performed such that desired concentrations of gases and nutrients in the culture medium are maintained and that efficient mass transfer to the growing tissue is provided. Dynamic cultivation procedures in either bioreactors or agitated Petri dishes can ideally meet these requirements as they increase diffusion processes by enhanced convection [3,103]. Though adipocytes constitute a highly metabolically active tissue, particularly sensitive to insufficient nutrient and oxygen supply, present *in vitro* approaches of adipose TE employ static culture conditions [82,85]. In contrast, application of dynamic cultivation techniques may help to improve nutrient and oxygen transfer to the cells and ultimately may result in improved properties of the engineered fat equivalents.

Current state – Summary and consequences [2]:

Encouraging data demonstrating fat pad formation *in vivo* have been published over the last couple of years [85,86]. However, long-term maintenance of engineered adipose tissue *in vivo* still remains elusive [85]. In order to clarify the potential reasons for the failure, standardized investigations within a tissue-like environment are required. A readily available 3-D *in vitro* model of adipogenesis developed through means of TE could facilitate the respective studies. Recently, first approaches were reported examining both adhesion and differentiation of preadipocytes on different 3-D polymeric matrices [85,87]. Though the first promising results could be gained with respect to adipogenesis under 3-D culture conditions, none of those studies resulted in the formation of a coherent fat-like tissue. Accordingly, an environment recreating the particular cell-cell and cell-ECM interactions present within native fat is still lacking. As the currently applied approaches partly failed, alternative strategies need

[2] For more details see also introduction of chapter 3 (3-D *in vitro*-Model of Adipogenesis – Comparison of Culture Conditions)

to be assessed with regard to their suitability for developing fat equivalents. For this purpose, the components critical to adipose TE have to be thoroughly evaluated.

The basis for the establishment of a standardized *in vitro* engineered fat construct would be to employ reproducible source materials. Specifically, the two major components, cells and 3-D matrices, have to be provided in reproducible quality. In order to circumvent the heterogeneity of primary cells, the use of well-characterized and uniform 3T3-L1 preadipocytes is suggested. Similarly, it seems reasonable to apply commercially available synthetic polymeric scaffolds, which ensure continuous conditions for 3-D cell culture. In terms of the remaining two parameters, i.e., tissue-inducing substances and culture methodologies, only very limited studies have been published. However, as described above, cell seeding and cultivation of the cell-polymer constructs may be tremendously advanced by choosing conditions, which have been shown to yield improved results in other tissues. In addition to addressing the key components of adipose TE, studies on further parameters may shed light on how construct characteristics can be advanced. For instance, the length of the cultivation period and the use of innovative synthetic polymers may significantly impact properties of the engineered tissues.

In summary, a coherent 3-D *in vitro* model of adipose tissue exhibiting typical features of fat cells, such as triglyceride biosynthesis, typical gene expression, and functionality is still lacking. Such a model system would likely contribute to advance the understanding of adipose tissue physiology, which in turn may help to improve fat grafting for clinical use and define novel therapeutic targets in the treatment of obesity. Therefore, the development of a standardized, coherent, and functional fat-like construct by means of TE is strongly recommended.

Goals of the thesis

Engineered adipose tissue equivalents are increasingly acknowledged to serve for both fat grafting and basic research of obesity. However, the current approaches do not allow for the formation of the desired coherent constructs. Therefore, this thesis focused on the establishment of a fat-like model system capable of overcoming the present limitations. On the way to accomplishing the overall objective, it was necessary to meet the following specific aims:

1. Establish suitable cultivation conditions for 3T3-L1 adipogenesis in 3-D cell culture.
2. Generate coherent adipose tissue constructs and characterize them with regard to fat-like properties after both short-term and long-term culture and under physiological conditions *in vivo*.
3. Investigate adipogenesis on alternative synthetic polymers with respect to their suitability for adipose TE.

1. Evaluation of cultivation conditions:

The first aim was to establish the four key components integral to generating cell-polymer constructs, namely cells, scaffold, tissue-inducing substances, and culture methodologies (see p. 18).

In order to ensure the reproducibility of the model, cells from the well-characterized 3T3-L1 cell line and commercially available poly(glycolic acid) (PGA) fiber meshes were employed. The highly porous scaffolds are provided in reproducible quality and have been successfully applied in other tissue engineering applications, such as cartilage [104,105]. To assess appropriate tissue-inducing substances, different cell culture media and hormonal induction protocols (including the PPARγ agonists indomethacin and troglitazone) were evaluated comprehensively (chapter 2). Subsequently, appropriate techniques for assembly of the constructs have been determined by comparing static and dynamic seeding procedures and by evaluation of distinct cultivation conditions, i.e., static culture and dynamic culture in either agitated well-plates or stirred bioreactors (chapter 3).

2. Generation and characterization of coherent adipose constructs:

The second aim was to generate and thoroughly investigate the fat-like properties of coherent constructs and to determine if the applied experimental conditions allow for completion of reorganization into tissues histologically comparable to native fat.

3T3-L1 cells are reported to undergo differentiation to mature adipocytes over a 4-6 day period following adipogenic treatment [44]. Accordingly, the differentiation time for the cell-polymer constructs was initially fixed for 8 to 10 days. Subsequent to the characterization of these "short-term" cultured constructs (chapter 4), it was furthermore assessed which impact prolonged differentiation periods (21 and 35 days) exert on adipose tissue properties (chapter 5). Finally, the question arose how the engineered constructs develop under physiological conditions *in vivo*. 3T3-L1 cells are regarded to not give rise to mature fat pads *in vivo* [48,106], in contrast to other preadipose cell lines such as 3T3-F442A. Nevertheless, it was aimed at investigating if the implantation of coherent 3T3-L1-polymer constructs exhibiting tissue-like interactions proves favorable and finally allows for reorganization into fat pads (chapter 5).

3. Investigation of biodegradable polymers:

Recently, poly(D,L-lactic acid)-poly(ethylene glycol)-monomethyl ether diblock copolymers (Me.PEG-PLA) have been developed for controlled cell-biomaterial interactions [107]. They were demonstrated to promote osteoblast differentiation and to modify 3T3-L1 adhesion behavior [108-110]. Accordingly, the third aim of this thesis was to investigate if the novel biomaterials feature advantageous properties with regard to adipose tissue engineering and may therefore be used as an alternative to the PGA polymers employed in all other experiments.

Prior to subjecting the processed Me.PEG-PLAs to cell culture, they have to be sterilized. As common sterilization procedures such as steam autoclave or heat sterilization are known to strongly affect Me.PEG-PLA properties, UV irradiation is used as an alternative sterilization method. However, potential alterations of polymer characteristics due to UV have not been extensively considered yet. Consequently, the impact of UV irradiation on Me.PEG-PLA properties was addressed thoroughly (chapter 6) before performing the particular experiments to study adipogenesis on these biomaterials (chapter 7).

References

1. Langer, R. and Vacanti, J. P. (1993). Tissue engineering. *Science* **260**, 920-926.

2. Patrick, C. W., Jr., Mikos, A. G., and McIntire, L., V (1998). Prospectus of Tissue Engineering. *In* "Frontiers in Tissue Engineering" (C. W. Patrick, A. G. Mikos, and L. McIntire, V, Eds.), Elsevier Science Ltd., Oxford.

3. Lalan, S., Pomerantseva, I., and Vacanti, J. P. (2001). Tissue engineering and its potential impact on surgery. *World J.Surg.* **25**, 1458-1466.

4. Freed, L. E. and Vunjak-Novakovic, G. (1998). Culture of organized cell communities. *Adv.Drug Delivery Rev.* **33**, 15-30.

5. Fuchs, J. R., Nasseri, B. A., and Vacanti, J. P. (2001). Tissue engineering: a 21st century solution to surgical reconstruction. *Ann.Thorac.Surg.* **72**, 577-591.

6. Kaihara, S. and Vacanti, J. P. (1999). Tissue engineering: toward new solutions for transplantation and reconstructive surgery. *Arch.Surg.(Chicago)* **134**, 1184-1188.

7. Tabata, Y. (2001). Recent progress in tissue engineering. *Drug.Discov.Today* **6**, 483-487.

8. Marler, J. J., Upton, J., Langer, R., and Vacanti, J. P. (1998). Transplantation of cells in matrices for tissue regeneration. *Adv.Drug Delivery Rev.* **33**, 165-182.

9. Nerem, R. M. (1991). Cellular engineering. *Ann.Biomed.Eng.* **19**, 529-545.

10. Stock, U. A. and Vacanti, J. P. (2001). Tissue engineering: current state and prospects. *Annu.Rev.Med.* **52**, 443-451.

11. Gregoire, F. M., Smas, C. M., and Sul, H. S. (1998). Understanding adipocyte differentiation. *Physiol.Rev.* **78**, 783-809.

12. Arner, P. (2003). The adipocyte in insulin resistance: key molecules and the impact of the thiazolidinediones. *Trends Endocrinol.Metab.* **14**, 137-145.

13. Trayhurn, P. and Beattie, J. H. (2001). Physiological role of adipose tissue: white adipose tissue as an endocrine and secretory organ. *Proc.Nutr.Soc.* **60**, 329-339.

14. Kim, S. and Moustaid-Moussa, N. (2000). Secretory, endocrine and autocrine/paracrine function of the adipocyte. *J.Nutr.* **130**, 3110S-3115S.

15. Diamond, F. B., Jr. and Eichler, D. C. (2002). Leptin and the adipocyte endocrine system. *Crit.Rev.Clin.Lab.Sci.* **39**, 499-525.

16. Billings, E. J. and May, J. W., Jr. (1989). Historical review and present status of free fat graft autotransplantation in plastic and reconstructive surgery. *Plast.Reconstr.Surg.* **83**, 368-381.

17. Smahel, J. (1986). Adipose tissue in plastic surgery. *Ann.Plast.Surg.* **16**, 444-453.

18. Katz, A. J., Llull, R., Hedrick, M. H., and Futrell, J. W. (1999). Emerging approaches to the tissue engineering of fat. *Clin.Plast.Surg.* **26**, 587-603.

19. Ellenbogen, R. (2000). Fat transfer: current use in practice. *Clin.Plast.Surg.* **27**, 545-556.

20. Yuksel, E., Weinfeld, A. B., Cleek, R., Wamsley, S., Jensen, J., Boutros, S., Waugh, J. M., Shenaq, S. M., and Spira, M. (2000). Increased free fat-graft survival with the long-term, local delivery of insulin, insulin-like growth factor-I, and basic fibroblast growth factor by PLGA/PEG microspheres. *Plast.Reconstr.Surg.* **105**, 1712-1720.

21. Patrick, C. W., Jr., Chauvin, P. B., and Robb, G. L. (1998). Tissue engineered adipose tissue. *In* "Frontiers in tissue engineering" (C. W. Patrick, Jr., A. G. Mikos, and L. V. McIntire, Eds.), Elsevier Science Ltd., Oxford.

22. Smahel, J. (1989). Experimental implantation of adipose tissue fragments. *Br.J.Plast.Surg.* **42**, 207-211.

23. Yuksel, E., Weinfeld, A. B., Cleek, R., Jensen, J., Wamsley, S., Waugh, J. M., Spira, M., and Shenaq, S. (2000). Augmentation of adipofascial flaps using the long-term local delivery of insulin and insulin-like growth factor-1. *Plast.Reconstr.Surg.* **106**, 373-382.

24. Kononas, T. C., Bucky, L. P., Hurley, C., and May, J. W., Jr. (1993). The fate of suctioned and surgically removed fat after reimplantation for soft-tissue augmentation: a volumetric and histologic study in the rabbit. *Plast.Reconstr.Surg.* **91**, 763-768.

25. Coleman, S. R. (1995). Long-term survival of fat transplants: controlled demonstrations. *Aesthetic.Plast.Surg.* **19**, 421-425.

26. Fagrell, D., Enestrom, S., Berggren, A., and Kniola, B. (1996). Fat cylinder transplantation: an experimental comparative study of three different kinds of fat transplants. *Plast.Reconstr.Surg.* **98**, 90-96.

27. Nguyen, A., Pasyk, K. A., Bouvier, T. N., Hassett, C. A., and Argenta, L. C. (1990). Comparative study of survival of autologous adipose tissue taken and transplanted by different techniques. *Plast.Reconstr.Surg.* **85**, 378-386.

28. Kopelman, P. G. (2000). Obesity as a medical problem. *Nature* **404**, 635-643.

29. MacDougald, O. A. and Mandrup, S. (2 A.D.). Adipogenesis: forces that tip the scales. *Trends Endocrinol.Metab.* **13**, 5-11.

30. Gregoire, F. M. (2001). Adipocyte differentiation: from fibroblast to endocrine cell. *Exp.Biol.Med.(Maywood)* **226**, 997-1002.

31. Sorisky, A. (1999). From preadipocyte to adipocyte: differentiation-directed signals of insulin from the cell surface to the nucleus. *Crit.Rev.Clin.Lab.Sci.* **36**, 1-34.

32. Rosen, E. D. and Spiegelman, B. M. (2000). Molecular regulation of adipogenesis. *Annu.Rev.Cell Dev.Biol.* **16**, 145-171.

33. Green, H. and Kehinde, O. (1974). Sublines of Mouse 3T3 Cells That Accumulate Lipid. *Cell* 113-116.

34. Hwang, C. S., Loftus, T. M., Mandrup, S., and Lane, M. D. (1997). Adipocyte differentiation and leptin expression. *Annu.Rev.Cell Dev.Biol.* **13**, 231-259.

35. Ntambi, J. M. and Kim, Y. C. (2000). Adipocyte differentiation and gene expression. *J.Nutr.* **130**, 3122S-3126S.

36. Kras, K. M., Hausman, D. B., Hausman, G. J., and Martin, R. J. (1999). Adipocyte development is dependent upon stem cell recruitment and proliferation of preadipocytes. *Obes.Res.* **7**, 491-497.

37. Zuk, P. A., Zhu, M., Mizuno, H., Huang, J., Futrell, J. W., Katz, A. J., Benhaim, P., Lorenz, H. P., and Hedrick, M. H. (2001). Multilineage cells from human adipose tissue: implications for cell-based therapies. *Tissue Eng.* **7**, 211-228.

38. Beresford, J. N., Bennett, J. H., Devlin, C., Leboy, P. S., and Owen, M. E. (1992). Evidence for an inverse relationship between the differentiation of adipocytic and osteogenic cells in rat marrow stromal cell cultures. *J.Cell Sci.* **102 (Pt 2)** , 341-351.

39. Pittenger, M. F., Mackay, A. M., Beck, S. C., Jaiswal, R. K., Douglas, R., Mosca, J. D., Moorman, M. A., Simonetti, D. W., Craig, S., and Marshak, D. R. (1999). Multilineage potential of adult human mesenchymal stem cells. *Science* **284**, 143-147.

40. Minguell, J. J., Erices, A., and Conget, P. (2001). Mesenchymal Stem Cells. *Exp.Biol.Med.(Maywood)* **226**, 507.

41. Vidal-Puig, A., Jimenez-Linan, M., Lowell, B. B., Hamann, A., Hu, E., Spiegelman, B., Flier, J. S., and Moller, D. E. (1996). Regulation of PPAR gamma gene expression by nutrition and obesity in rodents. *J.Clin.Invest.* **97**, 2553-2561.

42. Alexander, C. M., Selvarajan, S., Mudgett, J., and Werb, Z. (2001). Stromelysin-1 regulates adipogenesis during mammary gland involution. *J.Cell.Biol.* **152**, 693-703.

43. Lee, K., Villena, J. A., Moon, Y. S., Kim, K. H., Lee, S., Kang, C., and Sul, H. S. (2003). Inhibition of adipogenesis and development of glucose intolerance by soluble preadipocyte factor-1 (Pref-1). *J.Clin.Invest.* **111**, 453-461.

44. Rosen, E. D., Walkey, C. J., Puigserver, P., and Spiegelman, B. M. (2000). Transcriptional regulation of adipogenesis. *Genes Dev.* **14**, 1293-1307.

45. Morrison, R. F. and Farmer, S. R. (1999). Insights into the transcriptional control of adipocyte differentiation. *J.Cell.Biochem.* **76 Supplement 32/33**, 59-67.

46. Spiegelman, B. M. and Ginty, C. A. (1983). Fibronectin modulation of cell shape and lipogenic gene expression in 3T3-adipocytes. *Cell* **35**, 657-666.

47. MacDougald, O. A., Hwang, C. S., Fan, H., and Lane, M. D. (1995). Regulated expression of the obese gene product (leptin) in white adipose tissue and 3T3-L1 adipocytes. *Proc.Natl.Acad.Sci.U.S.A.* **92**, 9034-9037.

48. Mandrup, S., Loftus, T. M., MacDougald, O. A., Kuhajda, F. P., and Lane, M. D. (1997). Obese gene expression at in vivo levels by fat pads derived from s.c. implanted 3T3-F442A preadipocytes. *Proc.Natl.Acad.Sci.U.S.A.* **94**, 4300-4305.

49. Ailhaud, G., Grimaldi, P., and Negrel, R. (1992). Cellular and molecular aspects of adipose tissue development. *Annu.Rev.Nutr.* **12**, 207-233.

50. Hees, H. (1996). Bindegewebsarten. *In* "Grundriß und Atlas der Mikroskopischen Anatomie des Menschen, Band 1 Zytologie und Allgemeine Histologie" (H. Hees, Ed.), Gustav Fischer Verlag, Stuttgart.

51. Welsch, U. (2003). Bindegewebe. *In* "Lehrbuch Histologie" Urban & Fischer, Muenchen.

52. Engfeldt, P. and Arner, P. (1988). Lipolysis in human adipocytes, effects of cell size, age and of regional differences. *Horm.Metab.Res., Suppl.Ser.* **19**, 26-29.

53. Lefebvre, A. M., Laville, M., Vega, N., Riou, J. P., van Gaal, L., Auwerx, J., and Vidal, H. (1998). Depot-specific differences in adipose tissue gene expression in lean and obese subjects. *Diabetes* **47**, 98-103.

54. Shibasaki, M., Takahashi, K., Itou, T., Miyazawa, S., Ito, M., Kobayashi, J., Bujo, H., and Saito, Y. (2002). Alterations of insulin sensitivity by the implantation of 3T3-L1 cells in nude mice. A role for TNF-[Alpha;]? *Diabetologia* **45**, 518-526.

55. Arner, P. (2001). Free fatty acids--do they play a central role in type 2 diabetes? *Diabetes Obes.Metab.* **3 Supplement 1**, S11-S19.

56. Napolitano, L. (1963). The differentiation of white adipose cells. *J.Cell.Biol.* **18**, 663-679.

57. Alberts, B., Bray, D., Lewis, J., Raff, M., Roberts, K., and Watson, J. D. (1994). Cell junctions, cell adhesion, and the extracellular matrix. *In* "Molecular Biology of the Cell" (M. Robertson and R. Adams, Eds.), Garland Publishing, New York.

58. Morrison, R. F. and Farmer, S. R. (2000). Hormonal signaling and transcriptional control of adipocyte differentiation. *J.Nutr.* **130**, 3116S-3121S.

59. Trayhurn, P., Hoggard, N., Mercer, J. G., and Rayner, D. V. (1999). Leptin: fundamental aspects. *Int.J.Obes.* **23**, 22-28.

60. Hotamisligil, G. S. (2000). Molecular mechanisms of insulin resistance and the role of the adipocyte. *Int.J.Obes.* **24**, S23-S27.

61. Kahn, B. B. and Flier, J. S. (2000). Obesity and insulin resistance. *J.Clin.Invest.* **106**, 473.

62. Fasshauer, M., Klein, J., Neumann, S., Eszlinger, M., and Paschke, R. (2002). Hormonal regulation of adiponectin gene expression in 3T3-L1 adipocytes. *Biochem.Biophys.Res.Commun.* **290**, 1084-1089.

63. Schling, P., Mallow, H., Trindl, A., and Loffler, G. (1999). Evidence for a local renin angiotensin system in primary cultured human preadipocytes. *Int.J.Obes.* **23**, 336-341.

64. Shimomura, I., Funahashi, T., Takahashi, M., Maeda, K., Kotani, K., Nakamura, T., Yamashita, S., Miura, M., Fukuda, Y., and Takemura et, a. (1996). Enhanced expression of PAI-1 in visceral fat: possible contributor to vascular disease in obesity. *Nat.Med.* **2**, 800-803.

65. Ahima, R. S. and Flier, J. S. (2000). Adipose Tissue as an Endocrine Organ. *Trends Endocrinol.Metab.* **11**, 327-332.

66. Cowherd, R. M., Lyle, R. E., and McGehee, R. E., Jr. (1999). Molecular regulation of adipocyte differentiation. *Semin.Cell Dev.Biol.* **10**, 3-10.

67. Wu, Z., Puigserver, P., and Spiegelman, B. M. (1999). Transcriptional activation of adipogenesis. *Curr.Opin.Cell Biol.* **11**, 689-694.

68. Camp, H. S., Ren, D., and Leff, T. (2002). Adipogenesis and fat-cell function in obesity and diabetes. *Trends Mol.Med.* **8**, 442-447.

69. Tang, Q. Q., Otto, T. C., and Daniel Lane, M. (2003). Mitotic clonal expansion: A synchronous process required for adipogenesis. *Proc.Natl.Acad.Sci.U.S.A.* **100**, 44-49.

70. Hu, E., Tontonoz, P., and Spiegelman, B. M. (1995). Transdifferentiation of myoblasts by the adipogenic transcription factors PPAR gamma and C/EBP alpha. *Proc.Natl.Acad.Sci.U.S.A.* **92**, 9856-9860.

71. Lane, M. D., Tang, Q. Q., and Jiang, M. S. (1999). Role of the CCAAT enhancer binding proteins (C/EBPs) in adipocyte differentiation. *Biochem.Biophys.Res.Commun.* **266**, 677-683.

72. Spiegelman, B. M. and Farmer, S. R. (1982). Decreases in tubulin and actin gene expression prior to morphological differentiation of 3T3 adipocytes. *Cell* **29**, 53-60.

73. Kubo, Y., Kaidzu, S., Nakajima, I., Takenouchi, K., and Nakamura, F. (2000). Organization of extracellular matrix components during differentiation of adipocytes in long-term culture. *In Vitro Cell.Dev.Biol.:Anim.* **36**, 38-44.

74. Calvo, J. C., Rodbard, D., Katki, A., Chernick, S., and Yanagishita, M. (1991). Differentiation of 3T3-L1 preadipocytes with 3-isobutyl-1-methylxanthine and dexamethasone stimulates cell-associated and soluble chondroitin 4-sulfate proteoglycans. *J.Biol.Chem.* **266**, 11237-11244.

75. Kuri-Harcuch, W., Arguello, C., and Marsch-Moreno, M. (1984). Extracellular matrix production by mouse 3T3-F442A cells during adipose differentiation in culture. *Differentiation* **28**, 173-178.

76. Aratani, Y. and Kitagawa, Y. (1988). Enhanced synthesis and secretion of type IV collagen and entactin during adipose conversion of 3T3-L1 cells and production of unorthodox laminin complex. *J.Biol.Chem.* **263**, 16163-16169.

77. Patrick, C. W., Jr. (2001). Tissue engineering strategies for adipose tissue repair. *Anat.Rec.* **263**, 361-366.

78. Lee, K. Y., Halberstadt, C. R., Holder, W. D., and Mooney, D. J. (2000). Breast reconstruction. *In* "Principles of Tissue Engineering" (R. P. Lanza, R. Langer, and J. P. Vacanti, Eds.), Academic Press, San Diego.

79. Patrick, C. W., Jr. (2000). Adipose tissue engineering: the future of breast and soft tissue reconstruction following tumor resection. *Semin.Surg.Oncol.* **19**, 302-311.

80. Sugihara, H., Yonemitsu, N., Miyabara, S., and Yun, K. (1986). Primary cultures of unilocular fat cells: characteristics of growth in vitro and changes in differentiation properties. *Differentiation* **31**, 42-49.

81. Sugihara, H., Yonemitsu, N., Miyabara, S., and Toda, S. (1987). Proliferation of unilocular fat cells in the primary culture. *J.Lipid Res.* **28**, 1038-1045.

82. von Heimburg, D., Zachariah, S., Heschel, I., Kuhling, H., Schoof, H., Hafemann, B., and Pallua, N. (2001). Human preadipocytes seeded on freeze-dried collagen scaffolds investigated in vitro and in vivo. *Biomaterials* **22**, 429-438.

83. Kral, J. G. and Crandall, D. L. (1999). Development of a human adipocyte synthetic polymer scaffold. *Plast.Reconstr.Surg.* **104**, 1732-1738.

84. Huss, F. R. M. and Kratz, G. (2002). Adipose tissue processed for lipoinjection shows increased cellular survival in vitro when tissue engineering principles are applied. *Scand.J.Plast.Reconstr.Surg.* **36**, 166-171.

85. Patrick, C. W., Jr., Chauvin, P. B., Hobley, J., and Reece, G. P. (1999). Preadipocyte seeded PLGA scaffolds for adipose tissue engineering. *Tissue Eng.* **5**, 139-151.

86. Kawaguchi, N., Toriyama, K., Nicodemou-Lena, E., Inou, K., Torii, S., and Kitagawa, Y. (1998). De novo adipogenesis in mice at the site of injection of basement membrane and basic fibroblast growth factor. *Proc.Natl.Acad.Sci.U.S.A.* **95**, 1062-1066.

87. Huss, F. R. and Kratz, G. (2001). Mammary epithelial cell and adipocyte co-culture in a 3-D matrix: the first step towards tissue-engineered human breast tissue. *Cells Tissues Organs* **169**, 361-367.

88. Kimura, Y., Ozeki, M., Inamoto, T., and Tabata, Y. (2003). Adipose tissue engineering based on human preadipocytes combined with gelatin microspheres containing basic fibroblast growth factor. *Biomaterials* **24**, 2513-2521.

89. Sugihara, H., Toda, S., Yonemitsu, N., and Watanabe, K. (2001). Effects of fat cells on keratinocytes and fibroblasts in a reconstructed rat skin model using collagen gel matrix culture. *Br.J.Dermatol.* **144**, 244-253.

90. Toriyama, K., Kawaguchi, N., Kitoh, J., Tajima, R., Inou, K., Kitagawa, Y., and Torii, S. (2002). Endogenous adipocyte precursor cells for regenerative soft-tissue engineering. *Tissue Eng.* **8**, 157-165.

91. Tabata, Y., Miyao, M., Inamoto, T., Ishii, T., Hirano, Y., Yamaoki, Y., and Ikada, Y. (2000). De novo formation of adipose tissue by controlled release of basic fibroblast growth factor. *Tissue Eng.* **6**, 279-289.

92. Kimura, Y., Ozeki, M., Inamoto, T., and Tabata, Y. (2002). Time course of de novo adipogenesis in matrigel by gelatin microspheres incorporating basic fibroblast growth factor. *Tissue Eng.* **8**, 603-613.

93. Halberstadt, C., Austin, C., Rowley, J., Culberson, C., Loebsack, A., Wyatt, S., Coleman, S., Blacksten, L., Burg, K., and Mooney et, a. (2002). A hydrogel material for plastic and reconstructive applications injected into the subcutaneous space of a sheep. *Tissue Eng.* **8**, 309-319.

94. von Heimburg, D., Zachariah, S., Low, A., and Pallua, N. (2001). Influence of different biodegradable carriers on the in vivo behavior of human adipose precursor cells. *Plast.Reconstr.Surg.* **108**, 411-420.

95. Halbleib, M., Skurk, T., de Luca, C., von Heimburg, D., and Hauner, H. (2003). Tissue engineering of white adipose tissue using hyaluronic acid-based scaffolds. I: in vitro differentiation of human adipocyte precursor cells on scaffolds. *Biomaterials* **In Press, Corrected Proof**.

96. Widmer, M. S. and Mikos, A. G. (1998). Fabrication of biodegradable polymer scaffolds for tissue engineering. *In* "Frontiers in tissue engineering" (C. W. Patrick, Jr., A. G. Mikos, and L. V. McIntire, Eds.), Elsevier Science Ltd., Oxford.

97. Patrick, C. W., Jr., Zheng, B., Johnston, C., and Reece, G. P. (2002). Long-Term Implantation of Preadipocyte-Seeded PLGA Scaffolds. *Tissue Eng.* **8**, 283-293.

98. Shenaq, S. M. and Yuksel, E. (2002). New research in breast reconstruction: adipose tissue engineering. *Clin.Plast.Surg.* **29**, 111-125, vi.

99. Lehmann, J. M., Lenhard, J. M., Oliver, B. B., Ringold, G. M., and Kliewer, S. A. (1997). Peroxisome proliferator-activated receptors alpha and gamma are activated by indomethacin and other non-steroidal anti-inflammatory drugs. *J.Biol.Chem.* **272**, 3406-3410.

100. Sinha, D., Addya, S., Murer, E., and Boden, G. (1999). 15-Deoxy-delta(12,14) prostaglandin J2: a putative endogenous promoter of adipogenesis suppresses the ob gene. *Metab., Clin.Exp.* **48**, 786-791.

101. Slieker, L. J., Sloop, K. W., and Surface, P. L. (1998). Differentiation method-dependent expression of leptin in adipocyte cell lines. *Biochem.Biophys.Res.Commun.* **251**, 225-229.

102. Vunjak-Novakovic, G., Obradovic, B., Martin, I., Bursac, P. M., Langer, R., and Freed, L. E. (1998). Dynamic cell seeding of polymer scaffolds for cartilage tissue engineering. *Biotechnol.Prog.* **14**, 193-202.

103. Freed, L. E. and Vunjak-Novakovic, G. (2000). Tissue engineering bioreactors. *In* "Principles of Tissue Engineering" (R. P. Lanza, R. Langer, and J. P. Vacanti, Eds.), Academic Press, San Diego.

104. Gooch, K. J., Blunk, T., Courter, D. L., Sieminski, A. L., Bursac, P. M., Vunjak-Novakovic, G., and Freed, L. E. (2001). IGF-I and Mechanical Environment Interact to Modulate Engineered Cartilage Development. *Biochem.Biophys.Res.Commun.* **286** , 909-915.

105. Kellner, K., Schulz, M. B., Göpferich, A., and Blunk, T. (2001). Insulin in tissue engineering of cartilage: a potential model system for growth factor application. *J.Drug Targeting* **9**, 439-448.

106. Green, H. and Kehinde, O. (1979). Formation of normally differentiated subcutaneous fat pads by an established preadipose cell line. *J.Cell.Physiol.* **101**, 169-171.

107. Lucke, A., Tessmar, J., Schnell, E., Schmeer, G., and Göpferich, A. (2000). Biodegradable poly(D,L-lactic acid)-poly(ethylene glycol)-monomethyl ether diblock copolymers: Structures and surface properties relevant to their use as biomaterials. *Biomaterials* **21**, 2361-2370.

108. Göpferich, A., Peter, S. J., Lucke, A., Lu, L., and Mikos, A. G. (1999). Modulation of marrow stromal cell function using poly(D,L-lactic acid)- block-poly(ethylene glycol)-monomethyl ether surfaces. *J.Biomed.Mater.Res.* **46**, 390-398.

109. Lieb, E., Tessmar, J., Hacker, M., Fischbach, C., Rose, D., Blunk, T., Mikos, A. G., Göpferich, A., and Schulz, M. B. (2003). Poly(D,L-lactic acid)-poly(ethylene glycol)-monomethyl ether diblock copolymers control adhesion and osteoblastic differentiation of marrow stromal cells. *Tissue Eng.* **9**, 71-84.

110. Tessmar, J., Fischbach, C., Lucke, A., Blunk, T., and Göpferich, A. PEG-PLA diblock copolymers for the control of biomaterial-cell interaction. BioValley Tissue Engineering Symposium 2 (Freiburg). 25-11-1999.

Chapter 2

Evaluation of Culture Conditions: Influence of Cell Culture Media and Adipogenic Factors

Claudia Fischbach, Achim Göpferich, Torsten Blunk

Department of Pharmaceutical Technology, University of Regensburg,
93040 Regensburg, Germany

Introduction

The cell line 3T3-L1 represents one of the most frequently employed model systems for the study of adipocyte differentiation *in vitro*. It was established by Green et al. from the mouse fibroblast line 3T3 through the isolation of subclones that accumulate intracellular triglyceride droplets upon growth arrest [1]. As the resulting lipid containing cells resembled adipocytes, 3T3-L1 clones were proposed in 1973 for the first time as a valuable tool for the study of lipid accumulation and obesity [1]. For the past 30 years, 3T3-L1 preadipocytes have been extensively used to investigate the cellular and molecular mechanisms underlying adipocyte differentiation and, hence, they have been developed into a well characterized model system. In addition to providing abundant data concerning adipose conversion, reproducibility and high proliferation capacity are ensured. Due to these properties, 3T3-L1 cells appear to be a suitable cell source for establishing a 3-D *in vitro* model of adipogenesis. Nevertheless, prior to performing tissue engineering studies involving 3T3-L1, it was necessary to establish appropriate culture conditions for the growth and differentiation of the preadipocytes.

The methodologies described in the literature vary tremendously in terms of the media utilized and the composition of the hormonal cocktail triggering adipogenesis. DMEM supplemented with either 10% fetal bovine serum (FBS) or 10% calf serum (CS), as recommended by the supplier of 3T3-L1 (ATCC), is the most commonly utilized medium for the culture of 3T3-L1 cells. However, other formulations such as alpha-MEM/FBS or chemically defined serum-free media are also reported [2-4]. To the best of our knowledge, no study conducted thus far has aimed at comprehensively comparing different media. While the culture medium potentially has a great impact on the development of the cell cultures, it must be kept in mind that reported differences in adipose conversion are mainly due to varying hormonal induction. Nevertheless, composition of the cocktails reported in the literature is inconsistent as well. In general, the combination of a glucocorticoid, the cAMP enhancing agent isobutylmethylxanthin (IBMX), and pharmacological concentrations of insulin, which activates the IGF-1 receptor, have proven to be most effective in inducing the differentiation of 3T3-L1 [5-7]. However, some groups diverge from this protocol and add micromolar concentrations of indomethacin or troglitazone, two factors promoting the terminal differentiation of preadipocytes by activating PPARγ, a ligand-activated transcription factor known to play a pivotal role in adipogenesis [8-11]. With the aim of thoroughly

evaluating culture conditions for our particular purposes, it thus appears useful to not only assess the impact of the culture medium, but furthermore to investigate different induction protocols.

Therefore, the goal of our study was to thoroughly investigate the impact of the two commercially available media alpha-MEM and DMEM on adipogenesis with different induction protocols. Besides investigating the effects in two-dimensional (2-D) cell culture, adipose tissue formation was assessed in three-dimensional (3-D) cell-polymer constructs. Specifically, 3T3-L1 cell culture was performed either in alpha-MEM or in DMEM in both conventional 2-D conditions and 3-D polyglycolic acid fiber meshes. Adipose differentiation was routinely triggered with a hormonal cocktail consisting of corticosterone, IBMX, and insulin. In parallel, the influences of indomethacin and troglitazone were evaluated independently. In order to assess the characteristics of the differently cultivated cells, typical features of adipocyte differentiation were examined. Not only was the intracellular lipid accumulation investigated, but the expression of typical fat cell genes was analyzed on both the protein and the mRNA level as well. Finally, the tissue coherence of the generated 3-D cell-polymer constructs was histologically assessed in order to determine the suitability of the evaluated culture conditions for adipose tissue engineering.

Materials and methods

3T3-L1 preadipocytes were obtained from ATCC (Manassas, VA, USA). DMEM with 1.0 g/l glucose (Tab. 1), fetal bovine serum (FBS), and trypsin (1:250) were purchased from Biochrom KG Seromed (Berlin, Germany); phosphate buffered saline (PBS) and penicillin-streptomycin solution were from Life Technologies (Karlsruhe, Germany). MEM (alpha-modification), designated in the following as alpha-MEM (Tab. 1), corticosterone, indomethacin, and oil red O were purchased from Sigma-Aldrich (Deisenhofen, Germany). 3-isobutyl-1-methylxanthine (IBMX) was from Serva Electrophoresis GmbH (Heidelberg, Germany). Troglitazone and insulin were kindly provided by Dr. Thomas Skurk, Deutsches Diabetes Forschungsinstitut (Duesseldorf, Germany) and Hoechst Marion Roussel (Frankfurt a. M., Germany), respectively. Cell culture materials were obtained from Sarstedt AG & Co. (Nuembrecht, Germany) and BD Biosciences Labware (Heidelberg, Germany). Spinner flasks were self-made (250 ml volume, 6 cm bottom diameter with side arms for gas exchange). Silicon stoppers were obtained from Schuber & Weiss (München, Germany); needles were from Unimed (Lausanne, Switzerland). Polyglycolic acid (PGA) non-woven fiber meshes (12-14 µm fiber diameter; 96% porosity; 62 mg/cm^3 bulk density) were purchased from Albany Int. Research Co. (Mansfield, MA, USA) and die-punched into discs 5 mm in diameter and 2 mm thick. All other chemicals were acquired in analytical grade from Merck KGaA (Darmstadt, Germany).

Additional remarks table 1:
Numbered substances are in the medium as indicated below.
[1)] $CaCl_2 \cdot H_2O$; [2)] $MgSO_4 \cdot 7\ H_2O$; [3)] L-Cystine·2 HCl; [4)] L-Tyrosine·2 Na·2 H_2O; [5)] Pyridoxin·HCl
For comparison, calculations were performed to the total formula of the other medium.

Legend:

Essential amino acid
Conditionally essential amino acid
Vitamin-like substance

Enhanced concentration relative to the other medium

Table 1: Composition of alpha-MEM and DMEM (mg per l)

	Substance	alpha-MEM	DMEM
Minerals	NaCl	6,800	6,400
	KCl	400	400
	$CaCl_2$	200[1)]	200
	$MgSO_4$	97.67	97.69[2)]
	NaH_2PO_4	122	124
	$NaHCO_3$	2,200	3,700
Amino Acids	L-Alanine	25	-
	L-Arginine·HCl	126	84
	L-Asparagine·H_2O	50	-
	L-Aspartic Acid	30	-
	L-Cysteine·HCl·H_2O	100	-
	L-Cystine	24[3)]	48
	L-Glutamine	292	580
	L-Glutamic Acid	75	-
	Glycine	50	30
	L-Histidine·HCl·H_2O	42	42
	L-Isoleucine	52	105
	L-Leucine	52	105
	L-Lysine·HCl	72.5	146
	L-Methionine	15	30
	L-Phenylalanine	32	66
	L-Proline	40	-
	L-Serine	25	42
	L-Threonine	48	95
	L-Tryptophan	10	16
	L-Tyrosine	27.4[4)]	72
	L-Valine	46	94
Vitamins	L-Ascorbic Acid, Vit. C	50	-
	Biotin, Vit. H	0.1	-
	Choline chloride	1	4
	Folic acid, Vit. M	1	4
	Myo-Inositol	2	7.2
	Niacineamide, Vit. B3	1	4
	D-Pantothenic Acid, Vit. B5	1	4
	Pyridoxal·HCl, Vit. B6	1	4[5)]
	Riboflavin, Vit. B2	0.1	0.4
	Thiamine·HCl, Vit. B1	1	4
	Vitamin B12	1.36	-
	Thioctic Acid	0.2	-
Div.	D-Glucose	1,000	1,000
	$Fe(NO_3)_3$·9 H_2O	-	0.1
	Pyruvic Acid Na	110	110
	Phenolred	11	15

Cell culture:

3T3-L1 preadipocytes were expanded during 4 passages and frozen in liquid nitrogen. Subsequent to defrosting, the cells were further expanded; cells from the fourth passage (following cryo-storage) were used for experiments. Growth of stock cultures, cell plating (2-D), and cell seeding (3-D) was performed in DMEM/10% FBS, whereas proliferation, induction, and differentiation was conducted in both alpha-MEM and DMEM with serum, as indicated in (Tab. 2).

Table 2: Experimental set-up

Expansion	Plating (2-D) Seeding (3-D)	Proliferation	Induction	Differentiation
8 passages	12h (Plating) 2d (Seeding)	4d	2d	6d
		4d	2d	6d
10% FBS			**5% FBS**	

alpha-MEM (100 U/ml penicillin, 0.1 mg/ml streptomycin)
DMEM (100 U/ml penicillin, 0.1 mg/ml streptomycin)

For 2-D cell culture, preadipocytes were plated at a density of 5,000 cells per cm² and allowed to adhere overnight. After 12 hours, the medium was aspirated and the cells were fed with either alpha-MEM/10% FBS or DMEM/10% FBS. After four days of proliferation, adipogenesis was stimulated by administration of the particular hormonal cocktails designated in Tab. 3 to either alpha-MEM or DMEM. This induction time-point was referred to as day 0.

Table 3: Medium supplementation during induction and differentiation phase

Group	Induction		Differentiation	
control	5% FBS 1 µM insulin 0.1 µM corticosterone 0.5 mM IBMX	-	5% FBS 1 µM insulin	-
+ indomethacin		60 µM indomethacin		-
+ troglitazone		5 µM troglitazone		5 µM troglitazone

At day 2, the hormonal induction medium was replaced by differentiation medium alone (Tab. 3) and the cells were maintained under these conditions until day 8 and 10 (leptin ELISA) of adipogenesis, respectively. According to the differentiation protocols used in the

literature [10], troglitazone was supplemented with each medium change over the whole course of the experiment (Tab. 3). In summary, in this study 6 different groups were investigated, which were composed as follows: alpha-MEM – control, indomethacin, troglitazone; DMEM – control, indomethacin, troglitazone.

For the 3-D culture, PGA scaffolds were pre-wetted with 70% ethanol, and rinsed thoroughly with PBS. The scaffolds were pinned on needles (10 cm long, 0.5 mm diameter) and held in place with segments of silicone tubing (1 mm long). Four needles with two scaffolds each were inserted into a silicone stopper; the stopper was in turn placed into the mouth of a spinner flask containing a magnetic stir bar. The spinner flasks were filled with 100 ml culture medium and placed on a magnetic stir plate (Bellco Glas; Vineland, NJ, USA) at 80 rpm in an incubator (37°C, 5% CO_2). After 24 h, the medium was aspirated and the cell suspension containing $2x10^6$ cells per scaffold, i.e., $16x10^6$ per flask, was added to the flask. Stirring for two days at 80 rpm allowed for cell attachment to the polymer fibers. Cell-polymer constructs were transferred into 6-well plates (one construct and 5 ml culture medium per well) and cultured in the incubator dynamically on an orbital shaker at 50 rpm (Dunn Labortechnik GmbH; Asbach, Germany). Proliferation of the cell-seeded constructs was performed in DMEM and alpha-MEM supplemented with 10% FBS for 4 days (Tab. 2). Hormonal induction and adipose differentiation was conducted as stated above for 2-D cell culture (Tab. 2, 3).

In general, the cell culture medium was changed every other day. Cell harvesting was carried out consistent with the specific requirements of each analytical method described below.

Oil red O staining:

In order to visualize the accumulated cytoplasmic triglyceride droplets 8 days after hormonal stimulation of adipogenesis, oil red O staining was performed. For this purpose, the cells were washed with PBS. After subjecting the samples to an overnight fixation step in 10% buffered formalin, the adipocytes were stained as previously described [12].

Histology:

At day 8 of adipogenesis, fat-like constructs generated from the various 3-D cultures were fixed overnight in 10% buffered formalin. Subsequently, the specimen were dehydrated

and embedded in paraffin. Deparaffinized sections 5 µm thick were stained with hematoxylin and eosin (H&E) (Sigma-Aldrich; Deisenhofen, Germany). As this staining procedure using organic solvents led to lipid extraction from the cells, lipid storage was assessed by examining the size of blank areas which represented those spaces previously occupied by accumulated triglyceride droplets. Photographs were taken with a Dynax 600 si classic camera (Minolta Europe GmbH; Langenhagen, Germany) mounted on a Leica DM IRB light microscop (Leica Microsystems AG; Wetzlar, Germany).

Analysis of glycerol-3-phosphate dehydrogenase (GPDH):

At day 0, day 4, and day 8 of hormonal differentiation, 2-D cells and 3-D cell-polymer constructs were washed with PBS, harvested in lysis buffer (50 mM Tris, 1 mM EDTA, 1 mM mercaptoethanol, pH 7.5), and sonicated afterwards with a digital sonifier (Branson Ultrasonic Corporation; Danburg, CT, USA). The GPDH assay was performed as described in the literature [13,14]. Cytosolic protein concentration was determined after precipitation with trichloracetic acid using the Lowry assay [15]. GPDH activity was expressed as mU per mg protein.

Investigation of leptin secretion:

The leptin secretion of cells cultivated in 2-D and 3-D cell culture under different conditions was measured in cell culture media by using the Quantikine M immunoassay (R&D Systems; Wiesbaden, Germany) for mouse leptin. Media samples from day 8 to day 10 were taken and centrifuged for 5 min at 13,200 rpm (Centrifuge 5415 R, Eppendorf AG; Hamburg, Germany) to remove cell debris. The supernatants were frozen at –80°C until ELISA was conducted.

Reverse transcription polymerase chain reaction (RT-PCR):

In order to investigate gene expression, the cells were harvested at day 8 after hormonal stimulation with Trizol reagent (Invitrogen GmbH; Karlsruhe, Germany) and the total RNA was isolated according to manufacturers instructions. First-stranded cDNA was synthesized from total RNA by using random hexamers (Roche Diagnostics; Mannheim, Germany) and Superscript II RNase H- Reverse Transcriptase (Invitrogen GmbH; Karlsruhe, Germany). Subsequently, PCR was conducted with Sawady Taq-DNA-Polymerase (PeqLab; Erlangen,

Germany). Thereby, the amplification was carried out using specific primers and appropriate conditions for each gene (Tab. 4). Primers were purchased from Amersham Biosciences (Freiburg, Germany) and MWG-Biotech AG (Ebersberg, Germany). 18 S rRNA served as an internal control. Reverse transcription and PCR were performed using a Mastercycler Gradient (Eppendorf AG; Hamburg, Germany). The PCR products were analyzed by electrophoresis on agarose gels containing ethidium bromide, followed by imaging and densitometric scanning of the resulting bands using a Kodak EDAS 290 (Fisher Scientific; Schwerte, Germany).

Table 4: Primer sequences and PCR conditions for the investigated genes
Oligonucleotide sequences of mouse forward (sense) and reverse (antisense) primers. Gene amplification was performed by PCR according to the specified annealing temperatures (AT) and number of cycles for each gene. The reaction conditions of one cycle were as follows: denaturation for 45 sec at 94°C, annealing for 45 sec at the indicated temperatures, and extension for 1 min at 72°C.

Gene	Forward and reverse primers of examined genes	AT (°C) / Cycles
PPARγ	5′-AAC CTG CAT CTC CAC CTT ATT ATT CTG A-3′ 5′-GAT GGC CAC CTC TTT GCT CTG CTC CTG-3′	60 / 35
leptin	5′-GAC ACC AAA ACC CTC ATC AAG ACC-3′ 5′-GCA TTC AGG GCT AAC ATC CAA CT-3′	58,5 / 36
18 S	5′-TCA AGA ACG AAA GTC GGA GGT TCG-3′ 5′-TTA TTG CTC AAT CTC GGG TGG CTG-3′	60 / 22

Statistical analysis:

Statistical significance was determined by one-way analysis of variance ANOVA followed by Tukey post-hoc test (Software: SPSS 10.0 for Windows). The statistical significance level was set as indicated (either $p < 0.05$ or $p < 0.01$).

Results

Investigation of intracellular triglyceride (TG) storage:

At first, the lipid biosynthesis of differently cultivated adipocytes was assessed in conventional 2-D cell culture. Microscopic examination of oil red O stained adipocytes revealed that cultivation in alpha-MEM yielded enhanced triglyceride storage as compared to DMEM (Fig. 1). Whereas the number of differentiated cells did not vary between the two

media, alpha-MEM gave rise to larger lipid vacuoles, independent of the applied induction conditions. Investigation of the different hormonal protocols clarified that indomethacin treatment did not affect the size of the TG droplets as compared to control conditions (Fig. 1). In contrast, troglitazone supplementation resulted in adipocytes containing smaller lipid inclusions and, additionally, the number as well as the size of the attached cells was diminished relative to the control (Fig. 1). The differences due to the induction supplements were detected in both alpha-MEM and DMEM.

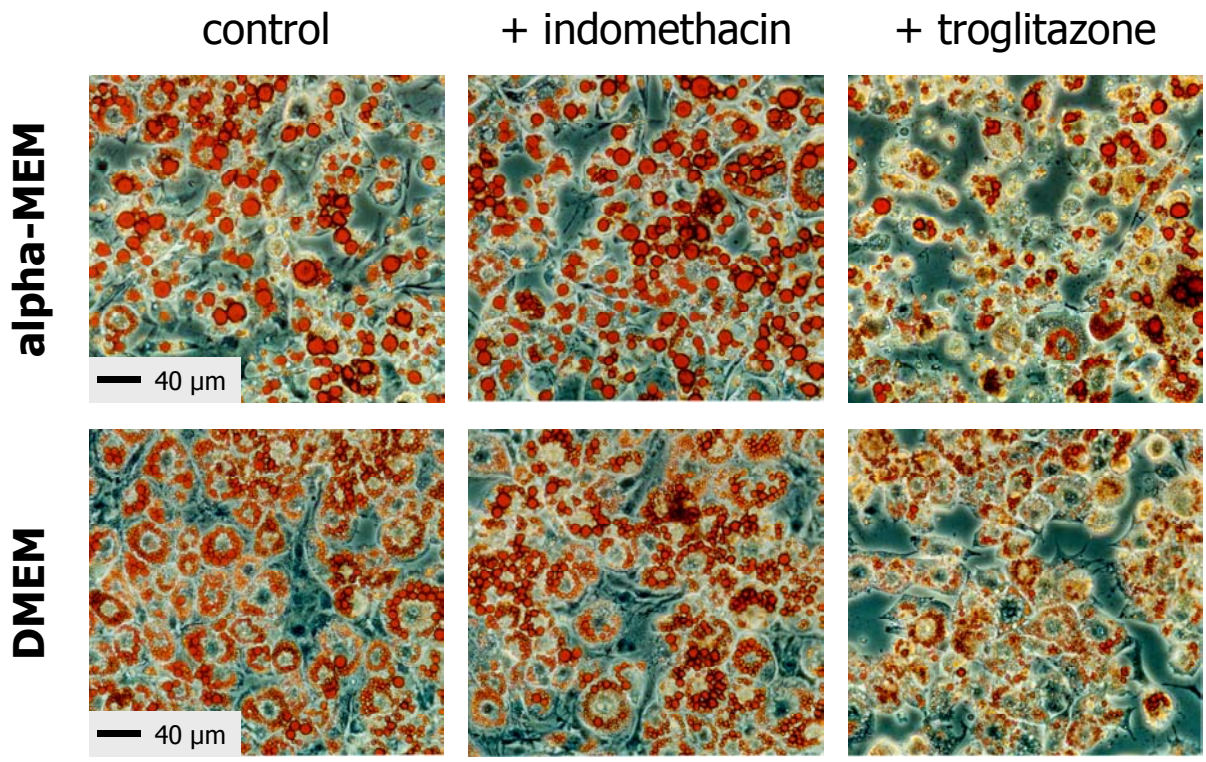

Fig. 1:
Triglyceride storage of adipocytes differentiated for 8 days under variable conditions in conventional 2-D cell culture was visualized by oil red O staining of intracellular lipid vacuoles. Bars represent 40 µm.

In 3-D cell culture, triglyceride storage was determined by microscopic examination of H&E stained cross-sections at day 8 of adipogenesis (Fig. 2). Comparison of constructs differentiated in the distinct media revealed the formation of coherent fat-like tissues with large lipid vacuoles in alpha-MEM, but not in DMEM (data not shown). The tissues developed in DMEM shrank over time and, hence, were smaller than those grown in alpha-MEM (data not shown). Investigation of the different induction protocols, as indicated below for alpha-MEM, revealed that the size of the accumulated lipid droplets (represented by blank spaces within the cell-polymer constructs) was similar for the control and the indomethacin

group. In contrast, troglitazone treatment resulted in smaller triglyceride inclusions being in good accordance with the findings described above for 2-D cultivation. Furthermore, the area of developed coherent tissue mass was diminished in the latter group as compared to both of the other conditions. Comparison of the control constructs and those differentiated according to the indomethacin protocol revealed no substantial distinctions with regard to the extent of formed fat-like tissue (Fig. 2).

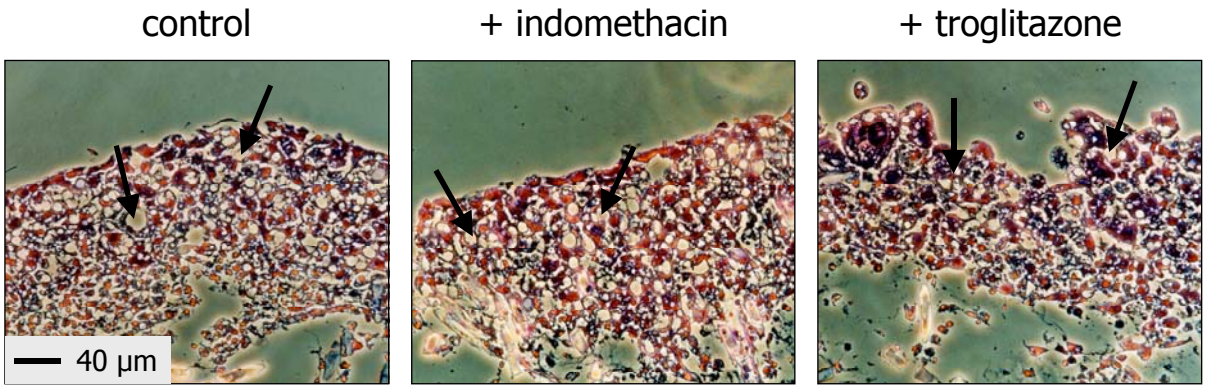

Fig. 2:
Triglyceride accumulation and tissue coherence of cell-polymer constructs generated with different induction protocols in alpha-MEM as detected by staining of histological cross-sections with hematoxylin and eosin (H&E). Arrows indicate spaces previously occupied by lipid droplets.

Subsequently, the activity of GPDH, a major enzyme involved in TG biosynthesis was determined. Measurement were normalized to cytoplasmic protein content to account for varying cell densities. The enzyme kinetics of all groups investigated indicated increased activity over the course of the experiment (Fig. 3). At day 4 and day 8, differentiation in alpha-MEM was demonstrated to yield significantly enhanced GPDH activities as compared to DMEM (Fig. 3).

In terms of the induction protocols, after 4 days and 8 days of differentiation in alpha-MEM, troglitazone treatment was shown to result in significantly enhanced GPDH activities ($p<0.01$) as compared to the control group and to the indomethacin group. In contrast, adipocytes cultivated in DMEM exhibited a significant ($p<0.01$) increase only at day 8 of adipogenesis. Significant differences were not detected between the control and additional indomethacin in either of the media (Fig. 3). Thus, culture in alpha-MEM combined with hormonal stimulation using the troglitazone cocktail gave rise to the highest GPDH values in 2-D culture.

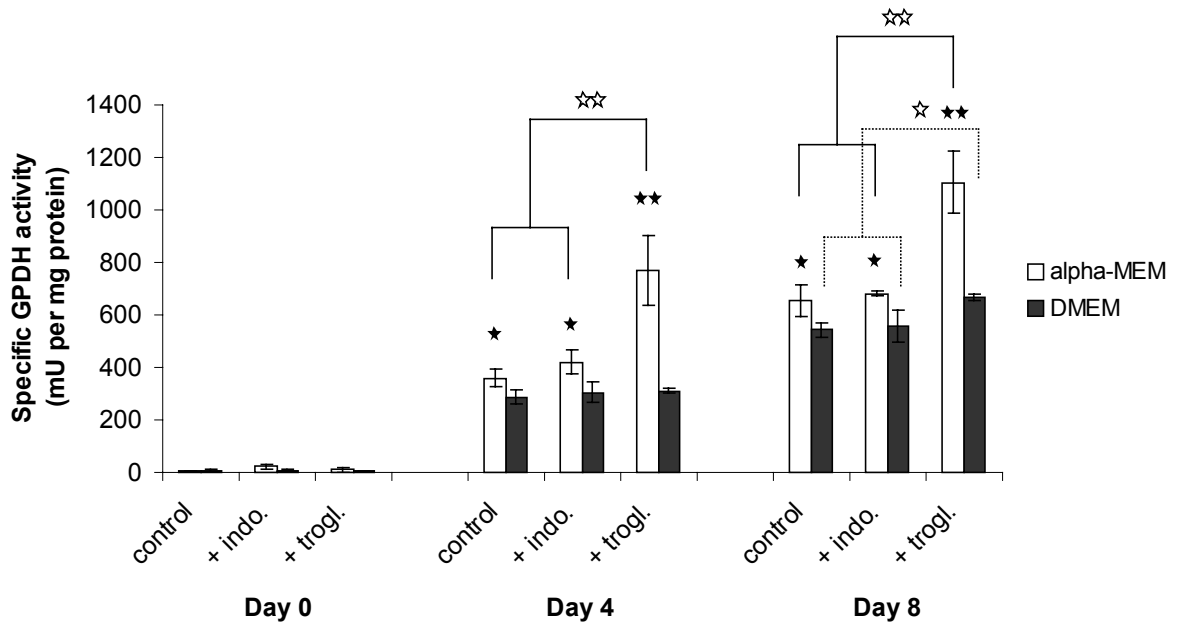

Fig. 3:
GPDH activity in 2-D conventional cell culture. Impact of different cell culture media and induction protocols were determined by analysis of GPDH kinetics subsequent to hormonal induction (referred to as day 0). Two independent experiments were conducted, representative result of one experiment is shown here. Statistically significant differences between alpha-MEM and DMEM are indicated by ★ ($p<0.05$) and ★★ ($p<0.01$), whereas significances resulting from different induction factors are denoted by ☆ ($p<0.05$) and ☆☆ ($p<0.01$).

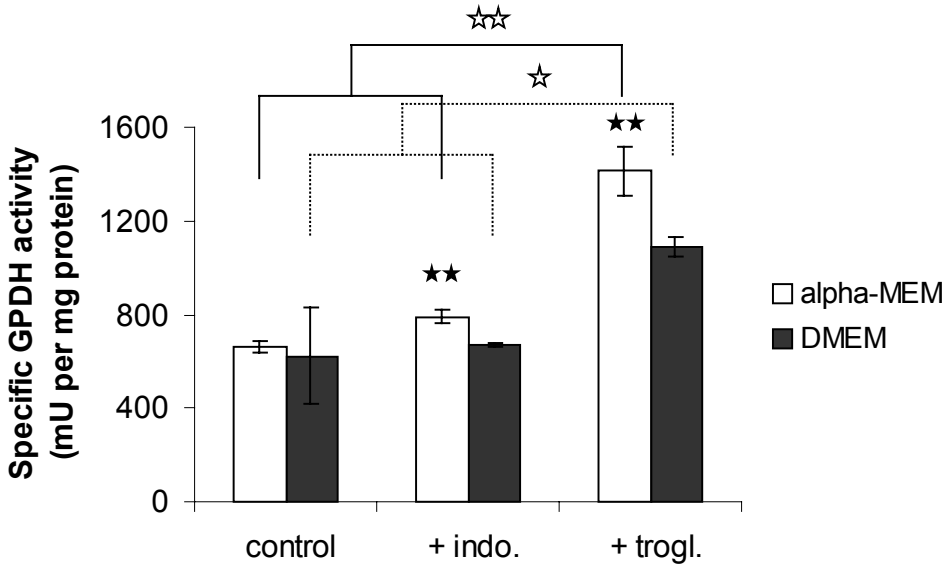

Fig. 4:
Impact of different cell culture media and induction protocols on GPDH activity in 3-D cell culture was determined at day 8 after hormonal induction. Data represent the mean ± SD of three constructs. Two independent experiments were conducted, a representative result of one experiment is shown here. Statistically significant differences ($p<0.01$) between alpha-MEM and DMEM are indicated by ★★. Additionally, significant differences resulting from different induction protocols are denoted by ☆ ($p<0.05$) and ☆☆ ($p<0.01$), respectively .

The differences in GPDH activity determined in 2-D cell culture were supported by the findings gained from measurement of 3-D cell-polymer constructs at day 8 of differentiation (Fig. 4).Again, as compared to DMEM, alpha-MEM was shown to yield significantly increased ($p<0.01$) enzyme activities for the indomethacin and the troglitazone group. Differentiation under control conditions did not reveal a statistically significant difference between alpha-MEM and DMEM. Comparison of the various induction protocols confirmed that troglitazone treatment provoked significantly enhanced GPDH values in both media as compared to hormonal induction under control conditions and with the addition of indomethacin.

Analysis of leptin secretion:

The satiety hormone leptin is secreted by mature adipocytes. As its expression is dependent upon the cellular differentiation status, we analyzed leptin secretion in order to gain insight into how different media and induction protocols regulate protein secretion. In addition to hormonal stimulation under control conditions, the effects of indomethacin and troglitazone addition were analyzed. Troglitazone, a PPARγ ligand, is known to down-regulate leptin secretion [9], but the effects of indomethacin on leptin levels are discussed controversially in the literature [8,9,16,17].

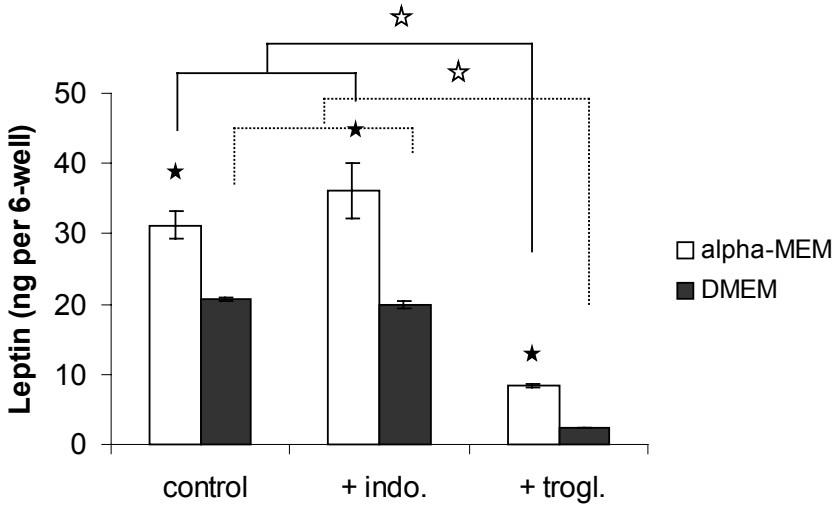

Fig. 5:
Leptin secretion in conventional 2-D cell culture. Impact of different cell culture media and induction protocols, as measured from cell culture media sampled form day 8 to 10 by ELISA. Three independent experiments were performed, representative result of one experiment is shown here. Values are expressed as mean ± SD (n=3). Statistically significant differences ($p<0.05$) between alpha-MEM and DMEM are indicated by ★, whereas significances ($p<0.01$) resulting from addition of indomethacin or troglitazone are denoted by ☆.

In 2-D cell culture media collected from day 8 to 10, alpha-MEM was clearly demonstrated to yield significantly ($p<0.01$) enhanced leptin concentrations as compared to DMEM, independent of the applied hormonal cocktail (Fig. 5). Analysis of different induction protocols furthermore proved that cellular leptin secretion was significantly inhibited ($p<0.01$) by troglitazone treatment. In contrast, indomethacin administration resulted in similar amounts of secreted leptin relative to hormonal stimulation under control conditions (Fig. 5). This result was obtained in both alpha-MEM and DMEM.

As alpha-MEM was shown in 2-D cell culture to yield improved leptin secretion as compared to DMEM, the impact of different induction protocols on 3-D protein secretion was not determined in both media, but only in alpha-MEM (Fig. 6). Comparison of the results with those examined in 2-D cell culture revealed that the ratio of leptin secretion under control conditions, additional indomethacin, and troglitazone treatment was strikingly similar (Fig. 6). Whereas supplementation with indomethacin did not result in statistically significant differences, leptin concentration in the medium was significantly ($p<0.01$) reduced by troglitazone (Fig. 6). It has to be noted, however, that values normalized to protein concentration were lower in 3-D cell culture as compared to conventional 2-D cell culture (values determined under control conditions: 35.3 ng leptin per mg protein (2-D) control 23.7 ng leptin per mg protein (3-D)).

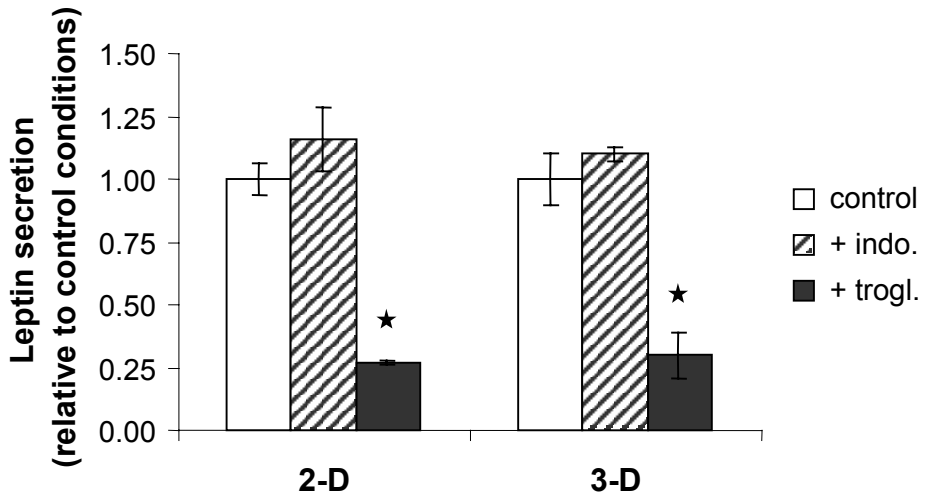

Fig. 6:
The influence of different hormonal induction protocols on leptin secretion in 2-D and 3-D cell culture media (alpha-MEM, sampled from day 8 to 10), as measured by ELISA. Data represent the mean ± SD (n=3). Statistically significant differences ($p < 0.01$) are denoted by ★. The mean leptin amount in the medium after "control" induction were 31.17 ± 1.94 ng per 6-well and 9.48 ± 0.95 ng per construct, respectively. Two independent experiments were conducted, representative result of one experiment is shown here.

Examination of mRNA gene expression:

In order to gain further insight into how the different media and induction protocols regulate leptin secretion, investigation of mRNA gene expression was performed by means of RT-PCR at day 8 of adipogenesis. As troglitazone belongs to the class of thiazolidinediones, which is described to inhibit leptin secretion through a mechanism involving PPARγ activation [17], we focused on analysis of PPARγ and leptin mRNA. Comparison of the distinct media and induction protocols was conducted in 2-D cell culture. Additionally, 3-D cell-polymer constructs were induced in alpha-MEM in order to verify the results determined in 2-D.

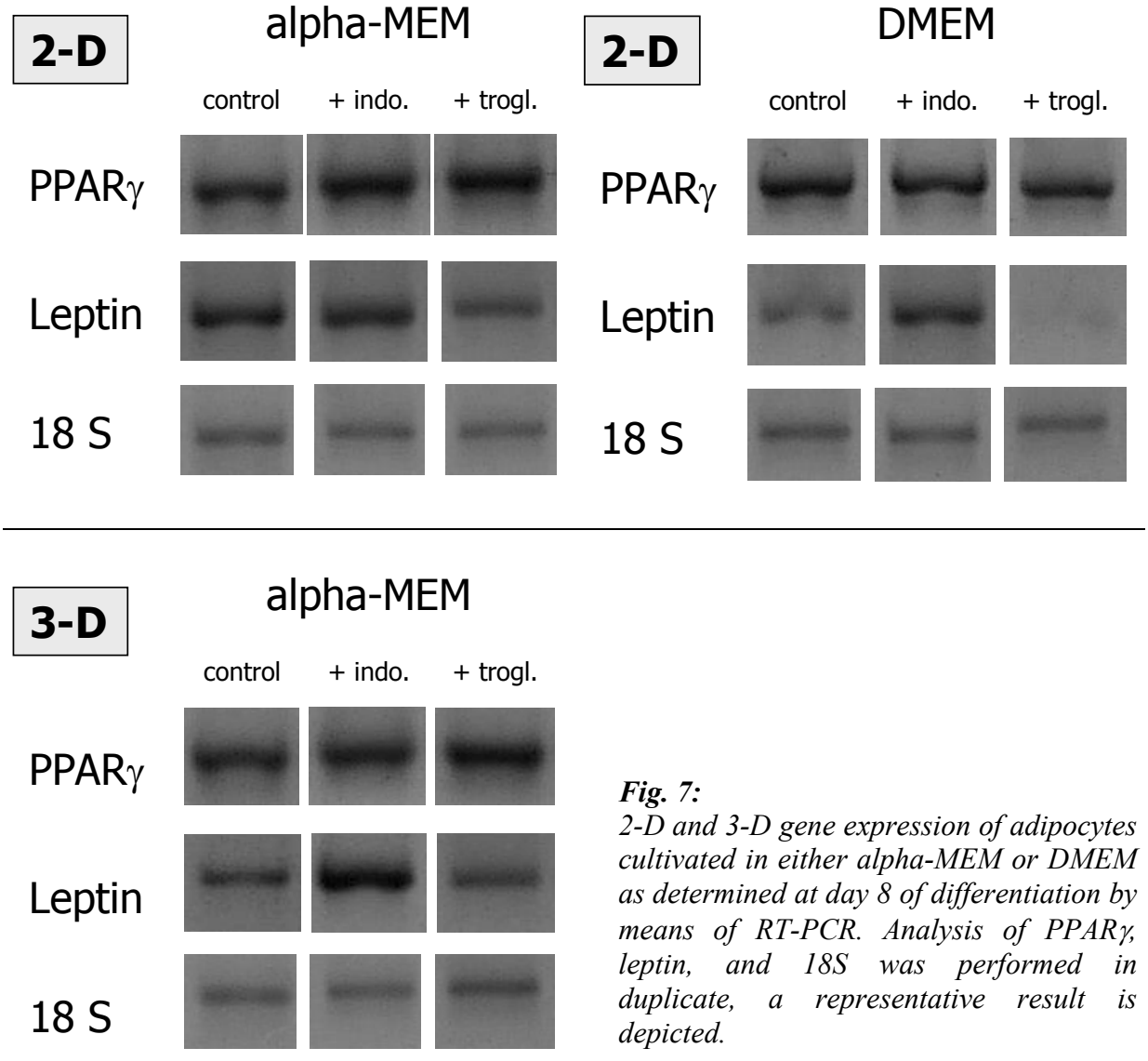

Fig. 7:
2-D and 3-D gene expression of adipocytes cultivated in either alpha-MEM or DMEM as determined at day 8 of differentiation by means of RT-PCR. Analysis of PPARγ, leptin, and 18S was performed in duplicate, a representative result is depicted.

Examination of PPARγ expression in 2-D cell culture revealed that all band intensities were slightly increased by alpha-MEM as compared to DMEM (Fig. 7). Furthermore, indomethacin and troglitazone supplementation resulted in a faint increase of PPARγ in alpha-MEM as compared to controls, whereas in DMEM the bands exhibited similar densities. Extent of leptin mRNA expression in 2-D cell culture was in good accordance with the findings determined by ELISA: gene expression on the transcriptional level was enhanced in alpha-MEM relative to DMEM (Fig. 7). Additionally, troglitazone supplementation caused a remarkable decrease in leptin expression in both media. Although indomethacin is equally known to act as a PPARγ ligand [11], the addition of indomethacin did not inhibit leptin expression relative to control conditions, neither in alpha-MEM nor in DMEM. On the contrary, administration of additional indomethacin to DMEM resulted in enhanced mRNA levels (Fig. 7).

Analysis of PPARγ expression in 3-D cell culture (grown in alpha-MEM) showed small differences as compared to 2-D conditions. In 3-D cell culture only troglitazone treatment mediated a faint intensification of bands, whereas in 2-D both indomethacin and troglitazone caused this effect. Furthermore, the levels of leptin mRNA appeared to be dissimilar from the 2-D levels. In particular, leptin expression was seemingly increased by induction with indomethacin, while troglitazone rather provoked a only weak reduction of leptin expression.

Evaluation of cytoplasmic protein content:

Subsequent to hormonal stimulation, 3T3-L1 preadipocytes undergo at least one round of cell division leading to the so called process of clonal expansion, which is regarded as a prerequisite for adipocyte differentiation [5,18,19]. With the objective of estimating whether alpha-MEM and DMEM result in different cellular amplification during clonal expansion, cytoplasmic protein content was analyzed before (day 0) and 2 days after hormonal stimulation (day 4) in conventional 2-D cell culture (Fig. 8).

At day 0, concentration of cellular protein was significantly enhanced in DMEM cultures, as compared to alpha-MEM ($p<0.01$, $p<0.05$). Four days after hormonal induction, however, the relations were reversed. In the control group, cytoplasmic protein content was significantly increased ($p<0.01$) in alpha-MEM relative to DMEM, whereas additional indomethacin treatment yielded similar values for both media (Fig. 8). Thus, the relative increase of protein content from day 0 to day 4 was significantly augmented through culture

in alpha-MEM (control: 4.5-fold, indomethacin: 4.5-fold) as compared to DMEM (control: 3.2-fold, indomethacin: 3.4-fold) (Fig. 8).

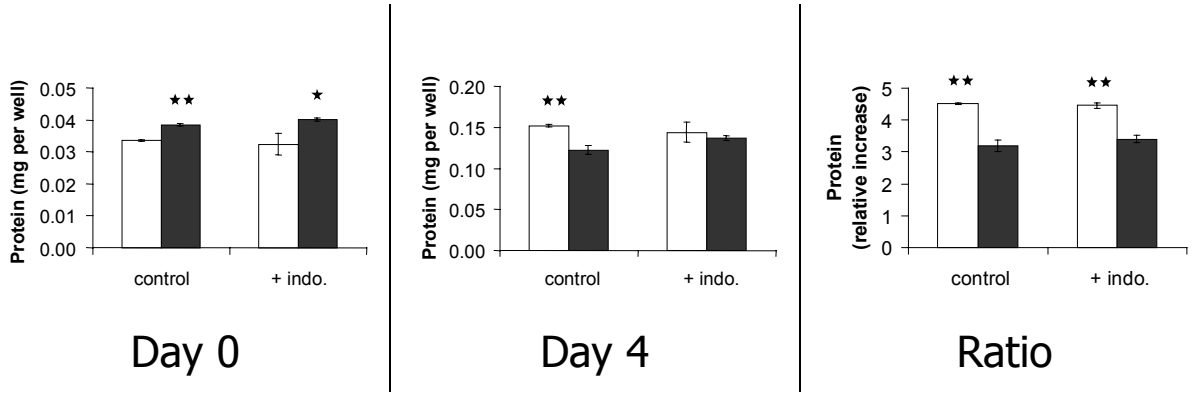

Fig. 8:
Cytoplasmic protein content of 3T3-L1 cells two-dimensionally grown in alpha-MEM (□) *and in DMEM* (■) *(in 24-well plates) was measured by the Lowry assay [15] at day 0 and day 4 of differentiation. Additionally, the relative increase of protein content (day 0 to day 4) is depicted. Values are denoted as means ± SD (n=3). Statistically significant differences between alpha-MEM and DMEM are indicated by ★ ($p<0.05$) and ★★ ($p<0.01$), respectively.*

Discussion

In addition to providing highly reproducible conditions, preadipocytes from the 3T3-L1 cell line are well characterized and easily available. Therefore, they represent an attractive cell source for tissue engineering of a 3-D model system of adipogenesis. However, prior to developing such a model system, the culture conditions reported in the literature have to be assessed with regard to their suitability for this particular purpose. Therefore, this study was conducted with the aim of simultaneously evaluating two media (DMEM and alpha-MEM) and three hormonal induction protocols (designated as control, indomethacin, and troglitazone) for their ability to promote 3T3-L1 differentiation in both 2-D and 3-D cell culture.

In this study, we could demonstrate that cultivation in alpha-MEM yielded superior results with regard to typical fat cell features as compared to DMEM, which is most frequently utilized for growth of 3T3-L1. In terms of hormonal induction, we showed that additional indomethacin (60 µM) treatment did not result in substantial differences relative to control stimulation with corticosterone, IBMX, and insulin. In contrast, supplementary

troglitazone (5 µM) resulted in adipocyte characteristics distinctly different from both the control and the indomethacin group.

Specifically, microscopic investigation of intracellular triglyceride storage in either 2-D or 3-D cell culture elucidated that the size of lipid inclusions was increased in alpha-MEM as compared to DMEM (Fig. 1). Quantitative determination of lipid biosynthesis through measurement of GPDH activity equally revealed enhanced triglyceride storage for adipocytes (2-D and 3-D) differentiated in alpha-MEM (Fig. 3, 4). Regarding the impact of different induction protocols on lipid accumulation, it was clarified that supplementation of indomethacin did not result in significant effects as compared to control conditions (Fig. 1-4). In contrast, additional troglitazone elicited increased GPDH enzyme activities and seemingly less attached cells exhibiting smaller triglyceride vacuoles indicating that vacuole size does not necessarily correlate to GPDH activity (Fig. 1-4). Our observations corresponded well with published data, describing the thiazolidinedione troglitazone as a synthetic ligand of PPARγ capable of stimulating terminal differentiation by activating this particular nuclear receptor [20,21]. The number and the size of the attached adipocytes may be explained by published data suggesting that thiazolidinediones stimulate apoptosis of mature fat cells and, concomitantly, promote differentiation of small adipocytes [20,22].

A further criterion used to assess the various culture conditions was the extent of cellular leptin expression. Leptin, a peptide hormone secreted by mature adipocytes, is involved in the regulation of food intake and energy expenditure. Its expression is dependent upon the cellular differentiation status [5,23] and, therefore, we attempted to gain insight into how the culture media and induction protocols modulate leptin expression on the protein as well as on the mRNA level. At first, leptin secretion was studied in 2-D cell culture. Thereby, increased leptin secretion was proven for alpha-MEM relative to DMEM independent of the induction protocol (Fig. 5), which led us to conclude that alpha-MEM may improve adipocyte maturation. Regarding different hormonal stimulation, it was furthermore demonstrated that medium supplementation with 60 µM indomethacin showed no significant effects as compared to control conditions, while 5 µM troglitazone substantially decreased leptin secretion (Fig. 5). 3-D cell culture in alpha-MEM was found to be similarly influenced by indomethacin and troglitazone treatment, thus confirming the aforementioned results (Fig. 6). According to the literature, troglitazone is clearly known to dramatically reduce leptin expression [16,17,22,24]. However, for 3T3-L1 cells indomethacin is discussed controversially. Whereas Sinha et al. reported inhibition of leptin expression by indomethacin [9], Slieker et al. demonstrated the opposite, namely up-regulation of leptin [8]. The results of

our study neither indicated stimulation nor inhibition of leptin secretion by indomethacin treatment. Besides other factors, leptin expression is reportedly linked to PPARγ activation, a key event of adipogenesis [17]. Because troglitazone, as well as indomethacin, represent PPARγ ligands [11,20], we aimed at additionally investigating leptin and PPARγ gene expression on the mRNA level. At first, the results of RT-PCR demonstrated the superiority of alpha-MEM over DMEM for both leptin and PPARγ expression (Fig. 7). Furthermore, it was shown in 2-D and 3-D cell culture (in alpha-MEM) that supplementary troglitazone slightly augmented PPARγ levels paralleling a decrease in leptin expression. In contrast, indomethacin treatment did not cause the inhibition of leptin mRNA, whereas it provoked enhanced PPARγ gene expression in 2-D cell culture (Fig. 7). In general, RT-PCR of leptin reflected the results determined by ELISA. In addition, PPARγ gene expression was documented to be affected only partly by the different cultivation conditions.

In terms of the histological characteristics of the tissues engineered in alpha-MEM, it could be assessed that the constructs stimulated according to the control and to the indomethacin protocol exhibited comparable properties with respect to tissue coherence and lipid droplet size (Fig. 2). In contrast, additional troglitazone resulted in less coherent tissue mass and smaller triglyceride inclusions (Fig. 2). The findings described above led us to regard hormonal stimulation with additional troglitazone as being inappropriate for adipose tissue engineering purposes.

With the aim of defining potential reasons for improved adipogenesis in alpha-MEM relative to DMEM, cytoplasmic protein was analyzed before and after hormonal stimulation. Thereby, it could be estimated whether clonal expansion, a prerequisite of adipocyte differentiation, is affected. Before induction, the protein content was diminished in alpha-MEM as compared to DMEM; after induction the relations were reversed and enhanced protein content was determined in alpha-MEM (Fig. 8). Accordingly, the calculated ratios indicating the relative increase of protein content after hormonal induction were increased in alpha-MEM. This finding prompted us to hypothesize that alpha-MEM may favor adipogenesis by enhancing cellular amplification during clonal expansion. However, future studies remain to be performed in order to examine this assumption more in detail.

The different adipogenic properties of the media are likely to be derived from their nutrient composition (Tab. 1). In general, DMEM contains fewer amino acids and vitamins. However, on the whole, nutrient concentrations are higher than those contained in alpha-MEM (Fig. 8). The most obvious difference between the media is that DMEM lacks vitamin

C and proline, two substances required for formation of adequate extracellular matrix (Tab. 1) [25]. Though proline represents a non-essential amino acid, it is thought that exogenous supply may prove beneficial as 3T3-L1 exhibit augmented collagen biosynthesis, which was demonstrated by increased incorporation ratio of ^{14}C-labeled proline into hydroxyproline residues of protein [26]. Vitamin C is equally involved in collagen biosynthesis. The factor acts via maintaining proline hydroxylase (and lysine hydroxylase) in its activated form [25]. Accordingly, a lack of vitamin C mediates incomplete hydroxylation of collagen resulting in inappropriately formed collagen fibers [25]. However, the formation of an adequate extracellular matrix is known to be crucial for the terminal differentiation of adipocytes [18,27,28]. For instance, collagen type IV is reported to be up-regulated during adipogenesis [29]. A direct connection between collagen IV biosynthesis, vitamin C, and adipogenesis was proven by Ono et al., showing that ascorbic acid phosphate stimulated type IV collagen synthesis and accelerated adipose conversion of 3T3-L1 cells [30]. Furthermore, Kawada et al. clarified that vitamin C significantly stimulated adipocyte conversion at concentrations above 10 µM [31]. Specifically, the addition of physiological concentrations of vitamin C (200 µM) to DMEM yielded triglyceride concentrations and GPDH activities over 400% of the control. As alpha-MEM contains 50 mg vitamin C per liter of medium, which corresponds to a molar concentration of 284 µM, it seems likely that vitamin C essentially contributes to the determined differences in adipogenesis. Finally, biotin represents a further candidate potentially contributing to the distinct adipogenic effects of the media. The vitamin acts as a coenzyme for many carboxylation reactions and is, for instance, decisively involved in the biosynthesis of fatty acids [32]. The activity of biotin-dependent carboxylases increases during adipogenesis and, therefore, the absence of biotin in DMEM (Tab. 1) may play a part in diminished adipogenesis relative to alpha-MEM [33,34]. Though the above mentioned factors possibly account for the determined differences other ingredients of the media may be responsible as well.

In summary, the results of our study indicate a substantially improved adipose conversion of 3T3-L1 cells in alpha-MEM as compared to DMEM. Comparison of the nutrient composition of the media suggests proline, vitamin C and biotin, contained in alpha-MEM but lacking in DMEM, as likely candidates that may account for this finding. The exact impact of these substances remains to be investigated in further studies. Evaluation of different hormonal induction protocols showed no significant distinction between control stimulation (corticosterone, IBMX, and insulin) and additional indomethacin (60 µM). In contrast, supplementary troglitazone (5 µM) yielded adipose tissue formation less suitable for

the tissue engineering of fat. Accordingly, the development of a 3-D model system of adipogenesis by means of tissue engineering is suggested to be conducted in alpha-MEM. Furthermore, adipocyte differentiation is recommended to be either initiated by treatment with the hormonal control cocktail or with additional indomethacin.

References

1. Green, H. and Kehinde, O. (1974). Sublines of Mouse 3T3 Cells That Accumulate Lipid. *Cell* 113-116.

2. Black, M. A. and Begin-Heick, N. (1995). Growth and maturation of primary-cultured adipocytes from lean and ob/ob mice. *J.Cell.Biochem.* **58**, 455-463.

3. Staiger, H., Haring, H. U., and Loffler, G. (2002). Serum-free differentiation of 3T3-L1 preadipocytes is characterized by only transient expression of peroxisome proliferator-activated receptor-gamma. *Biochem.Biophys.Res.Commun.* **296**, 125-128.

4. Schmidt, W., Poll-Jordan, G., and Loffler, G. (1990). Adipose conversion of 3T3-L1 cells in a serum-free culture system depends on epidermal growth factor, insulin-like growth factor I, corticosterone, and cyclic AMP. *J.Biol.Chem.* **265**, 15489-15495.

5. Hwang, C. S., Loftus, T. M., Mandrup, S., and Lane, M. D. (1997). Adipocyte differentiation and leptin expression. *Annu.Rev.Cell Dev.Biol.* **13**, 231-259.

6. Cowherd, R. M., Lyle, R. E., and McGehee, R. E., Jr. (1999). Molecular regulation of adipocyte differentiation. *Semin.Cell Dev.Biol.* **10**, 3-10.

7. Smith, P. J., Wise, L. S., Berkowitz, R., Wan, C., and Rubin, C. S. (1988). Insulin-like growth factor-I is an essential regulator of the differentiation of 3T3-L1 adipocytes. *J.Biol.Chem.* **263**, 9402-9408.

8. Slieker, L. J., Sloop, K. W., and Surface, P. L. (1998). Differentiation method-dependent expression of leptin in adipocyte cell lines. *Biochem.Biophys.Res.Commun.* **251**, 225-229.

9. Sinha, D., Addya, S., Murer, E., and Boden, G. (1999). 15-Deoxy-delta(12,14) prostaglandin J2: a putative endogenous promoter of adipogenesis suppresses the ob gene. *Metab., Clin.Exp.* **48**, 786-791.

10. Kim, Y. C., Gomez, F. E., Fox, B. G., and Ntambi, J. M. (2000). Differential regulation of the stearoyl-CoA desaturase genes by thiazolidinediones in 3T3-L1 adipocytes. *J.Lipid Res.* **41**, 1310-1316.

11. Lehmann, J. M., Lenhard, J. M., Oliver, B. B., Ringold, G. M., and Kliewer, S. A. (1997). Peroxisome proliferator-activated receptors alpha and gamma are activated by indomethacin and other non-steroidal anti-inflammatory drugs. *J.Biol.Chem.* **272**, 3406-3410.

12. Hausman, G. J. (1981). Techniques for studying adipocytes. *Stain Technol.* **56**, 149-154.

13. Bachmeier, M. and Loffler, G. (1995). Influence of growth factors on growth and differentiation of 3T3-L1 preadipocytes in serum-free conditions. *Eur.J.Cell Biol.* **68**, 323-329.

14. Pairault, J. and Green, H. (1979). A study of the adipose conversion of suspended 3T3 cells by using glycerophosphate dehydrogenase as differentiation marker. *Proc.Natl.Acad.Sci.U.S.A.* **76**, 5138-5142.

15. Lowry, O. H., Rosebrough, N. J., Farr, A. L., and Randall, R. J. (1951). Protein measurement with the Folin phenol reagent. *J.Biol.Chem.* **193**, 265-275.

16. Murata, M., Kaji, H., Takahashi, Y., Iida, K., Mizuno, I., Okimura, Y., Abe, H., and Chihara, K. (2000). Stimulation by eicosapentaenoic acids of leptin mRNA expression and its secretion in mouse 3T3-L1 adipocytes in vitro. *Biochem.Biophys.Res.Commun.* **270**, 343-348.

17. Kallen, C. B. and Lazar, M. A. (1996). Antidiabetic thiazolidinediones inhibit leptin (ob) gene expression in 3T3-L1 adipocytes. *Proc.Natl.Acad.Sci.U.S.A.* **93**, 5793-5796.

18. Gregoire, F. M., Smas, C. M., and Sul, H. S. (1998). Understanding adipocyte differentiation. *Physiol.Rev.* **78**, 783-809.

19. Tang, Q. Q., Otto, T. C., and Daniel Lane, M. (2003). Mitotic clonal expansion: A synchronous process required for adipogenesis. *Proc.Natl.Acad.Sci.U.S.A.* **100**, 44-49.

20. Houseknecht, K. L., Cole, B. M., and Steele, P. J. (2002). Peroxisome proliferator-activated receptor gamma (PPARgamma) and its ligands: a review. *Domest.Anim.Endocrinol.* **22**, 1-23.

21. Rosen, E. D. and Spiegelman, B. M. (2000). Molecular regulation of adipogenesis. *Annu.Rev.Cell Dev.Biol.* **16**, 145-171.

22. Okuno, A., Tamemoto, H., Tobe, K., Ueki, K., Mori, Y., Iwamoto, K., Umesono, K., Akanuma, Y., Fujiwara, T., and Horikoshi et, a. (1998). Troglitazone increases the number of small adipocytes without the change of white adipose tissue mass in obese Zucker rats. *J.Clin.Invest.* **101**, 1354-1361.

23. MacDougald, O. A., Hwang, C. S., Fan, H., and Lane, M. D. (1995). Regulated expression of the obese gene product (leptin) in white adipose tissue and 3T3-L1 adipocytes. *Proc.Natl.Acad.Sci.U.S.A.* **92**, 9034-9037.

24. Considine, R. V. (2001). Regulation of leptin production. *Rev.Endocr.Metab.Disord.* **2** , 357-363.

25. Stryer, L. (2003). Bindegewebsproteine. *In* "Biochemie" Spektrum Akademischer Verlag GmbH, Oxford.

26. Green, H. and Meuth, M. (1974). An established pre-adipose cell line and its differentiation in culture. *Cell* **3**, 127-133.

27. Ibrahimi, A., Bonino, F., Bardon, S., Ailhaud, G., and Dani, C. (1992). Essential role of collagens for terminal differentiation of preadipocytes. *Biochem.Biophys.Res.Commun.* **187**, 1314-1322.

28. Spiegelman, B. M. and Ginty, C. A. (1983). Fibronectin modulation of cell shape and lipogenic gene expression in 3T3-adipocytes. *Cell* **35**, 657-666.

29. Aratani, Y. and Kitagawa, Y. (1988). Enhanced synthesis and secretion of type IV collagen and entactin during adipose conversion of 3T3-L1 cells and production of unorthodox laminin complex. *J.Biol.Chem.* **263**, 16163-16169.

30. Ono, M., Aratani, Y., Kitagawa, I., and Kitagawa, Y. (1990). Ascorbic acid phosphate stimulates type IV collagen synthesis and accelerates adipose conversion of 3T3-L1 cells. *Exp.Cell Res.* **187**, 309-314.

31. Kawada, T., Aoki, N., Kamei, Y., Maeshige, K., Nishiu, S., and Sugimoto, E. (1990). Comparative investigation of vitamins and their analogues on terminal differentiation, from preadipocytes to adipocytes, of 3T3-L1 cells. *Comp.Biochem.Physiol.A Mol.Integr.Physiol.* **96**, 323-326.

32. Löffler, G. and Petrides, P. (1990). Vitamine. *In* "Biochemie und Pathobiochemie" Springer Verlag, Berlin.

33. Chang, H. I. and Cohen, N. D. (1983). Regulation and intracellular localization of the biotin holocarboxylase synthetase of 3T3-L1 cells. *Arch.Biochem.Biophys.* **225**, 237-247.

34. Freytag, S. O. and Utter, M. F. (1980). Induction of pyruvate carboxylase apoenzyme and holoenzyme in 3T3-L1 cells during differentiation. *Proc.Natl.Acad.Sci.U.S.A.* **77**, 1321-1325.

Chapter 3

3-D *in vitro*-Model of Adipogenesis – Comparison of Culture Conditions

Claudia Fischbach[1], Jochen Seufert[2], Harald Staiger[3], Michael Hacker[1], Markus Neubauer[1], Achim Göpferich[1], Torsten Blunk[1]

[1] Department of Pharmaceutical Technology,
University of Regensburg, 93040 Regensburg, Germany

[2] Division of Endocrinology, Metabolism and Molecular Medicine,
Medical Poliklinik, University of Würzburg, 97070 Würzburg, Germany

[3] Department of Endocrinology, Metabolism, and Pathobiochemistry,
Medical Clinic Tübingen, Eberhard-Karls-University, 72076 Tübingen, Germany

Tissue Eng. 2003, in press

Abstract

Recent *in vivo* and *in vitro* studies have demonstrated both promises and current limitations in tissue engineering of fat. Herein, we report the establishment of a well-defined 3-D *in vitro* model useful for systematic investigations of 3-D adipogenesis. Polyglycolic acid fiber meshes were dynamically seeded with 3T3-L1 preadipocytes; subsequently, cell-polymer constructs were hormonally induced and cultivation under three different conditions was evaluated. Regarding tissue coherence and intracellular lipid content, culture of cell-polymer constructs either dynamically in well plates or in stirred bioreactors yielded similar results which were distinctly improved compared to static conditions in well plates. On the protein and mRNA level, significantly increased expression of genes characteristic for a mature adipose phenotype was demonstrated for constructs dynamically cultured in well plates, as compared to static conditions. Furthermore, investigation of lipolysis under stimulating and inhibiting conditions demonstrated functionality of the dynamically differentiated constructs.

Using dynamic culture conditions, the presented *in vitro* model system is suggested as a valuable tool serving both fat tissue engineering and basic research by likely facilitating investigations into tissue-inherent features not possible to be appropriately conducted under conventional 2-D culture conditions.

Introduction

The demand for soft tissue equivalents in reconstructive and plastic surgery is continuously increasing [1], even though currently applied surgical techniques fail to produce fully satisfactory results. Clinical approaches to soft tissue reconstruction used in the augmentation of soft-tissue volume for the treatment of congenital deformities, posttraumatic repair, and breast cancer rehabilitation include the autografting of fat pads or injection of adipocyte cell suspensions obtained by liposuction [2-5]. There are, however, major problems associated with these techniques, such as low fat-graft survival and necrosis due to insufficient vascularization followed by progressive resorption of the graft over time [2,3,5-8]. Thus, growing viable and functional adipose tissue constructs by the means of tissue engineering would represent a promising strategy to develop alternative therapeutic approaches aimed at improved predictability, reproducibility, and long-term efficacy, as compared to current autologous fat transplantation procedures.

Over the last couple of years, several groups working in this field have published encouraging data demonstrating *de novo* tissue generation *in vivo*. For example, subcutaneous injection of basement membrane supplemented with bFGF as well as local delivery of insulin and IGF-1 by polymeric microspheres resulted in formation of visible fat pads *in vivo* [9-14]. Furthermore, adipose tissue development is reported for implanted preadipocyte-seeded scaffolds made from various biomaterials [15-18]. Taken together, tissue engineering strategies are useful for fat pad formation by recruitment of endogenous precursor cells as well as by implantation of preadipocytes. However, long-term maintenance of tissue engineered adipose tissue *in vivo* still remains elusive [16]. Although extensive investigations at the cellular and molecular level could possibly clarify the potential reasons for the failed grafts, the appropriate studies have not yet been performed. Until now, explant characterization has been simply carried out by histological examinations and detection of triglyceride accumulation. Furthermore, RT-PCR has also been recently utilized to analyze the expression of glycerol-3-phosphate dehydrogenase expression [9].

In addition to the above mentioned *in vivo* studies, the first *in vitro* investigations were performed by examining three-dimensional (3-D) adhesion behavior of preadipocytes on PLGA scaffolds, freeze-dried collagen scaffolds, and expanded polytetrafluorethylen meshes coated with collagen, albumin, and fibronectin, respectively [15,17,19]. Moreover, adipocytes in three-dimensional cultures were detected by oil red O staining of cells within polymer

scaffolds [15,19] and collagen gels [20]. However, detailed studies of adipogenesis in a tissue engineering context regarding not only lipid accumulation, but also expression of specific differentiation markers, as well as tissue functionality, are still lacking, even though especially this kind of approach may help to explain why previous studies partly failed.

Whereas differentiation control *in vivo* is complex and contingent on the implantation site as well as the gender and age of the patient [21-23], the development of a standardized *in vitro* engineered fat construct would facilitate investigations into characteristic tissue properties, e.g. 3-D cell-cell interactions. Thus, basic insights into the events occurring during 3-D adipogenesis could be gained at the molecular and cellular level. Therefore, our intention in this study was not to generate implantable fat, but to establish a 3-D *in vitro* model exhibiting typical features of white adipose tissue, such as triglyceride biosynthesis, expression of typical fat cell genes, and adipocyte functionality, which is useful for systematic investigations on adipose tissue formation. Such a 3-D model could serve in future studies as a valuable tool to investigate the effects of determinants such as different adipogenic factors, co-cultures, or extracellular matrix components under easily controllable and well-defined conditions. In turn, a thorough understanding of the development of engineered adipose tissue on a molecular and cellular level is likely to prove beneficial for future *in vivo* approaches to the engineering of fat.

In the current study, in order to establish such a well-defined 3-D adipogenesis model, we generated adipose tissue constructs using the murine preadipose cell line 3T3-L1 [24,25], one of the most frequently utilized and best characterized cell lines for the investigation of adipocyte differentiation *in vitro*, and commercially available 3-D polymer scaffolds made from polyglycolic acid. To trigger adipose differentiation, the cell-polymer constructs were induced with a hormonal cocktail according to protocols described in the literature. The main goal was to establish suitable conditions for the cultivation of the model. Specifically, static and cultivation in well plates and stirred bioreactors (spinner flasks) were investigated. To assess the properties of the differently cultivated cell-polymer constructs, typical features of adipogenic differentiation were examined. In detail, intracellular lipid accumulation was investigated. Furthermore, expression of typical fat cell genes was analyzed on both the protein and the mRNA level. Finally, lipolysis rate of the 3-D cultivated adipocytes was measured under different conditions to ascertain functionality of the generated tissues.

Materials and Methods

Materials:

3T3-L1 preadipocytes were obtained from ATCC (Manassas, VA, USA). DMEM with 1.0 g/l glucose, fetal bovine serum (FBS), and trypsin (1:250) were purchased from Biochrom KG Seromed (Berlin, Germany); phosphate buffered saline (PBS) and penicillin-streptomycin solution were from Life Technologies (Karlsruhe, Germany). MEM (alpha-modification), corticosterone, indomethacin, and oil red O were from Sigma-Aldrich (Deisenhofen, Germany). 3-isobutyl-1-methylxanthine (IBMX) was purchased from Serva Electrophoresis GmbH (Heidelberg, Germany). Insulin was kindly provided by Hoechst Marion Roussel (Frankfurt a. M., Germany). Cell culture materials were obtained from Sarstedt AG & Co. (Nuembrecht, Germany) and BD Biosciences Labware (Heidelberg, Germany).

Spinner flasks were self-made (250 ml volume, 6 cm bottom diameter, side arms for gas exchange). Silicon stoppers were obtained from Schuber & Weiss (München, Germany); needles were from Unimed (Lausanne, Switzerland). Polyglycolic acid (PGA) non-woven fiber meshes (12-14 µm fiber diameter; 96% porosity; 62 mg/cm^3 bulk density) were purchased from Albany Int. Research Co. (Mansfield, MA, USA) and die-punched into discs 5 mm in diameter and 2 mm thick.

Cell culture:

3T3-L1 preadipocytes were expanded during 4 passages and frozen in liquid nitrogen. Subsequent to defrosting, cells were further expanded; cells from the fourth and fifth passage were used for experiments. Stock cultures were grown in DMEM supplemented with 10% FBS, penicillin (100 U/ml), and streptomycin (0.1 mg/ml). For 2-D cell culture preadipocytes were plated on tissue culture polystyrene (TCPS) at a density of 5,000 cells per cm². For the 3-D culture, PGA scaffolds were pre-wetted with 70% ethanol, and rinsed thoroughly with PBS. In preliminary experiments, cell seeding was assessed by comparing two different static conditions and dynamic seeding in stirred bioreactors, respectively. For dynamic cell seeding in bioreactors (the method that was finally used in further experiments), the scaffolds were pinned onto needles (10 cm long, 0.5 mm diameter) and held in place with segments of silicone tubing (1 mm long). Four needles with two scaffolds each were inserted into a silicone stopper; the stopper was in turn placed into the mouth of a spinner flask containing a

magnetic stir bar. The spinner flasks were filled with 100 ml culture medium and put on a magnetic stir plate (Bellco Glas; Vineland, NJ, USA) at 80 rpm in an incubator (37°C, 5% CO_2). After 24 h, the medium was aspirated and the cell suspension containing either $0.5x10^6$, $2x10^6$, or $4x10^6$ cells per scaffold, was filled into the flask. Stirring for two days at 80 rpm allowed for cell attachment to the polymer fibers. Alternatively, for static cell seeding, the PGA scaffolds were either placed into centrifuge tubes (diameter of the bottom 5 mm) or pinned onto needles (similar set-up as described for dynamic seeding). Subsequently, cell suspensions ($2x10^6$ cells in 200 µl culture medium) were pipetted directly onto the polymer scaffolds followed by a 2 h incubation step to allow for cell attachment. Then, the culture medium was added and 12 h later the cell-seeded scaffolds were harvested.

For investigation of different cultivation conditions the cell-polymer constructs were transferred into 6-well plates (one construct and 5 ml culture medium per well) and cultured in the incubator either statically or on an orbital shaker at 50 rpm (Dunn Labortechnik GmbH; Asbach, Germany) (Fig. 1). Alternatively, the cell-seeded PGA scaffolds stayed and were cultured in the same bioreactors (100 ml culture medium, stirred at 80 rpm) used for the seeding procedure. Cultivation of constructs was performed in MEM (alpha-modification) supplemented with 10% FBS, penicillin (100 U/ml), and streptomycin (0.1 mg/ml).

Four days after seeding (3-D), adipogenesis was induced by adding 0.1 µM corticosterone, 0.5 mM IBMX, and 60 µM indomethacin to differentiation medium (MEM (alpha-modification), 5% FBS, 1 µM insulin, penicillin (100 U/ml), and streptomycin (0.1 mg/ml)) and referred to as day 0. After 2 days, the induction medium was replaced by differentiation medium alone. Cells were maintained under these conditions until the performance of analytical investigations.

Histology:

At day 9 of adipogenesis, differently treated specimens were fixed overnight in 10% buffered formalin, dehydrated and then embedded in paraffin. Deparaffinized sections of 5 µm were stained with hematoxylin and eosin (H&E) (Sigma-Aldrich; Deisenhofen, Germany). As this staining procedure using organic solvents led to lipid extraction from the cells, lipid storage was assessed by examining size of blank areas which represented those spaces previously occupied by accumulated triglyceride droplets. Photographs were taken with a Dynax 600 si classic camera (Minolta Europe GmbH; Langenhagen, Germany) mounted on a Leica DM IRB light microscop (Leica Microsystems AG; Wetzlar, Germany).

Oil red O staining:

On day 9 after hormonal induction of adipogenesis, oil red O staining of cytoplasmic triglyceride droplets was performed. For this purpose, 3-D cell-polymer constructs were washed with PBS. Subsequently, they were subjected to an overnight fixation step in 10% buffered formalin. The samples were stained as described [26].

Scanning electron microscopy (SEM):

At indicated points of time, washed cell-polymer constructs were fixed first for 15 min with 2.5% glutardialdehyde in PBS and then for 30 min with 1% osmium tetroxide (Carl Roth GmbH & Co.; Karlsruhe, Germany). After extensive rinsing and freezing at –80°C, samples were subjected to lyophilization (Christ Beta 2-16, Martin Christ Gefriertrocknungsanlagen; GmbH, Osterode am Harz, Germany).

For examination of lipid accumulation and 3-D tissue context, samples were mounted on aluminum stubs using conductive carbon tape and coated with gold - palladium (Polaron SC515, Fisons surface systems; Grinstead, UK). All micrographs were obtained at 10 kV on a DSM 950 (Zeiss; Oberkochen, Germany).

Analysis of triglyceride (TG) content:

To quantitatively determine the amount of intracellular TG at day 9 of adipogenesis, differently cultivated 3-D cell-polymer constructs were washed with PBS, harvested in 0.5% thesit, and sonicated with a digital sonifier (Branson Ultrasonic Corporation, Danburg, CT, USA). Subsequently, spectroscopic quantification of TG was performed using the enzyme coupled glycerol assay kit 337 (Sigma Diagnostics; Deisenhofen, Germany).

Glycerol-3-phosphate dehydrogenase (GPDH) measurement:

On day 9 of hormonal differentiation, 2-D cells and 3-D cell-polymer constructs were washed with PBS, harvested in lysis buffer (50 mM Tris, 1 mM EDTA, 1 mM mercaptoethanol, pH 7.5), and sonicated afterwards with a digital sonifier (Branson Ultrasonic Corporation, Danburg, CT, USA). The GPDH assay was performed as described in the literature[27,28]. Cytosolic protein concentration was determined after precipitation with

trichloracetic acid using the Lowry assay [29]. GPDH activity was expressed as mU per mg protein.

Leptin quantification:

Leptin concentrations in cell culture media of differently cultivated 3-D cell-polymer constructs were determined using a sandwich ELISA for mouse leptin. Media samples from day 8 to day 10 were taken and centrifuged for 5 min at 13,200 rpm (Centrifuge 5415 R, Eppendorf AG; Hamburg, Germany) to remove cell debris. The supernatants were frozen at –80°C until the Quantikine M immunoassay (R&D Systems; Wiesbaden, Germany) was performed.

Reverse transcription polymerase chain reaction (RT-PCR):

Total RNA was harvested from the cells with Trizol reagent (Invitrogen GmbH; Karlsruhe, Germany) and isolated according to manufacturers instructions. First-strand cDNA was synthesized from total RNA by using random hexamers (Roche Diagnostics; Mannheim, Germany) and Superscript II RNase H- Reverse Transcriptase (Invitrogen GmbH; Karlsruhe, Germany). Samples were incubated at 42°C for 50 min and heated afterwards for 15 min at 70°C to inactivate the enzyme. Subsequently, PCR was performed with Sawady Taq-DNA-Polymerase (PeqLab; Erlangen, Germany); initial denaturation occurred at 94°C for 120 sec, final extension at 72°C for 30 sec, and holding at 4°C. The amplification was carried out using specific primers and appropriate conditions for each gene (Tab. 1). 18 S rRNA served as internal control. Reverse transcription and PCR were performed using a Mastercycler Gradient (Eppendorf AG; Hamburg, Germany).

The PCR products were analyzed by electrophoresis through 2% agarose gels, stained with ethidium bromide. Finally, the gels were subjected to imaging and densitometric scanning of the resulting bands under UV light ($\lambda = 312$ nm) using a Kodak EDAS 290 (Fisher Scientific; Schwerte, Germany).

Measurement of lipolysis:

The lipolytic cell response of dynamically cultivated 3-D constructs was assessed by measuring the amount of glycerol released into the incubation buffer after treatment with agents stimulating or inhibiting lipolysis. Briefly, on day 9 after initiation of adipogenesis, 3-

D cultures were washed with serum-free medium and then maintained in the same medium for 2h to avoid interference with serum factors. Subsequently, medium was replaced by PBS supplemented with 3% fatty acid-free bovine serum albumin (Sigma-Aldrich; Deisenhofen, Germany). In addition to recording data on lipolysis under control conditions, stimulation and inhibition of glycerol release were conducted by adding 10 µM isoproterenol and 100 µM propranolol (both were from Sigma-Aldrich; Deisenhofen, Germany) to the incubation buffer, respectively. After 1h incubation (37°C, 5% CO_2), the conditioned media were frozen at –20°C until the enzyme coupled glycerol assay kit 337 (Sigma Diagnostics; Deisenhofen, Germany) was carried out.

Table 1: Primer sequences and PCR conditions for the investigated genes
Oligonucleotide sequences of mouse forward (sense) and reverse (antisense) primers. Gene amplification was performed by PCR according to the specified annealing temperatures (AT) and number of cycles for each gene. The reaction conditions of one cycle were composed as follows: denaturation for 45 sec at 94°C, annealing for 45 sec at the indicated temperatures, and extension for 1 min at 72°C.

Gene	Forward and reverse primers of examined genes	AT (°C) / Cycles
PPARγ	5′-AAC CTG CAT CTC CAC CTT ATT ATT CTG A-3′ 5′-GAT GGC CAC CTC TTT GCT CTG CTC CTG-3′	60 / 35
GLUT-4	5′-CCC CGC TGG AAT GAG GTT TTT GAG GTG AT-3′ 5′-CAG ACA GGG GCC GAA GAT TGG GAG ACA GT-3′	61 / 35
beta3-AR	5′-CAG TGG TGG CGT GTA GGG GCA GAT-3′ 5′-CGG GTT GAA GGC GGA GTT GGC ATA G-3′	63 / 36
angiotensinogen	5′-CTG GCC GCC GAG AAG CTA GAG GAT GAG GA-3′ 5′-GAG AGC GTG GGA AGA GGG CAG GGG TAA AGA G-3′	62 / 35
leptin	5′-GAC ACC AAA ACC CTC ATC AAG ACC-3′ 5′-GCA TTC AGG GCT AAC ATC CAA CT-3′	58,5 / 36
18 S	5′-TCA AGA ACG AAA GTC GGA GGT TCG-3′ 5′-TTA TTG CTC AAT CTC GGG TGG CTG-3′	60 / 22

Statistical analysis:

Statistical significance was assessed by one-way analysis of variance ANOVA followed by Tukey post-hoc test (Software: SPSS 10.0 for Windows). The statistical significance level was set at $p < 0.01$.

Results

Experimental set-up: dynamic vs. static conditions:

In order to preliminarily determine an appropriate cell seeding technique, PGA meshes were statically seeded by pipetting a cell suspension onto polymer meshes either being placed in centrifuge tubes or pinned onto needles. Alternatively, dynamic cell seeding in bioreactors (spinner flasks) was performed as described above (see Methods) [30]. Investigations of the obtained cell-polymer constructs, thereby, revealed that static conditions yielded less homogeneous distribution within the polymer meshes relative to dynamic conditions. Furthermore, the dynamic procedure resulted in densely seeded constructs, whereas the meshes generated by the static approaches displayed polymer fibers partially devoid of cells (data not shown). For these reasons, the dynamic seeding technique was regarded as being most suitable for the following experiments (Fig. 1).

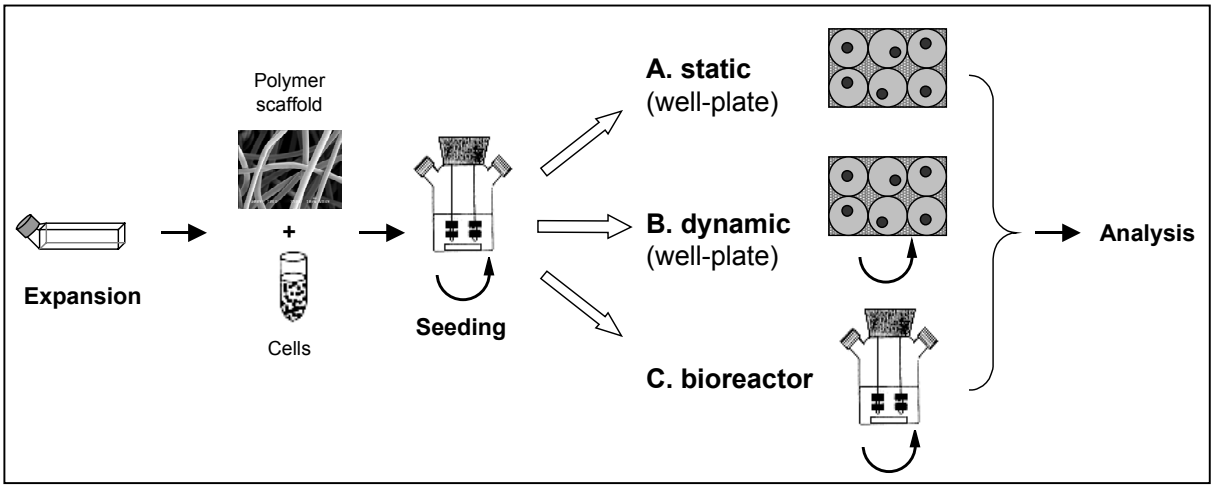

Fig. 1:
Experimental set-up: dynamic cell seeding of 3T3-L1 preadipocytes on PGA fiber meshes in spinner flasks is followed by comparison of different cultivation conditions. Cell-polymer constructs were cultivated A) statically, B) dynamically on an orbital shaker, and C) impaled to needles in stirred bioreactors. Subsequently, analysis of characteristic fat cell features on the tissue, cellular, and molecular level was conducted.

With the aim of developing tissue-like constructs exhibiting typical adipocyte characteristics, distinct cultivation techniques were evaluated to optimize properties of the resulting tissues. For this purpose, cell-polymer constructs were either cultured in well plates under conventional static conditions or dynamically on an orbital shaker, or pinned onto needles in stirred bioreactors (Fig. 1).

Tissue formation of the generated constructs:

Macroscopic investigation of constructs cultivated up to two weeks (fours days between seeding and induction, then up to ten days after induction) revealed that only hormonal treatment of seeded preadipocytes yielded white fat-like tissues (Fig. 2). In contrast, un-induced cell-polymer constructs did not result in fat formation. Furthermore, tissues coherent, firm and resistant enough to be moved with forceps similar to pieces of fat could only be created by dynamic cultivation on an orbital shaker and by culture in stirred bioreactors, respectively.

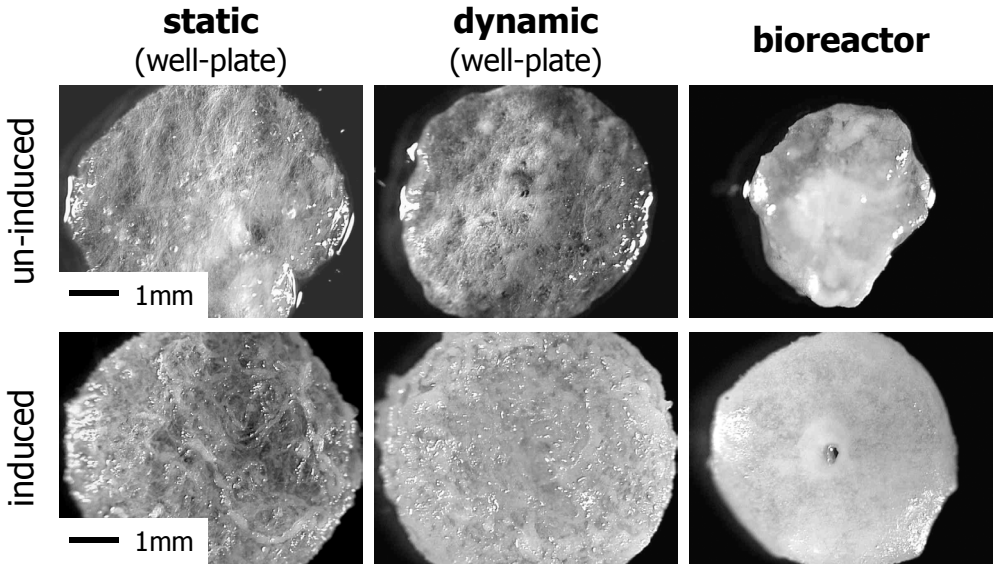

Fig. 2:
Macroscopic appearance of differently cultivated cell-polymer constructs (statically, dynamically, and in stirred bioreactors) 9 days after induction of differentiation. Bars represent 1 mm. Un-induced constructs served as controls.

In contrast, static conditions yielded constructs with inferior mechanical properties, i.e., they partially disintegrated upon handling. It has to be noted that cultivation in stirred bioreactors led to remarkable changes in the shape of the developed tissues compared to the original polymer shape and the shape of the constructs generated employing either well plate culture (Fig. 2). Using the bioreactors, the diameter of the constructs decreased to about 70% of the constructs derived from either culture in well plates. Additionally, the surface of the bioreactor-derived tissues appeared to be smoother than the surface from the matching static and dynamic ones.

Microscopic examination of the respective H&E stained cross-sections supported the macroscopic observations and evidenced that un-induced constructs did not result in coherent lipid containing tissues (Fig. 3), i.e., hormonal stimulation was necessary for significant

accumulation of lipid droplets (represented by blank spaces) within the constructs. However, tissue coherence within the generated constructs even after hormonal induction was only detectable on cross-sections of dynamic and bioreactor culture (Fig. 3). In contrast, static cultivation did not yield a tissue-like context and only a few small lipid vacuoles were detected (Fig. 3). In contrast to constructs dynamically cultured in well plates, outer areas of the bioreactor constructs exhibited a thin layer composed of undifferentiated cells.

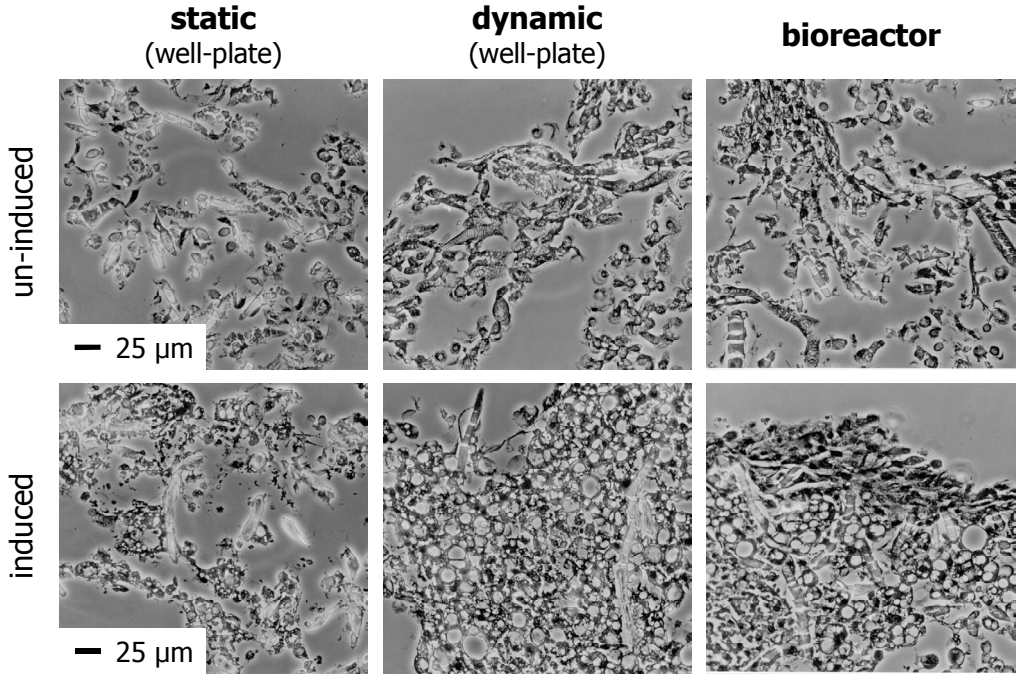

Fig. 3:
Tissue coherence and lipid inclusions of differentiated (9 days) 3T3-L1 cells in 3-D cell-polymer constructs cultivated under different conditions. Staining of histological cross-sections was conducted with hematoxylin and eosin (H&E). Un-induced cell-polymer constructs did not result in coherent tissue, whereas hormonally stimulated constructs yielded a tissue-like context. Blank spaces within H&E stained cells were caused by dissolving lipid inclusions with organic solvents during deparaffinization. Bars represent 25 µm.

Triglyceride (TG) accumulation of differently cultivated constructs:

Examination of oil red O stained intracellular lipid vesicles by light microscopy confirmed the results described above: Independent of the used cultivation technique, lack of hormonal stimulation of adipogenesis yielded only a few differentiated adipocytes whereas adipose induction resulted in a large number of fat cells containing intracellular lipid vacuoles (Fig. 4). Compared to static conditions, dynamically cultivated constructs and constructs harvested from stirred bioreactors exhibited larger, nearly unilocular fat droplets. However,

bioreactor constructs showed vacuoles with varying amount of accumulated lipid, whereas lipid vacuoles of dynamically cultivated constructs exhibited almost homogeneous droplet size (Fig. 4).

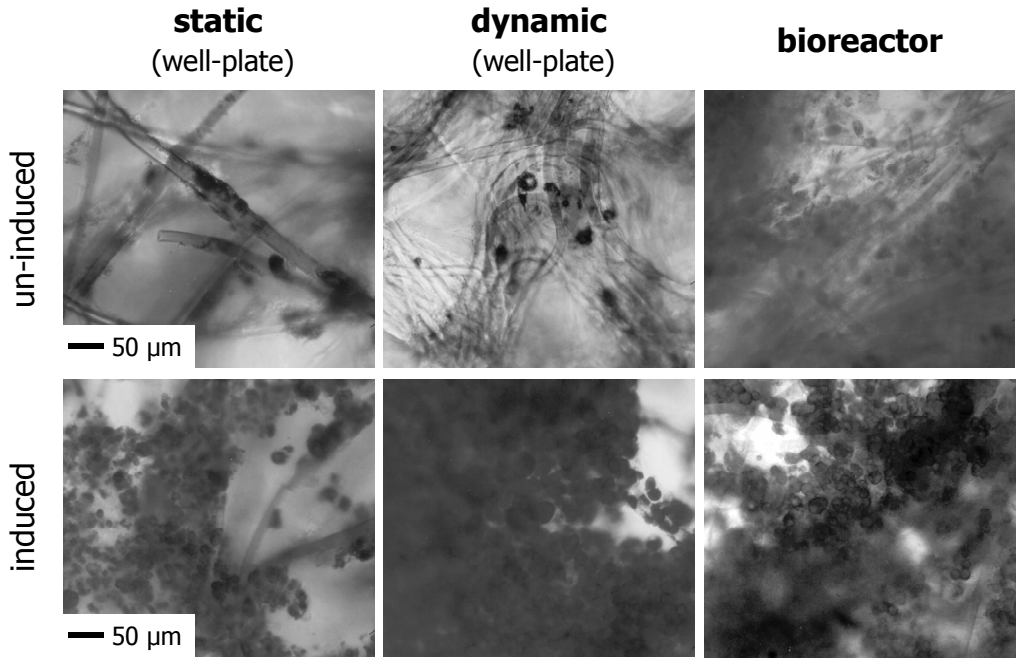

Fig. 4:
Lipid accumulation of 3T3-L1 cells on PGA fiber meshes, as observed by light microscopy. 3-D cell culture was either performed statically, dynamically, or in stirred bioreactors. At day 9 after hormonal induction, constructs were oil red O stained to better visualize size and amount of cytoplasmic lipid vesicles. Un-induced constructs served as controls. Bars represent 50 µm.

To determine changes in cell size and morphology provoked by lipid accumulation, kinetic investigations by the means of SEM were performed for dynamically cultivated constructs which had been hormonally induced to undergo differentiation. While adipogenesis proceeded during the course of the experiment, a gradual enlargement of cytoplasmic lipid vesicles, increase in cell size, and alterations in morphology (Fig. 5a) could be detected. Cells changed from a more spread towards a round cell shape and exhibited bulged cell membranes due to lipid storage (Fig. 5a). To determine if cells cultivated either statically or in bioreactors exhibit comparable morphological properties, the so generated constructs were subjected to SEM as well (at day 9 after hormonal induction). Static conditions led to less pronounced changes in cell morphology which was attributed to diminished TG biosynthesis rate (Fig. 5b). In contrast to dynamic and static culture in well plates, constructs obtained from bioreactor cultivation exhibited a smooth coherent surface which made it difficult to distinguish single cells (Fig. 5b). Lack of hormonal stimulation under either condition did not result in any detectable changes of cell size and morphology (Fig. 5b).

Fig. 5:
Appearance of 3-D cell-polymer constructs as visualized by SEM. Micrographs were taken from representative areas.

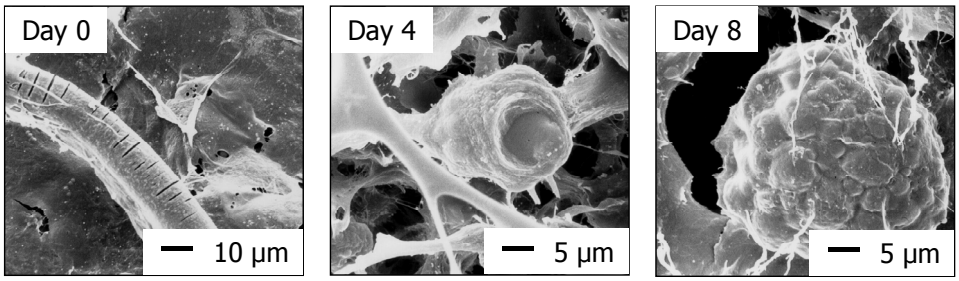

a) *Cellular lipid accumulation during adipose differentiation under dynamic conditions in well plates. The micrograph of day 0 exemplarily shows a PGA fiber and spread cells. An increase in cell size and changes in morphology with bulged cell membranes due to fat storage were observed. Bars represent 10 µm (day 0) and 5 µm (day 4 and 8), respectively.*

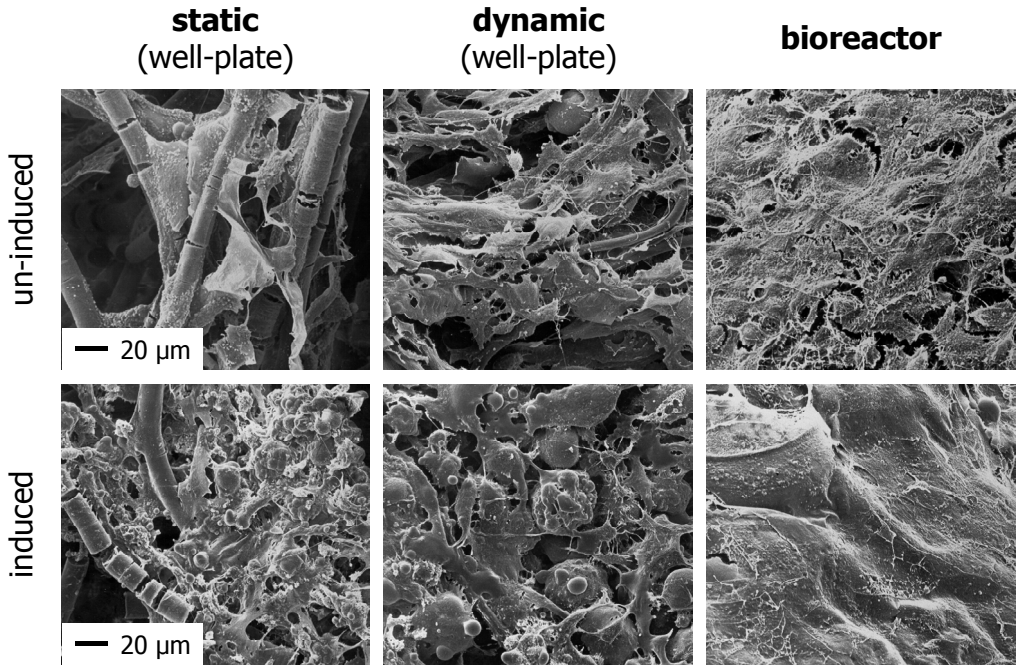

b) *Cell morphology resulting from cultivation of the cell-polymer constructs under different conditions. Well-rounded adipocytes with bulged cell membranes could only be observed after hormonal induction. Size and coherence of cells was decreased under static compared to dynamic conditions. In contrast to all other conditions, bioreactor cultivation yielded smooth construct surface. Bars represent 20 µm.*

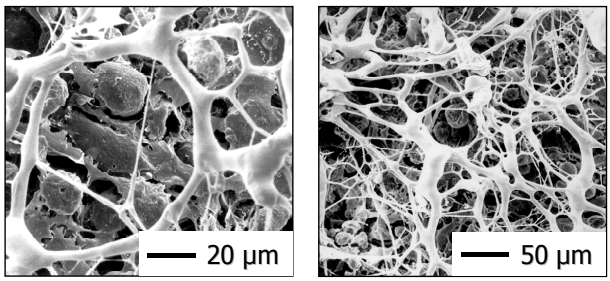

c) *Fibril deposition within the 3-D model system as observed 4 days after hormonal induction under dynamic conditions in well plates. Observed structures cannot be attributed to cells or polymer fibers and were accounted for as extracellular matrix fibrils deposited by the cells (see discussion). Bars represent 20 µm and 50 µm, respectively.*

To quantitatively assess lipid accumulation of the differently cultivated cell-polymer constructs, triglyceride (TG) content was measured. The results obtained from the assay supported our microscopic findings. Independent of the cultivation procedure, appropriate TG accumulation could only be achieved by hormonal stimulation of adipogenesis (Fig. 6).

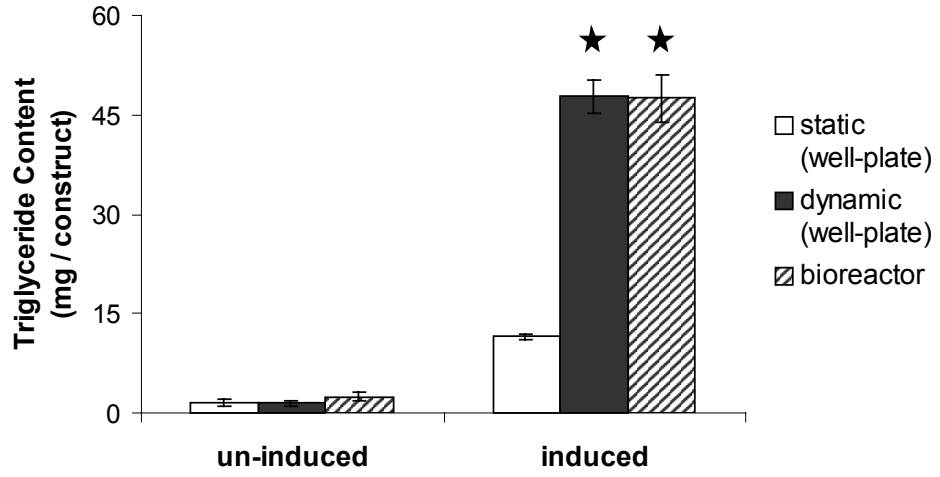

Fig. 6:
Triglyceride content of 3T3-L1 cells on PGA fiber meshes cultivated with and without hormonal induction of adipose differentiation under different conditions. Data represent the mean ± SD of three constructs. Statistically significant differences to static conditions ($p < 0.01$) are denoted by ★. Three independent experiments were conducted, representative result of one experiment is shown here.

Without treatment, no significant differences were determined between static (1.69±0.53 mg per construct) and dynamic conditions (1.46±0.46 mg per construct) in well plates and cultivation in bioreactors (2.42±0.67 mg per construct) (Fig. 6).With hormonal stimulation, cell-polymer constructs dynamically cultivated in well plates and constructs cultured in bioreactors exhibited equal content of intracellular TG (47.75±2.58 mg and 47.46±3.61 mg per construct, respectively), which was significantly larger than TG content of constructs cultured under static conditions (11.54±0.48 mg per construct) (Fig. 6).

Adipocyte gene expression on the protein and on the mRNA level:

With the objective of thoroughly investigating the most promising cultivation method with regard to adipose tissue formation, gene expression of constructs dynamically cultivated in well plates (hormonally induced) was analyzed. For comparison, the matching constructs from static culture were examined as well. In order to characterize the phenotype of the differently cultivated adipocytes, typical fat cell genes known to be expressed during adipose

differentiation were determined on both the protein and the mRNA level. At first, late markers of adipogenesis described to be expressed by mature fat cells were investigated on the protein level. For this purpose, activity of GPDH, a key enzyme of triacylglycerol biosynthesis, and the hormone leptin, known to be involved in hypothalamic regulation of satiety, were analyzed. Dynamic cultivation of the constructs proved to be beneficial for expression of both proteins (Fig. 7).

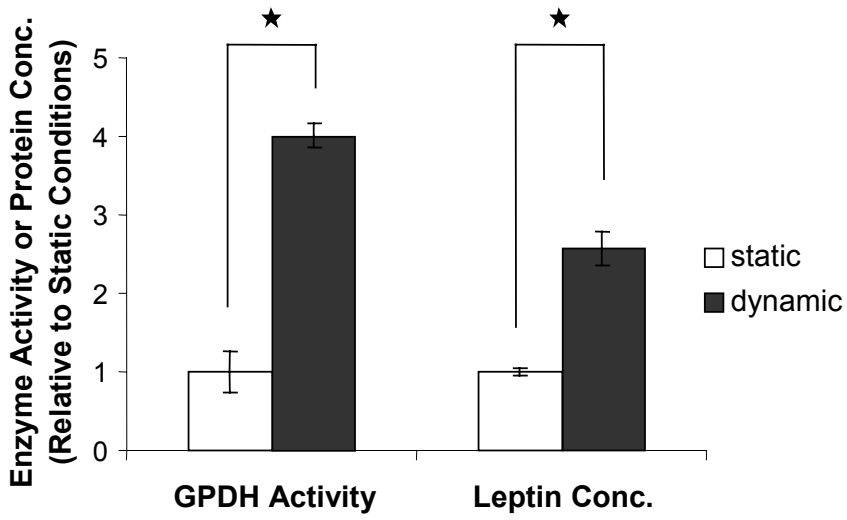

Fig. 7:
Effects of static or dynamic cultivation in well plates of 3-D cell-polymer constructs on glycerol-3-phosphate dehydrogenase (GPDH) activity and leptin secretion. GPDH, a key enzyme involved in triacylglycerol synthesis, was determined at day 8 after induction of adipogenesis and standardized per mg protein. Leptin concentration was assessed in the cell culture medium sampled from day 8 to 10 using a mouse leptin ELISA. Values are expressed as mean ± SD (n=3). Statistically significant differences to static conditions ($p < 0.01$) are denoted by ★. Absolute values for dynamic conditions were 791.19 ± 32.63 mU GPDH activity per mg protein and 7.86 ± 0.67 ng leptin per construct, respectively. Three independent experiments were conducted, representative results of one experiment are shown here.

Cultivation on the orbital shaker (791.19±32.63 mU per mg protein) resulted in a four-fold increase of GPDH activity compared to 3-D cultures statically maintained (197.23±49.85 mU per mg protein) (Fig. 7). Only dynamic conditions led to GPDH values that equaled activities of a conventional 2-D cell culture (data not shown; in 2-D, no difference between static and dynamic cultivation was observed). Measurement of leptin concentration in the culture medium of the constructs revealed a significant increase (2.5-fold) of secreted leptin in dynamic cultures (7.86±0.67 ng leptin per construct) relative to the matching static ones (3.05±0.15 ng leptin per construct) (Fig. 7).

Similar results were obtained by analyzing expression kinetics of adipocyte genes on the mRNA level. Compared to dynamic cultivation, static conditions were determined as being less suitable to develop constructs with appropriate adipocyte gene expression. For all investigated genes, dynamically generated tissues exhibited enhanced band intensities compared to the constructs created under static conditions. In particular, examination of the key transcription factor PPARγ, which plays a crucial role in the activation of many adipose tissue-specific genes, showed that dynamically cultivated specimens exhibit enhanced mRNA expression at day 4 and 8 (Fig. 8).

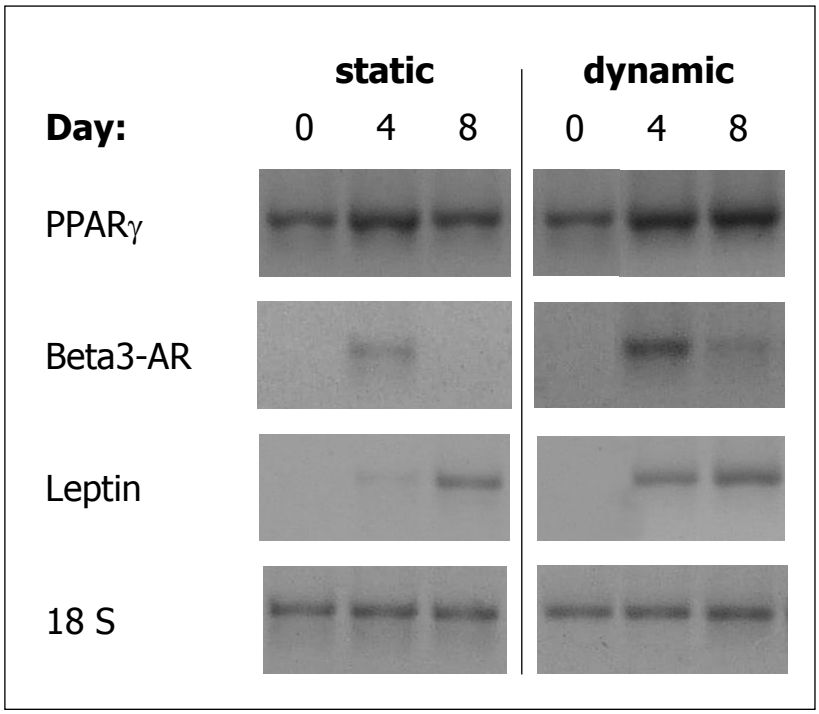

Fig. 8:
Evaluation of differential gene expression in static and dynamic 3-D cell culture in well plates at day 8 of adipose differentiation by means of RT-PCR. Examination of the characteristic fat cell genes PPARγ, beta3-adrenoreceptor, leptin, and the internal standard 18S was conducted in triplicate, one representative result is shown here.

Analysis of beta3-adrenoreceptor expression demonstrated superiority of dynamic conditions also at day 4 and 8, with highest expression at day 4 under both conditions (Fig. 8). Finally, the ob gene product leptin was already significantly expressed at day 4 under dynamic conditions, whereas under static condition it was hardly detectable then. (Fig. 8). 18 S served as internal standard. Compared to 2-D cell culture, which is commonly used for investigation of 3T3-L1 differentiation, only dynamic conditions yielded comparable

expression kinetics and band intensities (data not shown), thus demonstrating equivalence of the 3-D system with regard to appropriate gene expression.

Determination of adipocyte functionality within dynamic 3-D cell culture:

Finally, only the dynamically cultivated 3-D system, assessed as being most suitable to be used as an *in vitro* model, was analyzed with regard to adipocyte functionality. For this purpose, the lipolysis rate of 3-D differentiated constructs was studied under varying conditions. In addition to control conditions, a lipolysis stimulating factor, isoproterenol (10 µM), as well as a lipolysis inhibiting factor, propranolol (100 µM), were added to the constructs.

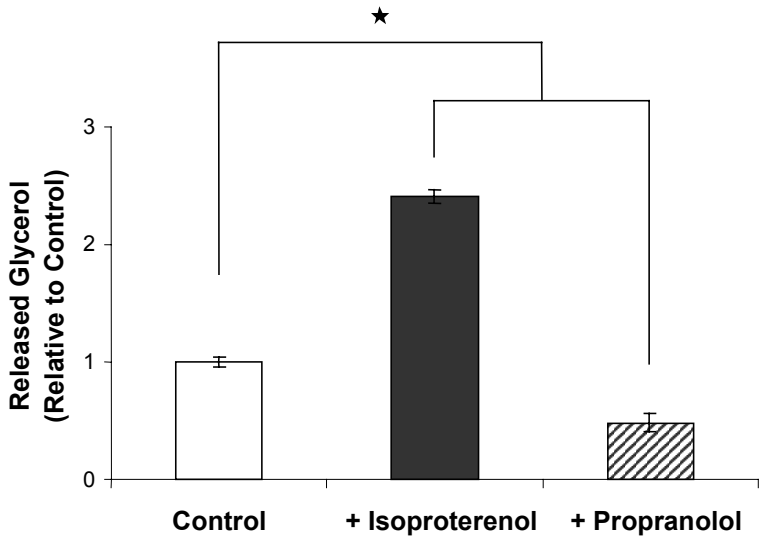

Fig. 9:
Functionality of 3-D 3T3-L1 adipocytes dynamically cultivated in well plates was demonstrated by treatment with a lipolysis stimulating (10 µM isoproterenol) as well as a lipolysis inhibiting (100 µM propranolol) agent and subsequent analysis of released glycerol. Three independent experiments were performed. Data are expressed as mean ± SD (n=3) of one representative experiment. Statistically significant differences to control conditions ($p < 0.01$) are denoted by ★. After 1h incubation, the mean value of control was 1.82 ± 0.08 µg glycerol per construct.

After 1 h incubation, levels of released glycerol provoked by intracellular TG cleavage were determined and compared to control conditions (1.82 ± 0.08 µg per construct). Addition of the β-adrenergic agonist isoproterenol caused an over 2-fold increase of glycerol levels (4.42 ± 0.24 µg per construct) demonstrating significant ($p<0.01$) stimulation of lipolysis (Fig. 9). Moreover, inhibition of lipolysis by the β-adrenergic antagonist propranolol was

detected, which diminished released glycerol to about 50% (0.92 ± 0.16 µg per construct) (Fig. 9). Hence, responsiveness of adipocytes in the 3-D constructs to both lipolysis stimulating and inhibiting factors could be demonstrated.

Discussion

To the best of our knowledge, for the first time this study reports the establishment of a well-defined 3-D *in vitro* model system exhibiting typical features of white adipose tissue, such as lipid accumulation, gene expression, and functionality. The focal point of the study, thereby, was the evaluation of distinct culture conditions. In future investigations, the model is supposed to easily enable systematic investigations of 3-D adipogenesis and, hence, may be a useful tool for tissue engineering of fat.

As none of the *in vitro* studies published so far provide detailed information on adipogenesis in a tissue engineering context, our intention was to create a standardized, easily manageable, and highly reproducible model system enabling the investigation of adipocyte differentiation in particular at the cellular and molecular level. To attain this goal we used preadipocytes of the 3T3-L1 cell line and highly porous PGA meshes as supportive framework. Despite the fact that 3T3-L1 preadipocytes actually do not reflect *in vivo* conditions, they serve as a homogeneous and highly proliferative cell source allowing to avoid the major drawbacks of primary cells such as cellular heterogeneity, low proliferation rates, and donor dependent differentiation capacity [31]. Commercially available PGA meshes were chosen as 3-D cell carriers as they are available in reproducible quality and have been successfully applied in other tissue engineering applications, such as cartilage [32,33].

Evaluating different cell seeding techniques in preliminary experiments, most appropriate results were achieved by dynamic cell seeding in spinner flasks over 2 days. This was in agreement with a report by Vunjak-Novakovic et al. [34], in which the same method also yielded superior results for seeding primary chondrocytes on PGA scaffolds, as compared to static seeding.

With the objective of investigating different cultivation conditions, the cell-seeded polymer constructs were either cultured statically or dynamically in well plates, or in stirred bioreactors. Simultaneously, the impact of hormonal induction on tissue formation was determined. Generated constructs were thoroughly characterized to assess their suitability for being used as 3-D model systems. For this purpose, the most obvious change during adipose tissue formation - lipid biosynthesis and storage – was determined by means of several

analytical methods, such as light and scanning electron microscopy, and measurement of triglyceride content. Thereby, it could be demonstrated that hormonal induction is crucial to the formation of fat-like constructs under either culture condition (Figs. 2-6). Evaluating different cultivation techniques showed that static cultivation in well plates is inferior to dynamic conditions with regard to the generation of adipose tissue, which was demonstrated on the tissue, cellular, and molecular level (Figs. 2-8). During differentiation of dynamically cultivated constructs, a more distinct enlargement of intracellular lipid vesicles was detected, which in turn led to an increase in cell size and nearly unilocular fat cells (Fig. 4, 5a). This phenomenon is sometimes difficult to realize in 2-D cell culture as lipid-filled cells are hardly able to stay at the bottom of a culture dish due to their buoyancy [35]. To assess the phenotype of adipocytes differentiated in static and dynamic culture in well plates, respectively, 3-D gene expression of some early and late markers of adipogenesis was investigated on the protein as well as on the mRNA level. Protein analysis of two late markers of adipogenesis, i.e., determination of GPDH activity and leptin secretion, revealed distinctly higher values for dynamic culture and, thus, additionally supported the findings that dynamically cultivated constructs feature advantageous characteristics compared to constructs derived from static cultures (Fig. 7). Similarly, enhanced PPARγ, beta3-adrenoreceptor, and leptin expression, examined by RT-PCR, contributed to confirm the superiority of the dynamic culture approach (Fig. 8). Compared to conventional 2-D cell culture, only dynamic conditions resulted in equivalent adipose gene expression (data not shown). By measuring lipolysis rate of the dynamically generated constructs, typical functionality of mature adipocytes was evidenced for the developed 3-D model system.

Comparison of constructs cultured either dynamically in well plates or in stirred bioreactors revealed a slight advantage of dynamic conditions in well plates (Figs. 2-5). As compared to constructs cultured under dynamic conditions in well plates, bioreactor constructs decreased in size and exhibited a less homogeneous lipid distribution (Fig. 4). In contrast to static and dynamic culture conditions, bioreactor derived constructs exhibited a smooth surface (Fig. 2, 5b). By investigation of H&E stained cross-sections, this observation could be attributed to a thin layer composed of undifferentiated cells exhibiting a fibroblastic appearance, which was potentially caused by shear stress generated by fluid flow preventing cells in the outer areas of the constructs from differentiation.

To conclude, it could be demonstrated that conventional static conditions, commonly applied in 2-D cell culture, were not sufficient to trigger adipose tissue formation within a 3-D context. Thorough evaluation of cultivation conditions demonstrated that only cultivation of

hormonally induced constructs under dynamic conditions and in stirred bioreactors, respectively, resulted in coherent cell-polymer constructs exhibiting fat-like appearance with large intracellular lipid droplets. However, our intention was not only to develop adipose tissue constructs but also to provide a model system which is easily manageable. As the bioreactor approach does not feature any advantages over dynamic cultivation in well plates but, on the contrary, entails enhanced experimental requirements, it is considered to be an inappropriate method to be routinely applied. For instance, in our current set-up the excess consumption of medium per construct (12.5 ml vs. 5 ml in dynamic culture) would notably increase the expenses of studies that involve the use of costly medium supplements such as growth factors. One fact that has to be considered in particular for larger studies is the need of bulky equipment and, thus, required space, because in one vessel only eight constructs can be generated which, furthermore, does not allow for individual treatment of each construct. In contrast, the dynamic 3-D culture system in well plates equally features adipose tissue formation but over and above it provides researchers with a simply manageable and undemanding *in vitro* model system, in which each construct can be treated individually, and is, therefore, regarded to be most suitable for the use in future studies.

The observed advantages of both dynamic cultivation and culture in bioreactors, as compared to static conditions, are likely due to convection-enhanced transport of nutrients and oxygen to and metabolic products away from the constructs. Alternatively, mechanical forces generated by fluid flow acting directly on the cells may be partially responsible for the observed effects. Also for other tissues, e.g. bone and cartilage, the mechanical environment is commonly acknowledged to decisively influence the development of engineered tissues cultured *in vitro* [36]. For instance, flow perfusion of 3-D cultivated marrow stromal osteoblasts tremendously improved bone formation by inducing *de novo* tissue modeling and formation of a biological matrix architecture [37]. Furthermore, tissue-engineered cartilage exposed to various mixing conditions exhibited increased biosynthesis of the characteristic ECM components collagen and GAG, as compared to static conditions [38].

Following establishment of the dynamic 3-D model system, further variations of the cell culture conditions were tested. To evaluate cell densities other than $2x10^6$ cells, cell seeding was additionally performed with $0.5x10^6$ and $4x10^6$ 3T3-L1 cells. Compared to $2x10^6$ cells, seeding with $4x10^6$ cells was not advantageous with regard to the formation of a coherent adipose tissue , whereas the use of $0.5x10^6$ cells yielded inferior constructs lacking tissue-like

strength (data not shown). Furthermore, scaffolds processed from poly(ethylene glycol)-poly(lactic acid) (PEG-PLA) copolymers [39] were tested to assess their suitability for adipose tissue engineering. The PEG-PLA polymers were previously synthesized in our lab [40]and have recently been shown to enhance marrow stromal cell differentiation towards the osteoblastic phenotype, depending on the PEG:PLA ratio [41]. Macroscopic and microscopic investigations of the resulting cell-polymer constructs, generated using dynamic cultivation in well plates, showed that tissue coherence was lacking. Determination of GPDH activity revealed no significant differences between different PEG-PLAs varying in their PEG:PLA ratios (data not shown). The obtained results clearly demonstrated that generation of adipose tissue constructs not only depends on the culture conditions but also on the choice of polymer and scaffold, respectively.

Adipose differentiation is accompanied by morphological changes from a fibroblastic appearance to a nearly spherical shape [42-44]. In addition, lipid accumulation of differentiated cells can finally lead to unilocular fat cells being in danger of detaching from a 2-D culture plate due to their buoyancy. As both observations give rise to a higher susceptibility to mechanical forces, e.g. occurring during medium aspiration, long-term studies on two-dimensionally cultured adipocytes are challenging to perform. In our 3-D model, long-term investigations are more likely to be enabled, as cells are cultivated in a tissue-like context and are, therefore, less susceptible to mechanical manipulations. Additionally, the cells may be stabilized by surrounding extracellular matrix (ECM) components which are synthesized by the cells. ECM interactions promoted within a 3-D tissue engineering environment are generally known to influence tissue properties. More specifically, ECM components were reported to play a regulatory role in adipogenesis, e.g., they facilitate morphological changes [31,43] and their synthesis is required for terminal differentiation of preadipocytes [45]. However, functions of and relations between different ECM components in adipose tissue have still to be fully clarified [31]. During adipose differentiation, ECM composition is altered [46-48] and in conventional 2-D cell culture increases in culture medium viscosity have been attributed to the release of synthesized ECM components [49]. One advantage of the 3-D system may be the prolonged cell-ECM contact, as secreted components such as laminin, collagens, and proteoglycans are possibly incorporated into the construct rather than being aspirated with every medium change. This assumption was supported by SEM images showing structures which were accounted for as ECM fibrils bound to the cell surface and in the intercellular space (Fig. 5c). Very similar

observations of fibrils have been described in the literature as long-spacing forms of collagen [50]. Future analysis of the presented 3-D constructs will aim at the identification of the observed structures and may facilitate new insights into the development of ECM in adipose tissue and its influence on long-term tissue development. Additional approaches to the elucidation of ECM effects in the newly established model system may include coating of polymer fibers with ECM molecules.

Basic research may also profit from the presented 3-D dynamic culture technique by further investigation of the endocrine functions of adipocytes. It has been reported that in some cases factors responsible for protein expression are seemingly absent from conventional cell culture. For example, *in vivo* production of TNFα and leptin by far exceed protein secretion in 2-D cell culture [51,52]. Our 3-D model will likely enable long-term *in vitro* investigations into factors typical for a coherent tissue. Although the established model system neither claims to completely reflect *in vivo* conditions nor to serve as a full substitute for animal studies, it is intended to be used to elucidate effects of isolated manipulations in a tissue-like context, e.g. examination of cell-ECM interactions. Furthermore, it offers the opportunity to investigate cell-cell interactions by co-culturing adipocytes with variable cell types in order to simulate *in vivo* effects exerted, for instance, by endothelial cells.

In summary, the established 3-D *in vitro* model of adipogenesis provides tissue engineering and basic research with a useful tool to systematically investigate processes involved in adipose tissue formation. Hence, it may serve as an alternative approach to elucidate 3-D effects expected to occur *in vivo* prior to performing further animal studies.

References

1. American Society of Plastic Surgeons (ASPS). 2001 Quick facts on cosmetic and reconstructive plastic surgery trends. www.plasticsurgery.org . 2002.

2. Katz, A. J., Llull, R., Hedrick, M. H., and Futrell, J. W. (1999). Emerging approaches to the tissue engineering of fat. *Clin.Plast.Surg.* **26**, 587-603.

3. Patrick, C. W., Jr., Chauvin, P. B., and Robb, G. L. (1998). Tissue engineered adipose tissue. *In* "Frontiers in tissue engineering" (C. W. Patrick, Jr., A. G. Mikos, and L. V. McIntire, Eds.), Elsevier Science Ltd., Oxford.

4. Markey, A. C. and Glogau, R. G. (2000). Autologous fat grafting: comparison of techniques. *Dermatol.Surg.* **26**, 1135-1139.

5. Har-Shai, Y., Lindenbaum, E. S., Gamliel-Lazarovich, A., Beach, D., and Hirshowitz, B. (1999). An integrated approach for increasing the survival of autologous fat grafts in the treatment of contour defects. *Plast.Reconstr.Surg.* **104**, 945-954.

6. Huss, F. R. M. and Kratz, G. (2002). Adipose tissue processed for lipoinjection shows increased cellular survival *in vitro* when tissue engineering principles are applied. *Scand.J.Plast.Reconstr.Surg.* **36**, 166-171.

7. Eremia, S. and Newman, N. (2000). Long-term follow-up after autologous fat grafting: analysis of results from 116 patients followed at least 12 months after receiving the last of a minimum of two treatments. *Dermatol.Surg.* **26**, 1150-1158.

8. Ersek, R. A. (1991). Transplantation of purified autologous fat: a 3-year follow-up is disappointing. *Plast.Reconstr.Surg.* **87**, 219-227.

9. Tabata, Y., Miyao, M., Inamoto, T., Ishii, T., Hirano, Y., Yamaoki, Y., and Ikada, Y. (2000). De novo formation of adipose tissue by controlled release of basic fibroblast growth factor. *Tissue Eng.* **6**, 279-289.

10. Kawaguchi, N., Toriyama, K., Nicodemou-Lena, E., Inou, K., Torii, S., and Kitagawa, Y. (1998). De novo adipogenesis in mice at the site of injection of basement membrane and basic fibroblast growth factor. *Proc.Natl.Acad.Sci.U.S.A.* **95**, 1062-1066.

11. Toriyama, K., Kawaguchi, N., Kitoh, J., Tajima, R., Inou, K., Kitagawa, Y., and Torii, S. (2002). Endogenous adipocyte precursor cells for regenerative soft-tissue engineering. *Tissue Eng.* **8**, 157-165.

12. Yuksel, E., Weinfeld, A. B., Cleek, R., Jensen, J., Wamsley, S., Waugh, J. M., Spira, M., and Shenaq, S. (2000). Augmentation of adipofascial flaps using the long-term local delivery of insulin and insulin-like growth factor-1. *Plast.Reconstr.Surg.* **106**, 373-382.

13. Yuksel, E., Weinfeld, A. B., Cleek, R., Wamsley, S., Jensen, J., Boutros, S., Waugh, J. M., Shenaq, S. M., and Spira, M. (2000). Increased free fat-graft survival with the long-term, local delivery of insulin, insulin-like growth factor-I, and basic fibroblast growth factor by PLGA/PEG microspheres. *Plast.Reconstr.Surg.* **105**, 1712-1720.

14. Yuksel, E., Weinfeld, A. B., Cleek, R., Waugh, J. M., Jensen, J., Boutros, S., Shenaq, S. M., and Spira, M. (2000). De novo adipose tissue generation through long-term, local delivery of insulin and insulin-like growth factor-1 by PLGA/PEG microspheres in an *in vivo* rat model: a novel concept and capability. *Plast.Reconstr.Surg.* **105**, 1721-1729.

15. Patrick, C. W., Jr., Chauvin, P. B., Hobley, J., and Reece, G. P. (1999). Preadipocyte seeded PLGA scaffolds for adipose tissue engineering. *Tissue Eng.* **5**, 139-151.

16. Patrick, C. W., Jr., Zheng, B., Johnston, C., and Reece, G. P. (2002). Long-Term Implantation of Preadipocyte-Seeded PLGA Scaffolds. *Tissue Eng.* **8**, 283-293.

17. von Heimburg, D., Zachariah, S., Heschel, I., Kuhling, H., Schoof, H., Hafemann, B., and Pallua, N. (2001). Human preadipocytes seeded on freeze-dried collagen scaffolds investigated *in vitro* and *in vivo*. *Biomaterials* **22**, 429-438.

18. von Heimburg, D., Zachariah, S., Low, A., and Pallua, N. (2001). Influence of different biodegradable carriers on the *in vivo* behavior of human adipose precursor cells. *Plast.Reconstr.Surg.* **108**, 411-420.

19. Kral, J. G. and Crandall, D. L. (1999). Development of a human adipocyte synthetic polymer scaffold. *Plast.Reconstr.Surg.* **104**, 1732-1738.

20. Huss, F. R. and Kratz, G. (2001). Mammary epithelial cell and adipocyte co-culture in a 3-D matrix: the first step towards tissue-engineered human breast tissue. *Cells, Tissues, Organs* **169**, 361-367.

21. Anderson, L. A., McTernan, P. G., Barnett, A. H., and Kumar, S. (2001). The effects of androgens and estrogens on preadipocyte proliferation in human adipose tissue: influence of gender and site. *J.Clin.Endocrinol.Metab.* **86**, 5045-5051.

22. Lefebvre, A. M., Laville, M., Vega, N., Riou, J. P., van Gaal, L., Auwerx, J., and Vidal, H. (1998). Depot-specific differences in adipose tissue gene expression in lean and obese subjects. *Diabetes* **47**, 98-103.

23. Engfeldt, P. and Arner, P. (1988). Lipolysis in human adipocytes, effects of cell size, age and of regional differences. *Horm.Metab.Res., Suppl.Ser.* **19**, 26-29.

24. Green, H. and Meuth, M. (1974). An established pre-adipose cell line and its differentiation in culture. *Cell* **3**, 127-133.

25. Green, H. and Kehinde, O. (1975). An established preadipose cell line and its differentiation in culture. II. Factors affecting the adipose conversion. *Cell* **5**, 19-27.

26. Hausman, G. J. (1981). Techniques for studying adipocytes. *Stain Technol.* **56**, 149-154.

27. Bachmeier, M. and Loffler, G. (1995). Influence of growth factors on growth and differentiation of 3T3-L1 preadipocytes in serum-free conditions. *Eur.J.Cell Biol.* **68**, 323-329.

28. Pairault, J. and Green, H. (1979). A study of the adipose conversion of suspended 3T3 cells by using glycerophosphate dehydrogenase as differentiation marker. *Proc.Natl.Acad.Sci.U.S.A.* **76**, 5138-5142.

29. Lowry, O. H., Rosebrough, N. J., Farr, A. L., and Randall, R. J. (1951). Protein measurement with the Folin phenol reagent. *J.Biol.Chem.* **193**, 265-275.

30. Vunjak-Novakovic, G., Obradovic, B., Martin, I., Bursac, P. M., Langer, R., and Freed, L. E. (1998). Dynamic cell seeding of polymer scaffolds for cartilage tissue engineering. *Biotechnol.Prog.* **14**, 193-202.

31. Gregoire, F. M., Smas, C. M., and Sul, H. S. (1998). Understanding adipocyte differentiation. *Physiol.Rev.* **78**, 783-809.

32. Kellner, K., Schulz, M. B., Göpferich, A., and Blunk, T. (2001). Insulin in tissue engineering of cartilage: a potential model system for growth factor application. *J.Drug Targeting* **9**, 439-448.

33. Gooch, K. J., Blunk, T., Courter, D. L., Sieminski, A. L., Vunjak-Novakovic, G., and Freed, L. E. (2002). Bone morphogenetic proteins-2, -12, and -13 modulate *in vitro* development of engineered cartilage. *Tissue Eng.* **8**, 591-601.

34. Vunjak-Novakovic, G., Freed, L. E., Biron, R. J., and Langer, R. (1996). Effects of Mixing on the Composition and Morphology of Tissue Engineered Cartilage. *AIChE J.* **42**, 850-860.

35. Sugihara, H., Yonemitsu, N., Miyabara, S., and Toda, S. (1987). Proliferation of unilocular fat cells in the primary culture. *J.Lipid Res.* **28**, 1038-1045.

36. Gooch, K. J., Blunk, T., Tennant, C. J., Vunjak-Novakovic, G., Langer, R., and Freed, L. E. (1998). Mechanical Forces and Growth Factors. *In* "Frontiers in Tissue Engineering" (C. W. Patrick, A. G. Mikos, and L. McIntire, V, Eds.), Pergamon, Oxford.

37. Bancroft, G. N., Sikavitsas, V. I., van den Dolder, J., Sheffield, T. L., Ambrose, C. G., Jansen, J. A., and Mikos, A. G. (2002). Fluid flow increases mineralized matrix

deposition in 3D perfusion culture of marrow stromal osteoblasts in a dose-dependent manner. *Proc.Natl.Acad.Sci.U.S.A.* **99**, 12600-12605.

38. Gooch, K. J., Blunk, T., Courter, D. L., Sieminski, A. L., Bursac, P. M., Vunjak-Novakovic, G., and Freed, L. E. (2001). IGF-I and Mechanical Environment Interact to Modulate Engineered Cartilage Development. *Biochem.Biophys.Res.Commun.* **286**, 909-915.

39. Hacker, M., Tessmar, J., Neubauer, M., Blunk, T., Göpferich, A., and Schulz, M. B. (2003). Towards biomimetic scaffolds: Anhydrous scaffold fabrication from biodegradable amine-reactive diblock copolymers. *Biomaterials* **in press**.

40. Lucke, A., Tessmar, J., Schnell, E., Schmeer, G., and Göpferich, A. (2000). Biodegradable poly(D,L-lactic acid)-poly(ethylene glycol)-monomethyl ether diblock copolymers: Structures and surface properties relevant to their use as biomaterials. *Biomaterials* **21**, 2361-2370.

41. Lieb, E., Tessmar, J., Hacker, M., Fischbach, C., Rose, D., Blunk, T., Mikos, A. G., Göpferich, A., and Schulz, M. B. (2003). Poly(D,L-lactic acid)-poly(ethylene glycol)-monomethyl ether diblock copolymers control adhesion and osteoblastic differentiation of marrow stromal cells. *Tissue Eng.* **9**, 71-84.

42. Spiegelman, B. M. and Farmer, S. R. (1982). Decreases in tubulin and actin gene expression prior to morphological differentiation of 3T3 adipocytes. *Cell* **29**, 53-60.

43. Spiegelman, B. M. and Ginty, C. A. (1983). Fibronectin modulation of cell shape and lipogenic gene expression in 3T3-adipocytes. *Cell* **35**, 657-666.

44. Antras, J., Hilliou, F., Redziniak, G., and Pairault, J. (1989). Decreased biosynthesis of actin and cellular fibronectin during adipose conversion of 3T3-F442A cells. Reorganization of the cytoarchitecture and extracellular matrix fibronectin. *Biol.Cell* **66**, 247-254.

45. Ibrahimi, A., Bonino, F., Bardon, S., Ailhaud, G., and Dani, C. (1992). Essential role of collagens for terminal differentiation of preadipocytes. *Biochem.Biophys.Res.Commun.* **187**, 1314-1322.

46. Kubo, Y., Kaidzu, S., Nakajima, I., Takenouchi, K., and Nakamura, F. (2000). Organization of extracellular matrix components during differentiation of adipocytes in long-term culture. *In Vitro Cell.Dev.Biol.:Anim.* **36**, 38-44.

47. Pierleoni, C., Verdenelli, F., Castellucci, M., and Cinti, S. (1998). Fibronectins and basal lamina molecules expression in human subcutaneous white adipose tissue. *Eur.J.Histochem.* **42**, 183-188.

48. Aratani, Y. and Kitagawa, Y. (1988). Enhanced synthesis and secretion of type IV collagen and entactin during adipose conversion of 3T3-L1 cells and production of unorthodox laminin complex. *J.Biol.Chem.* **263**, 16163-16169.

49. Calvo, J. C., Rodbard, D., Katki, A., Chernick, S., and Yanagishita, M. (1991). Differentiation of 3T3-L1 preadipocytes with 3-isobutyl-1-methylxanthine and dexamethasone stimulates cell-associated and soluble chondroitin 4-sulfate proteoglycans. *J.Biol.Chem.* **266**, 11237-11244.

50. Kuri-Harcuch, W., Arguello, C., and Marsch-Moreno, M. (1984). Extracellular matrix production by mouse 3T3-F442A cells during adipose differentiation in culture. *Differentiation* **28**, 173-178.

51. Rosen, E. D. and Spiegelman, B. M. (2000). Molecular regulation of adipogenesis. *Annu.Rev.Cell Dev.Biol.* **16**, 145-171.

52. Mandrup, S., Loftus, T. M., MacDougald, O. A., Kuhajda, F. P., and Lane, M. D. (1997). Obese gene expression at *in vivo* levels by fat pads derived from s.c. implanted 3T3-F442A preadipocytes. *Proc.Natl.Acad.Sci.U.S.A.* **94**, 4300-4305.

Chapter 4

Analysis of Differential Areas within 3-D Tissue-Engineered Fat Constructs

Claudia Fischbach, Michael Hacker, Barbara Weiser,
Torsten Blunk, Achim Göpferich

Department of Pharmaceutical Technology, University of Regensburg,
93040 Regensburg, Germany

To be submitted to Cells Tissues Organs

Introduction

Donor shortage problems have led to the emergence of the interdisciplinary field of tissue engineering (TE), which pursues the creation of biologically compatible substitutes to restore, maintain, or improve diseased tissue functions [1]. Originally intended to be used for transplantation and reconstructive purposes, TE approaches are increasingly recognized as a means of providing valuable three-dimensional (3-D) model systems applicable for basic research *in vitro*. Growing cells in a 3-D environment, e.g. in highly porous polymer scaffolds or gel systems, may lead to the recreation of the particular cell-cell and cell-extracellular matrix (ECM) interactions present within native tissues. Consequently, an environment resembling *in vivo* conditions can be imitated more thoroughly than in conventional two-dimensional (2-D) cell culture. Thereby, comprehensive investigations of cellular features characteristic for native tissues are enabled *in vitro*.

In recent years, a number of studies has been performed with the objective of demonstrating the advantages of 3-D cell culture techniques over conventional 2-D methodologies. For instance, it has been shown that dedifferentiated cartilage cells, yielded from monolayer proliferation, regained their differentiated phenotype when cultivated in a 3-D environment [2,3]. In these specific studies, the application of TE strategies proved to be beneficial to overcome the intrinsic drawbacks of conventional 2-D cell culture. Basic research of adipose tissue represents another scope potentially benefiting from a tissue-engineered 3-D culture system. It has been described that in some cases that adipose cell functions observed in animal studies are impaired *in vitro*; e.g. *in vivo* production of TNFα and leptin by far exceed protein secretion in 2-D cell culture [4,5]. Apparently, essential factors provided by the physiological environment are seemingly absent from conventional 2-D cell culture and thereby lead to the development of an incomplete adipose phenotype. In order to adequately address the potential reasons, it may, therefore, be helpful to conduct the particular investigations in a 3-D culture system, which is suitable for analyzing inherent tissue properties.

We recently reported the establishment of a 3-D *in vitro* model of adipogenesis consisting of 3T3-L1 preadipocytes, induced to undergo adipose differentiation, and highly porous polymer scaffolds made from polyglycolic acid (PGA) [6]. Generation of the model system under dynamic conditions resulted in a coherent fat-like construct, which exhibited the appropriate adipose characteristics and, thus, implied the promise for being of use for basic

research purposes. The first promising indications of improved adipose properties compared to conventional 2-D cell culture were obtained through microscopic examination of the 3-D model. Thereby, large lipid-filled, nearly unilocular adipocytes rarely detectable in monolayer cultures could be observed. However, microscopic investigation of cross-sections prepared from the constructs uncovered considerable differences of the outer areas relative to the inner ones. For other *in vitro* engineered tissues such as bone, this observation has been made before [7,8] and is also reported for human preadipocyte seeded collagen sponges [9]. Nevertheless, neither of those studies addressed the observed heterogeneity more in detail.

Therefore, the focus of this study was not only to thoroughly characterize the 3-D model, but to also address the non-uniform construct composition. Due to the preliminarily determined heterogeneity, a method was developed enabling separate investigation of the different construct parts. This approach allowed for more detailed evaluation as the results, hypothesized to depend on the particular construct part, could be related to a clearly defined area of the generated tissues. In detail, adipose tissue constructs were generated from 3T3-L1 preadipocytes and 3-D polyglycolic acid (PGA) fiber meshes. Subsequently, they were divided into outer and inner parts via a stainless-steel dermal punch and the resulting construct parts were characterized in terms of key features of adipose tissue. Afterwards, the gained results were compared to those obtained from adipocytes cultured under conventional 2-D conditions. At first, histological examination of entire adipose tissue constructs was performed in order to comprehensively assess spatial differences. Subsequently, intracellular lipid accumulation was quantitatively determined by measurement of triglyceride content and activity of glycerol-3-phosphate dehydrogenase (GPDH), a key enzyme involved in triglyceride biosynthesis. Expression analysis of a variety of fat cell genes, known to be characteristic for the adipose phenotype, was carried out on the mRNA level. Finally, lipolysis was determined under stimulating and inhibiting conditions in order to investigate the functionality of the adipocytes derived from the distinct construct parts.

Materials and Methods

Materials:

3T3-L1 preadipocytes were obtained from ATCC (Manassas, VA, USA). DMEM with 1.0 g/l glucose, fetal bovine serum (FBS), and trypsin (1:250) were purchased from Biochrom KG Seromed (Berlin, Germany); phosphate buffered saline (PBS) and penicillin-streptomycin

solution were from Life Technologies (Karlsruhe, Germany). α-MEM, corticosterone, indomethacin, and oil red O were from Sigma-Aldrich (Deisenhofen, Germany). 3-isobutyl-1-methylxanthine (IBMX) was purchased from Serva Electrophoresis GmbH (Heidelberg, Germany). Insulin was kindly provided by Hoechst Marion Roussel (Frankfurt a. M., Germany). Cell culture materials were obtained from Sarstedt AG & Co. (Nuembrecht, Germany) and BD Biosciences Labware (Heidelberg, Germany).

Spinner flasks were self-made (250 ml volume, 6 cm bottom diameter, side arms for gas exchange). Silicon stoppers were obtained from Schuber & Weiss (München, Germany); needles were from Unimed (Lausanne, Switzerland). Polyglycolic acid (PGA) non-woven fiber meshes (12-14 µm fiber diameter; 96% porosity; 62 mg/cm^3 bulk density) were purchased from Albany Int. Research Co. (Mansfield, MA, USA) and die-punched into discs 5 mm in diameter and 2 mm thick.

Cell culture:

3T3-L1 preadipocytes were expanded during 4 passages and frozen in liquid nitrogen. Subsequent to defrosting, the cells were further expanded; cells from the fourth passage (following cryo-storage) were used for experiments. Growth of stock cultures was performed in DMEM supplemented with 10% FBS, penicillin (100 U/ml), and streptomycin (0.1 mg/ml). For 2-D cell culture preadipocytes were plated on tissue culture polystyrene (TCPS) at a density of 5,000 cells per cm². Development of the 3-D model system was performed as previously described [6]. Briefly, expanded 3T3-L1 preadipocytes were dynamically seeded onto PGA scaffolds in stirred spinner flasks. Thereby, each flask comprised 8 scaffolds and 100 ml of a suspension containing 16x10^6 cells, i.e., 2x10^6 cells per scaffold. Stirring for two days at 80 rpm allowed for cell attachment to the polymer fibers. Cell-polymer constructs were transferred into 6-well plates (one construct and 5 ml culture medium per well) and cultured in the incubator (37°C, 5% CO_2) dynamically on an orbital shaker at 50 rpm (Dunn Labortechnik GmbH; Asbach, Germany). Cultivation of the cell-seeded constructs was performed in MEM (alpha-modification) supplemented with 10% FBS, penicillin (100 U/ml), and streptomycin (0.1 mg/ml). Four days after plating (2-D) and seeding (3-D), adipogenesis was induced by adding 0.1 µM corticosterone, 0.5 mM IBMX, and 60 µM indomethacin to differentiation medium (α-MEM, 5% FBS, 1 µM insulin, penicillin (100 U/ml), and streptomycin (0.1 mg/ml)) and referred to as day 0. After 2 days, the induction medium was

replaced by differentiation medium alone. Cultures were maintained under these conditions until cell harvest, whereby the culture medium was changed every other day.

Cell harvest:

9 days after hormonal induction of adipogenesis, 2-D and 3-D cells, respectively, were harvested under appropriate conditions according to the specific protocols described below in this section. To allow for separate investigation of the outer and inner areas of the cell-polymer constructs, entire constructs were aseptically divided by die-punching with a sterile stainless-steel dermal punch 3 mm in diameter (Aesculap; Tuttlingen, Germany). Thereby, a ring consisting of external tissue as well as a disc composed of internal areas was produced. Unless otherwise stated, subsequent analysis was independently carried out for entire constructs, outer rings and inner discs.

Histology:

Complete generated fat constructs were fixed overnight in 10% buffered formalin, dehydrated and then embedded in paraffin. To assess cellularity of different areas, deparaffinized sections of 5 µm were stained with hematoxylin and eosin (H&E) (Sigma-Aldrich; Deisenhofen, Germany). Due to lipid extraction from the cells by organic solvents used in routine staining procedures, examination of lipid storage was carried out with oil red O pre-stained specimen. For oil red O staining of cytoplasmic triglyceride droplets, 2-D cells, as well as complete 3-D cell-polymer constructs, were washed with PBS. Subsequently, they were subjected to an overnight fixation step in 10% buffered formalin. The fixed 2-D and 3-D samples were stained as described [10], but only the 3-D specimen were mounted in Tissue Tek (Sakura Finetek; Torrane, CA, USA). Finally, they were rapidly frozen and cut with a 2800 Frigocut E cryostat (Cambridge Instruments GmbH; Nussloch, Germany) in 12 µm sections, which could directly be investigated.

Immunohistological detection of the ECM component laminin was performed by staining of deparaffinized sections, 5 µm thick, with a rabbit anti-mouse laminin antibody (Novus Biologicals, Inc.; Littleton, CO, USA). The staining procedure was conducted as follows: Endogenous peroxidase activity was blocked by incubation in 1% H_2O_2. After extensive rinsing, antigen retrieval was performed by pepsin digestion. To prevent non-specific antibody binding, sections were incubated with 5% normal horse serum (Vector

Laboratories Inc.; Burlingame, CA, USA) in PBS. Subsequently, the primary antibody was applied at a dilution of 1:600 (in PBS with 5% horse serum) for 60 min at room temperature (RT). In control sections, the primary antibody was replaced by PBS with 5% normal horse serum. After washing with PBS, the sections were incubated with biotinylated horse anti-rabbit IgG antibody (1:100) (Vector Laboratories Inc.; Burlingame, CA, USA) for 30 min at RT. To form the streptavidin-biotin-peroxidase complex, the Vectastain Elite ABC-Kit was used. Peroxidase localization was performed with the DAB Substrate Kit for Peroxidase. Both kits were obtained from Vector Laboratories Inc.; Burlingame, CA, USA. Finally, the sections were counter-stained with hematoxylin and mounted in DPX Mountant (Fluka, Biochemika; Taufkirchen, Germany).

Scanning electron microscopy (SEM):

Entire cell-polymer constructs were washed with PBS. Afterwards, they were fixed for 15 min with 2.5% glutardialdehyde in PBS and for 30 min with 1% osmium tetroxide (Carl Roth GmbH & Co.; Karlsruhe, Germany). After extensive rinsing and freezing at –80°C, samples were subjected to lyophilization (Christ Beta 2-16, Martin Christ Gefriertrocknungsanlagen; GmbH, Osterode am Harz, Germany). For differential examination of internal and external areas, lyophilized samples were halved (Fig. 3) and mounted on aluminum stubs using conductive carbon tape and coated with gold - palladium (Polaron SC515, Fisons surface systems; Grinstead, UK). All micrographs were obtained at 10 kV on a DSM 950 (Zeiss; Oberkochen, Germany).

Glycerol-3-phosphate dehydrogenase (GPDH) measurement:

2-D cells and 3-D cell-polymer constructs (entire and die-punched) were washed with PBS, harvested in lysis buffer (50 mM Tris, 1 mM EDTA, 1 mM mercaptoethanol, pH 7.5), and sonicated afterwards with a digital sonifier. The GPDH assay was performed as described in the literature [11,12]. Cytosolic protein concentration was determined after precipitation with trichloracetic acid using the Lowry assay [13]. GPDH activity was normalized to protein content and is expressed as mU per mg protein.

Analysis of triglyceride (TG) content:

To facilitate the determination of TG content, 2-D cell cultures and die-punched samples of 3-D cell-polymer constructs were washed with PBS, harvested in 0.5% thesit, and sonicated with a digital sonifier (Branson Ultrasonic Corporation, Danburg, CT, USA). Subsequently, spectroscopic quantification of TG was performed using the enzyme coupled glycerol assay kit 337 (Sigma Diagnostics; Deisenhofen, Germany). Cytosolic protein concentration was determined after precipitation with trichloracetic acid using the Lowry assay[13]. TG content was normalized to protein content and is expressed as mg TG per mg protein.

Reverse transcription polymerase chain reaction (RT-PCR):

Subsequent to washing in PBS, harvest of 2-D and 3-D derived cells (from entire and die-punched constructs) was performed with Trizol reagent (Invitrogen GmbH; Karlsruhe, Germany). Total RNA was isolated according to manufacturers instructions.

Table 1: Primer sequences and PCR conditions for the investigated genes
Oligonucleotide sequences of mouse forward (sense) and reverse (antisense) primers. Gene amplification was performed by PCR according to the specified annealing temperatures (AT) and number of cycles for each gene. The reaction conditions of one cycle were composed as follows: denaturation for 45 sec at 94°C, annealing for 45 sec at the indicated temperatures, and extension for 1 min at 72°C.

Gene	Forward and reverse primers of examined genes	AT (°C) / Cycles
PPARγ	5′-AAC CTG CAT CTC CAC CTT ATT ATT CTG A-3′ 5′-GAT GGC CAC CTC TTT GCT CTG CTC CTG-3′	60 / 35
GLUT-4	5′-CCC CGC TGG AAT GAG GTT TTT GAG GTG AT-3′ 5′-CAG ACA GGG GCC GAA GAT TGG GAG ACA GT-3′	61 / 35
laminin-β1	5′-GCT GGA TCC GCT TGC AGC AGA GTG CAG CTG A-3′ 5′-CGC GAA TTC GCT AAG CAG GTG CTG TAA ACC G-3′	60 / 30
angiotensinogen	5′-CTG GCC GCC GAG AAG CTA GAG GAT GAG GA-3′ 5′-GAG AGC GTG GGA AGA GGG CAG GGG TAA AGA G-3′	62 / 35
beta3-AR	5′-CAG TGG TGG CGT GTA GGG GCA GAT-3′ 5′-CGG GTT GAA GGC GGA GTT GGC ATA G-3′	63 / 36
18 S	5′-TCA AGA ACG AAA GTC GGA GGT TCG-3′ 5′-TTA TTG CTC AAT CTC GGG TGG CTG-3′	60 / 22

First-strand cDNA was synthesized from total RNA by using random hexamers (Roche Diagnostics; Mannheim, Germany) and Superscript II RNase H- Reverse Transcriptase (Invitrogen GmbH; Karlsruhe, Germany). For reverse transcription, samples were incubated at 42°C for 50 min and heated afterwards for 15 min at 70°C to inactivate the enzyme. Subsequently, PCR was performed with Sawady Taq-DNA-Polymerase (PeqLab; Erlangen, Germany); initial denaturation occurred at 94°C for 120 sec, final extension at 72°C for 30 sec, and holding at 4°C. The amplification was carried out using specific primers and appropriate conditions for each gene (Tab. 1). 18 S rRNA served as internal control. Reverse transcription and PCR were performed using a Mastercycler Gradient (Eppendorf AG; Hamburg, Germany). The PCR products were analyzed by electrophoresis on 2% agarose gels containing ethidium bromide, followed by imaging and densitometric scanning of the resulting bands using UV light ($\lambda = 312$ nm) and a Kodak EDAS 290 (Fisher Scientific; Schwerte, Germany).

Determination of lipolysis rate:

The lipolytic cell response was assessed by measuring the amount of glycerol released into the incubation buffer after treatment with agents stimulating or inhibiting lipolysis. Briefly, 2-D cells and 3-D cell-polymer constructs (entire and die-punched) were washed with serum-free medium and then maintained in the same medium for 2 h to avoid interference with serum factors. Subsequently, medium was replaced by PBS supplemented with 3% fatty acid-free bovine serum albumin (Sigma-Aldrich; Deisenhofen, Germany). In addition to recording data on lipolysis under control conditions, stimulation and inhibition of glycerol release were conducted by adding 10 µM isoproterenol and 100 µM propranolol (both were from Sigma-Aldrich; Deisenhofen, Germany) to the incubation buffer, respectively. After 2h incubation (37°C, 5% CO_2), the conditioned media were frozen at –20°C until the enzyme coupled glycerol assay kit 337 (Sigma Diagnostics; Deisenhofen, Germany) was carried out.

Statistical analysis:

Statistical significance was assessed by one-way analysis of variance ANOVA followed by Tukey post-hoc test (Software: SPSS 10.0 for Windows). The statistical significance level was set at $p < 0.01$.

Results

Cellular composition of the constructs:

Microscopical examination of H&E stained paraffin sections prepared from entire constructs at day 9 after hormonal induction of adipogenesis revealed considerable heterogeneity of generated cell-polymer constructs (Fig. 1). Coherent adipose tissue, consisting of fully differentiated adipocytes, could only be observed in external regions of the scaffolds. In contrast, the internal areas comprised only a few undifferentiated cells. Furthermore, a cellular gradient within the external rim could be observed (Fig. 1).

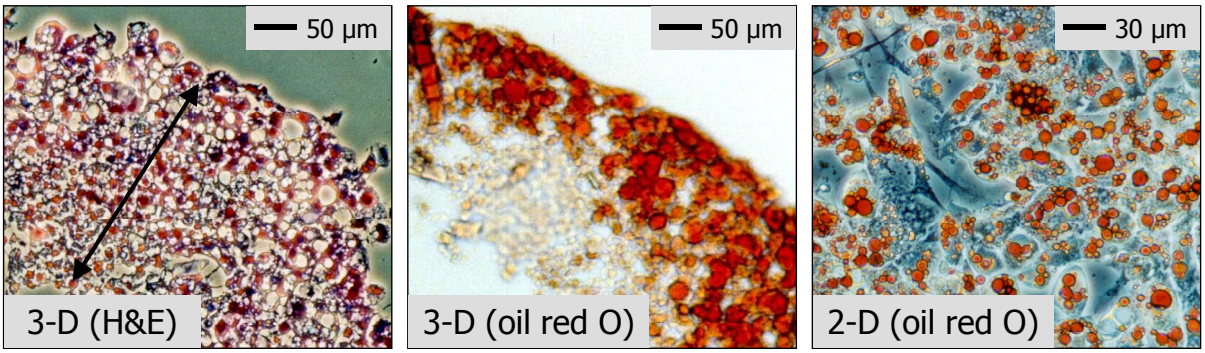

Fig. 1:
Cellular gradient within 3-D cell-polymer constructs as revealed by light microscopy of histological cross-sections and indicated by the arrow. In H&E stained sections, lipid vacuoles appear as blank spaces, whereas in oil red O stained cryo-sections, they become visible as red colored droplets. Towards interior areas of the constructs, size of intracellular lipid droplets declines and thereby demonstrates the dissimilarity of cells situated in outer and inner regions, respectively. Additionally, oil red O-stained 2-D cultivated adipocytes are shown to demonstrate homogeneous differentiation status within conventional cell culture. Bars represent 50 µm and 30 µm.

In particular, the more outside the cells were located the more intracellular lipid they had accumulated during differentiation. This observation was made by examining size of blank spaces in H&E stained paraffin sections, which were caused by dissolving lipid inclusions with organic solvents used during deparaffinization procedure (Fig. 1). These findings were strengthened by oil red O stained cryo-sections in which the lipid vacuoles were still intact. Thereby, a decrease in red colored lipid droplet size and color intensity could be revealed evidencing diminished fat storage of internally situated cells (Fig. 1). In contrast, 2-D differentiated adipocytes were evenly differentiated, which was demonstrated through detection of homogeneously distributed oil red O stained lipid inclusions over the whole culture dish surface (Fig. 1).

The above described differences in cellularity could be supported by immunohistochemical detection of laminin, a characteristic component of the adipocyte basement membrane. Microscopic investigation of the immuno-stained cross-sections elucidated that laminin was primarily synthesized by cells situated in the outer regions of the constructs (indicated by an intense black staining), whereas internally located cells secreted almost no laminin (demonstrated by a weak gray staining) (Fig. 2).

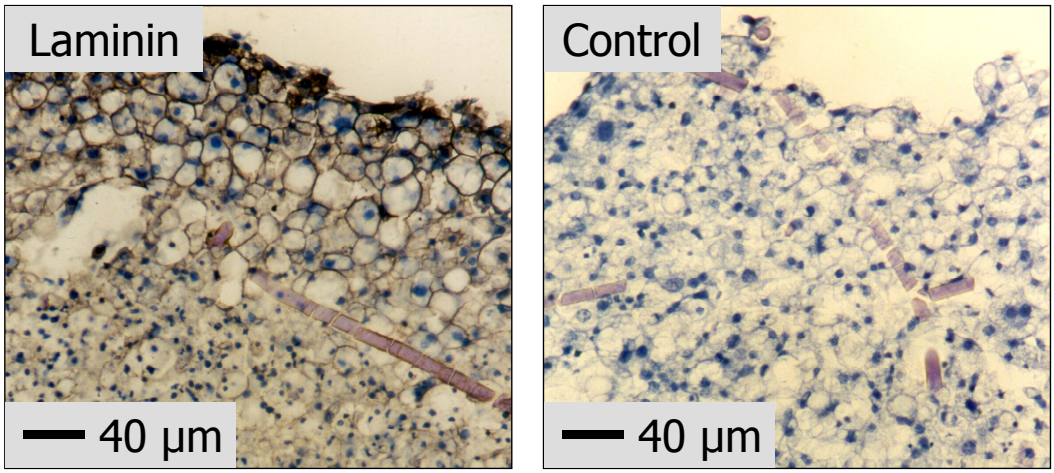

Fig. 2:
Immunostaining of laminin, a component of the adipocyte basement membrane. Cross sections obtained from cell-polymer constructs at day 9 of adipogenesis revealed a decrease of immunological laminin staining intensity towards inner construct areas. Thus, laminin protein expression is shown to be enhanced in outer regions. For staining of control sections, primary anti-laminin antibody was omitted. Scale bars indicate 40 µm.

As the typical composition of the adipocyte basement membrane does not arise until adipogenesis occurs [14], the results from the laminin staining confirm that only outer regions comprised mature adipocytes (see above). As a control, the staining procedure was performed without adding the primary anti-mouse laminin antibody. In these sections, no unspecific black staining was detected.

Heterogeneous cellularity of different scaffold areas was additionally proven by subjecting halved constructs (Fig. 3) to SEM examination. Well-differentiated cells exhibiting the typical morphology of large, rounded adipocytes with bulged cell membranes due to lipid accumulation were exclusively detected in the outer areas (top and edge) of cell-polymer constructs. In contrast, interior regions revealed only a few, relatively small fibroblastic cells that were hardly differentiated. Inner parts were mainly composed of degraded polymer fiber residues and structures that were accounted for as extracellular matrix fibrils deposited by the cells.

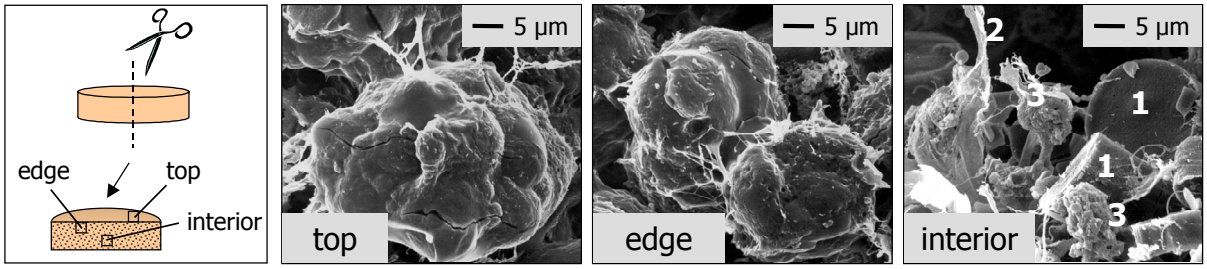

Fig. 3:
Cellularity of 3-D cell-polymer constructs as visualized by SEM subsequent to halving entire constructs. Investigating the top and edge areas of the constructs, differentiated adipocytes exhibiting bulged cell membranes due to fat storage were observed. In contrast, interior areas exhibited only a few cells that were hardly differentiated. Detected structures within internal parts were accounted for remnants of degraded PGA polymer fibers (1) and extracellular matrix fibrils (2) deposited by the cells (3). Micrographs were taken from representative areas. Bars represent 5 µm.

Lipid accumulation in different construct parts:

To investigate lipid accumulation, measurement of GPDH activity, a key enzyme involved in triacylglycerol biosynthesis, was performed. Compared to all other groups investigated, adipocytes derived from external areas of the 3-D constructs exhibited significantly ($p<0.01$) enhanced GPDH values (826.6 ± 15.2 mU/mg protein) (Fig. 4). In detail, values determined from 2-D differentiated cells (518.7 ± 11.3 mU/mg protein), from entire constructs (672.3 ± 65,8 mU/mg protein), and from interior areas (551.5 ± 26.1 mU/mg protein) were significantly lower as compared to those measured from external parts (Fig. 4). In the figure, specific GPDH activities are depicted. Addition of absolute GPDH activities measured from outer rings and inner discs resulted in similar activities as determined from entire constructs (data not shown).

To facilitate a quantitative analysis of lipid accumulation, the intracellular TG content of 2-D and 3-D differentiated adipocytes was investigated. Again, an advantage of externally situated cells over all other groups could be assessed (Fig. 5). Specifically, adipocytes derived from outer areas accumulated statistically significant ($p<0.01$) increases in intracellular lipid content (37.2 ± 0.1 mg/mg protein) as compared to cells cultivated within conventional 2-D cell culture (20.8 ± 4.5 mg/mg protein) (Fig. 5). Additionally, lipid content of entire constructs (26.4 ± 0.4 mg/mg protein) and inner discs (26.5 ± 1.4) was significantly lower as well (Fig. 5). As done for GPDH activities, TG content was normalized to protein

concentration. Adding the absolute TG amounts of external and internal areas yielded equal values as measured from entire constructs (data not shown).

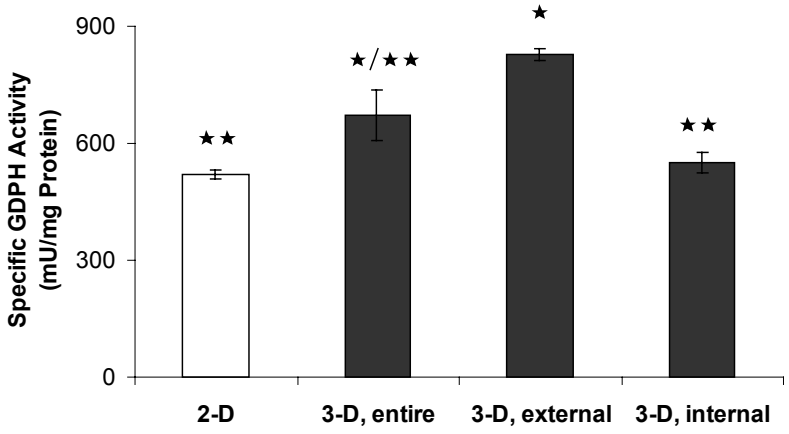

Fig. 4:
Activity of GPDH, a key enzyme involved in triacylglycerol synthesis, as determined 9 days after hormonal induction of adipogenesis and standardized per mg protein. Values are expressed as mean ± SD (n=3). Statistically significant differences ($p < 0.01$) to 2-D cultured cells are indicated by ★ whereas significance ($p < 0.01$) to 3-D cells derived from external parts of constructs is denoted by ★★. Three independent experiments were conducted, representative results of one experiment are shown here.

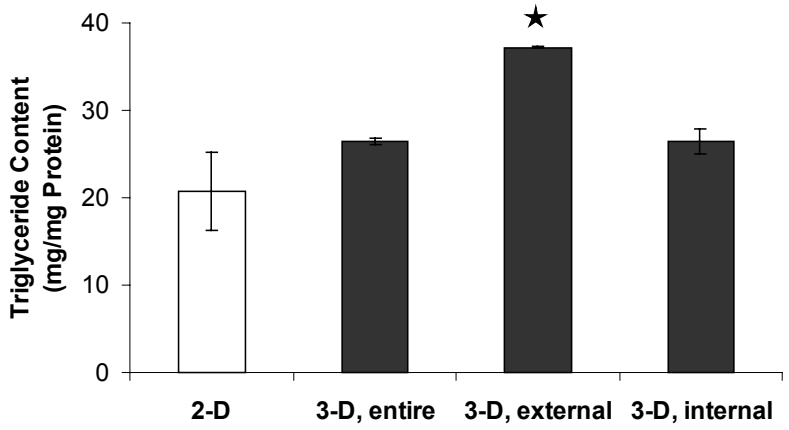

Fig. 5:
Triglyceride content of cells situated within disparate areas of differentiated cell-polymer constructs, as analyzed by an enzyme coupled colorimetric assay. Absolute values were standardized per mg protein and represented as mean ± SD (n=3). Statistically significant difference ($p < 0.01$) is indicated by ★. Two independent experiments were performed, representative results of one experiment are depicted.

Differential gene expression within the constructs:

To elucidate differences in adipose gene expression between conventional 2-D cell culture and distinct areas of the 3-D culture system, RT-PCR investigations of certain characteristic fat cell genes were performed. Generally, 2-D cells and adipocytes derived from 3-D entire constructs expressed most of the examined genes to a comparable extent. However, by dividing the constructs into outer and inner parts, cells from external regions could be demonstrated to exhibit superior properties in terms of gene expression as compared to the cells from inner parts.

In detail, examination of PPARγ, a key transcription factor of adipogenesis, revealed no difference in the extent of gene expression between 2-D cells and adipocytes derived from external areas. Only a slight decrease of gene expression was densitometrically assessed for 3-D cells from entire constructs and internal areas (Fig. 6). Analysis of glucose transporter 4 (Glut-4), catalyzing glucose uptake in adipocytes, displayed decreased gene expression for cells situated internally. All other groups exhibited similar gene expression (Fig. 6). Assuming differences in the organization of extracellular matrix (ECM) components between 2-D and 3-D, we investigated mRNA levels of laminin being a central component of adipocytes basement membrane. In 3T3-L1 adipocytes, laminin-8 (α4, β1, γ1) has been reported to be the specific isoform [15]. At first, laminin-8 expression was checked by using paired primers for α4, β1, and γ1. After demonstrating appropriate expression (data not shown), laminin-β1 mRNA was examined. Amplified fragments of 2-D adipocytes yielded bands more intensely stained than those detected in 3-D groups. However, laminin-β1 expression in externally located 3-D adipocytes was enhanced over cells from entire constructs. This effect was even more pronounced relative to cells from interior regions (Fig. 6). Investigation of the vascular function related protein angiotensinogen revealed comparable gene expression for 3-D entire constructs and outer areas. Thereby, the determined densities of angiotensinogen expression were slightly increased as compared to both 2-D cultivated adipocytes and 3-D cells from inner parts (Fig. 6). Finally, RT-PCR has been performed for beta3-adrenoreceptor. Relative to other 3-D areas, outer construct parts exhibited enhanced mRNA expression. Compared to adipocytes from 2-D cell culture equivalent staining intensities were assessed. Amplification of beta3-AR fragments harvested from entire constructs and interior parts yielded bands that were either weakly stained or undetectable (Fig. 6).

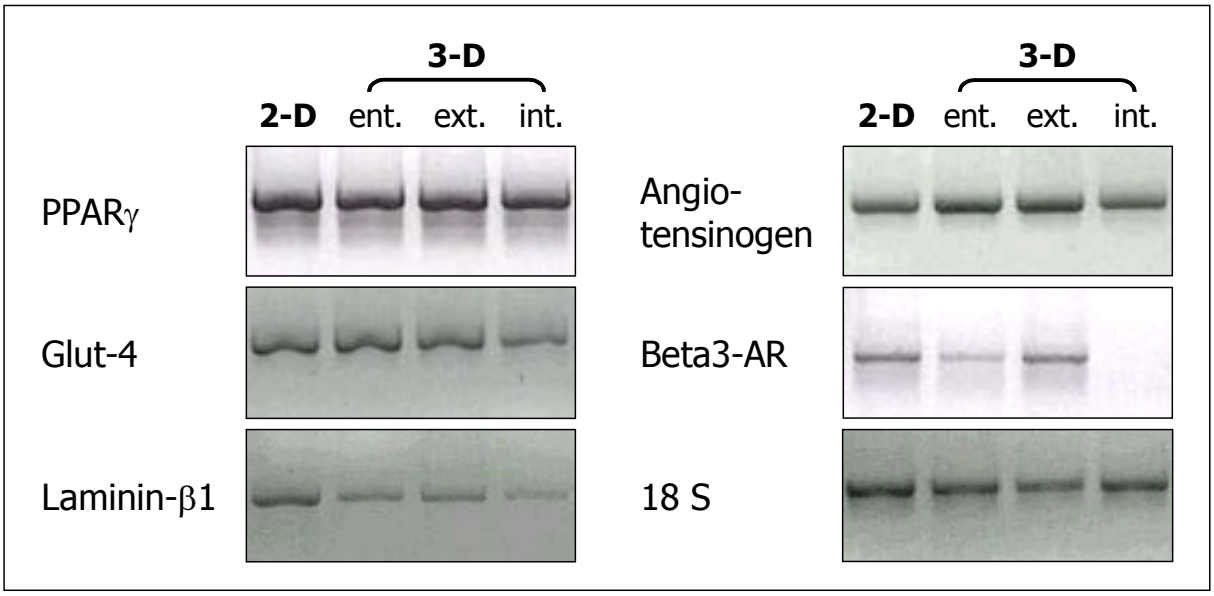

Fig. 6:
Gene expression on the mRNA level as examined by RT-PCR. Analysis of cells derived from 2-D cell culture and different areas of 3-D constructs was carried out at day 9 of adipogenesis. Resulting bands are shown for PPARγ, GLUT-4, laminin-β1, angiotensinogen, beta3-AR, and the internal standard 18 S. RT-PCR was performed in triplicate, representative results of one experiment are shown here.

Lipolytic cell response of differently situated adipocytes:

3-D cell polymer constructs are apparently composed of dissimilarly differentiated cells (see above). However, only mature adipocytes exhibit full functionality. In order to assess cellular functionality within distinct construct areas, the extent of lipolytic cell response was analyzed. The lipolysis rates of the respective construct parts were determined by analyzing the concentration of glycerol released into the incubation buffer. Under control conditions, cells from all groups exhibited basal lipolysis rates. However, only entire constructs and external parts responded significantly ($p<0.01$) to addition of a lipolysis stimulating factor (10 µM isoproterenol) (Fig. 7). Both groups released 3.49-fold more glycerol as compared to control conditions. In contrast, cell response of internal areas did not change significantly (1.41-fold increase) (Fig. 7). Accordingly, significant inhibition of lipolysis, facilitated by supplementing 100 µM propranolol, could only be triggered in adipocytes from complete constructs (0.47-fold decrease) and outer rings (0.51-fold decrease). Again, cells from inner discs did not change glycerol release significantly (0.64-fold decrease) (Fig. 7). Comparison of absolute values (control conditions: 1.90 ± 0.03 µg (entire), 1.10 ± 0.02 µg (external), and

0.60 ± 0.03 µg (internal)) furthermore demonstrated that externally situated cells contributed to a major extent to the overall lipolytic cell response of entire constructs.

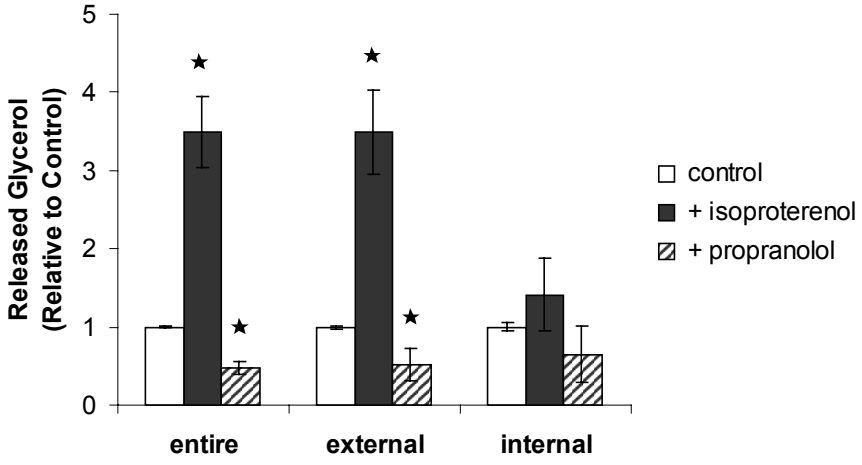

Fig. 7:
Functionality of 3T3-L1 adipocytes within differential sites of 3-D cell-polymer constructs as assessed by analysis of released glycerol subsequent to treatment with a lipolysis stimulating (10 µM isoproterenol) and a lipolysis inhibiting (100 µM propranolol) agent. Three independent experiments were performed. Data are expressed as mean ± SD (n=3) of one representative experiment. Statistically significant differences to control conditions ($p < 0.01$) are denoted by ★. Absolute values under control conditions were 1.90 ± 0.03 µg (entire), 1.10 ± 0.02 µg (external), and 0.60 ± 0.03 µg (internal).

Discussion

The focus of the presented study was to thoroughly characterize engineered adipose tissue constructs after differentiation over 9 days. In particular, it was aimed at comprehensively evaluating the fat-like properties in differential areas of the constructs and to compare the gained results with those determined from conventional 2-D cell culture.

It is commonly acknowledged that *in vitro* engineered tissues may be subject to insufficient nutrient and oxygen supply and may therefore suffer from the limitation to consist of differential areas [16]. However, to the best of our knowledge, no study has been conducted so far addressing this heterogeneity more in detail. Adipose tissue constructs were generated from PGA polymer meshes and 3T3-L1 preadipocytes as previously described [6]. As preliminary analysis indicated a heterogeneous composition, we intended to take this potential restriction particularly into consideration and examined not only entire constructs but also different construct parts divided by die-punching with a stainless-steel dermal punch.

Thereby, potential differences could be assessed in detail allowing to better figure out the usefulness of the adipose equivalents for basic research.

At first, histological investigations of entire constructs were performed in order to determine preliminarily detected differences of the generated constructs more in detail. By means of light and scanning electron microscopy, a cellular gradient was observed, which revealed that only outer construct areas consisted of well-differentiated, lipid-filled adipocytes, whereas interior regions mainly contained fibroblastic, less-differentiated cells (Fig. 1, 3). Accordingly, laminin, a component of the basement membrane secreted by adipocytes, could only be detected in outer regions of the constructs (Fig. 2). With the objective of comprehensively evaluating the microscopically detected gradient, entire constructs as well as the separated parts were analyzed with regard to triglyceride accumulation, expression of typical fat cell genes, and functionality of the differently located cells. All applied methodologies revealed that the outer rings featured appropriate properties with respect to fat-like characteristics, whereas the inner parts displayed inferior quality (Fig. 4-7). By analyzing entire constructs, a mixture of those distinct areas was recorded and, thus, yielded impaired overall results compared to the findings measured from external parts alone. In detail, the determination of GPDH activity and intracellular triglyceride content showed that outwardly located adipocytes exhibited enhanced lipogenesis relative to the cells harvested from either entire constructs or inner parts (Fig. 4, 5). In terms of adipocyte gene expression, cells situated in interior areas expressed diminished Glut-4, laminin-β1, angiotensinogen, and beta3-AR mRNA levels as compared to the cells derived from complete constructs and the corresponding external rings (Fig. 6). In contrast, gene expression of adipocytes derived from outer regions was either equivalent to that of entire constructs (PPARγ, Glut-4, laminin-β1, and angiotensinogen) or was enhanced (beta3-AR). Analysis of functionality further demonstrated that both entire constructs and outer parts yielded basal lipolysis rates under control conditions and appropriate cell response subsequent to supplementation of stimulating or inhibiting factors (Fig. 7). In contrast, internal ones did not exhibit a significant cell response to either stimulating or inhibiting conditions.

Consequently, only external areas of the constructs displayed a coherent adipose tissue consisting of mature adipocytes featuring lipid accumulation, secretion of a laminin containing basement membrane, appropriate gene expression, and functionality. Therefore, to demonstrate the potential of the 3-D culture approach for basic research, these results were used for comparison with conventional 2-D cell culture. Encouraging data were obtained by measurement of both GPDH activity and intracellular triglyceride content revealing increased

lipid accumulation of 3-D cultivated cells relative to that determined from 2-D cultured ones. Investigation of gene expression by means of RT-PCR showed that laminin-1β mRNA levels were increased in 2-D cultures as compared to 3-D. This observation may be attributed to the fact that the ECM secreted by 3-D cultivated cells is largely kept incorporated within the constructs, which in turn may lead to down-regulation of laminin-1β. In contrast, ECM synthesized in 2-D cell culture is more likely to be aspirated with every medium change, which can be supported by the finding that preadipocyte differentiation in 2-D cell culture results in enhanced medium viscosity [17]. As a consequence, the cells possibly up-regulate laminin-β1 mRNA to maintain the levels required for a physiological environment.

The heterogeneous composition of the *in vitro* engineered adipose tissue constructs may be ascribed to both the insufficient nutrient and oxygen supply to the internally situated cells and the inadequate removal of catabolites away from them [16,18]. Furthermore, tissue-inducing factors are required for appropriate fat formation. In detail, preadipocytes are reported to only undergo adipogenesis when stimulated with an hormonal cocktail containing either pharmacological concentrations of insulin or IGF-1, a glucocorticoid, and a cAMP-enhancing agent [14,19,20]. *In vivo*, the supply of substances would be regulated by diffusion processes and simultaneous onset of vascularization [18,21], whereas *in vitro*-cultures are dependent upon diffusion processes alone. Hence, the quality of the interior areas of the engineered cell-polymer constructs is generally limited to the maximum distance over which factors can effectively diffuse to the cells (app. 100-200 µm [22]). Accordingly, it seems likely that restricted local concentrations of nutrients, oxygen, and tissue-inducing substances, necessary to trigger appropriate adipocyte differentiation and structural reorganization, contributed to the underdevelopment of interior areas. Although dynamic culture conditions (as used in our approach) are known to considerably improve mass transfer of essential biochemical factors as compared to static culture [23-25], they appear to not be adequate enough to allow for homogeneous tissue quality. Hence, efforts have to be undertaken to engineer adipose tissue equivalents homogeneously composed of coherent fat-like structures throughout the whole construct. This challenge is most likely to be met by enhancing the transfer of nutrients, oxygen, and adipogenesis stimulating factors into the constructs, e.g. through cultivation in perfusion reactors or by development of cell carriers with modified pore size and pore structure [25,26]. Furthermore, the engineering of smaller constructs may prove beneficial. By exhibiting a larger surface to volume ratio, more cells are in direct

contact with the culture medium and, thus, are likely to develop into larger coherent tissue structures relative to the overall construct volume.

In summary, engineered fat-like constructs were shown to exhibit typical adipose tissue characteristics, which were comparable to those of conventional 2-D cell culture. Nevertheless, die-punching of the constructs allowed for a more precise analysis of the results. Thereby, it could be assessed that the constructs consisted of well- and less-differentiated areas. By comparing adipocytes derived from high quality outer parts with fat-cells differentiated under 2-D conditions, a slight advantage could be revealed with respect to lipid accumulation and laminin-β1 expression. However, only the 3-D culture approach allowed for formation of a coherent tissue-like context. Until meeting the challenge of engineering homogenous fat equivalents, it is suggested that future experiments aimed at elucidating intrinsic adipose tissue properties will be conducted with separated outer parts, rather than entire constructs. Taking into consideration the above mentioned findings, significance for basic research was clearly demonstrated. Nevertheless, it must be noted that the histological cross-sections did not reveal unilocular signet-ring cells. As this lack may be attributed to insufficient cultivation time, future studies over prolonged periods of differentiation will be required and eventually contribute to improving the exhibition of fat-like characteristics.

References

1. Langer, R. and Vacanti, J. P. (1993). Tissue engineering. *Science* **260**, 920-926.

2. Martin, I., Vunjak-Novakovic, G., Yang, J., Langer, R., and Freed, L. E. (1999). Mammalian Chondrocytes Expanded in the Presence of Fibroblast Growth Factor 2 Maintain the Ability to Differentiate and Regenerate Three-Dimensional Cartilaginous Tissue. *Exp.Cell Res.* **253**, 681-688.

3. Murphy, C. L. and Sambanis, A. (2001). Effect of oxygen tension and alginate encapsulation on restoration of the differentiated phenotype of passaged chondrocytes. *Tissue Eng.* **7**, 791-803.

4. Mandrup, S., Loftus, T. M., MacDougald, O. A., Kuhajda, F. P., and Lane, M. D. (1997). Obese gene expression at in vivo levels by fat pads derived from s.c. implanted 3T3-F442A preadipocytes. *Proc.Natl.Acad.Sci.U.S.A.* **94**, 4300-4305.

5. Rosen, E. D. and Spiegelman, B. M. (2000). Molecular regulation of adipogenesis. *Annu.Rev.Cell Dev.Biol.* **16**, 145-171.

6. Fischbach, C., Seufert, J., Staiger, H., Hacker, M., Neubauer, M., Gopferich, A., and Blunk, T. (2003). 3-D *in vitro*-Model of Adipogenesis – Comparison of Culture Conditions. *Tissue Eng.* **in press**.

7. Abukawa, H., Terai, H., Hannouche, D., Vacanti, J. P., Kaban, L. B., and Troulis, M. J. (2003). Formation of a mandibular condyle in vitro by tissue engineering. *J.Oral Maxillofac.Surg.* **61**, 94-100.

8. Sikavitsas, V. I., Bancroft, G. N., and Mikos, A. G. (2002). Formation of three-dimensional cell/polymer constructs for bone tissue engineering in a spinner flask and a rotating wall vessel bioreactor. *J.Biomed.Mater.Res.* **62**, 136-148.

9. von Heimburg, D., Zachariah, S., Heschel, I., Kuhling, H., Schoof, H., Hafemann, B., and Pallua, N. (2001). Human preadipocytes seeded on freeze-dried collagen scaffolds investigated in vitro and in vivo. *Biomaterials* **22**, 429-438.

10. Hausman, G. J. (1981). Techniques for studying adipocytes. *Stain Technol.* **56**, 149-154.

11. Bachmeier, M. and Loffler, G. (1995). Influence of growth factors on growth and differentiation of 3T3-L1 preadipocytes in serum-free conditions. *Eur.J.Cell Biol.* **68**, 323-329.

12. Pairault, J. and Green, H. (1979). A study of the adipose conversion of suspended 3T3 cells by using glycerophosphate dehydrogenase as differentiation marker. *Proc.Natl.Acad.Sci.U.S.A.* **76**, 5138-5142.

13. Lowry, O. H., Rosebrough, N. J., Farr, A. L., and Randall, R. J. (1951). Protein measurement with the Folin phenol reagent. *J.Biol.Chem.* **193**, 265-275.

14. Gregoire, F. M., Smas, C. M., and Sul, H. S. (1998). Understanding adipocyte differentiation. *Physiol.Rev.* **78**, 783-809.

15. Niimi, T., Kumagai, C., Okano, M., and Kitagawa, Y. (1997). Differentiation-dependent expression of laminin-8 (alpha 4 beta 1 gamma 1) mRNAs in mouse 3T3-L1 adipocytes. *Matrix Biol.* **16**, 223-230.

16. Freed, L. E. and Vunjak-Novakovic, G. (1998). Culture of organized cell communities. *Adv.Drug Delivery Rev.* **33**, 15-30.

17. Calvo, J. C., Rodbard, D., Katki, A., Chernick, S., and Yanagishita, M. (1991). Differentiation of 3T3-L1 preadipocytes with 3-isobutyl-1-methylxanthine and dexamethasone stimulates cell-associated and soluble chondroitin 4-sulfate proteoglycans. *J.Biol.Chem.* **266**, 11237-11244.

18. Cassell, O. C. S., Hofer, S. O. P., Morrison, W. A., and Knight, K. R. (2002). Vascularisation of tissue-engineered grafts: the regulation of angiogenesis in reconstructive surgery and in disease states. *Br.J.Plast.Surg.* **55**, 603-610.

19. Smith, P. J., Wise, L. S., Berkowitz, R., Wan, C., and Rubin, C. S. (1988). Insulin-like growth factor-I is an essential regulator of the differentiation of 3T3-L1 adipocytes. *J.Biol.Chem.* **263**, 9402-9408.

20. Cowherd, R. M., Lyle, R. E., and McGehee, R. E., Jr. (1999). Molecular regulation of adipocyte differentiation. *Semin.Cell Dev.Biol.* **10**, 3-10.

21. Yuksel, E., Weinfeld, A. B., Cleek, R., Wamsley, S., Jensen, J., Boutros, S., Waugh, J. M., Shenaq, S. M., and Spira, M. (2000). Increased free fat-graft survival with the long-term, local delivery of insulin, insulin-like growth factor-I, and basic fibroblast growth factor by PLGA/PEG microspheres. *Plast.Reconstr.Surg.* **105**, 1712-1720.

22. Polverini, P. J. (2002). Angiogenesis in health and disease: insights into basic mechanisms and therapeutic opportunities. *J.Dent.Educ.* **66**, 962-975.

23. Gooch, K. J., Kwon, J. H., Blunk, T., Langer, R., Freed, L. E., and Vunjak-Novakovic, G. (2001). Effects of mixing intensity on tissue-engineered cartilage. *Biotechnol.Bioeng.* **72**, 402-407.

24. Bancroft, G. N., Sikavitsas, V. I., van den Dolder, J., Sheffield, T. L., Ambrose, C. G., Jansen, J. A., and Mikos, A. G. (2002). Fluid flow increases mineralized matrix deposition in 3D perfusion culture of marrow stromal osteoblasts in a dose-dependent manner. *Proc.Natl.Acad.Sci.U.S.A.* **99**, 12600-12605.

25. Freed, L. E. and Vunjak-Novakovic, G. (2000). Tissue engineering bioreactors. *In* "Principles of Tissue Engineering" (R. P. Lanza, R. Langer, and J. P. Vacanti, Eds.), Academic Press, San Diego.

26. Widmer, M. S. and Mikos, A. G. (1998). Fabrication of biodegradable polymer scaffolds for tissue engineering. *In* "Frontiers in tissue engineering" (C. W. Patrick, Jr., A. G. Mikos, and L. V. McIntire, Eds.), Elsevier Science Ltd., Oxford.

Chapter 5

Tissue Engineering Allows for Development of 3T3-L1 Cells into Fat Pads *in vitro* and *in vivo*

Claudia Fischbach[1], Thilo Spruß[2], Barbara Weiser[1],
Achim Göpferich[1], Torsten Blunk[1]

[1] Department of Pharmaceutical Technology, University of Regensburg, 93040 Regensburg, Germany

[2] Department of Pharmaceutical Chemistry, University of Regensburg, 93040 Regensburg, Germany

To be submitted to Exp. Cell Res.

Abstract

To develop therapeutic approaches for the prevention and treatment of obesity, a thorough understanding of adipose tissue development is required. Although the potentially large impact of cell-cell and cell-extracellular matrix interactions on adipogenesis still remains to be clarified, the presently used preadipocyte culture models lack a tissue-like context and are, therefore, unsuitable for addressing such interactions. Herein, we report that tissue engineering allows for the reorganization of the 3T3-L1 cell line into fat-like tissues that are histologically comparable to native fat. After cell-seeding of 3-D polymeric scaffolds, the resulting constructs were hormonally stimulated and differentiated for either 9, 21, or 35 days *in vitro*. Histological investigation revealed that only long-term culture yielded tissues exhibiting the typical composition of unilocular signet ring adipocytes enveloped by a basement membrane. Analysis of triglyceride storage strongly supported the microscopic observations. Despite apparent dissimilarities in tissue coherence, the constructs did not vary substantially with regard to gene expression (mRNA and protein level) and lipolysis. However, tissue formation did increase leptin secretion. *In vivo*, only the implantation of differentiated 3-D constructs was demonstrated to yield vascularized fat-pads.

This study demonstrated for the first time the development of 3T3-L1 into fat-pads *in vitro* and *in vivo*. The presented model system is suggested as a useful tool to address tissue-inherent interactions under both standardized *in vitro* and physiological conditions.

Introduction

Although obesity is known to represent a major risk factor for metabolically related disorders, such as cardiovascular diseases and type 2 diabetes mellitus, its prevalence has dramatically increased over the last decades [1-3]. Until a few years ago, adipose tissue was commonly viewed as a passive depot for the storage of energy and obesity was accepted to result from excess calorie storage when energy intake exceeds nutritional requirements. However, the link between the regulation of adipose tissue mass and metabolic syndromes remained elusive until it was discovered that adipose tissue additionally operates as an endocrine organ secreting a variety of signaling molecules [4,5]. Meanwhile, adipocytes are convincingly recognized to target physiological and pathological processes by releasing factors known to have an impact on immunological responses, vascular function, and appetite regulation [1]. Because there is increasing evidence that obesity is not only due to an increase in adipocyte cell size (hypertrophy) but also caused by *de novo* differentiation of adipocytes (hyperplasia) [6,7], many studies have been conducted with the aim of gaining thorough insight into how adipose conversion is regulated. By elucidating the factors and signaling pathways critical for adipose differentiation, they distinctly improved the existent knowledge. However, the mechanisms underlying adipogenesis are not fully clarified yet and, thus, require further examination. For instance, even though a few studies indicated a pivotal role for cell-cell and cell-extracellular matrix (ECM) interactions, the respective aspects have not yet been comprehensively addressed [1].

The use of 3T3-L1 cells, an extensively used model system for analysis of adipocyte differentiation *in vitro*, may prove beneficial to facilitate investigations into interactions among adipose cells and their ECM. Indeed, conventional 2-D cell culture of those cells does not feature the typical 3-D cell-cell and cell-ECM interactions present within real fat and, thus, only partly reflects physiological conditions. In order to enable studies on adipose tissue formation within an environment better resembling *in vivo* conditions, we recently established a 3-D model system consisting of 3T3-L1 cells and polyglycolic acid (PGA) polymeric fiber meshes [8]. By evaluating various tissue engineering strategies, we determined the appropriate culture conditions suitable for generating coherent fat-like constructs. The tissues accordingly developed were analyzed extensively and demonstrated typical characteristics of adipose tissue, e.g. triglyceride storage, appropriate adipocyte gene expression, and functionality. However, histological examination showed that they lacked large signet ring cells and, thus, only faintly resembled natural fat. Apparently, the time span investigated (9

days of differentiation) allowed for formation of the mature adipose phenotype, however, it was not adequate to complete cellular reorganization into appropriate tissue structures, which are necessary for addressing the tissue-inherent interactions. As the size of the adipocytes increases during triglyceride accumulation, the detection of undersized cells prompted us to presume that an insufficient cultivation period led to restriction of the fat cell size and, in turn, to the observed differences in tissue coherence.

Therefore, the focus of this study was to cultivate the cell-polymer constructs over prolonged periods of time to generate 3-D fat-like constructs consisting of unilocular signet ring cells *in vitro*. Subsequently, the correlation between the properties of the engineered tissues and the culture period were investigated. Finally, the tissue development under *in vivo* conditions was assessed. Specifically, adipose tissue constructs were generated *in vitro* and harvested at day 9, 21, and 35 after hormonal induction of adipogenesis. Afterwards, they were thoroughly analyzed in terms of appropriate adipose tissue formation. For this purpose, construct appearance was assessed macroscopically as well as by histological staining for cellularity and laminin, a characteristic component of the ECM synthesized by adipocytes. Furthermore, lipid accumulation was determined by measurement of intracellular triglyceride content and the activity of glycerol-3-phosphate dehydrogenase (GPDH). Appropriate gene expression was analyzed for various typical fat-cell genes by means of RT-PCR. Additionally, leptin, a peptide hormone secreted by mature adipocytes, was quantitatively investigated with ELISA. The functionality of the constructs cultivated for different periods was studied by investigating their lipolysis rates. To examine the development of the engineered tissues *in vivo*, they were implanted subcutaneously (s.c.) into nude mice. Until now, 3T3-L1 cells have not been shown to give rise to mature fat pads *in vivo* [9,10], in contrast to other preadipose cell lines such as 3T3-F442A. Because the previously reported studies were performed by s.c. injection of a 3T3-L1 single cell suspension, we aimed at investigating if the implantation of coherent 3T3-L1-polymer constructs exhibiting tissue-like interactions proves helpful and finally allows for reorganization into fat pads. For this purpose, the constructs were implanted and, subsequent to their excision, histologically investigated regarding adipose tissue formation.

Materials and methods

Materials:

3T3-L1 preadipocytes were obtained from ATCC (Manassas, VA, USA). DMEM, fetal bovine serum (FBS), and trypsin (1:250) were purchased from Biochrom KG Seromed (Berlin, Germany); phosphate buffered saline (PBS) and penicillin-streptomycin solution were from Life Technologies (Karlsruhe, Germany). MEM (alpha-modification), corticosterone, indomethacin, and oil red O were from Sigma-Aldrich (Deisenhofen, Germany). 3-isobutyl-1-methylxanthine (IBMX) was purchased from Serva Electrophoresis GmbH (Heidelberg, Germany). Insulin was kindly provided by Hoechst Marion Roussel (Frankfurt a. M., Germany). Cell culture materials were obtained from Sarstedt AG & Co. (Nuembrecht, Germany) and BD Biosciences Labware (Heidelberg, Germany). Polyglycolic acid (PGA) non-woven fiber meshes (12-14 µm fiber diameter; 96% porosity; 62 mg/cm^3 bulk density) were purchased from Albany Int. Research Co. (Mansfield, MA, USA). Scaffolds were prepared by die-punching into discs 5 mm in diameter and 2 mm thick. Spinner flasks were self-made.

Engineering of the cell-polymer constructs in vitro:

Development of the 3-D model system was performed as previously described [8]. Briefly, 3T3-L1 preadipocytes expanded in DMEM supplemented with 10% FBS, penicillin (100 U/ml), and streptomycin (0.1 mg/ml) were dynamically seeded onto PGA scaffolds in stirred spinner flasks. Thereby, each flask contained 8 scaffolds and 100 ml of a suspension with 16x10^6 cells, i.e., 2x10^6 cells per scaffold. Stirring for two days at 80 rpm allowed for cell attachment to the polymer fibers. Cell-polymer constructs were transferred into 6-well plates (one construct and 5 ml culture medium per well) and cultured in an incubator (37°C, 5% CO_2) dynamically on an orbital shaker at 50 rpm (Dunn Labortechnik GmbH; Asbach, Germany). Cultivation of the cell-seeded constructs was performed in MEM (alpha-modification) supplemented with 10% FBS, penicillin (100 U/ml), and streptomycin (0.1 mg/ml). Four days after seeding, adipogenesis was induced by adding 0.1 µM corticosterone, 0.5 mM IBMX, and 60 µM indomethacin to differentiation medium (MEM (alpha-modification), 5% FBS, 1 µM insulin, penicillin (100 U/ml), and streptomycin (0.1 mg/ml)) and referred to as day 0. After 2 days, the induction medium was replaced by

differentiation medium alone. Constructs were maintained under these conditions until day 9, 21, and 35 of adipogenesis, respectively. Finally, the generated tissues were harvested according to the specific requirements of each analytical method described below.

2-D cell culture:

For investigation of mRNA gene expression and leptin secretion, 3T3-L1 preadipocytes were cultivated in conventional 2-D cell culture for 9, 21, and 35 days after initiation of adipogenesis. For this purpose, the cells were plated in 6-well plates at a density of 5,000 cells per cm². Cultivation was performed in MEM (alpha-modification) supplemented with 10% FBS, penicillin (100 U/ml), and streptomycin (0.1 mg/ml). Four days after plating adipogenesis was hormonally induced as described above. Cells were maintained in differentiation medium until harvest.

Macroscopic and microscopic investigation of the generated tissues:

In order to macroscopically assess adipose tissue formation, the generated constructs were washed and fixed in 10% buffered formalin and then stained with oil red O as previously described [11]. Pictures were taken with a Panasonic F15 CCD video camera. For histological investigations, the fixed constructs were dehydrated, paraffin-embedded, and finally cut into sections of 5 µm. Due to lipid extraction from the cells caused by the use of organic solvents during dehydration, lipid storage was assessed by examining size of blank areas, which represented those spaces previously occupied by accumulated triglyceride droplets. To assess cellularity, the sections were routinely stained with hematoxylin and eosin (H&E) (Sigma-Aldrich; Deisenhofen, Germany). For detection of the ECM component laminin, the sections were immuno-stained with a rabbit anti-mouse laminin antibody (Novus Biologicals, Inc.; Littleton, CO, USA). For this purpose, endogenous peroxidase activity was blocked by incubation in 1% H_2O_2. After extensive rinsing, antigen retrieval was performed by pepsin digestion. To prevent non-specific antibody binding, sections were incubated with 5% normal horse serum (Vector Laboratories Inc.; Burlingame, CA, USA) in PBS. Subsequently, the primary antibody was applied at a dilution of 1:600 (in PBS with 5% horse serum) for 60 min at room temperature (RT). In control sections, the primary antibody was replaced by PBS with 5% normal horse serum. After washing with PBS, the sections were incubated with biotinylated horse anti-rabbit IgG antibody (1:100) (Vector Laboratories Inc.; Burlingame, CA, USA) for 30 min at RT. To form the streptavidin-biotin-peroxidase complex, the

Vectastain Elite ABC-Kit was used. Peroxidase localization was performed with the DAB Substrate Kit for Peroxidase. Both kits were obtained from Vector Laboratories Inc.; Burlingame, CA, USA. Finally, the sections were counter-stained with hematoxylin and mounted with DPX Mountant (Fluka, Biochemika; Taufkirchen, Germany).

Quantitative analysis of intracellular triglyceride (TG) accumulation:

The intracellular TG accumulation was quantified by measuring both the glycerol-3-phosphate dehydrogenase (GPDH) activity and the TC content. First, all cell-polymer constructs were washed with PBS. To measure GPDH activity, they were immersed in lysis buffer (50 mM Tris, 1 mM EDTA, 1 mM mercaptoethanol, pH 7.5) and sonicated with a digital sonifier. The GPDH assay was performed as described in the literature [12,13]. For analysis of the intracellular TG content, the constructs were placed into 0.5% thesit and sonicated. Subsequently, spectroscopic quantification of TG was performed using the enzyme coupled glycerol assay kit 337 (Sigma Diagnostics; Deisenhofen, Germany). Cytosolic protein concentration of all samples was determined after precipitation with trichloracetic acid using the Lowry assay [14]. GPDH activity and TG content were expressed as mU GPDH per mg protein and mg TG per mg protein, respectively.

Reverse transcription polymerase chain reaction (RT-PCR):

RT-PCR of cells (2-D and 3-D) cultivated for 9, 21, and 35 days was conducted as recently described [8]. In brief, mRNA isolation was performed with Trizol reagent (Invitrogen GmbH; Karlsruhe, Germany). First-strand cDNA was synthesized from total RNA by using random hexamers (Roche Diagnostics; Mannheim, Germany) and Superscript II RNase H- Reverse Transcriptase (Invitrogen GmbH; Karlsruhe, Germany). Subsequently, PCR was conducted with Sawady Taq-DNA-Polymerase (PeqLab; Erlangen, Germany). Thereby, the amplification was carried out using specific primers and appropriate conditions for each gene (Tab. 1). 18 S rRNA served as internal control. Reverse transcription and PCR were performed using a Mastercycler Gradient (Eppendorf AG; Hamburg, Germany). The PCR products were analyzed by electrophoresis with ethidium bromide containing agarose gels, followed by imaging and densitometric scanning of the resulting bands using a Kodak EDAS 290 (Fisher Scientific; Schwerte, Germany).

Table 1: Primer sequences and PCR conditions for the investigated genes
Oligonucleotide sequences of mouse forward (sense) and reverse (antisense) primers. Gene amplification was performed by PCR according to the specified annealing temperatures (AT) and number of cycles for each gene. The reaction conditions of one cycle were composed as follows: denaturation for 45 sec at 94°C, annealing for 45 sec at the indicated temperatures, and extension for 1 min at 72°C.

Gene	Forward and reverse primers of examined genes	AT (°C) / Cycles
PPARγ	5′-AAC CTG CAT CTC CAC CTT ATT ATT CTG A-3′ 5′-GAT GGC CAC CTC TTT GCT CTG CTC CTG-3′	60 / 35
GLUT-4	5′-CCC CGC TGG AAT GAG GTT TTT GAG GTG AT-3′ 5′-CAG ACA GGG GCC GAA GAT TGG GAG ACA GT-3′	61 / 35
beta3-AR	5′-CAG TGG TGG CGT GTA GGG GCA GAT-3′ 5′-CGG GTT GAA GGC GGA GTT GGC ATA G-3′	63 / 36
leptin	5′-GAC ACC AAA ACC CTC ATC AAG ACC-3′ 5′-GCA TTC AGG GCT AAC ATC CAA CT-3′	58,5 / 36
laminin-1β	5′-GCT GGA TCC GCT TGC AGC AGA GTG CAG CTG A-3′ 5′-CGC GAA TTC GCT AAG CAG GTG CTG TAA ACC G-3′	60 / 30
18 S	5′-TCA AGA ACG AAA GTC GGA GGT TCG-3′ 5′-TTA TTG CTC AAT CTC GGG TGG CTG-3′	60 / 22

Leptin quantification:

Leptin concentrations in cell culture media of 2-D cultivated cells and 3-D entire constructs were determined after days 9 and 35 using a sandwich ELISA for mouse leptin. To furthermore investigate the assumption that leptin may be retained within the constructs due to limited diffusion, sterile die-punching with a stainless-steel dermal punch 3 mm in diameter (Aesculap; Tuttlingen, Germany) was conducted in order to enlarge the surface in contact with the culture medium. Subsequently, the resulting parts were analyzed in terms of leptin release as well. After 2 days of incubation (day 9-11 and 35–37) media samples were taken and centrifuged to remove cell debris. The supernatants were frozen at –80°C until the Quantikine M immunoassay (R&D Systems; Wiesbaden, Germany) was performed.

Measurement of Lipolysis:

The lipolytic cell response of the constructs was assessed by measuring the amount of glycerol released into the incubation buffer under control conditions and subsequent to stimulation with 10 µM isoproterenol (Sigma-Aldrich; Deisenhofen, Germany). Briefly, on

day 9 and 35 after initiation of adipogenesis, the tissues were washed with serum-free medium and then maintained in the same medium for 2 h to avoid interference with serum factors. Subsequently, medium was replaced by PBS supplemented with 3% fatty acid-free bovine serum albumin (Sigma-Aldrich; Deisenhofen, Germany). After 1 h incubation, the conditioned buffer was frozen at –20°C until the enzyme coupled glycerol assay kit 337 (Sigma Diagnostics; Deisenhofen, Germany) was conducted.

In vivo study:

Blank control scaffolds and cell-polymer constructs (either undifferentiated or differentiated for 35 d), were implanted s.c. into the right flank of immunodeficient NMRI (nu/nu) mice randomly bred in the nude mouse laboratory at the University of Regensburg under pathogen-free conditions at 26°C, 70% relative humidity, and a 12 h light/dark cycle. The wound was closed with surgical clips and the animals were returned to the housing facility, where they had free access to food and water. Weighing was performed twice a week in order to check the sanitary constitution of the mice. After 1 and 3 weeks, the animals were sacrificed by cervical dislocation and the constructs, easily identifiable, were excised. Subsequently, fixation of the tissues was conducted for 15 min with 2.5% glutardialdehyde in PBS and, additionally, overnight in 10% buffered formalin. Afterwards, the fixed tissues were paraffin embedded and cut into 5 µm sections. Finally, the sections were stained for histological analysis according to the Masson and Goldner method modified by Jerusalem [15].

Statistical analysis:

Statistical significance was assessed by one-way analysis of variance ANOVA followed by Tukey post-hoc test (Software: SPSS 10.0 for Windows). The statistical significance level was set as indicated separately for each methodology.

Results

Determination of tissue properties:

In order to assess how the prolongation of culture time affects the properties of the adipose constructs, macroscopic and microscopic investigations were performed. Compared to blank control scaffolds, the macroscopic appearance of un-stained cell-polymer constructs

differentiated for 9, 21, and 35 days clearly indicated tissue formation (Fig. 1). Oil red O staining of the constructs further indicated that the generated tissues were composed of lipid containing cells (Fig. 1). Relative to day 9, the constructs cultivated for 21 days exhibited a smoother surface, which referred to the enhanced lipid content of the cells as indicated by a darker color of oil red O-stained constructs (Fig. 1). Between 21 and 35 days, the shrinking of the constructs was observed and was attributed to the degradation of the PGA scaffold occurring within an aqueous environment after app. 4 weeks (data not shown) (Fig. 1). Consequently, the cells lost their additional support and compacted to some extent. However, after doing so, the shape of the tissues remained stable (data not shown). In addition to their diminished size, the constructs cultivated for 35 days similarly exhibited a smooth surface and a dark oil red O-staining, as observed after 21 days.

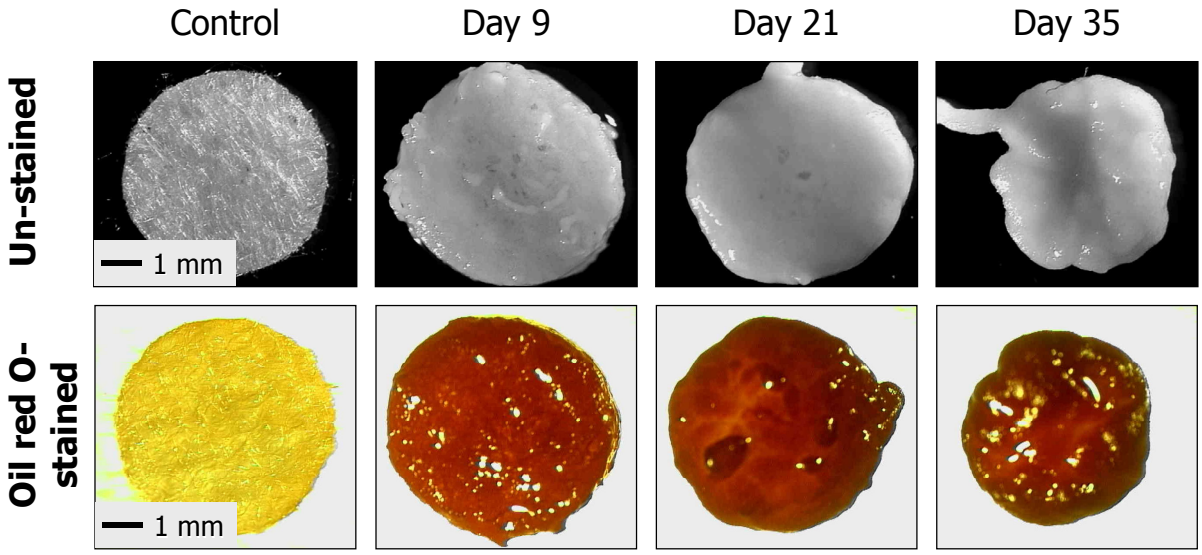

Fig. 1:
Macroscopic appearance of the cell-polymer constructs cultivated for different periods of time (9 days, 21 days, and 35 days) after induction of adipogenesis. The increased fat content of the engineered tissues was visualized by oil red O-staining. Scale bars represent 1 mm. Un-seeded, blank PGA scaffolds served as controls.

To investigate tissue coherence on the histological level, the sections were stained for cellularity and the ECM component laminin. H&E staining after 9 days of adipogenesis revealed that the tissues were composed of lipid containing cells supported by PGA polymer fibers (Fig. 2). However, the development of mature fat comparable to real adipose tissue could not be determined; due to less fat content, the observed adipocytes did not exhibit the typical signet ring form and their size was only app. 40% of the cell size detected in native fat from rats femora. At day 21, the tissues consisted of cells exhibiting both relatively small and

large lipid vacuoles (app. up to 70% of the cell size present in native fat) and of polymer fibers residues detected occasionally. Thereby, certain areas of the sections were assessed to rather resemble real fat, whereas others did not. However, substantial similarity could not be observed until 35 days subsequent to initiation of differentiation. At this time-point, the engineered constructs were comparable to real fat with regard to cellularity, adipocyte size, and tissue coherence in general (Fig. 2).

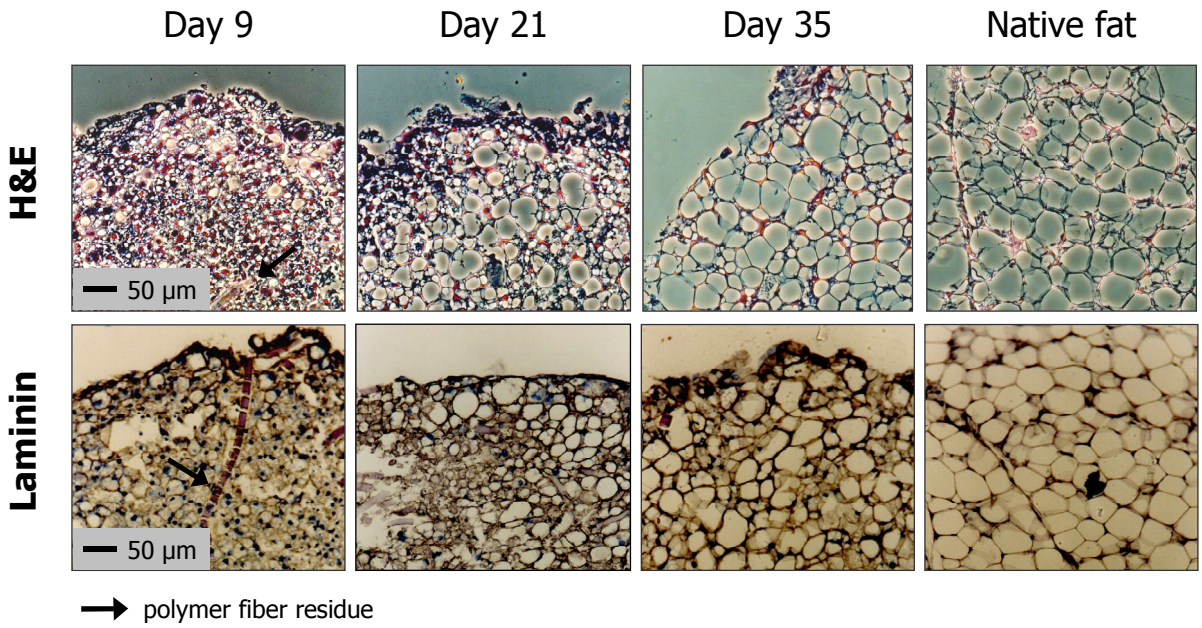

Fig. 2:
The histological composition of the generated tissues was analyzed at day 9, day 21, and day 35 of differentiation by hematoxylin & eosin (H&E) staining for cellularity and immuno-detection of the ECM component laminin. Blank spaces within the cells were caused by dissolving lipid inclusions with organic solvents during deparaffinization. With increasing culture time, the tissues were demonstrated to be more and more composed of unilocular signet ring cells and to increasingly exhibit the typical pattern of laminin staining comparable to native fat. Scale bars represent 50 µm. Native fat from rats is depicted for comparison.

As degradation of the PGA scaffolds occurred earlier, no remnants of polymer fibers were detectable in sections prepared at day 35 of construct differentiation. Analysis of laminin showed expression of the characteristic ECM protein at all time-points investigated. However, the staining intensity determined from samples harvested at day 21 and 35, respectively, was increased as compared to that observed at day 9 (Fig. 2). Furthermore, the typical staining pattern of a small rim around the adipocytes, characterizing the disposition of the laminin containing basement membrane, was exclusively detected at later time-points (day 21 and day 35).

Investigation of triglyceride (TG) storage:

With the aim of determining the extent of intracellular TG accumulation after 9, 21, and 35 days of differentiation, the constructs were analyzed with regard to the specific activity of GPDH, a key enzyme involved in TG biosynthesis, and their TG content. Thereby, the GPDH activity of the constructs measured at the respective time-points remained the same (Fig. 3). No significant differences were detected between day 9 (672.3±65.8 mU per mg protein), day 21 (624.2±50.3 mU per mg protein), and day 35 (643.7±12.4 mU per mg protein). In contrast, intracellular TG content remarkably increased over time (Fig. 3). Between day 9 (31.4±4.0 mg per mg protein) and day 21 (44.0±5.2 mg per mg protein) of adipogenesis, already a significant rise in accumulated TG ($p < 0.05$) was measured. Until the harvest of the constructs at day 35 after differentiation, substantially ($p < 0.01$) more TG (177.1±5.9 mg/mg protein) was stored within the cells as compared to those harvested on either day 9 or 21. These findings were in good accordance with the observed alterations in macroscopic and histological tissue consistence (Fig. 2).

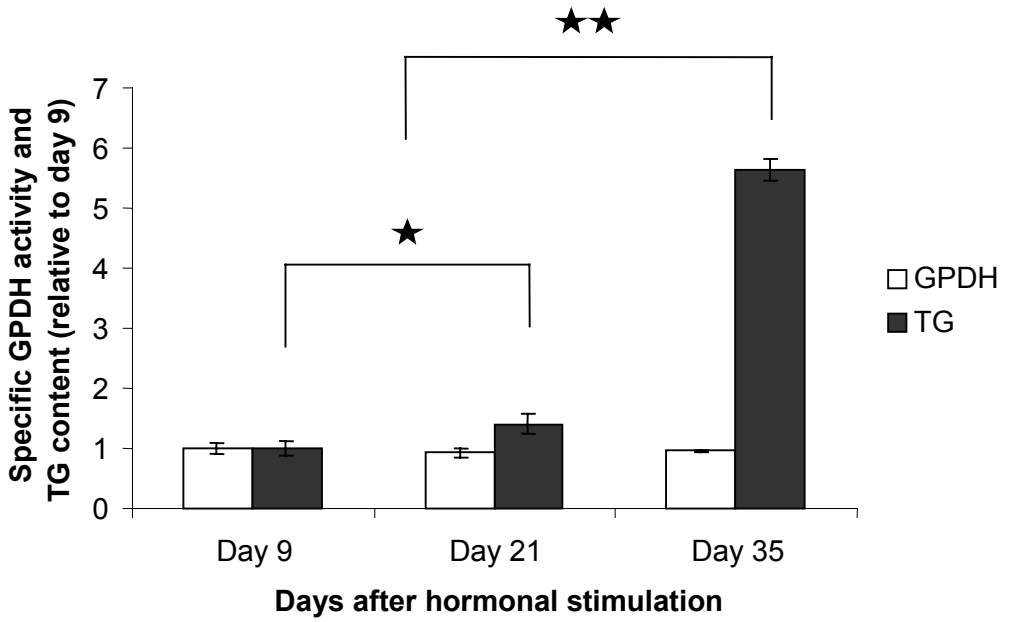

Fig. 3:
TG storage of the cell-polymer constructs differentiated for 9 days, 21 days, and 35 days. Whereas GPDH activity, which reflects the rate of TG biosynthesis, did not change significantly, the intracellular TG content was shown to be augmented with increasing time of cultivation. Data represent the mean ± SD of three constructs. Statistically significant differences are denoted by ★ ($p < 0.05$) and ★★ ($p < 0.01$). Absolute values at day 9 were 672.3 ± 65.8 mU GPDH activity per mg protein and 31.4 ± 4.0 mg TG per mg protein. Three independent experiments were conducted, representative results of one experiment are shown here.

Gene expression of adipocytes cultivated for prolonged periods of time:

To elucidate if the macroscopically and microscopically detected alterations in construct coherence, caused through extended culture time, are accompanied by changes in cellular mRNA gene expression, RT-PCR of various fat-cell genes was performed. Furthermore, we investigated gene expression of adipocytes conventionally cultured in 2-D in order to determine potential differences between cells situated within a tissue-like context and those maintained under conventional 2-D conditions. For the transcription factor PPARγ, the glucose transporter Glut-4, and the satiety hormone leptin, no difference in mRNA gene expression could be detected; neither for adipocytes cultivated for different periods of time (9, 21, and 35 days) nor between cells differentiated in 2-D cell culture or under 3-D conditions (Fig. 4). In contrast, analysis of the adrenoreceptor β3 revealed an increase of mRNA levels at day 21 for both 2-D and 3-D cells, as compared to day 9 (Fig. 4).

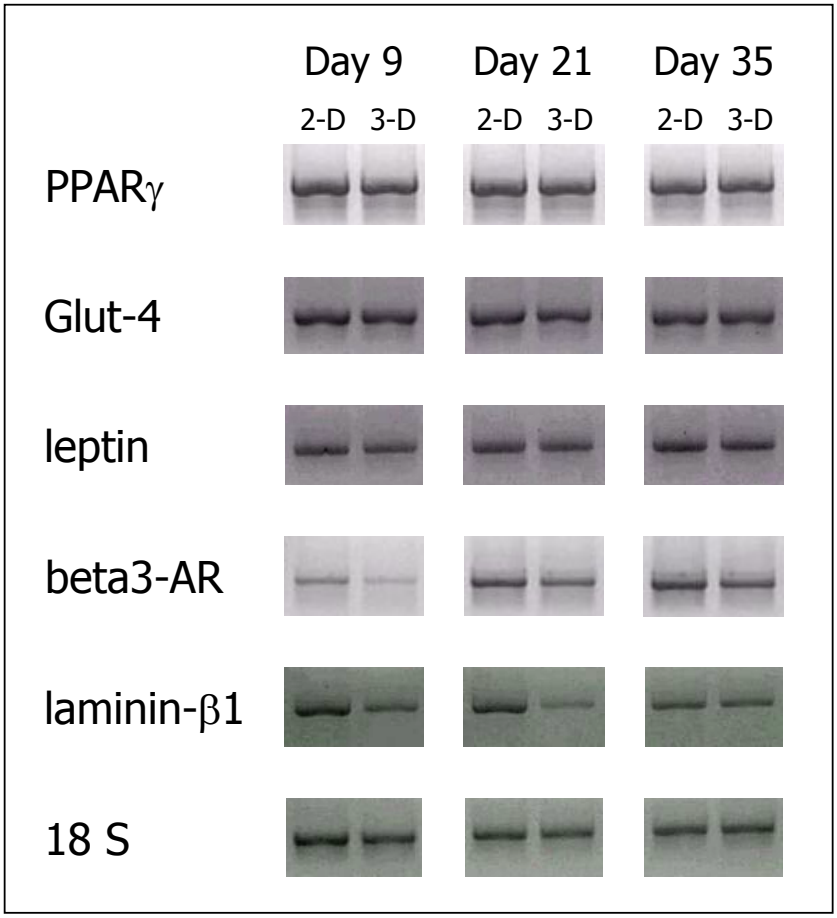

Fig. 4:
Gene expression of 3T3-L1 adipocytes cultivated in 2-D and 3-D cell culture as investigated by means of RT-PCR at day 9, day 21 and day 35 after hormonal stimulation. Examination of the characteristic fat cell genes PPARγ, Glut-4, leptin, beta3-adrenoreceptor, laminin-1β, and the internal standard 18S was performed in triplicate, one representative result is shown

here.

Between days 21 and 35, no further enhancement was determined. Furthermore, 2-D gene expression was slightly enhanced over 3-D at all points of time investigated. Expression of laminin-β1, a component of the basement membrane synthesized by 3T3-L1 adipocytes [16], was also augmented in 2-D adipocytes but, in contrast, it decreased with prolonged culture time for 2-D as well as for 3-D differentiated cells (Fig. 4). 18 S served as internal standard.

Investigation of leptin secretion:

Measurement of secreted leptin at day 11 did not reveal significant differences between cells cultivated in 2-D cell culture (53.5±10.0 ng per mg protein) or in the developed entire constructs (30.9±6.0 ng per mg protein) (Fig. 5). However, comparison of protein secretion of the divided parts (69.2±21.9 ng per mg protein) clarified a significant increase relative to that determined from entire constructs ($p < 0.05$). After 37 days again, cells either differentiated in 2-D cell culture (44.9±1.8 ng per mg protein) or in 3-D entire constructs (45.8±13.2 ng per mg protein) did not exhibit a significant difference. But the amount of leptin released from the die-punched parts (86.5±7.9 ng per mg protein), was significantly increased (approx. 2-fold) over those determined from both other groups – 2-D cells and entire constructs ($p < 0.01$) (Fig. 5). Comparison of the values determined after 11 days and 37 days of differentiation showed no significant variations.

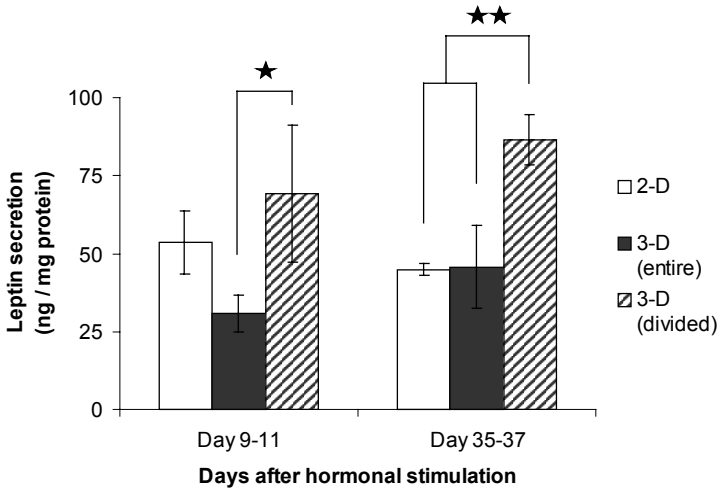

Fig. 5:
Impact of culture time on leptin secretion of 3T3-L1 adipocytes. To investigate if leptin is partially retained within the constructs, the release from constructs divided by die-punching was determined. Leptin was measured in the cell culture medium sampled after 2 days (day 9-11; day 35-37) by a mouse leptin ELISA. Values are expressed as mean ± SD (n=3). Statistically significant differences are indicated by ★ ($p < 0.05$) and ★★ ($p < 0.01$). Three independent

experiments were conducted, a representative result of one experiment is shown here.

Measurement of lipolysis:

Analysis of lipolysis was conducted by examining the amount of released glycerol under control conditions and subsequent to stimulation with 10 µM isoproterenol. Compared to un-stimulated samples (day 9: 1.75±0.11 mg per construct; day 35: 1.97±0.04 mg per construct), isoproterenol treatment led to a significant increase ($p < 0.01$) of released glycerol at both day 9 (3.4-fold) and day 35 (3.1-fold) (Fig. 6). As no differences were detected between lipolysis after 9 days and 35 days of differentiation, retained functionality of long-term constructs was demonstrated.

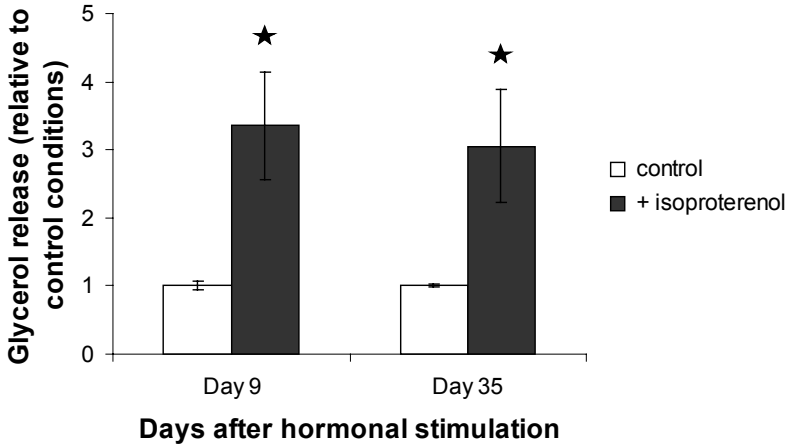

Fig. 6:
Lipolytic cell response of tissues cultivated for 9 days and 35 days after hormonal stimulation as determined by analysis of released glycerol under control conditions and subsequent to stimulation with 10 µM isoproterenol. Three independent experiments were performed. Data are expressed as mean ± SD (n=3) of one representative experiment. Statistically significant differences to control conditions ($p < 0.01$) are denoted by ★. Absolute values for control conditions were 1.75±0.11 mg glycerol per construct (day 9) and 1.97±0.04 mg glycerol per construct (day 35).

Development of the engineered tissues in vivo:

Blank PGA meshes, constructs seeded with un-differentiated preadipocytes, and cell-polymer constructs differentiated for 35 days were implanted into nude mice for the purpose of investigating their development *in vivo*. Excision of the tissues after 1 week revealed that explants from all investigated groups were infiltrated by fibroblasts and small blood vessels (Fig. 7). Removal of the tissues 3 weeks subsequent to implantation evidenced progressive

scaffold degradation by detection of abridged fiber remnants. The formation of adipose tissue occurred in neither the control group nor after implantation of preadipocyte-seeded scaffolds. In contrast, cells with intracellular lipid vacuoles were observed in samples, which were differentiated prior to implantation. In particular, engineered fat-like constructs differentiated for 35 days before implantation resulted in appropriate adipose tissue formation, as indicated by large, unilocular fat cells and neovascularization (Fig. 7).

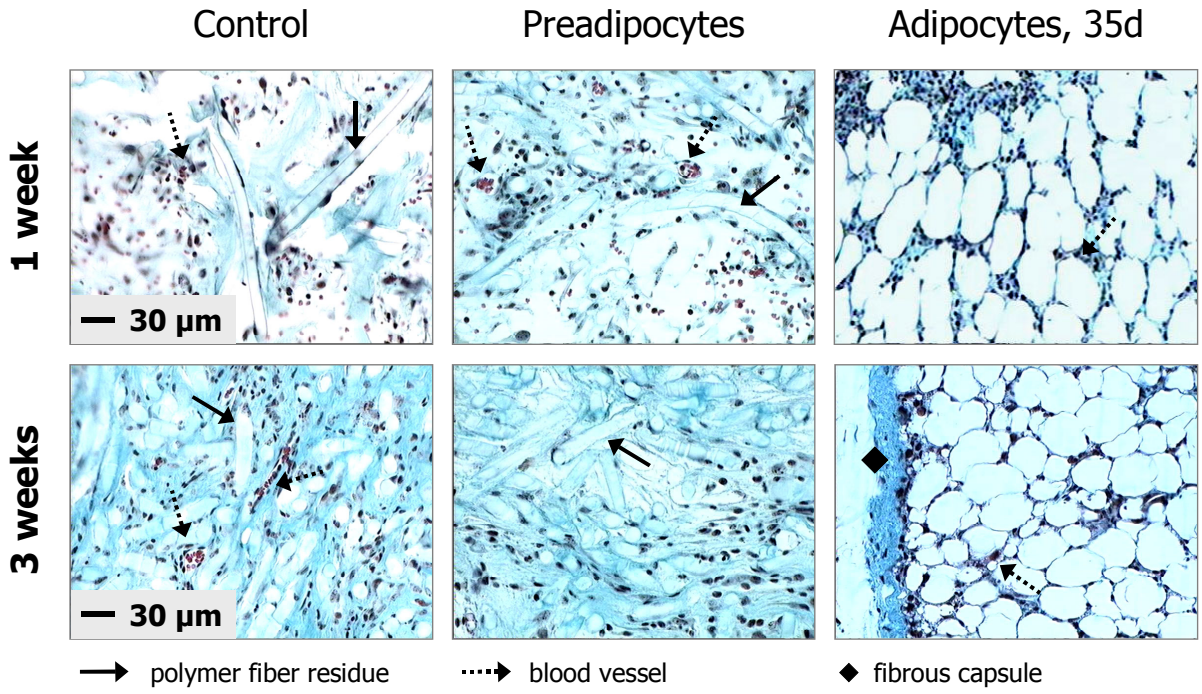

Fig. 7:
In vivo development of blank PGA meshes (control), constructs seeded with un-differentiated preadipocytes, and fat-like constructs (differentiated for 35 days) 1 week and 3 weeks after implantation into nude mice. Blank control scaffolds and preadipocyte-seeded constructs were invaded by fibroblasts and small blood vessels. However, appropriate adipose tissue development indicated by large unilocular fat cells and neovascularization was only observed for cell-polymer constructs, which had been differentiated prior to implantation. Due to the degradation of the PGA scaffold after app. 4 weeks, no polymer fiber residues were detectable in the latter group.

In order to investigate the integration of constructs that have not yet completed cellular reorganization, constructs differentiated for 9 days were implanted as well. Subsequent to excision, they were also shown to form adipose tissue, though, their development took longer and their appearance did not resemble that of native fat until 5 weeks after implantation (data not shown). Taken together, differentiation of 3T3-L1 prior to implantation is crucial for reorganization of these cells and finally allows for formation of fat pads *in vivo*.In general, the detection of polymer fiber residues, fibrous tissue capsules surrounding the explants, and large aneuploid cell nuclei, a characteristic of 3T3-L1 cells, evidenced that, in fact, the

implanted constructs were excised. No apparent polymer fiber remnants were visible in 35 d-differentiated constructs, because at the time-point of implantation scaffold degradation was already finalized which could be proven by histological sections analyzed from constructs cultivated *in vitro* (see data described above).

Discussion

For some years, obesity has been commonly acknowledged to be associated with differentiation of adipocyte precursors into fat cells and microenvironmental signals, such as cell-cell and cell-extracellular matrix (ECM) interactions, are generally accepted to decisively contribute to this process. However, only limited information is available regarding the specific 3-D interplay between cells and their ECM occurring within adipose tissue. In order to gain thorough insight into how these relations modulate adipocyte differentiation, it is essential to provide a microenvironment featuring typical properties of adipose tissue. The data of this study indicate that tissue engineering offers the potential to create an appropriate context approximating the physiological environment. For the first time, the development of a coherent fat-like tissue consisting of unilocular fat cells could be demonstrated *in vitro*. Furthermore, we showed that s.c. implantation of engineered 3-D 3T3-L1 constructs allows for their reorganization into vascularized fat pads *in vivo*.

Specifically, the focus of this study was to investigate, if the prolongation of culture time leads to completion of adipose tissue formation *in vitro*. For this purpose, the constructs were engineered as recently described using 3T3-L1 preadipocytes and PGA polymer fiber meshes [8]. To subsequently investigate the influence of different culture times on the fat-like characteristics of the tissues, the cell-polymer constructs were allowed to differentiate for a period of 9, 21, and 35 days. Macroscopic investigation of tissue coherence with and without oil red O staining revealed that the constructs first adopted the smooth and fatty appearance typical for adipose tissue after 21 days of differentiation (Fig. 1). However, on the histological level, only the tissues cultured for 35 days exhibited a tissue structure almost completely composed of unilocular signet ring cells and were, thus, comparable to native fat (Fig. 2). Our supposition that culture over 35 days enables the development of fat-like tissues could be supported by the characteristic laminin staining pattern of a thin rim around each cell, which is an essential part of the formation of an appropriate adipocyte basement membrane (Fig. 2). Shrinking of the tissues cultured for 35 days could be explained by degradation of the supporting polymer meshes occurring between day 21 and day 35. However, despite loosing their mechanical support from the polymer mesh, the created constructs were, upon gross

examination using forceps and scalpel, as firm and resistant as native pieces of fat tissue, indicating that a coherent tissue was formed and that the cells were held together by tissue-like interactions alone. The macroscopic and microscopic observation that prolonged culture time mediated an expansion of the intracellular lipid vacuoles was confirmed by quantitative analysis of intracellular triglyceride content. Although an increase was already measured between day 9 and day 21, the amount examined at day 35 was significantly enhanced as compared to earlier points of time (4-fold compared to day 21) (Fig. 3). This result well reflected the histological composition of the 35 day-constructs showing mature fat cells with large unilocular lipid vacuoles (Fig. 2). In contrast, the activity of GPDH, a key enzyme of triglyceride biosynthesis, remained stable over the whole course of the experiment, indicating that differences in TG content are attributable to factors other than GPDH (Fig. 3).

According to the literature, adipocytes develop a mature adipose phenotype after 4-6 days subsequent to initiation of differentiation [17]. Analysis of the characteristic fat cell genes PPARγ, Glut-4, and leptin on the mRNA level verified that the adipocytes featured a mature phenotype at all time-points investigated independent of culture conditions either in a tissue-like context or in conventional 2-D cell culture (Fig. 4). However, slight differences could be detected for the adrenoreceptor β3 and laminin-β1, a component of laminin-8 (α4, β1, γ1), the specific isoform synthesized by 3T3-L1 [16]. Expression of the ß3-AR was demonstrated to be up-regulated with increasing culture time (Fig. 4). As ß3-ARs have previously been shown to be essential for lipolytic response of adipocytes cultivated *in vitro* [18], an enhancement of the intracellular lipid storage possibly induced this rise. Furthermore, ß3-AR receptors are present on the cell surface, such that enlargement of the adipocyte membrane during culture time leads to a decrease in receptor density, which in turn may cause an up-regulation of the respective gene expression. The diminished expression of ß3-AR in 3-D relative to 2-D, have not yet been deduced. Decreased expression of laminin-β1 in 3-D, as compared to 2-D, may be explained by the tissue-like context retaining the protein and, thus, preventing its aspiration with every medium change (Fig. 4). Being in permanent contact with the ECM may lead to down-regulation of mRNA expression. After 35 days, 2-D cells also revealed diminished laminin-β1 expression, which may be also caused by partial retention of ECM. Determination of leptin, a protein only secreted by fully differentiated cells, additionally proved the mature adipose phenotype after 9 days and its maintenance during long-term culture until day 35. Comparison of protein secretion in 2-D and 3-D (entire constructs) did not elucidate any significant differences (Fig. 5). However, when investigating divided constructs, the measured concentration of secreted leptin was enhanced (2-fold)

relative to that determined from 2-D cells (day 35) and 3-D entire constructs (day 9 and 35), which may be attributed to the fact that leptin was partially retained within the entire constructs due to limited diffusion. This phenomenon does not occur in 2-D cell culture and, therefore, it seems reasonable to suspect that leptin expression on the protein level is increased in a tissue-like environment. A comparable observation has been made by Mandrup et al. [10], detecting strongly diminished leptin expression *in vitro* (conventional 2-D culture) as compared to *in vivo* conditions. Tissue-inherent factor(s) or conditions were cited as an explanation for this finding. Hence, the proposed model system may contribute to elucidate the respective events under standardized conditions *in vitro*

To finally examine the development of the engineered tissues *in vivo*, they were implanted s.c. into nude mice. Thereby, it could be shown that it is essential to differentiate the constructs prior to insertion. Whereas blank control meshes and preadipocyte-seeded scaffolds did not result in adipose tissue formation *in vivo*, 3T3-L1 cell-polymer constructs differentiated before implantation were demonstrated for the first time to yield fat pads *in vivo* histologically comparable to native fat (Fig. 7). The infiltration of blood vessels furthermore showed neovascularization of the implants. Accordingly, it could be clarified that in contrast to the injection of a single cell suspension [10], 3T3-L1 cells are capable of giving rise to vascularized fat pads *in vivo* when implanted in the form of differentiated tissue-like constructs.

To conclude, the formation of coherent tissues histologically comparable to native fat was shown *in vitro* after long-term culture of 35 days and *in vivo* after implantation of differentiated constructs. Although the *in vitro* cultivated constructs exhibited a mature adipocyte phenotype already at day 9 and day 21 of differentiation, appropriate tissue formation could not be observed until after 35 days. The developed fat-like model system offers the valuable option of investigating specific questions under well-defined conditions *in vitro* and, in parallel, to use the same constructs for performing *in vivo* studies. Thereby, the correlation of the results determined under both *in vitro* and *in vivo* conditions may be enabled. Specifically, adipose tissue formation can be investigated isolated from other cell types *in vitro*, but after implantation further aspects mediated by the *in vivo* context can be evaluated as well, e.g. the impact of substances secreted by endothelial cells. These kinds of experiments may especially help to define potential reasons for diminished leptin expression in conventional 2-D cell culture as compared to *in vivo* conditions [10].

Furthermore, the model system could be utilized to contribute to the elucidation of 3-D cell-cell and cell-ECM interactions underlying the formation of adipose tissue and thus, to

participate in clarifying potential causes of obesity. In particular, it provides a tool to comprehensively investigate the ECM remodeling crucial for appropriate adipose differentiation. It has been reported that inappropriate modulation leads to the suppression of 3T3-L1 differentiation, e.g. by impairing adipogenic signaling or by interfering with cytoskeletal and morphological changes known to be essential for adipose conversion [19-21]. Alterations in the composition and structural organization of ECM are mediated in part by proteolytic activity of distinct matrix metalloproteinases (MMPs). MMPs furthermore contribute to the regulation of adipose differentiation by releasing matrix-bound growth factors (e.g TGF-β) or by altering the activity and availability of various cytokines, hormones, and growth factors (e.g. IGF-1) [22]. Due to their effect on the integrity and function of the ECM, these enzymes are meanwhile recognized as novel modulators of adipogenesis. Although they are known to be differentially expressed during adipogenesis [23-25], their role in obesity-related adipose tissue formation remains to be clarified more in detail. As the proposed 3-D model of fat provides a tissue-like context histologically comparable to real fat, it will presumably prove useful in addressing the actions of MMPs and other modulators of adipogenesis.

In conclusion, for the first time we demonstrated that application of tissue engineering strategies facilitates 3T3-L1 cells to develop into fat-pads *in vitro* as well as *in vivo*. In future studies, the fat-like constructs are suggested for use as model systems suitable for investigating adipose tissue-inherent interactions under both standardized conditions *in vitro* and physiological settings *in vivo*. In particular, the model will be of use for addressing interactions between cells and ECM, as well as interactions between adipocytes and other cell types, e.g. endothelial cells and, thus, may contribute to the elucidation of tissue-derived factors influencing, for instance, expression of secretory factors such as leptin.

References

1. Gregoire, F. M., Smas, C. M., and Sul, H. S. (1998). Understanding adipocyte differentiation. *Physiol.Rev.* **78**, 783-809.

2. Kopelman, P. G. (2000). Obesity as a medical problem. *Nature* **404**, 635-643.

3. Arner, P. (2003). The adipocyte in insulin resistance: key molecules and the impact of the thiazolidinediones. *Trends Endocrinol.Metab.* **14**, 137-145.

4. Morrison, R. F. and Farmer, S. R. (1999). Insights into the transcriptional control of adipocyte differentiation. *J.Cell.Biochem.* **76 Supplement 32/33**, 59-67.

5. Diamond, F. B., Jr. and Eichler, D. C. (2002). Leptin and the adipocyte endocrine system. *Crit.Rev.Clin.Lab.Sci.* **39**, 499-525.

6. Rosen, E. D. and Spiegelman, B. M. (2000). Molecular regulation of adipogenesis. *Annu.Rev.Cell Dev.Biol.* **16**, 145-171.

7. Gregoire, F. M. (2001). Adipocyte differentiation: from fibroblast to endocrine cell. *Exp.Biol.Med.(Maywood)* **226**, 997-1002.

8. Fischbach, C., Seufert, J., Staiger, H., Hacker, M., Neubauer, M., Gopferich, A., and Blunk, T. (2003). 3-D *in vitro*-Model of Adipogenesis – Comparison of Culture Conditions. *Tissue Eng.* **in press**.

9. Green, H. and Kehinde, O. (1979). Formation of normally differentiated subcutaneous fat pads by an established preadipose cell line. *J.Cell.Physiol.* **101**, 169-171.

10. Mandrup, S., Loftus, T. M., MacDougald, O. A., Kuhajda, F. P., and Lane, M. D. (1997). Obese gene expression at in vivo levels by fat pads derived from s.c. implanted 3T3-F442A preadipocytes. *Proc.Natl.Acad.Sci.U.S.A.* **94**, 4300-4305.

11. Hausman, G. J. (1981). Techniques for studying adipocytes. *Stain Technol.* **56**, 149-154.

12. Bachmeier, M. and Loffler, G. (1995). Influence of growth factors on growth and differentiation of 3T3-L1 preadipocytes in serum-free conditions. *Eur.J.Cell Biol.* **68**, 323-329.

13. Pairault, J. and Green, H. (1979). A study of the adipose conversion of suspended 3T3 cells by using glycerophosphate dehydrogenase as differentiation marker. *Proc.Natl.Acad.Sci.U.S.A.* **76**, 5138-5142.

14. Lowry, O. H., Rosebrough, N. J., Farr, A. L., and Randall, R. J. (1951). Protein measurement with the Folin phenol reagent. *J.Biol.Chem.* **193**, 265-275.

15. Romeis Benno (1989). Faerbung des kollagenen Bindegewebes. *In* "Romeis Mikroskopische Technik" (Boeck Peter, Ed.), Urban und Schwarzenberg, Muenchen.

16. Niimi, T., Kumagai, C., Okano, M., and Kitagawa, Y. (1997). Differentiation-dependent expression of laminin-8 (alpha 4 beta 1 gamma 1) mRNAs in mouse 3T3-L1 adipocytes. *Matrix Biol.* **16**, 223-230.

17. Rosen, E. D., Walkey, C. J., Puigserver, P., and Spiegelman, B. M. (2000). Transcriptional regulation of adipogenesis. *Genes Dev.* **14**, 1293-1307.

18. Preitner, F., Muzzin, P., Revelli, J. P., Seydoux, J., Galitzky, J., Berlan, M., Lafontan, M., and Giacobino, J. P. (1998). Metabolic response to various beta-adrenoceptor agonists in beta3-adrenoceptor knockout mice: evidence for a new beta-adrenergic receptor in brown adipose tissue. *Br.J.Pharmacol.* **124**, 1684-1688.

19. Gagnon, A. M., Chabot, J., Pardasani, D., and Sorisky, A. (1998). Extracellular matrix induced by TGFbeta impairs insulin signal transduction in 3T3-L1 preadipose cells. *J.Cell.Physiol.* **175**, 370-378.

20. Mondal, D., Larussa, V. F., and Agrawal, K. C. (2001). Synergistic antiadipogenic effects of HIV type 1 protease inhibitors with tumor necrosis factor alpha: suppression of extracellular insulin action mediated by extracellular matrix-degrading proteases. *AIDS Res.Hum.Retroviruses* **17**, 1569-1584.

21. Spiegelman, B. M. and Ginty, C. A. (1983). Fibronectin modulation of cell shape and lipogenic gene expression in 3T3-adipocytes. *Cell* **35**, 657-666.

22. Sternlicht, M. D. and Werb, Z. (2001). How matrix metalloproteinases regulate cell behavior. *Annu.Rev.Cell Dev.Biol.* **17**, 463-516.

23. Chavey, C., Mari, B., Monthouel, M. N., Bonnafous, S., Anglard, P., Van Obberghen, E., and Tartare-Deckert, S. (2003). Matrix Metalloproteinases Are Differentially Expressed in Adipose Tissue during Obesity and Modulate Adipocyte Differentiation. *J.Biol.Chem.* **278**, 11888-11896.

24. Croissandeau, G., Chretien, M., and Mbikay, M. (2002). Involvement of matrix metalloproteinases in the adipose conversion of 3T3-L1 preadipocytes. *Biochem.J.* **364**, 739-746.

25. Alexander, C. M., Selvarajan, S., Mudgett, J., and Werb, Z. (2001). Stromelysin-1 regulates adipogenesis during mammary gland involution. *J.Cell.Biol.* **152**, 693-703.

Chapter 6

Does UV Irradiation Affect Polymer Properties Relevant to Tissue Engineering?

Claudia Fischbach[1], Jörg Tessmar[1], Andrea Lucke[1], Edith Schnell[2], Georg Schmeer[2], Torsten Blunk[1], Achim Göpferich[1]

[1] Department of Pharmaceutical Technology, University of Regensburg, 93040 Regensburg, Germany

[2] Department of Physical and Theoretical Chemistry, University of Regensburg, 93040 Regensburg, Germany

Surf. Sci. 491 (2001), pp. 333-345

Abstract

For most tissue engineering approaches aiming at the repair or generation of living tissues, the interaction of cells and polymeric biomaterials is of paramount importance. Prior to contact with cells or tissues, biomaterials have to be sterilized. However, many sterilization procedures such as steam autoclave or heat sterilization are known to strongly affect polymer properties. UV irradiation is used as an alternative sterilization method in many tissue engineering laboratories on a routine basis, however, potential alterations of polymer properties have not been extensively considered.

In this study we investigated the effects of UV irradiation on spin-cast films made from biodegradable poly(D,L-lactic acid)-poly(ethylene glycol)-monomethyl ether diblock copolymers (Me.PEG-PLA) which have recently been developed for controlled cell-biomaterial interaction. After 2 hours of UV irradiation, which is sufficient for sterilization, no alterations in cell adhesion to polymer films were detected, as demonstrated with 3T3-L1 preadipocytes. This correlated with unchanged film topography and molecular weight distribution. However, extended UV irradiation for 5-24 hours elicited drastic responses regarding Me.PEG-PLA polymer properties and interactions with biological elements: Large increases in unspecific protein adsorption and subsequent cell adhesion were observed. Changes in polymer surface properties could be correlated with the observed alterations in cell/protein-polymer interactions. AFM analysis of polymer films revealed a marked "smoothing" of the polymer surface after UV irradiation. Investigations using GPC, ^{1}H-NMR, mass spectrometry, and a PEG-specific colorimetric assay demonstrated that polymer film composition was time-dependently affected by exposure to UV irradiation, i.e., that large amounts of PEG were lost from the copolymer surface.

The data indicates that sterilization using UV irradiation for 2 hours is an appropriate technique for the recently synthesized Me.PEG-PLA diblock copolymers. However, the study also serves as an example that it is indispensable to control the duration of exposure to UV irradiation for a given biomaterial in order not to compromise polymer properties relevant to tissue engineering purposes.

Introduction

Biodegradable polymers such as poly(α-hydroxyesters) are well established biomaterials in the field of tissue engineering. Their use as membrane or scaffold material providing 2-D and 3-D matrices for cell adhesion and subsequent development of transplantable tissues is commonly acknowledged [1]. A major challenge in guided tissue regeneration is to control the interactions between polymeric carrier and cells [2]. Polymer bulk and surface properties, e.g., chemical composition, hydrophobicity, and topography, determine cell adhesion [3-6] and may also influence cell differentiation [3], which in turn may decisively influence tissue development. A key prerequisite for the use of polymeric cell carriers both in vitro and in vivo is sterility. Therefore an effective and non-destructive sterilization method is needed that maintains the characteristics of the carrier. Because of the susceptibility of many biodegradable polymers to degradation and deformation of highly porous polymer scaffolds at high temperature and pressure, steam autoclave and heat sterilization cannot be applied [7]. Ethylene oxide (ETO) or γ-irradiation are used for sterilization in some tissue engineering approaches, however, also with these methods significant changes in properties of biodegradable poly(α-hydroxyesters) such as degradation and shrinking have been observed [5,8]. Furthermore, the potential toxicity of residual ETO [9] has to be considered. An established alternative sterilization method is UV irradiation which is used in many tissue engineering laboratories. The treatment with UV light represents a simple and cheap but effective procedure [10]. However, UV light has also been reported to degrade polymers such as polyethylene or polypropylene [11,12]. Therefore, it appears logical to test polymers and cell carriers for their susceptibility to changes in polymer properties generated by exposure to UV irradiation.

Previously, in an approach to control cell-polymer interactions we have synthesized a range of biocompatible, biodegradable diblock copolymers consisting of a hydrophilic, water-soluble poly(ethylene glycol)-monomethyl ether (Me.PEG) block and a hydrophobic, biodegradable poly(D, L-lactic acid) (PLA) block (Me.PEGx-PLAy) [13]. It was demonstrated that increasing PEG content reduced unspecific protein adsorption from culture medium and subsequently resulted in decreased unspecific cell adhesion and a shift in cell morphology from a spreaded to a more rounded cell shape [3]. Furthermore, changes in copolymer composition showed an additional impact on cell differentiation of rat marrow stromal cells towards the osteogenic lineage [3]. The composition of copolymers could even

be altered in such a way that cell adhesion on polymeric membranes was completely suppressed [3], which may be used in certain tissue engineering applications. Additionally, their protein adsorption-reducing properties may make these polymers candidates for the use in controlled protein drug delivery, where unintentional protein adsorption to carrier material is a major obstacle [14,15]. For any of these applications, maintenance of surface properties is an indispensable prerequisite.

In this study, we investigated effects of UV sterilization on properties of Me.PEG-PLA diblock copolymers. For this purpose Me.PEG-PLA films were prepared and exposed to UV light for varying periods of time. Specifically, first we examined the effects on interactions of polymeric films with biological elements, i.e., cell adhesion and protein adsorption. Subsequently, effects on polymer film topography and copolymer composition, especially possible cleavage of PEG chains, were investigated in order to find possible causes for the observed alterations in interactions with the biological environment. The study was expected to shed more light on the suitability of UV irradiation as sterilization method for newly developed biomaterials without compromising relevant polymer properties.

Materials and methods

Materials:

Me.PEGx-PLAy diblock copolymers (Fig. 1) were synthesized and their composition and molecular weight were determined as previously described [13]. In case of these polymers, x and y represent the weight-average molecular weight (MW) in kDa of the Me.PEG and PLA block, respectively. Me.PEG5-PLA20, for example, consists of a Me.PEG block of MW 5,000 covalently bound to a PLA block of MW 20,000. The two different diblock copolymers used in this study were Me.PEG5-PLA20 and Me.PEG2-PLA20. Resomer R202 (PLA17), an endcapped poly(D,L-lactic acid) with equal amounts of D- and L-lactic acid units and MW 17,000 was a gift from Boehringer Ingelheim, Ingelheim, Germany. The water used for the investigations was double-distilled. All other chemicals were used in analytical grade or higher.

Fig. 1:
Structure of Me.PEGx-PLAy: m is the number of ethylene glycol units in Me.PEG, n is the number of lactic acid units of the PLA part of the copolymer.

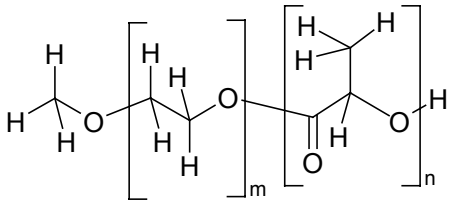

For investigation of cell adhesion 3T3-L1 preadipocytes were obtained from ATCC (American Type Culture Collection), Rockville, MD/USA. Stock cultures used for experiments were grown as described [16]. Newborn calf serum (NCS), Trypsin (1:250) and DMEM were purchased from Biochrom, Berlin, Germany; PBS and penicillin-streptomycin solution were from Gibco, Life Technologies, Karlsruhe, Germany. Cell culture materials were from Sarstedt, Nümbrecht, Germany, and Corning Costar, Bodenheim, Germany.

Manufacture and UV treatment of polymer films:

Thin polymer films were obtained by spin casting of polymer solutions on carriers of different materials (Table 1). The use of different film carriers was necessary due to the specific requirements of the different investigation techniques. With AFM, it could be shown that the surface structure of the polymer films were not affected by the different carrier materials.

Table 1: Manufacture of polymer films
Carriers for polymer films used for the different investigations and amounts of spin cast polymer solution to give films with equivalent polymer/surface ratio.

carrier	size	polymer solution	investigations
polypropylene disks	13 mm ∅	50 µl	cell adhesion
glass cover slips	18 x 18 mm^2	70 µl	GPC, ^{1}H-NMR
V2A steel disks	10 x 10 mm^2	70 µl	XPS
V2A steel disks	18 mm ∅	90 µl	AFM

The polymer solutions were obtained by dissolving 50 mg of the polymer in 1 ml of methylene chloride and the solutions were cast on the disks fixed on a platform rotating at 1,950 rpm. Different amounts of the polymer solutions had to be cast on the different carriers to give films of equivalent polymer/surface ratio. For XPS investigations, spin casting was carried out under laminar air flow (UVF 6.12 S, BDK Luft- und Reinraumtechnik GmbH, Sonnenbuehl-Gengkingen, Germany) to avoid any surface contamination. In all other cases, the films were manufactured in a fume hood. The films were allowed to dry under ambient conditions for two hours, followed by at least 24 hours drying under vacuum at room temperature in a desiccator to remove residual solvent. During vacuum drying, the pressure

was kept below 0.1 mbar using a RV5 two stage vacuum pump from Edwards (Crawley, West Sussex, UK).

For UV treatment the polymer films were put under a 30 Watts mercury-vapor UV-C lamp (TUV 30 W LL, Philips Lighting B.V., Roosendaal, The Netherlands) integrated in the laminar air flow hood with a distance of 60 cm between films and lamp. The films were treated with UV light for either 2, 5, 10, 15 or 24 hours. Non-irradiated films were used as controls in all investigations.

Except for films used for cell adhesion experiments and for determination of polymer molecular weight, polymer films were washed by incubation with double-distilled water at 37 °C to remove water-soluble parts of the polymer after UV treatment. After 5 hours of incubation, the films were taken out of the water and frozen at –80 °C. Control films were treated the same way. Prior to further analysis, the films were freeze-dried over 24 h. For freeze-drying, the frozen polymer films were stored in a desiccator which was cooled with dry ice and evacuated using a RV5 two stage vacuum pump (Edwards, Crawley, West Sussex, UK). When the pressure was as low as 10^{-2} mbar after approximately 12-18 h of drying, the dry ice was removed and the drying continued with a pressure of 10^{-2} mbar until the desiccator had reached room temperature.

The solution resulting from the incubation of polymer films with water was used for the determination of water-soluble polymer fractions.

Investigation of cell adhesion:

Cell adhesion on untreated and UV treated polymer films was investigated by scanning electron microscopy (SEM) and cell counting. Polypropylene disks coated with polymer films before and after UV treatment were put in 12-well plates. For cell seeding stock cultures of preadipocytes (3T3-L1) were trypsinized and diluted with serum containing cell culture medium in such a way that for SEM investigations 160 µL of cell suspension contained 10,000 cells per cm^2, i.e., 13,300 cells/film and for cell counting experiments 160 µL of cell suspension contained 5,000 cells per cm^2, i.e. 6,500 cells/film. The obtained suspension was applied to polymer films. The adhered cells were examined 5 h after seeding. For SEM, the adherent cells were fixed on the polymer films with glutardialdehyde and osmiumtetroxide and freeze-dried. The dried polymer films were glued to aluminium sample holders using Leit Tabs (Ted Pella Inc., Redding, CA, USA) and gold-sputtered for 4 minutes under argon atmosphere using a Polaron Automatic Sputter Coater E 5200 from Polaron Equipment Ltd.

(Watford, UK). The coated samples were analyzed using a JSM-840 Scanning Microscope from Jeol Ltd. (Tokyo, Japan). For cell counting the adherent cells were fixed on the polymer films with formaldehyde and then counted on photographs of 5 representative areas on each film. At least 4 films were counted for each experimental group. Statistical analysis was done by ANOVA followed by Tukey post-hoc test (Software: SPSS 10.0 for Windows). The statistical significance level was set at $p<0.05$.

Investigation of protein adsorption (XPS):

Protein adsorption to washed and freeze-dried polymer films before and after UV treatment was investigated by incubation of polymer films with a 10 % solution of newborn calf serum (NCS) in double-distilled water, the same concentration as in cell culture experiments. Polymer films were incubated with the NCS solution for 1 h, rinsed three times with water, frozen at –80 C, and freeze-dried over 24 h as describe above. The analysis of adsorbed protein on the surface of polymer films was carried out by XPS.

The surface composition of polymer films was determined by X-ray photoelectron spectroscopy (XPS) on a Phi 5600 XPS system from Physical Electronics, Ismaning, Germany, using an $Al_{K\alpha}$ source. For each sample, a survey scan was performed using $Al_{K\alpha}$ radiation (1,486.6 eV), with a step size of 0.8 eV and with the sample at 45° to the electron beam to detect the elements present in the polymer surface. Data were analyzed with the Phi PC software package provided by the manufacturer. The presence of nitrogen on the polymer surface content indicated the presence of adsorbed protein as the polymers themselves contain no nitrogen.

Determination of polymer surface topography (AFM):

The topography of the freeze-dried polymer films before and after UV treatment was investigated by atomic force microscopy (AFM) with an Autoprobe CP (Park Scientific Instruments, Sunnyvale, CA) including a hardware corrected scanner with 100 µm maximum lateral and 7.5 µm vertical scanning range. At a scan rate of 0.5 to 1.0 line per second, measurements were performed in intermittent contact mode using boron doped Ultralevers (Park Scientific Instruments, Sunnyvale, CA) with a nominal force constant of 3.2 N/m at the resonant frequency of approximately 90 kHz. The surface was investigated at 20 °C using a peltier element between scanner and sample. Under the chosen conditions, the observed

features were stable in all four scanning directions as well as during multiple scans and at varying scan sizes. Cantilevers and parameters were checked for proper function by scanning the surface of a cover slide. Lateral calibrations were performed on a 1 µm gold grating. All images represent topographic data which were obtained from the z-position of the scanner controlled by the z-scanner feedback loop at a gain of 0.25 to 0.75 arbitrary units. The raw data were reprocessed with the PSI ProScan Image Processing software package (Park Scientific Instruments, Sunnyvale, CA) before plotting, using plane-fit filters only.

Determination of polymer film composition (GPC):

The average molecular weights of the polymers were determined using gel permeation chromatography (GPC). A combination of two columns, a pre-column (Phenogel 5 µm, 50 x 7.8 mm) and an analytical column (Phenogel 100 Å, 5 µm, 300 x 7.8 mm, from Phenomenex, Torrance, CA), was used with chloroform as mobile phase (flux: 1.0 ml/min) thermostated at 35 °C in a 10AVP HPLC system (Shimadzu, Duisburg, Germany). In a typical GPC experiment, 10 polymer films of each experimental group were pooled in order to generate a sufficient signal. Films (not washed) were dissolved in 2 ml $CHCl_3$ and filtered through a chloroform resistant filter with a pore diameter of 0.2 µm (Spartan 30/A (regenerated nitrocellulose membrane) from Schleicher & Schuell, Dassel, Germany). 50 µl of each sample were injected and analyzed using a RID 10A refractive index detector (Shimadzu, Duisburg, Germany). The weight and number average molecular weights were calculated relative to the calibration with poly(ethylene glycol) molecular weight standards (Polymer Laboratories, Darmstadt, Germany) using the Class VP GPC software package included with Class VP 5.03 Software (Shimadzu, Duisburg, Germany). All GPC-investigations (polymer film composition and water-soluble polymer fraction) were done with the same analytical column in order to obtain comparable results for molecular weight calculation. It has to be taken into account that calculated molecular weights are extrapolated values relative to the used PEG standards. Nevertheless, the calculated polydispersity indices can be used as a semi-quantitative measure for peak broadening. The actual molecular weights were determined by ^{1}H-NMR which confirmed the expected values.

Determination of polymer film composition (^{1}H-NMR):

For the determination of changes in the polymer composition, ^{1}H-NMR spectra of the polymer films were obtained. Washed polymer films were dissolved in $CDCl_3$ and ^{1}H-NMR spectra were taken at 400.13 MHz with tetramethylsilane (TMS) as internal standard using a Bruker ARX400 spectrometer (Bruker, Rheinstetten, Germany). Special attention was paid that areas that contain peaks relevant to quantification were properly phased. The signal of the three chemically equivalent hydrogen atoms of the methyl ether at the end of the Me.PEG block is located at 3.4 ppm. Its integral is used as internal standard to calculate the number average ratio of the Me.PEG and PLA blocks in the polymer. ^{1}H-NMR spectra were analyzed with regard to PEG/PLA ratio of the polymer using Win-NMR 6.0 software (Bruker-Franzen, Rheinstetten, Germany).

Determination of water-soluble polymer fraction:

The water-soluble fraction (cleavage products) of the polymer before and after UV treatment was washed from polymer films as described above. The solution was used for determining the molecular weight distribution of the water-soluble fraction of the polymer by GPC. The solution was freeze-dried for 24 h and the freeze-dried residues were dissolved in 200 µl $CHCl_3$ and analyzed using the GPC system and settings described above. For comparison of the water-soluble polymer fraction with poly(ethylene glycol)-monomethyl ether (MW 5,000, from Sigma, Steinheim, Germany) (Me.PEG5), a solution of Me.PEG5 in $CHCl_3$ was prepared and analyzed using the same GPC system.

Additionally, the solution of the water-soluble fraction was analyzed for PEG content using a colorimetric assay after Baleux [17] and a mass spectrometer TSQ 7000 (Thermo-quest/Finnigan, San Jose, CA) with an electrospray ionization unit.

Results

For the study of the effects of UV irradiation on protein adsorption and subsequent cell adhesion Me.PEG5-PLA20 and Me.PEG2-PLA20 films were used. In order to investigate into the causes of these observed effects, exemplarily Me.PEG5-PLA20 was employed in a range of characterization methods to study potential changes in polymer properties after varying UV irradiation times.

Cell adhesion (SEM, Cell counting):

After 5 hours of incubation, 3T3-L1 preadipocytes readily adhered to PLA control films, many of them displaying a well spreaded morphology (Fig. 2a). UV irradiation for up to 24 hours did not affect cell adhesion on PLA films (Fig. 3). In drastic contrast, no cell adhesion at all was observed on non-irradiated Me.PEG2-PLA20 (Fig. 3) and Me.PEG5-PLA20 films (data not shown). Also, after 2 hours of UV irradiation and subsequent incubation with cell suspension, on both Me.PEG-PLA films no cell adhesion was detected (Figs. 2b, 3). However, exposure to UV light for 5, 10, and 24 hours led to increasing cell adhesion with time on both Me.PEG-PLA films. After 24 hours of irradiation, Me.PEG5-PLA20 displayed substantial cell adhesion (Fig. 2c), though still a lower cell number and less spreaded cells as compared to PLA films (Fig. 2a). Me.PEG2-PLA20, after 24 hours of UV irradiation (Figs. 2d, 3), exhibited a significantly ($p<0,05$) increased cell adhesion compared to 0-10h irradiated polymer films that was not distinguishable from that on PLA films (Figs. 2a, 3).

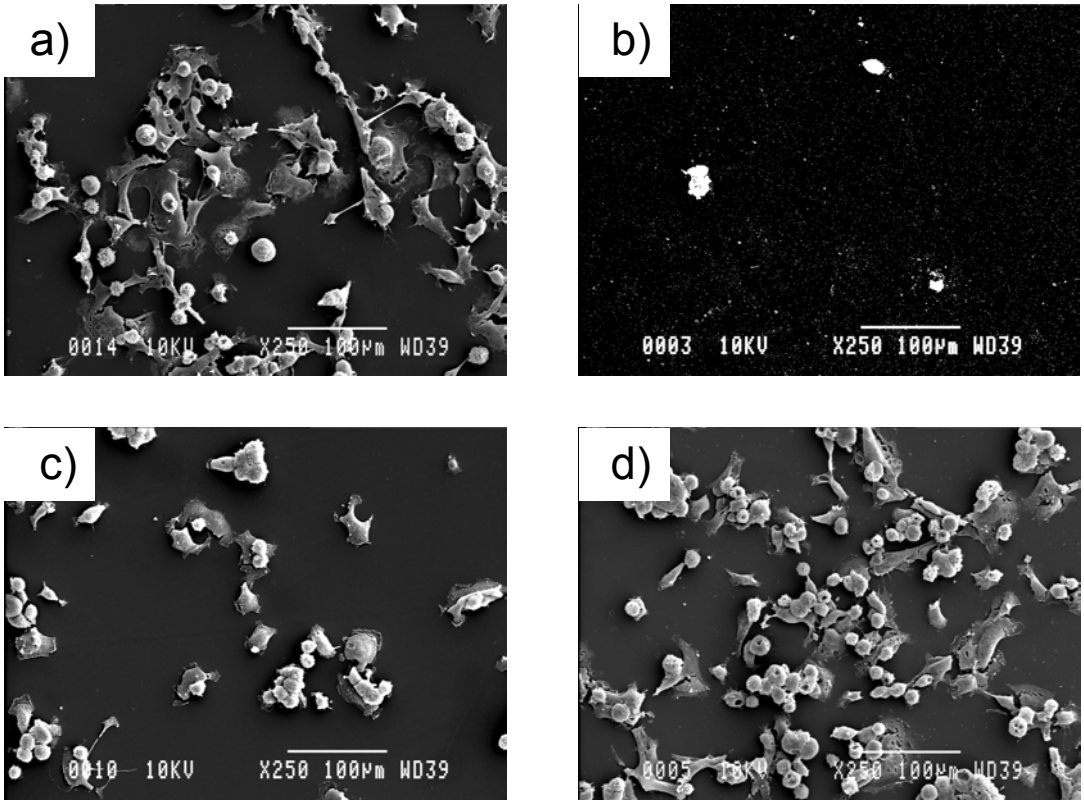

Fig. 2:
3T3-L1 preadipocyte adhesion behavior on different polymer surfaces visualized by scanning electron microscopy (original magnification x250): (a) PLA, 0h UV; (b) Me.PEG2-PLA20, 2h UV (exemplarily shown; no adhesion was also observed on non-irradiated Me.PEG2-PLA20, non-irradiated Me.PEG5-PLA20, and on 2h irradiated Me.PEG5-PLA20); (c) Me.PEG5-PLA20, 24h UV; (d) Me.PEG2-PLA20, 24h UV. Bars represent 100 µm.

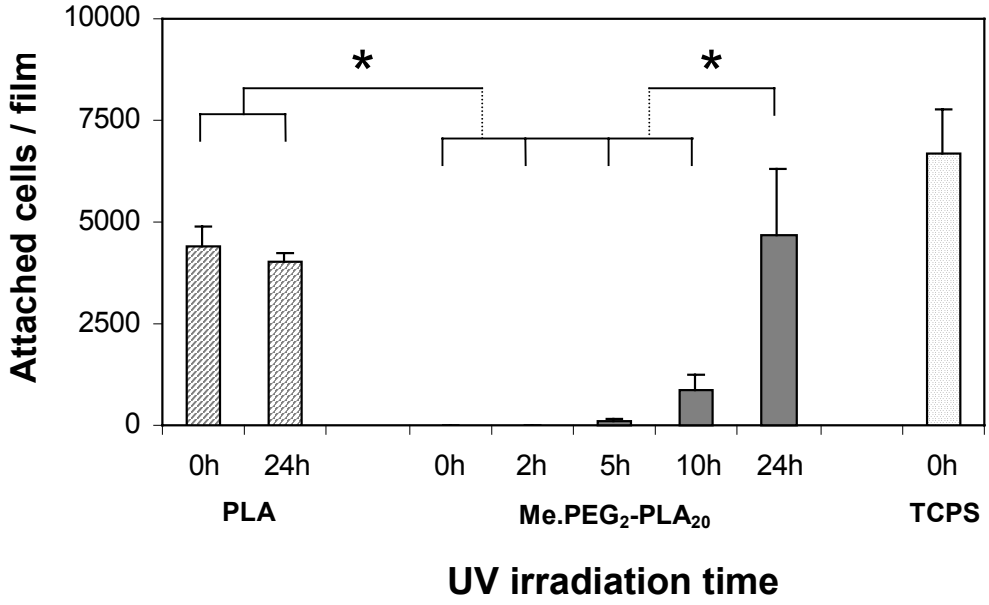

Fig. 3:
Number of attached 3T3-L1 preadipocytes on 0-24h UV irradiated polymer films. Films were incubated with a suspension of 6,500 cells/film. Four films per experimental group were counted, error bars represent the standard deviation; statistically significant differences ($p<0,05$) between groups are indicated by an asterisk. Between PLA (0h and 24h UV) and Me.PEG2-PLA20 (24h UV) no significant differences were detected. Untreated tissue culture polystyrene (TCPS) is shown as comparison.

Protein adsorption (XPS):

XPS was employed in order to analyze protein adsorption on polymeric films from a serum-containing solution. As the polymers themselves contain no nitrogen, the N_{1s} signal in the spectra at 398.1 eV could be taken as a semi-quantitative measure for adsorbed serum proteins. Both non-irradiated PEG-PLA films, Me.PEG2-PLA20 (Fig. Fig. 4a, Table 2) and Me.PEG5-PLA20 (Fig. 4c, Table 2), exhibited small amounts of adsorbed proteins, being hardly detectable on Me.PEG5-PLA20 (Fig 4c). UV irradiation for 24 hours resulted in marked increases of nitrogen peaks indicating increased protein adsorption on Me.PEG2-PLA20 films (Fig. 4b, Table 2) as well as on Me.PEG5-PLA20 (Fig. 4d, Table 2). Additionally, the carbon-to-oxygen ratio increased on both surfaces after irradiation (Table 2), which may also be attributed to increased protein adsorption (on average in proteins carbon content is higher than oxygen content).

Table 2: Protein adsorption on polymer films (XPS)
Carbon, oxygen, and nitrogen content of polymer film surfaces (non-irradiated or irradiated for 24 hours) from XPS survey scans after incubation with serum solution. As investigated polymers do not contain nitrogen, the nitrogen signal can be taken as a measure for protein adsorption.

Polymer	UV (h)	C [%]	O [%]	C/O	N [%]
Me.PEG2-PLA20	0	64.6	31.5	2.1	4.0
	24	66.2	25.4	2.6	8.4
Me.PEG5-PLA20	0	61.6	38.1	1.6	0.3
	24	64.2	29.2	2.2	6.7

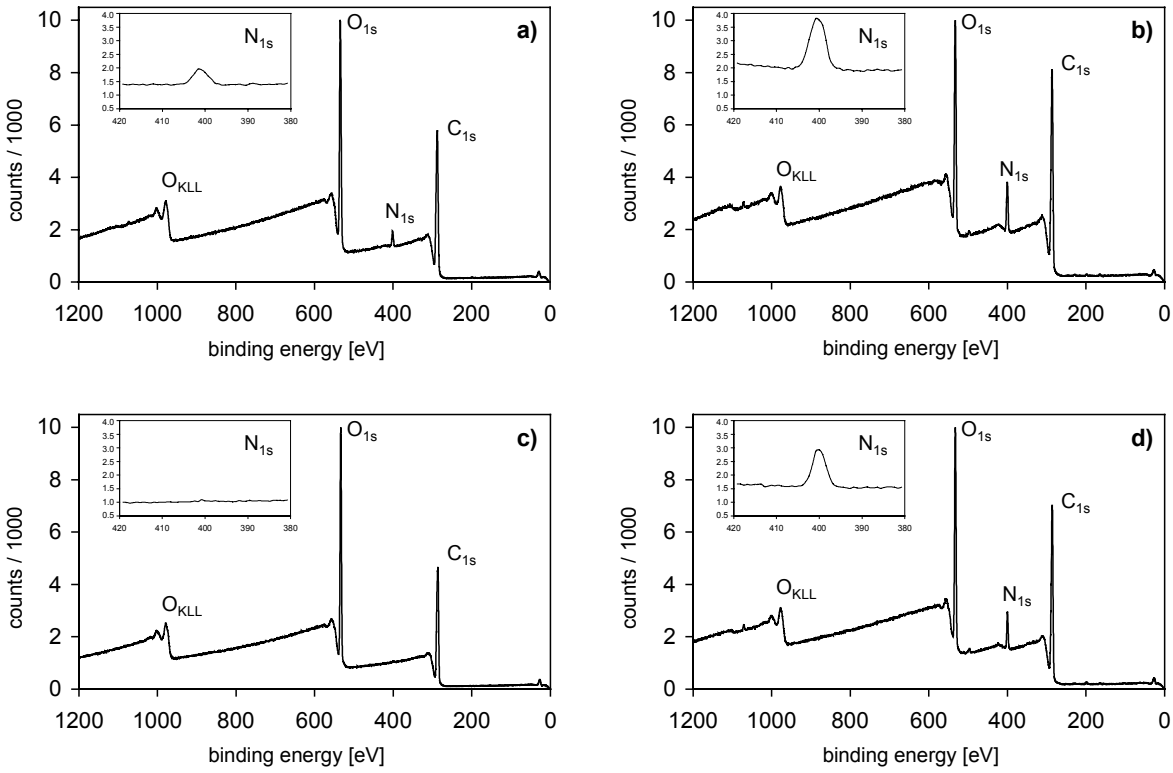

Fig. 4:
XPS spectra of polymer films after incubation with NCS protein solution:
(a) Me.PEG2-PLA20, 0h UV; (b) Me.PEG2-PLA20, 24h UV; (c) Me.PEG5-PLA20, 0h UV; (d) Me.PEG5-PLA20, 24h UV. Inserted spectra show the nitrogen signal at high resolution. As investigated polymers do not contain nitrogen, the nitrogen signal can be taken as a measure for protein adsorption.

Polymer film topography (AFM):

To elucidate the topography of native and irradiated copolymer surfaces AFM analysis was carried out on films that had been washed and freeze-dried afterwards. The obtained three-dimensional atomic force micrographs demonstrated that surface roughness markedly depended on UV irradiation time (Fig. 5a-e).

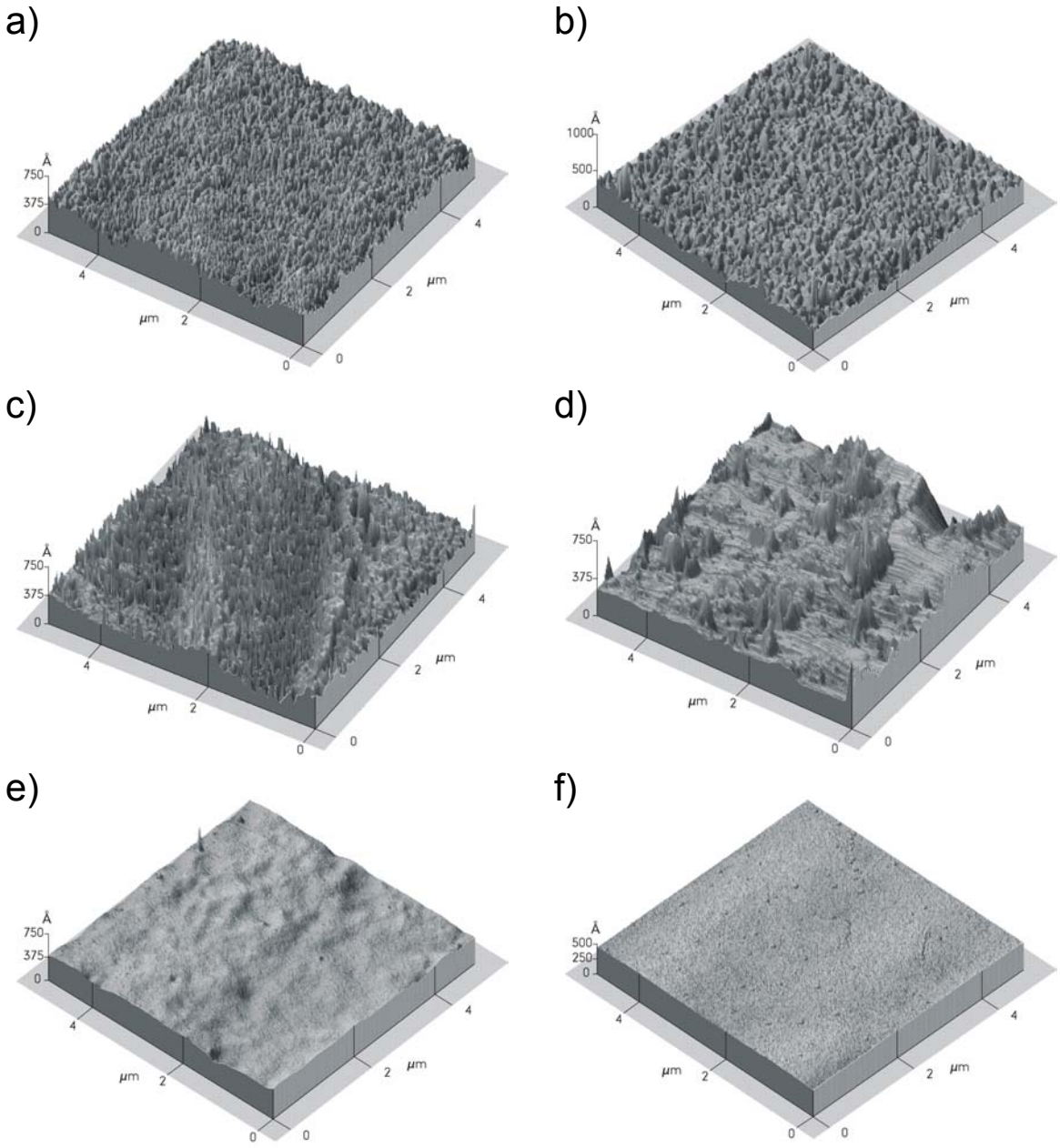

Fig. 5:
AFM imaging: irradiation time-dependent changes in surface topography of Me.PEG5-PLA20 films, compared to a non-irradiated PLA film: (a) Me.PEG5-PLA20, 0h UV; (b) Me.PEG5-PLA20, 2h UV; (c) Me.PEG5-PLA20, 5h UV; (d) Me.PEG5-PLA20, 10h UV; (e) Me.PEG5-PLA20, 24h UV; (f) PLA, 0h UV.

Non-irradiated Me.PEG5-PLA20 films (Fig. 5a) showed high surface roughness likely due to preferential orientation of PEG chains to the surface. After 2 hours of UV irradiation there were hardly any changes detectable in film topography (Fig. 5b). However, with increasing exposure to UV light smoothing of certain surface areas could be observed (Fig. 5c and d). The films irradiated for 24 hours (Fig. 5e) even showed a smooth surface with hardly any noticeable structures which rather compared to a pure PLA film (Fig. 5f) than to the rough original PEG-PLA films.

Polymer film composition (GPC):

For molecular weight distributions of Me.PEG5-PLA20 films, as determined by GPC, a semi-quantitative trend was observed with increasing UV irradiation time. After 2 hours of exposure to UV light there was only a slight change in molecular weight distribution detectable as compared to non-irradiated films (Fig. 6). However, after 5 hours a shift to lower molecular weights and a broader molcular weight distribution were observed (Fig. 6). This trend continued with time and was measured for up to 24 hours (Fig. 6). Broadening of molecular weight distribution was also reflected by the calculated polydispersity indices (PI): After 0 and 2 hours of irradiation PIs were similar, i.e., 1.33 and 1.38, respectively (Table 3). Five hours of irradiation already led to a PI of 1.8 and values increased further to PIs of approx. 2 for irradiation for 15 and 24 hours (Table 3).

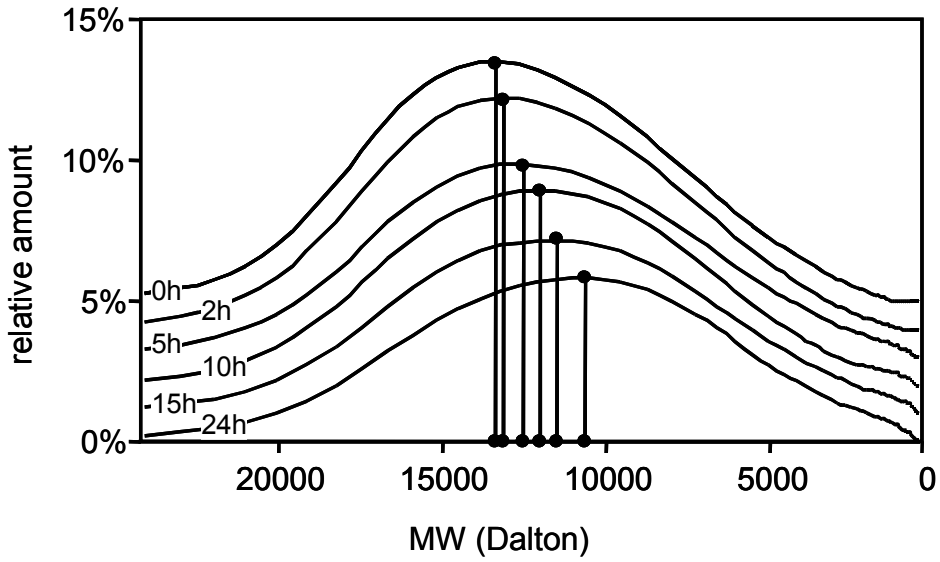

Fig. 6:
Molecular weight (MW) distribution of whole non-washed polymer films (Me.PEG5-PLA20) irradiated for 0-24 hours. GPC-MW was calculated relative to PEG standards. For better visualization absolute values were shifted by 1%.

Table 3: Molecular weight distributions in polymer films (GPC)
Weight average molecular weight (Mw), number average molecular weight (Mn) and polydispersity indices (PI = Mw/Mn) of Me.PEG5-PLA20 polymer films as determined using GPC. PI data of Me.PEG5-PLA20 and Me.PEG (MW 5,000) polymer powder are added below.

Polymer	UV (h)	Mw	Mn	PI
Me.PEG5-PLA20	0	10,647	7,982	1.33
films	2	10,337	7,509	1.38
	5	9,221	5,121	1.80
	10	9,050	4,923	1.84
	15	8,410	4,127	2.04
	24	7,991	3,973	2.01
Me.PEG5-PLA20	-	10,945	8,639	1.27
Me.PEG (MW 5,000)	-	3,464	2,768	1.25

Polymer film composition (^{1}H-NMR):

The influence of UV irradiation on Me.PEG5-PLA20 film composition was also investigated using ^{1}H-NMR, of which a typical spectrum is shown in Fig. 7. Exemplarily, Me.PEG5-PLA20 films were irradiated for 10 hours and compared to non-irradiated films. UV irradiation led to a decrease in PEG/PLA ratio, indicating a preferential loss of PEG from the surface (Table 4). Furthermore, the ratio between hydrogen signals of the PEG block and the methyl ether at the end of the PEG chain (internal standard) remained constant, suggesting that PEG chains are preferentially cleaved as a whole from the copolymer (Table 4).

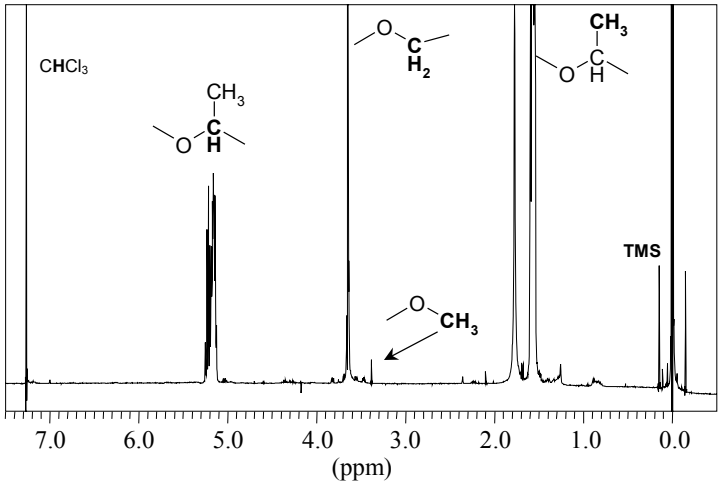

Fig. 7:
^{1}H-NMR spectrum of Me.PEG5-PLA20.

Table 4: Polymer film composition (^{1}H-NMR)
Number average molecular weight (Mn) of PEG and PLA parts in washed Me.PEG5-PLA20 films (non-irradiated or irradiated for 10 h) as calculated from integral values obtained with ^{1}H-NMR. (Integral values of PEG and PLA were calculated based on the set methyl ether integral.)

UV (h)	Integral			Mn		PEG:PLA
	MeO-	PEG	PLA	PEG	PLA	
0	3.000	483.76	310.16	5,328	22,351	0.24
10	3.000	483.45	371.56*)	5,324	26,775*)	0.20
Theoretical composition				5,000	20,000	0.25

*) Please note that the methyl ether (MeO) with its three protons at the end of the Me.PEG block was used as internal standard to calculate the integrals and average molecular weights of the PEG and PLA parts. The integral of the methyl ether, therefore, was set to 3.000, regardless if the original polymer or the irradiated polymer after possible cleavage of PEG including the methyl ether was analyzed. This is the reason why the calculated number average molecular weight of the PLA part after irradiation can be larger than that of the original PLA part. However, for conclusions drawn from this data only the ratio PEG/PLA was considered.

Water-soluble (cleaved) polymer fraction (GPC):

After UV irradiation, polymer films were washed with water; the resulting washing solution was separated from the polymer film and investigated for degradation products. GPC data showed a marked increase of the amount of cleavage products with increasing UV irradiation time (Fig. 8).

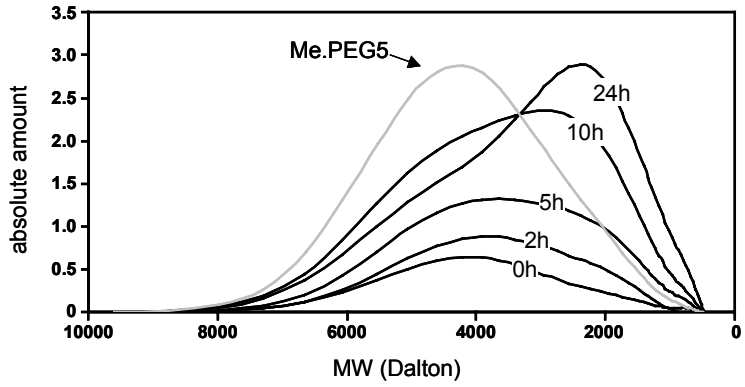

Fig. 8:
Molecular weight (MW) distribution of water-soluble polymer fraction (cleavage products) obtained from the washing solution of irradiated polymer films (Me.PEG5-PLA20). Me.PEG (MW 5,000) as used for copolymer synthesis was measured for comparison. GPC-MW were calculated relative to PEG standards.

Especially at early time points detected molecules had a molecular weight in the range of PEG 5,000. For extended UV irradiation for up to 24 hours a shift to lower molecular weights and broadening of molecular weight distribution was observed (Fig. 8). Analysis of cleaved polymer chains for poly(ethylene glycol) using the colorimetric assay after Baleux showed that with increasing irradiation time PEG content in the washing solution increased (data not shown), which correlated well with GPC data. Mass spectrometry measurements confirmed the abundant presence of poly(ethylene glycol) in the washing solution: Detected signals exhibited a mass difference of about 44 calculated for single charged ions, which is characteristic for the repeating unit of PEG (C_2H_40) (data not shown).

Discussion

The aim of our study was to investigate into the suitability of UV irradiation as a sterilization method for recently developed Me.PEG-PLA diblock copolymers which were synthesized for the use as biomaterials in tissue engineering and drug delivery.

The results showed that after 2 hours of UV irradiation, which is a sufficient time period for sterilization [18], cell adhesion to polymer films, polymer film topography, and chemical composition were maintained as compared to non-irradiated films. However, extended UV irradiation for 5-24 hours was demonstrated to exert drastic effects on Me.PEG-PLA polymer properties. Large increases in unspecific protein adsorption and subsequent cell adhesion were observed which correlated well with physicochemical characterization such as changing polymer film topography and chemical composition.

Of key importance for the success of most tissue engineering approaches is the interaction of cells with biomaterials. Especially polymer surface properties are known to determine the degree of cell adhesion and influence cell shape and cell differentiation [3-6]. Therefore, in this study the determination of cell adhesion was a key parameter for the judgement of the suitability of UV irradiation as sterilization technique. We investigated two extreme examples of block copolymers which have previously been synthesized in order to suppress any unspecific, e.g., fibroblastic, cell adhesion, which may be useful in certain in vivo tissue engineering approaches when materials are processed into membranes or films to prevent ingrowth of undesired cell types [6]. Additionally, these Me.PEG-PLA diblock copolymers have served as a base for the development of activated biomaterials to which cell-specific, e.g., osteoblast-specific, adhesion peptides can be covalently bound [19]. Again, for the use of these activated copolymers it is important that unspecific cell adhesion is

suppressed. Our investigation showed that after 2 hours of UV irradiation no cell adhesion was observed which was the same as on non-irradiated films. Extended irradiation for 5-24 hours led to increasing cell adhesion on both films, i.e., destruction of the desired surface properties.

As proteins adsorbed to a biomaterial represent a major factor mediating cell adhesion to the material [20,21], we compared irradiated and non-irradiated polymer surfaces with regard to protein adsorption using XPS. Previously it has been shown that in films of the Me.PEG-PLA diblock copolymers poly(ethylene glycol) (PEG) chains were preferentially oriented to the polymer surface [13]. PEG is generally known to substantially reduce protein adsorption [22,23], which has also previously been shown for the Me.PEG-PLA copolymers as compared to films made from pure PLA [3]. In the present study effects of UV irradiation for 24 hours were investigated and marked increases in protein adsorption after irradiation were observed. As these results suggested a loss of PEG from the surface, polymeric films were subjected to physicochemical characterization in order to further elucidate the causes of observed effects.

AFM imaging was employed to monitor polymer film topography. The observed changes after different time periods of UV irradiation correlated well with observed changes in cell adhesion. Hardly any changes in surface roughness were detected after 2 hours of irradiation. After extended exposure to UV light, however, characteristic structures previously interpreted as PEG chains [13,21] were lost from the surface. After 24 hours of UV irradiation smoothing of the surface was so drastic that resulting AFM images rather compared to pure PLA surfaces than to the original Me.PEG5-PLA20 surface.

The molecular weight distributions were analyzed as one measure to monitor changes in polymer bulk properties. Whereas after 2 hours of UV irradiation only slight changes were observed, after extended periods of exposure marked shifts towards lower molecular weights were observed. After washing of irradiated films to remove water- soluble cleavage products the remaining films were further characterized with regard to their composition. Comparing the results of ^{1}H-NMR measurements of non-irradiated and irradiated films a decrease in PEG/PLA ratio after irradiation was detected, indicating a preferential loss of PEG from the surface (Table 4). Additionally, the constant ratio between hydrogen signals of the PEG block and the methyl ether at the end of the PEG (Table 4) suggested that PEG chains were cleaved as a whole from the copolymer. This is in agreement with the interpretation of XPS and AFM data indicating that PEG is lossed from the surface leaving a surface with a strongly increased

PLA fraction. An increased hydrophobicity, as expected with reduced PEG content on the surface, was reflected by higher contact angles after UV irradiation (data not shown).

To further investigate cleavage products from the copolymer, films were irradiated and washed afterwards, and washing solutions were analyzed. GPC measurements showed that the amounts of water-soluble cleavage products increased with enhanced UV irradiation time. The peak of degradation products occurred at the same retention time as Me.PEG (MW 5,000) used for the synthesis of the diblock copolymers, suggesting that at least a large part of the detected substances may consist of PEG chains. Analysis of the cleaved polymer chains with a PEG-specific colorimetric assay revealed PEG separation increasing with UV irradiation time. Moreover, mass spectrometry measurements verified the abundant presence of poly(ethylene glycol) in the washing solution, thus, assuring the cleavage of PEG from the copolymer.

In conclusion, our study indicates that it is appropriate to use UV irradiation for up to 2 hours as sterilization technique for the investigated Me.PEG-PLA copolymers. However, UV treatment for extended periods of time (5 and more hours) drastically enhanced cell adhesion on polymer films. The observed degradation of Me.PEG-PLA responsible for the altered cell behavior may be explained by different mechanisms. Contributing factors may include photooxidation that happens to many man-made polymers on different pathways [11] and cleavage of ester bonds common in biodegradable polymers [24]. In both cases the high energy of UV irradiation may play an important role in the activation of these reactions. Large amounts of PEG are lost from the surface, mainly as whole chains as used for synthesis. Loss of PEG results in surfaces with higher PLA content representing, therefore, better substrates for protein adsorption which in turn mediates enhanced cell adhesion. Therefore, the results of our study imply that it is of paramount importance to carefully control sterilization times and monitor properties of new biomaterials, either developed for control of cell-biomaterial interaction in tissue engineering or for suppression of undesired protein adsorption in protein drug delivery, when they are subjected to UV sterilization.

References

1. Hubbell, J. A. (1995). Biomaterials in tissue engineering. *Biotechnology N.Y.* **13**, 565-576.

2. Langer, R. and Vacanti, J. P. (1993). Tissue engineering. *Science* **260**, 920-926.

3. Göpferich, A., Peter, S. J., Lucke, A., Lu, L., and Mikos, A. G. (1999). Modulation of marrow stromal cell function using poly(D,L-lactic acid)-*block*-poly(ethylene glycol)-mono methylether surfaces. *J.Biomed.Mater.Res.* **46**, 390-398.

4. Lampin, M., Warocquier, C., Legris, C., Degrange, M., and Sigot-Luizard, M. F. (1997). Correlation between substratum roughness and wettability, cell adhesion, and cell migration. *J.Biomed.Mater.Res.* **36**, 99-108.

5. Zhang, M., Desai, T., and Ferrari, M. (1998). Proteins and cells on PEG immobilized silicon surfaces. *Biomaterials* **19**, 953-960.

6. Cima, L. G. (1994). Polymer substrates for controlled biological interactions. *J.Cell Biochem.* **56**, 155-161.

7. Holy, C. E., Cheng, C., Davies, J. E., and Shoichet, M. S. (2001). Optimizing the sterilization of PLGA scaffolds for use in tissue engineering. *Biomaterials* **22**, 25-31.

8. Bittner, B., Mäder, K., Kroll, C., Borchert, H. H., and Kissel, T. (1999). Tetracycline-HCL-loaded poly(D,L-lactide-co-glycolide) microspheres prepared by a spray drying technique: influence of y-irradiation on radical formation and polymer degradation. *J.Controlled Release* **59**, 23-32.

9. Bousquet, J. and Michel, F. B. (1991). Allergy to formaldehyde and ethylene-oxide. *Clin.Rev.Allergy* **9**, 357-370.

10. UV-Technik, Speziallampen GmbH. Desinfektion mit UV-Strahlung: Strahlenquellen, technische Hinweise und Anwendung. 2000. Wümbach, Germany, UV-Technik Speziallampen GmbH.

11. McKellar, J. F. and Allen, N. S. (1979). "Photochemistry of man-made polymers," Applied Science Publishers, Barking, England.

12. Praschak, D., Bahners, T., and Schollmeyer, E. (1998). PET surface modifications by treatment with monochromatic excimer UV lamps. *Appl.Phys.A:Mater.Sci.Process.* **A66**, 69-75.

13. Lucke, A., Teβmar, J., Schnell, E., Schmeer, G., and Göpferich, A. (2000). Biodegradable poly(D,L-lactic acid)-poly(ethylene glycol)-monomethyl ether diblock copolymers: structures and surface properties relevant to their use as biomaterials. *Biomaterials* **21**, 2361-2370.

14. Schwendeman, S. P., Cardamone, M., Brandon, M. R., Klibanov, A., and Langer, R. (1996). Stability of proteins and their delivery from biodegradable polymer microspheres. *In* "Microparticulate Systems for the Delivery of Proteins and Vaccines" (S. Cohen and H. Bernstein, Eds.), Marcel Dekker, New York.

15. Fu, K., Klibanov, A. M., and Langer, R. (2000). Protein stability in controlled-release systems. *Nat.Biotechnol.* **18**, 24-25.

16. Staiger, H. and Löffler, G. (1998). The role of PDGF-dependent suppression of apoptosis in differentiating 3T3-L1 preadipocytes. *Eur.J.Cell Biol.* **77**, 220-227.

17. Baleux, M. B. and Champetier, M. G. (1972). Dosage colorimétrique d'agents de surface non ioniques poloxyéthylenes à l'aide d'une solution iodo-iodurée. *C.R.Acad.Sc.Paris* **274**, 1617-1620.

18. Abshire, R. L. and Dunton, H. (1981). Resistance of seletected strains of pseudomonas aeruginosa to low-intensity ultraviolet radiation. *Appl.Environ.Microbiol.* **41**, 1419-1423.

19. Tessmar, J., Mikos, A. G., and Göpferich, A. A new biodegradable polymer for the modification of surfaces: NH_2-poly(ethylene glycol)-poly(D,L-lactic acid). Sixth World Biomaterials Congress Transactions, 595. 2000.

20. Kim, B. S., Nikolovski, J., Bonadio, J., Smiley, E., and Mooney, D. J. (1999). Engineered smooth muscle tissues: regulating cell phenotype with the scaffold. *Exp.Cell Res.* **251**, 318-328.

21. Tziampazis, E., Kohn, J., and Moghe, P. V. (2000). PEG-variant biomaterials as selectively adhesive protein templates: model surfaces for controlled cell adhesion and migration. *Biomaterials* **21**, 511-520.

22. Jeon, S. I., Lee, J. H., Andrade, J. D., and de Gennes, P. G. (1991). Protein-surface interactions in the presence of polyethylene oxide. *J.Colloid Interface Sci.* **142**, 149-158.

23. Gref, R., Lück, M., Quellec, P., Marchand, M., Dellacherie, E., Harnisch, S., Blunk, T., and Müller, R. H. (2000). "Stealth" corona-core nanoparticles surface-modified by polythylene glycol (PEG): influences of the corona (PEG chain length and surface density) and of the core composition on phagocytic uptake and plasma protein adsorption. *Colloids Surf.B Biointerfaces* **18**, 301-313.

24. Göpferich, A. (1996). Mechanisms of polymer degradation and erosion. *Biomaterials* **17**, 103-114.

Chapter 7

Adipogenesis on Different Polymeric Materials

Claudia Fischbach, Jörg Tessmar, Michael Hacker, Sigrid Drotleff,
Torsten Blunk, Achim Göpferich

Department of Pharmaceutical Technology, University of Regensburg,
93040 Regensburg, Germany

Introduction

In tissue engineering, polymer matrices are frequently used to guide new tissue formation [1]. The generation of appropriate constructs for different fields of application can be optimized at three different levels: A) the cells, B) the polymer scaffolds, and C) the methodologies employed for construct assembly [2]. On the scaffold level, advances in polymer chemistry as well as polymer processing have led to the development of tailored 3-D matrices allowing to distinctly modify the characteristics of the created tissues. Not only are the physical and mechanical properties of the constructs tunable, for example by adjusting the porosity and degradation rate of the construct, but it is also being increasingly recognized that the polymer itself may influence cellular features including cell adhesion and differentiation. In order to investigate the impact of the polymer with relatively simple experimental procedures, many groups culture cells in 2-D on various polymer films. Using this approach, surface roughness and surface energy have been demonstrated as being critical to direct cell adhesion [3-5]. Nevertheless, cellular characteristics are known to be modulated through the chemical composition of the polymers. For instance, an increase in the hydrophobicity of the biomaterials leads to an enhanced cell adhesion and proliferation [6,7], caused by an increased adsorption of adhesion-mediating serum proteins such as fibronectin onto the polymer surface [8,9]. However, depending on the type and conformation of the adsorbed proteins, the adherent cells interact differently depending on the polymer surface and, hence, may adopt dissimilar phenotypes [9]. This can be explained, in part, by the fact that the adsorbed adhesive proteins dictate via which integrin receptors the cells attach to the substrate. Integrins are known to affect cellular differentiation by mediating cytoskeletal reorganization [10] and, thereby, allowing for changes in cell morphology. In turn, cell shape is reported to impact the differentiation of many cell types [11,12]. To conclude, one can, therefore, hypothesize that specific protein adsorption, controlled by tailored polymer constructs, may facilitate the differentiation of cells into the desired phenotype and, thus, guide the formation of the desired tissue.

Currently, polyglycolic acid (PGA), polylactic acid (PLA), and their respective copolymers (PLGA) are the most widely used polymers in tissue engineering [2,13]. This is due, in part, to their reported biocompatibility, as proven by their long-standing use as suture materials in humans, as well as their favorable properties with regard to processing and degradation [2]. These materials are not suitable for guiding specific tissue formation,

however, because of unspecific protein adsorption, which allows for the infiltration of undesired cell types, such as fibroblasts, into the tissue engineered construct. With the aim of preventing such unspecific protein adsorption, we synthesized poly(D,L-lactic acid)-poly(ethylene glycol)-monomethyl ether (Me.PEG-PLA) diblock co-polymers by attaching hydrophilic poly(ethylene glycol) blocks to poly(lactic acid) blocks [14]. Subsequently, unspecific protein adsorption was demonstrated to be reduced with increasing PEG content [14,15]. In terms of cell behavior, the resulting polymers have recently been described to further the differentiation of marrow stromal cells towards the osteoblastic phenotype [16,17]. Furthermore, the novel biomaterials have been shown to substantially influence the adhesion of 3T3-L1 preadipocytes; although fewer preadipocytes attached to Me.PEG-PLA_y films as compared to pure PLA films, the adhered cells exhibited a more rounded cell shape [15,18]. As adipose differentiation is accompanied by cytoskeletal reorganization to cells exhibiting a spherical appearance [12,19], this observation prompted us to hypothesize that Me.PEG-PLA may promote 3T3-L1 differentiation into adipocytes.

Therefore, the focus of this study was to address this hypothesis and to evaluate if the block-co-polymer is suitable for guiding adipose differentiation. To this end, we processed polymer films for 2-D cell culture and examined the typical features of adipose differentiation. Specifically, adipogenesis was investigated on hydrophilic films made from $Me.PEG_2PLA_{20}$ (MW (PEG): 2 kDa; MW (PLA): 20 kDa) and on hydrophobic films prepared from PLGA (molar ratio of PLA:PGA was 75:25). Conventional tissue culture polystyrene (TCPS) served for comparison. Adipose conversion was triggered by treatment with a hormonal cocktail according to protocols evaluated in preceding experiments (see Chapter 2). Following a differentiation phase of 9 days, adipocyte properties were analyzed. In detail, intracellular lipid accumulation was investigated. Furthermore, expression of typical fat cell genes was examined on both the protein and the mRNA level. In order to assess the functionality of the cells on different surfaces, the lipolysis rate of the adipocytes was measured under different conditions. Finally, the polymers were used in the form of 3-D porous scaffolds in order to investigate their impact on 3-D adipose differentiation, as compared to the polyglycolic acid (PGA) fiber meshes used so far.

Materials and methods

Materials:

For the fabrication of hydrophilic polymer films, poly(D,L-lactic acid)-poly(ethylene glycol)-monomethyl ether ($Me.PEG_2PLA_{20}$) diblock copolymers were synthesized in our lab as previously described [14]. The polymers consist of a hydrophilic, water-soluble poly(ethylene glycol)-monomethyl ether (Me.PEG) block of 2 kDa and a hydrophobic, biodegradable poly(D, L-lactic acid) (PLA) block of 20 kDa, as indicated by the subscripted numbers (Fig. 1A).

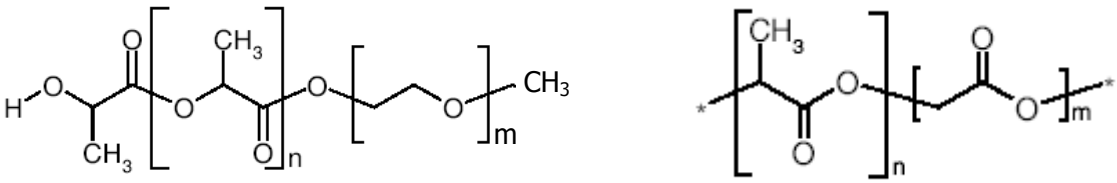

A) $Me.PEG_2PLA_{20}$ **B) PLGA**

Fig. 1:
Structure of the investigated polymers:
m and n is the number of the respective monomer units used for synthesis of copolymers
A) m = ethylene glycol, n = lactic acid; B) m = glycolic acid, n = lactic acid

To prepare hydrophobic polymer films, PLGA (Resomer®, RG 756) featuring a molar ratio of 75:25 (P(D,L)LA:PGA) was used (Fig. 1B). It was kindly provided by Boehringer Ingelheim (Ingelheim, Germany). Polypropylene sheets employed to prepare carriers for film manufacture were a kind gift from Dr. Stricker, Targor Application Technology (Ludwigshafen, Germany).

For cell experiments 3T3-L1 preadipocytes were obtained from ATCC (Manassas, VA, USA). Stock cultures were grown as described [20]. Fetal bovine serum (FBS), and trypsin (1:250) were purchased from Biochrom KG Seromed (Berlin, Germany); phosphate buffered saline (PBS) and penicillin-streptomycin solution were from Life Technologies (Karlsruhe, Germany). MEM (alpha-modification), corticosterone, indomethacin, and oil red O were purchased from Sigma-Aldrich (Deisenhofen, Germany). 3-isobutyl-1-methylxanthine (IBMX) was from Serva Electrophoresis GmbH (Heidelberg, Germany). Insulin was a gift from Hoechst Marion Roussel (Frankfurt a. M., Germany). Cell culture materials were obtained from Sarstedt AG & Co. (Nuembrecht, Germany) and BD Biosciences Labware (Heidelberg, Germany). Polyglycolic acid (PGA) non-woven fiber meshes (12-14 µm fiber

diameter; 96% porosity; 62 mg/cm^3 bulk density) were purchased from Albany Int. Research Co. (Mansfield, MA, USA) and die-punched into discs 5 mm in diameter and 2 mm thick.

Preparation of polymer films:

Thin polymer films were manufactured by spin casting of polymer solutions onto transparent polypropylene (PP) discs 13 mm in diameter. In cell culture medium, the films detached from commonly used glass cover slips and, therefore, PP carriers prepared from PP-sheets by die-punching were employed instead. That the surface structure of the polymer films is not affected by the carrier material has been shown in previous studies [15]. For spin casting, 50 mg of the polymer material was dissolved in 1 ml of methylene chloride and subsequently, 50 µl of the resulting solutions were cast onto the disks fixed on a platform rotating at 1,950 rpm. To remove residual solvent, the films were allowed to dry under ambient conditions for two hours, followed by at least 24 hours drying under vacuum at room temperature in a desiccator. During vacuum drying, the pressure was kept below 0.1 mbar using a RV5 two stage vacuum pump from Edwards (Crawley, West Sussex, UK). Subsequently, the polymer-coated PP disks were stuck to 24-well plates using a biocompatible silicon glue (Elastosil E4 Transparent, Drawin Vertriebs GmbH; Ottobrunn, Germany) followed by an additional overnight drying step. For final sterilization, the well plates, containing the polymer films, were exposed to UV irradiation for 1 hour under conditions described earlier [15].

Manufacture of Me.PEG$_2$PLA$_{20}$ and PLGA polymer scaffolds:

Me.PEG$_2$PLA$_{20}$ and PLGA polymers were processed to scaffolds as recently described [21]. Briefly, the polymers were dissolved in organic solvents (Me.PEG$_2$PLA$_{20}$ in a mixture of ethyl methyl ketone and tetrahydrofurane; PLGA in ethyl ester). Subsequently, triglyceride microspheres, prepared by a melt dispersion technique and classified by sieving, were added to the solution to yield pores of a defined size. The resulting dispersion was transferred into teflon molds 8 mm in diameter and, then, the molds were immersed in warm hexane in order to precipitate the polymer and extract the porogen particles. The resulting polymer cylinders were vacuum-dried and cut into scaffolds 2 mm thick using a self-made micro-saw.

Cell culture:

For 2-D cell culture, 3T3-L1 preadipocytes were plated at a density of 5,000 cells per cm². Subsequently, the cells were cultured in MEM (alpha-modification) supplemented with 10% FBS, penicillin (100 U/ml), and streptomycin (0.1 mg/ml). After four days, adipogenesis was stimulated by administration of 0.1 µM corticosterone, 0.5 mM IBMX, and 60 µM indomethacin contained in differentiation medium (MEM (alpha-modification), 5% FBS, 1 µM insulin, penicillin (100 U/ml), and streptomycin (0.1 mg/ml)). This time-point was referred to as day 0. At day 2, the hormonal induction medium was replaced by differentiation medium alone and the cells were maintained under these conditions until day 9 or 10 (leptin ELISA) of adipogenesis. Throughout the course of the experiment, the cell culture medium was changed every other day. Cell harvesting was conducted according to the specific requirements of each analytical method described below.

3-D cell culture was performed as previously reported [20]. In brief, 3T3-L1 preadipocytes were dynamically seeded onto the polymer scaffolds in stirred spinner flasks. Thereby, each flask comprised 8 scaffolds and 100 ml of a suspension containing $16x10^6$ cells, i.e., $2x10^6$ cells per scaffold. Stirring for two days at 80 rpm allowed for cell attachment to the polymer matrices. Cell-polymer constructs were transferred into 6-well plates (one construct and 5 ml culture medium per well) and cultured in the incubator dynamically on an orbital shaker at 50 rpm (Dunn Labortechnik GmbH; Asbach, Germany). Cultivation of the cell-seeded constructs was performed in MEM (alpha-modification) supplemented with 10% FBS, penicillin (100 U/ml), and streptomycin (0.1 mg/ml). Hormonal induction and adipose differentiation was performed according to the conditions described above for 2-D cell culture.

Oil red O staining:

In order to visualize accumulated cytoplasmic triglyceride droplets 9 days after hormonal stimulation of adipogenesis, oil red O staining was performed. For this purpose, the cells were washed with PBS. After subjecting the samples to an overnight fixation step in 10% buffered formalin, the adipocytes were stained as previously described [22].

Analysis of glycerol-3-phosphate dehydrogenase (GPDH):

At day 9 of hormonal differentiation, 2-D cells and 3-D cell-polymer constructs were washed with PBS, harvested in lysis buffer (50 mM Tris, 1 mM EDTA, 1 mM mercaptoethanol, pH 7.5), and sonicated with a digital sonifier (Branson Ultrasonic Corporation; Danburg, CT, USA). The GPDH assay was performed as described in the literature [23,24]. Cytosolic protein concentration was determined after precipitation with trichloracetic acid using the Lowry assay [25]. GPDH activity was expressed as mU per mg protein.

Measurement of triglyceride (TG) content:

Nine days after hormonal stimulation of adipogenesis, the intracellular TG content was quantitatively determined. For this purpose, the cells cultivated on different polymeric surfaces, were washed with PBS, scraped using 0.5% thesit, and sonicated with a digital sonifier (Branson Ultrasonic Corporation; Danburg, CT, USA). The spectroscopic quantification of TG was performed using the enzyme coupled glycerol assay kit 337 (Sigma Diagnostics; Deisenhofen, Germany). Values are expressed as mg TG per µg cytosolic protein as determined according to the Lowry assay [25].

Investigation of leptin secretion:

The leptin secretion of cells cultivated on different polymer films and on TCPS, respectively, was measured in cell culture media using the Quantikine M immunoassay (R&D Systems; Wiesbaden, Germany) for mouse leptin. Media samples from day 8 to day 10 were taken and centrifuged for 5 min at 13,200 rpm (Centrifuge 5415 R, Eppendorf AG; Hamburg, Germany) to remove cell debris. The supernatants were frozen at –80°C until an ELISA was conducted. Additionally, the cells were scraped off and cytosolic protein concentration was determined after precipitation with trichloracetic acid using the Lowry assay [25]. Finally, the measured amount of secreted leptin was normalized to cellular protein.

Reverse transcription polymerase chain reaction (RT-PCR):

In order to investigate the gene expression on different materials, the cells were harvested at day 9 and RT-PCR was performed as reported earlier [20]. In brief, mRNA

isolation was conducted with Trizol® reagent (Invitrogen GmbH; Karlsruhe, Germany). First-strand cDNA was synthesized from total RNA by using random hexamers (Roche Diagnostics; Mannheim, Germany) and Superscript II RNase H- Reverse Transcriptase (Invitrogen GmbH; Karlsruhe, Germany). Subsequently, PCR was conducted with Sawady Taq-DNA-Polymerase (PeqLab; Erlangen, Germany). Thereby, the amplification was carried out using specific primers and appropriate conditions for each gene (Tab. 1). Primers were purchased from Amersham Biosciences (Freiburg, Germany) and MWG-Biotech AG (Ebersberg, Germany). 18 S rRNA served as internal control. Reverse transcription and PCR were performed using a Mastercycler Gradient (Eppendorf AG; Hamburg, Germany). The PCR products were analyzed by electrophoresis through ethidium bromide containing agarose gels, followed by imaging and densitometric scanning of the resulting bands using a Kodak EDAS 290 (Fisher Scientific; Schwerte, Germany).

Table 1: Primer sequences and PCR conditions for the investigated genes
Oligonucleotide sequences of mouse forward (sense) and reverse (antisense) primers. Gene amplification was performed by PCR according to the specified annealing temperatures (AT) and number of cycles for each gene. The reaction conditions of one cycle were composed as follows: denaturation for 45 sec at 94°C, annealing for 45 sec at the indicated temperatures, and extension for 1 min at 72°C.

Gene	Forward and reverse primers of examined genes	AT (°C) / Cycles
PPARγ	5′-AAC CTG CAT CTC CAC CTT ATT ATT CTG A-3′ 5′-GAT GGC CAC CTC TTT GCT CTG CTC CTG-3′	60 / 35
GLUT-4	5′-CCC CGC TGG AAT GAG GTT TTT GAG GTG AT-3′ 5′-CAG ACA GGG GCC GAA GAT TGG GAG ACA GT-3′	61 / 35
beta3-AR	5′-CAG TGG TGG CGT GTA GGG GCA GAT-3′ 5′-CGG GTT GAA GGC GGA GTT GGC ATA G-3′	63 / 36
angiotensinogen	5′-CTG GCC GCC GAG AAG CTA GAG GAT GAG GA-3′ 5′-GAG AGC GTG GGA AGA GGG CAG GGG TAA AGA G-3′	62 / 35
leptin	5′-GAC ACC AAA ACC CTC ATC AAG ACC-3′ 5′-GCA TTC AGG GCT AAC ATC CAA CT-3′	58,5 / 36
VEGF*)	5′-ATA GCG GAT GGA AAA CCC TGC-3′ 5′-TAT CGC CTA CCT TTT GGG ACG 3′	60 / 40
18 S	5′-TCA AGA ACG AAA GTC GGA GGT TCG-3′ 5′-TTA TTG CTC AAT CTC GGG TGG CTG-3′	60 / 22

*) PCR for VEGF was conducted according to Ref. [26] (denaturation for 30 sec at 94°C, annealing for 60 sec at 60°C, and extension for 2 min at 68°C).

Quantification of lipolysis rate:

The lipolytic cell response of cells cultured on either polymer films or TCPS was determined by analyzing the amount of glycerol released into the incubation buffer after treatment with agents stimulating or inhibiting lipolysis. On day 9 after initiation of adipogenesis, the cells were washed with serum-free medium and then maintained in the same medium for 2h to avoid interference with serum factors. Subsequently, medium was replaced by PBS supplemented with 3% fatty acid-free bovine serum albumin (BSA) (Sigma-Aldrich; Deisenhofen, Germany). In addition to recording data on lipolysis under control conditions, stimulation and inhibition of glycerol release were conducted by adding 10 µM isoproterenol and 100 µM propranolol (both were from Sigma-Aldrich; Deisenhofen, Germany) to the incubation buffer, respectively. After 1h incubation (37°C, 5% CO_2), the conditioned media were frozen at –20°C until the enzyme coupled glycerol assay kit 337 (Sigma Diagnostics; Deisenhofen, Germany) was carried out. As the assay buffer interfered with the Lowry protein assay, absolute values were normalized to the cytoplasmic protein concentration, as determined from GPDH samples (mean of three samples).

Statistical analysis:

Statistical significance was determined by one-way analysis of variance ANOVA followed by Tukey post-hoc test (Software: SPSS 10.0 for Windows). The statistical significance level was set as indicated (either $p < 0.05$ or $p < 0.01$).

Results

Assessment of intracellular triglyceride (TG) storage:

With the aim of examining intracellular lipid droplets on the different polymeric substrates (TCPS, PLGA, and Me.PEG_2PLA_{20}), oil red O staining was performed. Subsequent microscopic investigations revealed remarkable lipid accumulation on all materials investigated (Fig. 2). However, whereas adipocytes cultured on TCPS and PLGA exhibited comparable properties with regard to the number of adherent cells, the size of the accumulated TG droplets, and their respective cell morphology, adipocytes differentiated on Me.PEG_2PLA_{20}-films looked notably different. Besides detecting a smaller number of

attached cells, a distinct increase in the size of the intracellular lipid vacuoles could be observed. Furthermore, the fat cells exhibited a less spread, more spherical shape pointing at diminished adhesion strength, as compared to TCPS and PLGA (Fig. 2).

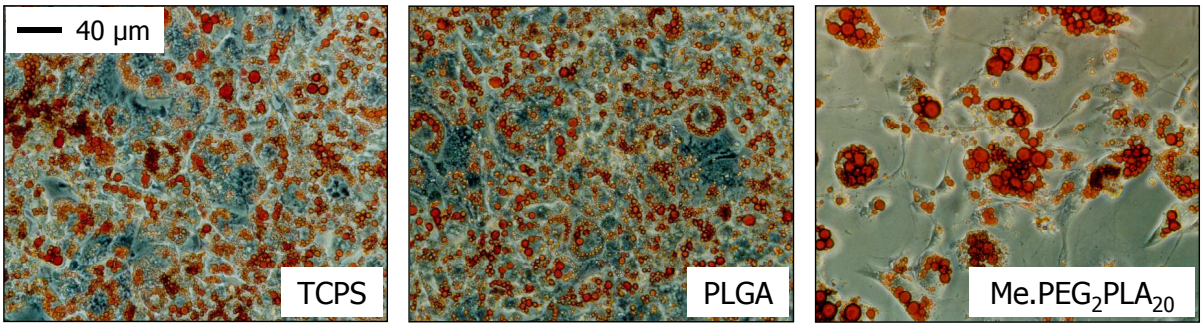

Fig. 2:
3T3-L1 adipocytes differentiated for 9 days on conventional tissue culture polystyrene (TCPS) and on polymer films prepared from PLGA and Me.PEG$_2$PLA$_{20}$. In order to better visualize intracellular triglyceride droplets the cells were stained with oil red O.

With the objective of quantifying the microscopically detected differences in TG storage, the activity of GPDH, a key enzyme of TG biosynthesis, as well as intracellular TG content, were measured. In order to take into account the different numbers of adherent adipocytes, the obtained values were normalized to cytoplasmic protein. The kinetics of the GPDH activity showed an increasing lipid biosynthesis during adipogenesis (Fig. 3); at all time-points investigated, however, no significant difference could be seen between the cells differentiated on TCPS, PLGA, or Me.PEG$_2$PLA$_{20}$.

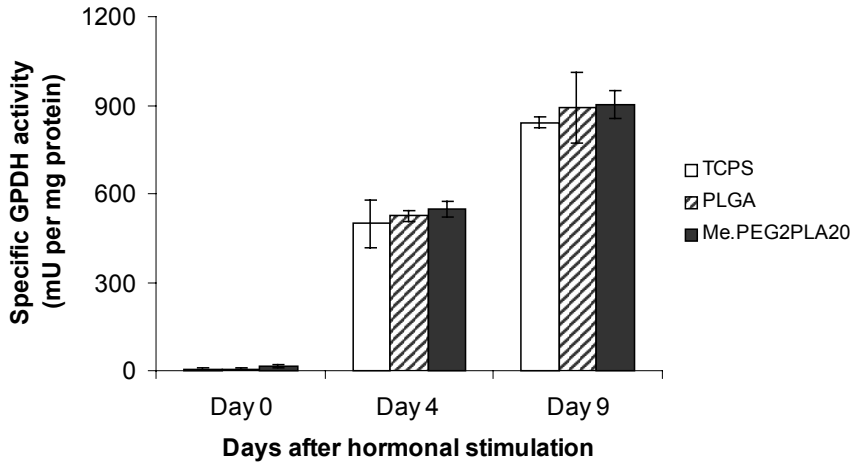

Fig. 3:
Impact of different culture materials on triglyceride biosynthesis of 3T3-L1 cells as investigated by kinetic measurement of GPDH activity. Subsequent to hormonal treatment, increasing enzyme activities were analyzed. However, no significant differences could be determined for adipogenesis either on TCPS, PLGA, or Me.PEG$_2$PLA$_{20}$. Data represent the average ± SD of three measurements.

The microscopically observed differences were also not detectable in the analysis of TG content (Fig. 4). The amount of intracellular TG found in cultures on $Me.PEG_2PLA_{20}$ (70.8 ± 6.1 mg per µg protein) were not significantly different relative to that accumulated in conventional TCPS cultures (75.6 ± 9.3 mg per µg protein). In contrast, the lipid concentration in adipocytes differentiated on PLGA-films (92.8 ± 0.3 mg per µg protein) was slightly enhanced over both TCPS ($p < 0.05$) and $Me.PEG_2PLA_{20}$ ($p < 0.01$) (Fig. 4).

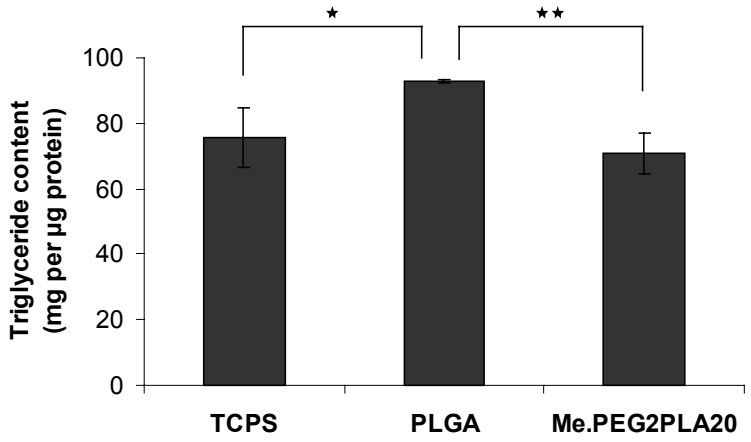

Fig. 4:
Intracellular triglyceride (TG) content of 3T3-L1 adipocytes cultivated on TCPS, PLGA, and $Me.PEG_2PLA_{20}$ as measured 9 days after hormonal induction of adipose conversion. Data were normalized relative to cellular protein and are represented as an average ± SD of three measurements. Different levels of significance are indicated by ★ ($p<0.05$) and ★★ ($p<0.01$).

Analysis of leptin secretion:

Leptin, a peptide hormone produced by adipocytes, is involved in the regulation of food intake and energy expenditure. As its expression in 3T3-L1 is known to be dependent upon the cellular differentiation status [27,28], leptin secretion of adipocytes cultured on different substrates was investigated. In order to take the distinct cell densities into account, the absolute values of leptin were normalized to cytoplasmic protein (Fig. 5). Two-day secretion rates (day 8-10) of cells cultivated on TCPS (47.8 ± 7.3 ng per mg protein) and PLGA (46.2 ± 5.3 ng per mg protein) were comparable. In contrast, the leptin concentration measured in culture medium of cells differentiated on $Me.PEG_2PLA_{20}$ (103.2 ± 32.0 ng per mg protein), was significantly enhanced as compared to both TCPS and PLGA (Fig. 5).

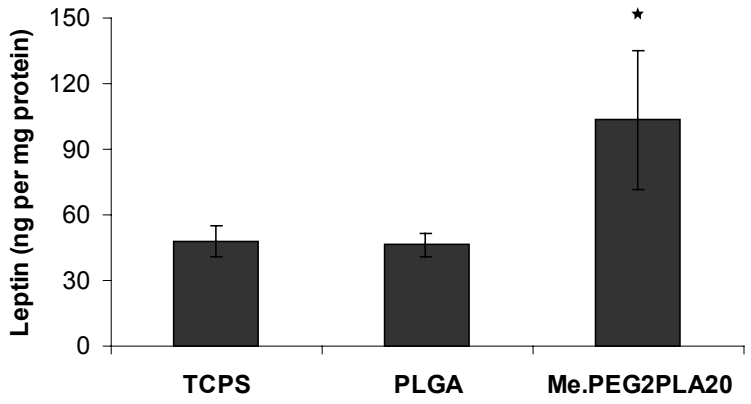

Fig. 5:
Effects of different cell culture substrates on 2-day leptin secretion of differentiated 3T3-L1 adipocytes. Leptin concentration was analyzed in samples of the cell culture medium taken at day 10 using a mouse leptin ELISA. Absolute values were referred to cellular protein. Data are expressed as mean ± SD (n=3). Statistically significant differences ($p < 0.05$) are denoted by ★.

Investigation of gene expression on the mRNA level:

In order to comprehensively investigate adipocytes differentiated for 9 days on either TCPS, PLGA, or Me.PEG$_2$PLA$_{20}$, RT-PCR was performed on a subset of characteristic fat cell genes. An investigation of gels revealed no substantial differences in the mRNA gene expression of the key transcription factor PPARγ, the glucose transporter Glut-4 or the adrenoreceptor beta3 (Fig. 6). Furthermore, the secretory protein angiotensinogen, which modulates cardiovascular functions, the satiety hormone leptin, and the vascular endothelial growth factor VEGF did not exhibit any differences either (Fig. 6). For further clarification, gene expression relative to the internal standard 18 S was calculated and is depicted in the form of diagrams (Fig. 6). It must be noted that the primers used to analyze VEGF (according to Ref. [26]), allowed amplification of the major three isoforms synthesized by alternative splicing (VEGF$_{120}$, VEGF$_{164}$, VEGF$_{188}$) and, thus, yielded 3 bands on the gels. For analysis of relative gene expression, their densities were added and the resulting sums were compared to 18 S.

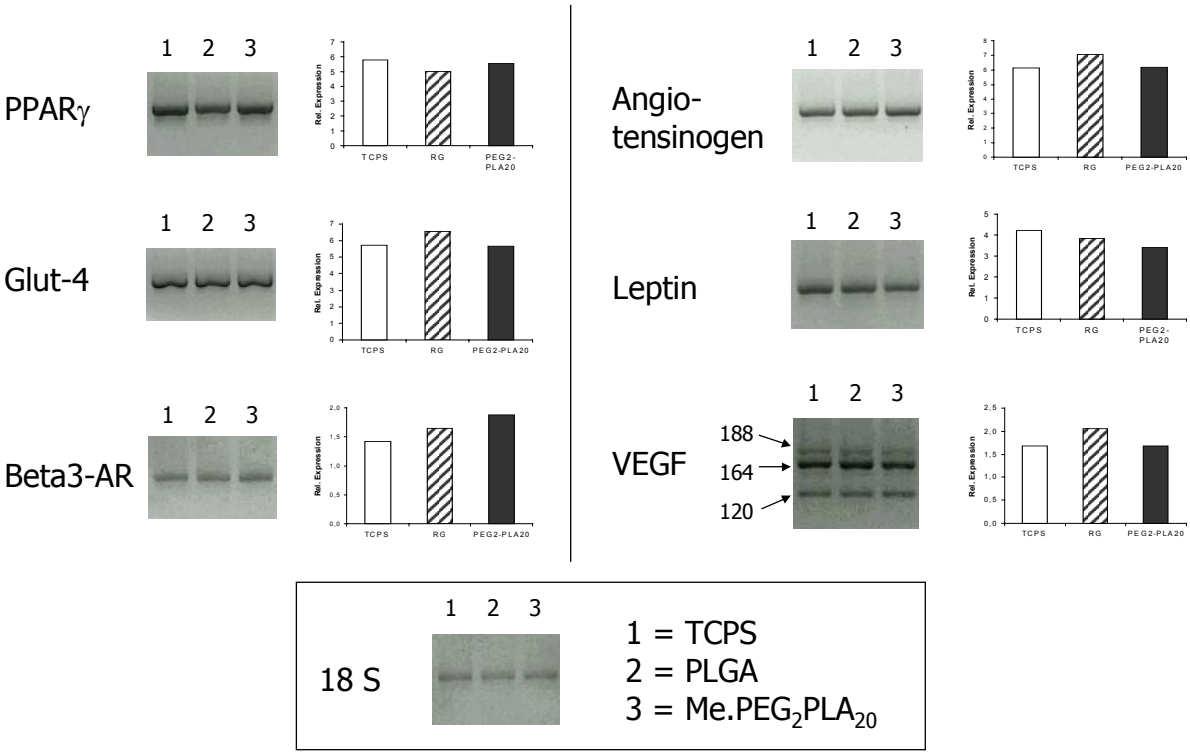

Fig. 6:
The impact of different culture surface materials on the expression of characteristic fat cell genes was examined on the mRNA level by means of RT-PCR. Invstigation of PPARγ, Glut-4, beta3-adrenoreceptor, angiotensinogen, leptin, VEGF and the internal standard 18 S was conducted in triplicate, one representative result is shown here. The primers used to investigate VEGF enabled detection of the major three isoforms synthesized by alternative splicing ($VEGF_{120}$, $VEGF_{164}$, $VEGF_{188}$).

Measurement of lipolysis:

In order to investigate the differently cultured adipocytes with regard to their lipolytic response, the amount of released glycerol was analyzed under control conditions, subsequent to stimulation with 10 µM isoproterenol and after inhibition with 100 µM propranolol. The assay buffer containing 3% BSA interfered with the Lowry protein assay. Therefore, the amount of released glycerol was normalized relative to the protein values determined from GPDH samples instead. On all materials investigated, isoproterenol treatment led to a significant increase ($p < 0.01$) of released glycerol, as compared to control conditions (Fig. 7). However, the administration of propranolol did not result in inhibition of lipolysis. No significant differences were detected between lipolysis of adipocytes differentiated on either TCPS, PLGA, or $Me.PEG_2PLA_{20}$ films (Fig. 7).

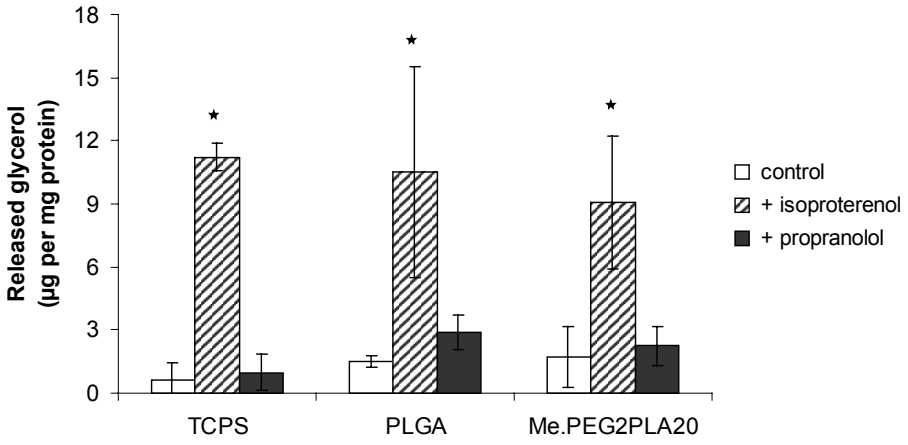

Fig. 7:
Lipolytic cell response of 3T3-L1 adipocytes, differentiated on different culture material, was assessed by analysis of released glycerol under control conditions and subsequent to treatment with a lipolysis stimulating (10 µM isoproterenol) as well as a lipolysis inhibiting agent (100 µM propranolol). Data represent the mean ± SD (n=3). Statistically significant differences to control conditions ($p<0.01$) are indicated by ★.

Evaluation of adipogenesis on different polymeric scaffolds:

Adipogenesis on 3-D matrices made from PLGA and Me.PEG_2PLA_{20} was assessed by investigating GPDH, which represents a late marker of differentiation. Commercially available PGA fiber meshes, routinely applied in 3-D experiments, served for comparison.

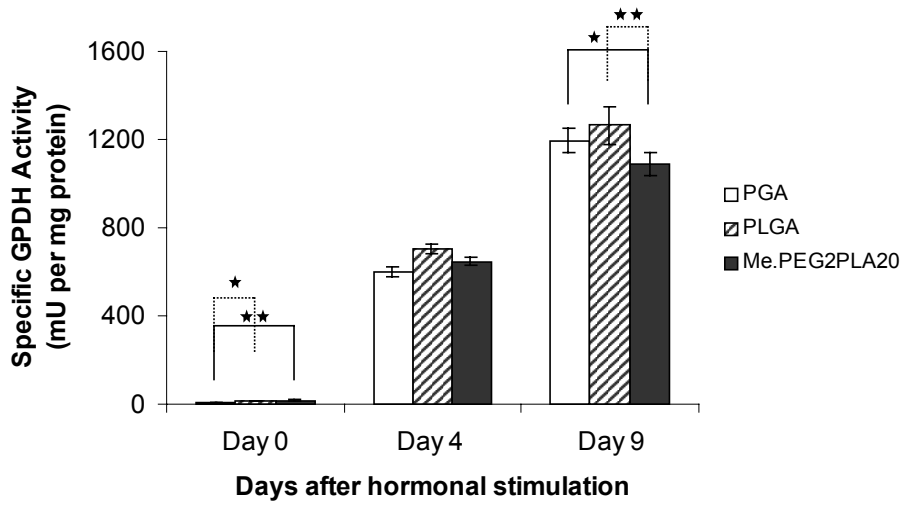

Fig. 8:
Comparison of 3-D adipogenesis on scaffolds made from PGA, PLGA, and Me.PEG_2PLA_{20} as determined by the kinetic measurement of GPDH activity. Subsequent to hormonal treatment, increasing enzyme activities were observed on all materials. Statistically significant differences, denoted by ★ ($p<0.05$) and ★★ ($p<0.01$), could be determined at day 0 and day 9. Data represent the average ± SD of three measurements.

As determined for adipogenesis on 2-D polymer films, increasing culture time resulted in a substantial rise in enzyme activity. After 4 days of adipogenesis, no differences in GPDH activity were detected between the different cell-polymer constructs (PGA: 599.2 ± 53.7 mU per mg protein, PLGA: 703.9 ± 84.4 mU per mg protein, Me.PEG$_2$PLA$_{20}$: 648.1 ± 49.6 mU per mg protein). However, at day 9, activity examined from Me.PEG$_2$PLA$_{20}$ scaffolds (1,088.5 ± 51.5 mU per mg protein) was slightly diminished relative to those investigated from PGA meshes (1,195.0 ± 7.3 mU per mg protein) ($p < 0.05$) and from PLGA scaffolds (1,265.6 ± 45.9 mU per mg protein) ($p < 0.01$).

Discussion

There is increasing evidence that the biomaterials used to create cell-polymer constructs in tissue engineering strongly affect the cellular phenotype. This observation appears to be attributable to the polymer properties known to direct the adsorption of adhesion-mediating proteins and, thereby, to modulate the features of the cells [8-11]. Accordingly, the adhesion of 3T3-L1 preadipocytes was demonstrated in previous experiments to depend on substrate hydrophobicity; i.e., hydrophilic Me.PEG$_2$PLA$_{20}$-films induced the adhered cells to adopt a spherical cell shape, whereas hydrophobic ones (PLA and PLGA) rather favored cell spreading [15,18]. As differentiation of 3T3-L1 preadipocytes is reported to be accompanied by cytoskleletal remodeling to rounded cells [12,19], the objective of this study was to investigate Me.PEG$_2$PLA$_{20}$ with regard to its capability of stimulating the differentiated adipose phenotype. Conventional TCPS and hydrophobic polymer films made from PLGA served as comparison.

The results of our study indicate that hydrophilic Me.PEG$_2$PLA$_{20}$ polymers only partially feature the hypothesized ability to distinctly promote adipogenesis. In terms of phenotype, we could demonstrate that adipocytes differentiated on Me.PEG$_2$PLA$_{20}$-films looked dissimilar as compared to PLGA and TCPS, i.e., they exhibited pronounced spherical morphology and larger intracellular lipid vacuoles. Methodologies employed to define the visible difference on the cellular and molecular level revealed enhanced leptin secretion relative to PLGA and TCPS. All investigated other parameters, however, yielded comparable results for all substrates. Equally, 3-D adipogenesis, which was estimated by only measuring GPDH activity, was not demonstrably improved on Me.PEG$_2$PLA$_{20}$-scaffolds, as compared to either PLGA scaffolds or PGA meshes.

In detail, the investigation of triglyceride (TG) storage was performed by oil red O staining of intracellular lipid droplets and, additionally, by biochemical assays to measure GPDH activity, a key enzyme of lipogenesis, and the intracellular TG content itself. While fewer adipocytes were attached to Me.PEG$_2$PLA$_{20}$-films, as compared to TCPS and PLGA, the cells exhibited a more spherical morphology and contained larger TG vacuoles (Fig. 2). The visible differences, however, were neither reflected by GPDH activity nor by intracellular TG content (Fig. 3, 4). Actually, TG measurement showed that adipocytes cultivated on PLGA-films contained the highest amount of stored TG (Fig. 4). This result, seemingly contradicting the microscopic observations, may be explained by the shape of the cells. On Me.PEG$_2$PLA$_{20}$, adipocytes round up easily and the distance between the accumulated TG vacuoles is thereby decreased. Hence, lipid droplets may coalesce more easily as compared to droplets in spread cells and, therefore, the amount of stored TG may only appear to be enhanced. In order to investigate a further marker characterizing mature adipocytes [27,28], the secretion rate of the satiety hormone leptin was investigated by ELISA. Thereby, enhanced concentrations of leptin were determined in media of Me.PEG$_2$PLA$_{20}$ cultures (Fig. 5), indicating altered adipocyte properties on Me.PEG$_2$PLA$_{20}$ films. With the aim of thoroughly examining the adipose phenotype on the different polymeric substrates, gene expression was furthermore analyzed on the mRNA level using RT-PCR. None of the typical fat cell genes investigated elucidated a substantial difference in gene expression of cells either cultured on TCPS, PLGA, or Me.PEG$_2$PLA$_{20}$ (Fig. 6). In order to assess the functionality of the differently cultivated cells, their lipolysis rate was examined. On all of the materials evaluated, isoproterenol treatment caused a significant increase in released glycerol as compared to control conditions (Fig. 7). In contrast, propranolol administration did not elicit the expected inhibitory effect. Nevertheless, no difference could be manifested for lipolytic cell response on the different substrates.

Me.PEG$_2$PLA$_{20}$ and PLGA were also processed into 3-D matrices, in order to examine the impact of the materials on 3-D differentiation. Subsequently, adipogenesis was estimated by both analyzing GPDH activity and by comparison with the recently established 3-D model system using PGA fiber meshes [20]. 3T3-L1 differentiation on all polymeric scaffolds resulted in appropriate triglyceride biosynthesis, as shown by GPDH activities, which were kinetically determined after hormonal stimulation (Fig. 8). At day 9, enzyme activities measured from Me.PEG$_2$PLA$_{20}$ constructs were similar to those assessed on PLGA, and PGA matrices. However, despite exhibiting values typical for late stages of adipogenesis, Me.PEG$_2$PLA$_{20}$ constructs contained fewer adhered cells, such that tissue coherence is likely

impaired. In order to comprehensively assess PEG_2PLA_{20} matrices with regard to their usefulness for adipose tissue engineering, further studies will be required.

In conclusion, we could demonstrate 3T3-L1 conversion into adipocytes on hydrophilic as well as on hydrophobic polymeric materials. Although substrate hydrophilicity strongly affected cell adhesion and adipocyte morphology, the key parameters of adipogenesis remained unchanged as compared to hydrophobic conditions. However, leptin secretion was increased on $Me.PEG_2PLA_{20}$, which may be ascribed to the spherical cell shape. In earlier reports, leptin expression was described as being dependent on tissue-derived factor(s) [29]. In an *in vivo* context, adipocytes interact differently with their environment, e.g. by adopting a round shape they are subject to 3-D cell-cell and cell-extracellular matrix (ECM) interactions. Hence, the rounded cells possibly express a distinct subset of the integrin ECM receptors as compared to cells in conventional 2-D cell culture. Recent evidence indicate that integrins, in turn, substantially contribute to the regulation of cellular gene expression [10]. On hydrophilic surfaces such as $Me.PEG_2PLA_{20}$, the cells are loosely attached and, thus, allowed to adopt a round shape, which is thought to positively affect their phenotype by better reflecting *in vivo* conditions. Although the methodologies employed so far were not suitable for elucidating the particular alterations, future studies, e.g. on integrins, may shed light on the reasons leading to altered morphology and enhanced leptin expression on $Me.PEG_2PLA_{20}$. The respective experiments may thereby participate in elucidating tissue-derived factors influencing leptin expression.

The data from this study indicate that $Me.PEG_2PLA_{20}$ polymers allow for adipogenesis of 3T3-L1 cells. However, they do not feature the hypothesized advantageous properties over PGA or PLGA polymers with respect to adipose tissue development. Nevertheless, by promoting rounding up of cells, $Me.PEG_2PLA_{20}$ polymer films are suggested as a valuable tool to investigate the impact of cell morphology on adipocyte properties isolated from other influences. The respective studies are thought to decisively contribute to gaining insight into how the cell shape affects adipocyte properties.

References

1. Langer, R. and Vacanti, J. P. (1993). Tissue engineering. *Science* **260**, 920-926.

2. Marler, J. J., Upton, J., Langer, R., and Vacanti, J. P. (1998). Transplantation of cells in matrices for tissue regeneration. *Adv.Drug Delivery Rev.* **33**, 165-182.

3. Thapa, A., Miller, D. C., Webster, T. J., and Haberstroh, K. M. (2003). Nano-structured polymers enhance bladder smooth muscle cell function. *Biomaterials* **24**, 2915-2926.

4. Kay, S., Thapa, A., Haberstroh, K. M., and Webster, T. J. (2002). Nanostructured polymer/nanophase ceramic composites enhance osteoblast and chondrocyte adhesion. *Tissue Eng.* **8**, 753-761.

5. Hallab, N. J., Bundy, K. J., O'Connor, K., Moses, R. L., and Jacobs, J. J. (2001). Evaluation of metallic and polymeric biomaterial surface energy and surface roughness characteristics for directed cell adhesion. *Tissue Eng.* **7**, 55-71.

6. Burmeister, J. S., McKinney, V. Z., Reichert, W. M., and Truskey, G. A. (1999). Role of endothelial cell-substrate contact area and fibronectin-receptor affinity in cell adhesion to HEMA/EMA copolymers. *J.Biomed.Mater.Res.* **47**, 577-584.

7. Khang, G., Lee, S. J., Lee, J. H., Kim, Y. S., and Lee, H. B. (1999). Interaction of fibroblast cells on poly(lactide-co-glycolide) surface with wettability chemogradient. *Biomed.Mater.Eng.* **9**, 179-187.

8. Webb, K., Hlady, V., and Tresco, P. A. (2000). Relationships among cell attachment, spreading, cytoskeletal organization, and migration rate for anchorage-dependent cells on model surfaces. *J.Biomed.Mater.Res.* **49**, 362-368.

9. Altankov, G., Thom, V., Groth, T., Jankova, K., Jonsson, G., and Ulbricht, M. (2000). Modulating the biocompatibility of polymer surfaces with poly(ethylene glycol): effect of fibronectin. *J.Biomed.Mater.Res.* **52**, 219-230.

10. Boudreau, N. J. and Jones, P. L. (1999). Extracellular matrix and integrin signalling: the shape of things to come. *Biochem.J.* **339 (Pt 3)**, 481-488.

11. Martin, I., Vunjak-Novakovic, G., Yang, J., Langer, R., and Freed, L. E. (1999). Mammalian Chondrocytes Expanded in the Presence of Fibroblast Growth Factor 2 Maintain the Ability to Differentiate and Regenerate Three-Dimensional Cartilaginous Tissue. *Exp.Cell Res.* **253**, 681-688.

12. Spiegelman, B. M. and Farmer, S. R. (1982). Decreases in tubulin and actin gene expression prior to morphological differentiation of 3T3 adipocytes. *Cell* **29**, 53-60.

13. Fuchs, J. R., Nasseri, B. A., and Vacanti, J. P. (2001). Tissue engineering: a 21st century solution to surgical reconstruction. *Ann.Thorac.Surg.* **72**, 577-591.

14. Lucke, A., Tessmar, J., Schnell, E., Schmeer, G., and Göpferich, A. (2000). Biodegradable poly(D,L-lactic acid)-poly(ethylene glycol)-monomethyl ether diblock copolymers: Structures and surface properties relevant to their use as biomaterials. *Biomaterials* **21**, 2361-2370.

15. Fischbach, C., Tessmar, J., Lucke, A., Schnell, E., Schmeer, G., Blunk, T., and Göpferich, A. (2001). Does UV irradiation affect polymer properties relevant to tissue engineering? *Surf.Sci.* **491**, 333-345.

16. Göpferich, A., Peter, S. J., Lucke, A., Lu, L., and Mikos, A. G. (1999). Modulation of marrow stromal cell function using poly(D,L-lactic acid)- block-poly(ethylene glycol)-monomethyl ether surfaces. *J.Biomed.Mater.Res.* **46**, 390-398.

17. Lieb, E., Tessmar, J., Hacker, M., Fischbach, C., Rose, D., Blunk, T., Mikos, A. G., Göpferich, A., and Schulz, M. B. (2003). Poly(D,L-lactic acid)-poly(ethylene glycol)-monomethyl ether diblock copolymers control adhesion and osteoblastic differentiation of marrow stromal cells. *Tissue Eng.* **9**, 71-84.

18. Tessmar, J., Fischbach, C., Lucke, A., Blunk, T., and Göpferich, A. PEG-PLA diblock copolymers for the control of biomaterial-cell interaction. BioValley Tissue Engineering Symposium 2 (Freiburg). 25-11-1999.

19. Gregoire, F. M., Smas, C. M., and Sul, H. S. (1998). Understanding adipocyte differentiation. *Physiol.Rev.* **78**, 783-809.

20. Fischbach, C., Seufert, J., Staiger, H., Hacker, M., Neubauer, M., Göpferich, A., and Blunk, T. (2003). 3-D *in vitro*-Model of Adipogenesis – Comparison of Culture Conditions. *Tissue Eng.* **in press**.

21. Hacker, M., Tessmar, J., Neubauer, M., Blunk, T., Göpferich, A., and Schulz, M. B. (2003). Towards biomimetic scaffolds: Anhydrous scaffold fabrication from biodegradable amine-reactive diblock copolymers. *Biomaterials* **in press**.

22. Hausman, G. J. (1981). Techniques for studying adipocytes. *Stain Technol.* **56**, 149-154.

23. Bachmeier, M. and Loffler, G. (1995). Influence of growth factors on growth and differentiation of 3T3-L1 preadipocytes in serum-free conditions. *Eur.J.Cell Biol.* **68**, 323-329.

24. Pairault, J. and Green, H. (1979). A study of the adipose conversion of suspended 3T3 cells by using glycerophosphate dehydrogenase as differentiation marker. *Proc.Natl.Acad.Sci.U.S.A.* **76**, 5138-5142.

25. Lowry, O. H., Rosebrough, N. J., Farr, A. L., and Randall, R. J. (1951). Protein measurement with the Folin phenol reagent. *J.Biol.Chem.* **193**, 265-275.

26. El Awad, B., Kreft, B., Wolber, E. M., Hellwig-Burgel, T., Metzen, E., Fandrey, J., and Jelkmann, W. (2000). Hypoxia and interleukin-1beta stimulate vascular endothelial growth factor production in human proximal tubular cells. *Kidney Int.* **58**, 43-50.

27. MacDougald, O. A., Hwang, C. S., Fan, H., and Lane, M. D. (1995). Regulated expression of the obese gene product (leptin) in white adipose tissue and 3T3-L1 adipocytes. *Proc.Natl.Acad.Sci.U.S.A.* **92**, 9034-9037.

28. Hwang, C. S., Loftus, T. M., Mandrup, S., and Lane, M. D. (1997). Adipocyte differentiation and leptin expression. *Annu.Rev.Cell Dev.Biol.* **13**, 231-259.

29. Mandrup, S., Loftus, T. M., MacDougald, O. A., Kuhajda, F. P., and Lane, M. D. (1997). Obese gene expression at in vivo levels by fat pads derived from s.c. implanted 3T3-F442A preadipocytes. *Proc.Natl.Acad.Sci.U.S.A.* **94**, 4300-4305.

Chapter 8

Summary and Conclusions

Summary and Conclusions

Adipose tissue has long been considered a passive organ primarily responsible for the storage and release of energy. Recent scientific advances have dramatically altered our understanding and suggest that this ubiquitous tissue is a secretory organ exerting far-ranging effects on a variety of physiological functions [1-3]. In order to gain a more complete comprehension of adipogenesis holding the promise of improved treatment strategies for obesity, adipose tissue is increasingly addressed by basic research [4]. Furthermore, it is employed as natural filling material for the restoration of soft tissue defects in plastic and reconstructive surgery [5,6]. In both fields, however, the presently applied strategies possess major limitations. Generation of fat equivalents through means of TE holds great promise to overcome these shortcomings by allowing for investigations of adipogenesis within a tissue-like context. So far, none of the current approaches succeeded in engineering such constructs. Therefore, the ultimate goal of this thesis was to develop a coherent fat-like model system applicable to investigate adipocyte differentiation under standardized conditions *in vitro* and *in vivo*.

In order to provide reproducible experimental conditions, the 3-D model system was composed of the well-characterized preadipocyte cell line 3T3-L1 and commercially available PGA fiber meshes as highly porous polymeric cell carrier. The first aim on the way to establish the model system was to evaluate appropriate cultivation conditions (chapter 2, 3). Subsequently, coherent constructs were generated in either short-term (chapter 4) or long-term culture (chapter 5) and comprehensively characterized with regard to fat-like properties on the histological, cellular, and molecular level. Furthermore, their development was assessed under physiological conditions *in vivo* (chapter 5) Finally, alternative polymers were investigated with regard to their usefulness for adipose tissue engineering (chapter 7). Before studying adipogenesis on these biomaterials, the impact of sterilizing UV irradiation on Me.PEG-PLA characteristics was thoroughly addressed in order to ensure unchanged polymer properties even after exposure to UV light (chapter 6).

Specifically, appropriate culture conditions were determined by evaluating both tissue-inducing substances (chapter 2) and culture methodologies (chapter 3) with regard to their suitability for generating coherent fat-like constructs. At first, it was thoroughly investigated to what extent the two commercially available media alpha-MEM and DMEM impact adipogenesis. Simultaneously, three different hormonal induction protocols (control

(corticosterone, IBMX, and insulin), control + 60 µM indomethacin, control + 5 µM troglitazone) were examined (chapter 2). The results of the study indicated that adipose conversion of 3T3-L1 cells was substantially improved in alpha-MEM as compared to DMEM. Furthermore, hormonal induction under control conditions and additional indomethacin equally resulted in appropriate differentiation properties, which were shown to prove suitable for the TE of fat. In contrast, supplementary troglitazone was considered as being less suitable for this purpose. Accordingly, the further experiments towards the development of a 3-D model system of adipogenesis were conducted in alpha-MEM and adipocyte differentiation was initiated by treatment with a hormonal cocktail consisting of corticosterone, IBMX, insulin, and indomethacin.

With the objective of properly assembling fat-like constructs, distinct static and dynamic cultivation conditions were evaluated (chapter 3). In detail, cell seeding was performed either statically by pipetting a cell suspension onto the scaffolds or dynamically by subjecting the meshes to mixing conditions in stirred bioreactors. The dynamic procedure, as compared to the static one, yielded more uniform cell distribution and more densely seeded constructs. For these reasons, it was regarded as being most suitable for the following experiments. Distinct cultivation conditions were examined by culturing the cell-polymer constructs either statically or dynamically in well-plates or in stirred bioreactors. Thereby, it could be shown that static cultivation in well plates is inferior to dynamic conditions with regard to the generation of adipose tissue. As the bioreactor approach did not feature any advantages over dynamic cultivation in well plates but, on the contrary, entailed enhanced experimental requirements, it was considered to be an inappropriate method to be routinely applied. Consequently, assembly of the constructs was performed by dynamic cell seeding in stirred bioreactors followed by dynamic cultivation in agitated well-plates.

The next aim was to employ the established cultivation conditions for the generation of coherent fat-like constructs, which were subsequently characterized comprehensively. At first, adipose tissue properties were investigated after short-term culture over 9 days (chapter 4). In addition to featuring tissue-like coherence, the engineered constructs were thereby shown to exhibit typical characteristics of mature adipocytes, which were comparable to those of conventional 2-D cell culture. In order to dissect the results more precisely, the constructs were die-punched. Thereby, it could be assessed that they were composed of well-differentiated cells in outer areas and less differentiated ones in internal parts. Furthermore, as compared to native fat, the adipocytes had not yet adopted the typical signet-ring form of unilocular cells. In order to address this distinction, the constructs were differentiated for

prolonged periods of time (up to 35 days) (chapter 5). Analysis of the resulting tissues elucidated completion of reorganization to structures histologically comparable to those of native adipose tissue. The microscopic observations could be supported by investigations on the cellular and the molecular level. Thereby, for the first time, the formation of a coherent fat-like tissue consisting of unilocular cells and ECM containing laminin as a key component of the basement membrane could be demonstrated *in vitro*. Finally, the question arose how the engineered constructs progress under physiological conditions *in vivo* (chapter 5). Injection (s.c.) of a 3T3-L1 single cell suspension has not been shown to develop into mature fat pads *in vivo* [7,8]. Therefore, it was aimed at investigating if implantation of 3T3-L1 in the form of coherent tissue-like constructs helps to overcome this limitation and ultimately allows for reorganization into fat pads. Not only were differentiated constructs s.c. implanted into nude mice but also PGA meshes seeded with undifferentiated 3T3-L1 preadipocytes. Subsequent to their excision, it could be shown for the first time that 3T3-L1 cells, when transplanted in the form of differentiated TE constructs, yielded vascularized fat pads histologically comparable to native fat. In contrast, blank control meshes and preadipocyte-seeded scaffolds did not result in adipose tissue formation *in vivo*.

Recently, Me.PEG-PLAs diblock copolymers have been developed for controlled cell-biomaterial interactions [9]. They were demonstrated to promote osteoblast differentiation and to modify 3T3-L1 adhesion behavior [10-12]. To examine these novel biomaterials in terms of their suitability for adipose TE, they were processed into both 2-D polymer films and 3-D scaffolds. Prior to contact with the cells, the carriers were sterilized by UV irradiation. In order not to compromise the polymer properties relevant to TE, an appropriate duration of exposure to UV light had to be assessed. For this purpose, films were subjected to UV irradiation for different periods of time and subsequently polymer properties were extensively addressed (chapter 6). The results indicated that UV treatment for 2 hours is an appropriate technique for sterilization of the Me.PEG-PLAs. However, UV irradiation for extended periods of time (5 and more hours) drastically altered the properties of the polymer films. Hence, adipogenesis on Me.PEG-PLAs was studied on cell carriers, which were previously sterilized by exposure to UV light for 2 hours (chapter 7). Although Me.PEG2-PLA20 polymers were thereby demonstrated to allow for adipogenesis of 3T3-L1 cells, the data from this study did not reveal the hypothesized advantage over PGA or PLGA polymers with respect to adipose tissue development. Nevertheless, by promoting rounding up of cells, Me.PEG2-PLA20 polymer films are suggested as a valuable tool to investigate the sole impact of cell morphology on adipocyte properties.

In summary, this thesis for the first time demonstrated the development of a coherent fat-like tissue *in vitro*. By comprehensively evaluating various strategies of TE it was possible to stimulate 3-D cultivated 3T3-L1 preadipocytes to differentiate into mature adipocytes and, above all, to induce their reorganization into constructs histologically comparable to native fat. Furthermore, it could be shown, that s.c. implantation of these engineered tissues into nude mice allows for development of vascularized fat pads *in vivo*. So far, 3T3-L1 cells, in contrast to 3T3-F442A, were considered to not give rise to adipose tissue *in vivo*. Hence, TE was proven useful to establish a valuable tool for investigation of adipogenesis within a tissue-like environment *in vitro* and *in vivo*. By recreating 3-D cell-cell and cell-ECM interactions as they are present within real tissues, a model system has become available entailing particular significance for both fat grafting and basic research. Application of the model *in vitro* is suggested to elucidate the impact of isolated manipulations under standardized conditions. Additionally, *in vivo* studies can be performed enabling verification of the results determined *in vitro* and furthermore analysis of effects mediated through the physiological surrounding.

The model system presented here could be used in future studies directed at clarifying the tissue-derived factors(s) potentially involved in appropriate expression of certain fat cell genes. For example, *in vivo* production of leptin by far exceed protein secretion in 2-D cell culture [8,13]. Therefore, it is thought that basic research may profit from the 3-D model as further investigations of the endocrine functions of adipocytes can be carried out in a tissue-like context. Alternatively, the model system may be used for co-culture experiments. For instance, a combination of adipocytes and endothelial cells may prove helpful to define novel strategies for improved neovascularization of fat-grafts. This is likely to serve plastic and reconstructive surgery by potentially improving cell survival rates and, thus, success of fat transplantation. Furthermore, basic research may benefit from such a co-culture approach by possibly gaining a more complete comprehension of how both cell types interact with each other. Detailed insights into these interactions, in turn, is suggested to contribute to a better understanding of adipose tissue physiology and development of obesity.

References

1. Gregoire, F. M., Smas, C. M., and Sul, H. S. (1998). Understanding adipocyte differentiation. *Physiol.Rev.* **78**, 783-809.

2. Diamond, F. B., Jr. and Eichler, D. C. (2002). Leptin and the adipocyte endocrine system. *Crit.Rev.Clin.Lab.Sci.* **39**, 499-525.

3. Morrison, R. F. and Farmer, S. R. (2000). Hormonal signaling and transcriptional control of adipocyte differentiation. *J.Nutr.* **130**, 3116S-3121S.

4. Sorisky, A. (1999). From preadipocyte to adipocyte: differentiation-directed signals of insulin from the cell surface to the nucleus. *Crit.Rev.Clin.Lab.Sci.* **36**, 1-34.

5. Billings, E. J. and May, J. W., Jr. (1989). Historical review and present status of free fat graft autotransplantation in plastic and reconstructive surgery. *Plast.Reconstr.Surg.* **83**, 368-381.

6. Smahel, J. (1986). Adipose tissue in plastic surgery. *Ann.Plast.Surg.* **16**, 444-453.

7. Green, H. and Kehinde, O. (1979). Formation of normally differentiated subcutaneous fat pads by an established preadipose cell line. *J.Cell.Physiol.* **101**, 169-171.

8. Mandrup, S., Loftus, T. M., MacDougald, O. A., Kuhajda, F. P., and Lane, M. D. (1997). Obese gene expression at in vivo levels by fat pads derived from s.c. implanted 3T3-F442A preadipocytes. *Proc.Natl.Acad.Sci.U.S.A.* **94**, 4300-4305.

9. Lucke, A., Tessmar, J., Schnell, E., Schmeer, G., and Göpferich, A. (2000). Biodegradable poly(D,L-lactic acid)-poly(ethylene glycol)-monomethyl ether diblock copolymers: Structures and surface properties relevant to their use as biomaterials. *Biomaterials* **21**, 2361-2370.

10. Göpferich, A., Peter, S. J., Lucke, A., Lu, L., and Mikos, A. G. (1999). Modulation of marrow stromal cell function using poly(D,L-lactic acid)- block-poly(ethylene glycol)-monomethyl ether surfaces. *J.Biomed.Mater.Res.* **46**, 390-398.

11. Lieb, E., Tessmar, J., Hacker, M., Fischbach, C., Rose, D., Blunk, T., Mikos, A. G., Göpferich, A., and Schulz, M. B. (2003). Poly(D,L-lactic acid)-poly(ethylene glycol)-monomethyl ether diblock copolymers control adhesion and osteoblastic differentiation of marrow stromal cells. *Tissue Eng.* **9**, 71-84.

12. Tessmar, J., Fischbach, C., Lucke, A., Blunk, T., and Göpferich, A. PEG-PLA diblock copolymers for the control of biomaterial-cell interaction. BioValley Tissue Engineering Symposium 2 (Freiburg). 25-11-1999.

13. MacDougald, O. A., Hwang, C. S., Fan, H., and Lane, M. D. (1995). Regulated expression of the obese gene product (leptin) in white adipose tissue and 3T3-L1 adipocytes. *Proc.Natl.Acad.Sci.U.S.A.* **92**, 9034-9037.

Appendix

1. List of abbreviations

AFM	atomic force microscopy
α-Mem	modified Eagle's medium, alpha-modification
Ang	angiotensinogen
AT	annealing temperature
ATCC	American Type Culture Collection
beta3-AR	beta 3-adrenoreceptor
bFGF	basic fibroblast growth factor
BSA	bovine serum albumin
cAMP	cyclic adenosin 3´,5´´-monophosphate
cDNA	complementary deoxyribonucleic acid
C/EBPs	CCAAT/enhancer binding proteins
CS	calf serum
3-D; 2-D	three-dimensional; two-dimensional
DMEM	Dulbecco´s modified Eagle's medium
DNA	deoxyribonucleic acid
ECM	extracellular matrix
ELISA	enzyme linked immuno sorbent assay
ETO	ethylene oxide
FBS	fetal bovine serum
FFA	free fatty acids
GLUT-4	glucose transporter 4
GPC	gel permeation chromatography
GPDH	glycerol-3-phosphate dehydrogenase
H&E	hematoxylin and eosin
^{1}H-NMR	proton nuclear magnetic resonance
IBMX	3-isobutyl-1-methylxanthine
IGF-1	insulin like growth factor 1
IL-6	interleukin 6
IRS	insulin receptor substrate
kDa	kilodalton
Me.PEG	poly(ethylene glycol)-monomethyl ether
Me.PEG-PLA	poly(D,L-lactic acid)-poly(ethylene glycol)-monomethyl ether diblock copolymer
MMP	matrix metallo-proteinase

MW	molecular weight
Mn	number average molecular weight
Mw	weight average molecular weight
NCS	newborn calf serum
PAI-1	plasminogen activator inhibitor 1
PBS	phosphate-buffered saline
RT-PCR	reverse transcription polymerase chain reaction
PEG	poly(ethylene glycol)
PGA	polyglycolic acid
PI	polydispersity index
PLA	polylactic acid
PLGA	poly (lactic-co-glycolic acid)
PP	polypropylene
PPARγ	peroxisome proliferator-activated receptor γ
RNA	ribonucleic acid
rRNA	ribosomal ribonucleic acid
rpm	rotations per minute
RT-PCR	reverse transcription polymerase chain reaction
s.c.	subcutaneously
Scd-1	stearoyl-CoA desaturase 1
SD	standard deviation
SEM	scanning electron microscopy
TCPS	tissue culture polystyrene
TE	tissue engineering
TG	triglyceride
TMS	tetramethylsilane
TNFα	tumor necrosis factor α
UV	ultraviolet light
VEGF	vascular endothelial growth factor
WAT	white adipose tissue
XPS	X-ray photoelectron spectroscopy

2. Primer Sequences and PCR Conditions

Gene	Forward and reverse primers of examined genes	AT (°C) / Cycles
Angiotensinogen	5′-CTG GCC GCC GAG AAG CTA GAG GAT GAG GA-3′ 5′-GAG AGC GTG GGA AGA GGG CAG GGG TAA AGA G-3′	62 / 35
Beta3-AR	5′-CAG TGG TGG CGT GTA GGG GCA GAT-3′ 5′-CGG GTT GAA GGC GGA GTT GGC ATA G-3′	63 / 36
GLUT-4	5′-CCC CGC TGG AAT GAG GTT TTT GAG GTG AT-3′ 5′-CAG ACA GGG GCC GAA GAT TGG GAG ACA GT-3′	61 / 35
Laminin-α4[1)]	5′-CAT GGG ATC CTA TTG GCC TG-3′ 5′-CAC ATA GCC GCC TTC TGT GG-3′	60 / 30
Laminin-β1	5′-GCT GGA TCC GCT TGC AGC AGA GTG CAG CTG A-3′ 5′-CGC GAA TTC GCT AAG CAG GTG CTG TAA ACC G-3′	60 / 30
Laminin-γ1	5′-GCG GGA TCC CCA ATG ACA TTC TCA ACA AC-3′ 5′-GCA GAT ATC GGG CTT CTC GAT AGA CGG GG-3′	60 / 30
Leptin	5′-GAC ACC AAA ACC CTC ATC AAG ACC-3′ 5′-GCA TTC AGG GCT AAC ATC CAA CT-3′	58,5 / 36
PPARγ	5′-AAC CTG CAT CTC CAC CTT ATT ATT CTG A-3′ 5′-GAT GGC CAC CTC TTT GCT CTG CTC CTG-3′	60 / 35
VEGF[2)]	5′-ATA GCG GAT GGA AAA CCC TGC-3′ 5′-TAT CGC CTA CCT TTT GGG ACG 3′	60 / 40
18 S	5′-TCA AGA ACG AAA GTC GGA GGT TCG-3′ 5′-TTA TTG CTC AAT CTC GGG TGG CTG-3′	60 / 26

Step	Temp. (°C)	Duration (sec)	Cycles
Initial denaturation	94	120	1
Denaturation	94	45	as indicated
Annealing	as indicated	45	
Extension	72	60	
Terminal extension	72	30	1

PCR for laminin and VEGF were conducted according to:

[1)] Niimi, T., Kumagai, C., Okano, M., and Kitagawa, Y. (1997). Differentiation-dependent expression of laminin-8 (alpha 4 beta 1 gamma 1) mRNAs in mouse 3T3-L1 adipocytes. *Matrix Biol.* **16**, 223-230.
(denaturation for 30 sec at 94°C, annealing for 60 sec at 60°C, and extension for 60 sec at 72°C)

[2)] El Awad, B., Kreft, B., Wolber, E. M., Hellwig-Burgel, T., Metzen, E., Fandrey, J., and Jelkmann, W. (2000). Hypoxia and interleukin-1beta stimulate vascular endothelial growth factor production in human proximal tubular cells. *Kidney International* **58**, 43-50.
(denaturation for 30 sec at 94°C, annealing for 60 sec at 60°C, and extension for 2 min at 68°C).

3. Chemicals and Instruments

Chemicals:

Cell Culture		
Fetal bovine serum (FBS)	Biochrom KG seromed	Berlin, Germany
DMEM, 1.0 g glucose	Biochrom KG seromed	Berlin, Germany
MEM, alpha-modification	Sigma-Aldrich	Deisenhofen, Germany
10,000 U/ml penicillin, 10,000 µg/ml streptom.	Invitrogen GmbH	Karlsruhe, Germany
PBS	Invitrogen GmbH	Karlsruhe, Germany
DMSO	Merck KGaA	Darmstadt, Germany
Ethanol	Merck KGaA	Darmstadt, Germany
NaHCO3	Sigma-Aldrich	Deisenhofen, Germany
Trypsin 1:250	Biochrom KG seromed	Berlin, Germany
3-isobutyl-1-methylxanthine	Serva Electrophoresis GmbH	Heidelberg, Germany
Corticosterone	Sigma-Aldrich	Deisenhofen, Germany
Insulin, porcine	Hoechst Marion Roussel	Frankfurt am Main, Germany
Troglitazone	gift from T. Skurk	DDF, Duesseldorf, Germany
Indomethacin	Sigma-Aldrich	Deisenhofen
GPDH-Assay		
Substances Z2-Buffer	Merck KGaA	Darmstadt, Germany
NADH, disodium salt, grade II	Roche Diagnostics	Mannheim, Germany
Dihydroxyacetone phosphate	Sigma-Aldrich	Deisenhofen, Germany
Mercaptoethanol	Sigma-Aldrich	Deisenhofen, Germany
Triethanolamin	Merck KGaA	Darmstadt, Germany
Cuvets	Sarstedt AG & Co.	Nuembrecht, Germany
Lowry		
Albumin, bovine, lyophilized, >98%, Fraction V	Sigma-Aldrich	Deisenhofen, Germany
Trichloressigsäure	Carl Roth GmbH & Co.	Karlsruhe, Germany
Substances Z2-Buffer	Merck KGaA	Darmstadt, Germany
Folin-Ciocalteu reagent	Merck KGaA	Darmstadt, Germany
Bradford		
Serva Blue G 250	Serva Electrophoresis GmbH	Heidelberg, Germany
H3PO4	Merck KGaA	Darmstadt, Germany
Ethanol	Carl Roth GmbH & Co.	Karlsruhe, Germany
Albumin, bovine, lyophilized, >98%, Fraction V	Sigma-Aldrich	Deisenhofen, Germany
Oil red O staining		
Oil Red O	Sigma-Aldrich	Deisenhofen, Germany
Formaldehyde	Merck KGaA	Darmstadt, Germany
Isopropanol	Carl Roth GmbH & Co.	Karlsruhe, Germany
SEM		
Glutardialdehyde	Sigma-Aldrich	Deisenhofen, Germany
Osmium tetroxide	Carl Roth GmbH & Co.	Karlsruhe, Germany
PBS	Invitrogen GmbH	Karlsruhe, Germany
Lipolysis		
Albumine bovine Fraction V, Fatty acid free	Sigma-Aldrich	Deisenhofen, Germany
Isoproterenol	Sigma-Aldrich	Deisenhofen, Germany
DL-Propranolol, HCl	Sigma-Aldrich	Deisenhofen, Germany
PBS	Invitrogen GmbH	Karlsruhe, Germany
Triglyceride (GPO-Trinder) Nr. 337	Sigma Diagnostics	St. Louis, MO, USA
Cuvets	Sarstedt AG & Co.	Nuembrecht, Germany

DNA-Assay		
DNA-Na salt	Sigma-Aldrich	Deisenhofen, Germany
Hoechst 33258 dye	Polysciences	Warrington, PA, USA
Substances for TEN-Puffer	Merck KGaA	Darmstadt, Germany
Substances for Phosphat and Papain-Puffer	Merck KGaA	Darmstadt, Germany
Trizma, base, HCl	Sigma-Aldrich	Deisenhofen, Germany
Glycine	Sigma-Aldrich	Deisenhofen, Germany
EDTA	Sigma-Aldrich	Deisenhofen, Germany
Papainase	CellSystem	St. Katharinen, Germany
Leptin-ELISA		
Quantikine M	R&D Systems GmbH	Wiesbaden, Germany
RT-PCR		
Trizol	Invitrogen GmbH	Karlsruhe, Germany
Chloroform	Carl Roth GmbH & Co.	Karlsruhe, Germany
Isopropanol	Carl Roth GmbH & Co.	Karlsruhe, Germany
Diethyl pyrocarbonate	Sigma-Aldrich	Deisenhofen
Superscript II RNase H- Reverse Transcriptase	Invitrogen GmbH	Karlsruhe, Germany
RNaseOUT	Invitrogen GmbH	Karlsruhe, Germany
Primer "random" pdN6	Roche Diagnostics	Mannheim, Germany
Peq Gold dNTP-Set	PeqLab	Erlangen, Germany
Sawady Taq-DNA-Polymerase	PeqLab	Erlangen, Germany
Agarose	Invitrogen GmbH	Karlsruhe, Germany
Glycerol	Merck KGaA	Darmstadt, Germany
EDTA	Sigma-Aldrich	Deisenhofen
Bromphenolblau	Serva Electrophoresis GmbH	Heidelberg, Germany
Xylene cyanole FF	Sigma-Aldrich	Deisenhofen
TAE-Buffer	Sigma-Aldrich	Deisenhofen
Ethidium bromide	Sigma-Aldrich	Deisenhofen
Histology		
Formaldehyde	Merck KGaA	Darmstadt, Germany
Hematoxylin	Sigma-Aldrich	Deisenhofen
Tissue Tek	Sakura Finetek	Torrane, CA, USA
rabbit anti-mouse laminin antibody	Novus Biologicals, Inc.	Littleton, CO, USA
H2O2	Merck KGaA	Darmstadt, Germany
normal horse serum	Vector Laboratories Inc.	Burlingame, CA, USA
biotinylated horse anti-rabbit IgG antibody	Vector Laboratories Inc.	Burlingame, CA, USA
Vectastain Elite ABC-Kit	Vector Laboratories Inc.	Burlingame, CA, USA
DAB Substrate Kit for Peroxidase	Vector Laboratories Inc.	Burlingame, CA, USA
DPX Mountant	Fluka, Biochemika	Taufkirchen, Germany
Western Blot		
High Molecular Weigth Standard Mixture for SDS Gel Electrophoresis (SDS-6H)	Sigma Diagnostics	St. Louis, MO, USA
ECL	Amersham Biosciences	Freiburg, Germany
C/EBPalpha, polyclonal (14AA)	Santa Cruz Inc.	Heidelberg, Germany
PPARgamma, monoclonal (E-8)	Santa Cruz Inc.	Heidelberg, Germany
Polymerfilms		
Silikon-Kleber: Elastosil E4 Transparent (Best.-Nr.: 70107016)	Drawin Vertriebs GmbH	Ottobrunn, Germany

Instruments:

Cell Culture		
Magnetic stir plate	Bellco Glas	Vineland, NJ, USA
Nuaire US Autoflow, CO2 Water-Jacketed Incubator	Zapf Instruments	Sarstedt, Germany
Stuart Scientific Mini Orbital Shaker SO5	Dunn Labortechnik GmbH	Asbach, Germany
LF-Box: Hera safe	Kendro Laboratory Products GmbH	Hanau, Germany
Pipetus-akku	Hirschmann Laborgeräte GmbH & Co.KG	Eberstadt, Germany
Beckmann GS-15 R Centrifuge	Beckmann Instruments Inc.	Fullerton, CA, USA
Needles 0.5x100 mm, (Punktionskanülen, Best.-Nr. 13.201)	Unimed	Lausanne, Switzerland
GPDH-Assay		
sonifier	Branson Ultrasonic Corporation	Danburg, CT, USA
cell scraper	Biochrom KG seromed	Berlin, Germany
Centrifuge 5415 R	Eppendorf AG	Hamburg, Germany
spectrophotometer: Uvicon 941	Bio-Tek Kontron Instruments	Neufahrn, Germany
cuvets	Sarstedt AG & Co.	Nuembrecht, Germany
-20°C freezer: Privileg Oeko	Quelle AG	Fuerth, Germany
refrigerator: Senator automatic	Gustav Schickedanz KG	Fuerth, Germany
Lowry		
Vortex mixer: Heidolph Reax control	Heidolph Instruments GmbH & Co. KG	Schwabach, Germany
Centrifuge 5415 R	Eppendorf AG	Hamburg, Germany
spectrophotometer: Uvicon 941	Bio-Tek Kontron Instruments	Neufahrn, Germany
cuvets	Sarstedt AG & Co.	Nuembrecht, Germany
Bradford		
CS-9301 PC Dual wavelength flying spot scanning densitometer	Shimadzu Deutschland GmbH	Duisburg, Germany
96 well plates		
SEM		
lyophilization: Christ Beta 2-16	Martin Christ Gefriertrocknungs-anlagen GmbH	Osterode am Harz, Germany
gold-coater (Rose): Polaron E 520 automatic sputter coater	Polaron Equipment Ltd.	Watford, UK
gold-palladium (Zoologie): Polaron SC515	Fisons surface systems	Grinstead, UK
Microscop (Rose): JEOL JSM-840	Jeol Ltd.	Tokio, Japan
Microscop (Zoologie): DSM 950	Carl Zeiss	Oberkochen, Germany
Lipolysis		
spectrophotometer: Uvicon 941	Bio-Tek Kontron Instruments	Neufahrn, Germany
cuvets	Sarstedt AG & Co.	Nuembrecht, Germany

DNA-Assay		
spectrophotometer: Uvicon 941	Bio-Tek Kontron Instruments	Neufahrn, Germany
water bath	Memmert	Schwabach, Germany
spectrofluorometer: RF-1501	Shimadzu Deutschland GmbH	Duisburg, Germany
Polystyrene Fluorimeter cuvets	Sigma-Aldrich	Deisenhofen, Germany
Centrifuge 5415 R	Eppendorf AG	Hamburg, Germany
Leptin-ELISA		
CS-9301 PC Dual wavelength flying spot scanning densitometer	Shimadzu Deutschland GmbH	Duisburg, Germany
Centrifuge 5415 R	Eppendorf AG	Hamburg, Germany
-80°C freezer: Hera freeze	Kendro Laboratory Products GmbH	Hanau, Germany
RT-PCR		
Centrifuge 5415 R	Eppendorf AG	Hamburg, Germany
thermocycler: Mastercycler Gradient	Eppendorf, AG	Hamburg, Germany
spectrophotometer: Uvicon 941	Bio-Tek Kontron Instruments	Neufahrn, Germany
Microwave Privileg 8018	Quelle AG	Fuerth, Germany
electrophoresis power supply: Power PAC 200	Bio-Rad Laboratories GmbH	Muenchen, Germany
electrophoresis chambers: Wide Mini-Sub Cell GT	Bio-Rad Laboratories GmbH	Muenchen, Germany
shaker: SM	Edmund Buehler Laborgeraetebau	Tuebingen, Germany
Transilluminator 312 nm: Fisherbrand FT-20/312	Herolab GmbH Laborgeraete	Wiessloch, Germany
Kodak Electrophoresis Documentation & Analysis System EDAS 290	Fisher Scientific GmbH	Schwerte, Germany
Histology		
cryotome: 2800 Frigocut E	Cambridge Instruments GmbH	Nussloch, Germany
microscope: Leica DM IRB	Leica Microsystems AG	Wetzlar, Germany
camera: Dynax 600 si classic	MINOLTA Europe GmbH	Langenhagen, Germany
microscope slides: SuperFrost rosa (76x26 mm)	Carl Roth GmbH & Co.	Karlsruhe, Germany
Western Blot		
Centrifuge 5415 R	Eppendorf AG	Hamburg, Germany
Ultraschallbad: Sonorex RK 106 Transistor	Bandelin Electronic KG	Berlin, Germany
-80°C freezer: Hera freeze	Kendro Laboratory Products GmbH	Hanau, Germany

4. Curriculum Vitae

Name:	Claudia Fischbach
Date of birth:	17.03.1973
Place of birth:	Dohna, Germany
Nationality:	German

Education

07/1992	**Dossenberger Gymnasium, *Günzburg*** Abitur
09/1992 – 04/1993	**PTA School, *Augsburg*** Apprenticeship as pharmaceutical technical assistant.
05/1993 – 05/1997	**Ludwig-Maximilians-University, *Munich*** Study of Pharmacy.

Professional Experience

05/1997 – 10/1997	**Boehringer Ingelheim, *Biberach*** Traineeship in pharmaceutical industry.
11/1997 – 07/1998	**Bahnhofsapotheke, *Krumbach*** Traineeship in a public pharmacy.
07/1998	Aquisition of the license to practice as pharmacist.
10/1998 - present	**University of Regensburg, *Regensburg*** PhD program at the Department of Pharmaceutical Technology, Prof. Achim Göpferich Subject: Tissue Engineering of Adipose Tissue.

Scholarship

11/2002 - present	**HWP Scholarship** Hochschul- und Wissenschaftsprogramm Programm zur Förderung der Chancengleichheit von Frauen in Forschung und Lehre.

5. List of Publications

Publications:

1. Fischbach, C., Tessmar, J., Lucke, A., Schnell, E., Schmeer, G., Blunk, T., and Göpferich, A. Does UV irradiation affect polymer properties relevant to tissue engineering? Surf Sci 2001: 491: 333-345. **(Chapter 6)**

2. Tessmar, J., Fischbach, C., Lucke, A., Schnell, E., Schmeer, G., Blunk, T., and Göpferich, A. Reaktive PEG-PLA Diblockcopolymere zur Kontrolle der Wechselwirkungen zwischen Zellen und Biomaterial. In: Wisser A, Nachtigall W, eds. Biona report 14. Mainz: Akademie der Wissenschaften und der Literatur, 2002: 66-68.

3. Maschke A., Lucke, A., Vogelhuber, W., Fischbach, C., Appel, B., Blunk, T., and Göpferich, A. Lipids: An Alternative Material for Protein and Peptide Release. In: Svenson Sonke, ed. Carrier Based Drug Delivery. American Chemical Society, 2002.

4. Lieb, E., Tessmar, J., Hacker, M., Fischbach, C., Rose, D., Blunk, T., Mikos, A.G., Göpferich, A., and Schulz, M.B. Poly(D,L-lactic acid)-poly(ethylene glycol)-monomethyl ether diblock copolymers control adhesion and osteoblastic differentiation of marrow stromal cells. Tissue Eng 2003: 9: 71-84.

5. Fischbach, C., Seufert, J., Staiger, H., Hacker, M., Neubauer, M., Göpferich, A., and Blunk, T. 3-D in vitro-Model of Adipogenesis – Comparison of Culture Conditions. Tissue Eng 2003: in press. **(Chapter 3)**

6. Fischbach, C., Hacker, M., Neubauer, M., Blunk, T., and Göpferich, A. Analysis of Differential Areas within 3-D Tissue-Engineered Fat Constructs. Cells Tissues Organs: to be submitted. **(Chapter 4)**

7. Fischbach, C., Spruss, T., Neubauer, M., Weiser, B., Göpferich, A., and Blunk, T. Tissue Engineering Allows for Development of 3T3-L1 cells into Fat Pads *in vitro* as well as *in vivo*. Exp Cell Res: to be submitted. **(Chapter 5)**

Conference abstracts:

1. Tessmar, J., Fischbach, C., Lucke, A., Blunk, T., and Göpferich, A. PEG-PLA Diblockcopolymere zur Kontrolle der Wechselwirkungen zwischen Zellen und Materialoberfläche. Jahrestagung der Deutschen Gesellschaft für Biomaterialien [Aachen]. 1999.

2. Tessmar, J., Fischbach, C., Lucke, A., Blunk, T., and Göpferich, A. PEG-PLA diblock copolymers for the control of biomaterial-cell interaction. BioValley Tissue Engineering Symposium 2 [Freiburg]. 1999.

3. Tessmar, J., Fischbach, C., Lucke, A., Blunk, T., and Göpferich, A. Reaktive PEG-PLA Diblockcopolymere zur Kontrolle der Wechselwirkungen zwischen Zellen und Biomaterial. Workshop: Biologisch komponierte Materialien und Systeme [Saarbrücken]. 1999.

4. Tessmar, J., Lucke, A., Schnell, E., Fischbach, C., Schmeer, G., Blunk, T., and Göpferich, A. Biomimetic biodegradable Polymers for Drug Delivery and Tissue Engineering Applications. Annual Congress of APV 46 [Berlin]. 2000.

5. Lucke, A., Tessmar, J., Fischbach, C., Blunk, T., Schnell, E., Schmeer, G., and Göpferich, A. The Effect of Me.PEG-PLA Diblock Copolymer Composition on Surface Properties and Cell Adhesion. World Biomaterials Congress 6 [Kamuela, Hawaii]. 2000.

6. Fischbach, C., Tessmar, J., Lucke, A., Schnell, E., Schmeer, G., Blunk, T., and Göpferich, A. UV Sterilization Affects PEG-PLA Polymer Surface Properties and Results in Modified Cell Adhesion. DPhG Jahrestagung D 2.34 [Münster]. 2000.

7. Lieb, E., Tessmar, J., Fischbach, C., Blunk, T., Schulz, M. B., and Göpferich, A. Me.PEG-PLA Diblock Copolymers Modulate Adhesion and Shape of Rat Marrow Stromal Cells for Bone Tissue Engineering. Third Biennal Tissue Engineering Society international Meeting 182 [Orlando, Florida, USA]. 2000.

8. Lieb, E., Tessmar, J., Fischbach, C., Blunk, T., Schulz, M. B, and Göpferich, A. PEG-PLA Diblock Copolymers Modulate cell behaviour for Tissue engineering of Bone. DPhG Jahrestagung 2000 D2.33 [Münster, Germany]. 2000.

9. Lieb, E., Tessmar, J., Fischbach, C., Blunk, T., Schulz, M. B, and Göpferich, A. PEG-PLA Diblock Copolymers Modulate Adhesion of Rat Marrow Stromal Cells for Tissue Engineering of Bone. Item 2000 P 105 [Innsbruck, Austria]. 2000.

10. Fischbach, C., Tessmar, J., Lucke, A., Schnell, E., Schmeer, G., Blunk, T., and Göpferich, A. Does UV Irradiation Affect Polymer Properties Relevant to Tissue Engineering? Controlled Release Society German Chapter Annual Meeting 2 [Saarbrücken]. 2001.

11. Fischbach, C., Seufert, J., Neubauer, M., Lazariotou, M., Göpferich, A., and Blunk, T. 3T3-L1 preadipocytes on three-dimensional polymer scaffolds as a model for fat tissue engineering. Biennial Meeting of the European Tissue Engineering Society ETES 2001 P-40 [Freiburg]. 2001.

12. Neubauer, M., Fischbach, C., Lieb, E., Hacker, M., Tessmar, J., Schulz, M.B., Göpferich, A., and Blunk, T.. Adipogenesis of Rat Marrow Stromal Cells in Two- and Three-Dimensional Cell Culture. ETES 2001 P-139 [Freiburg]. 2001.

13. Fischbach, C., Seufert, J., Neubauer, M., Lazariotou, M., Göpferich, A., and Blunk, T. Towards a Three-Dimensional *in vitro*-Model of Adipogenesis. Keystone Symposia 2002 "Molecular Control of Adipogenesis and Obesity" 136 [Keystone]. 2002.

14. Neubauer, M., Fischbach, C., Lieb, Esther, Hacker, M., Tessmar, J., Schulz, M., Goepferich, A., and Blunk, T. Exposure to Basic Fibroblast Growth Factor Enhances Adipogenesis of Rat Marrow Stromal Cells *in vitro*. Keystone Symposia 2002 "Molecular Control of Adipogenesis and Obesity" J 321 [Keystone]. 2002.

15. Neubauer, M., Tessmar, J., Hacker, M., Fischbach, C., Schulz, M., Blunk, T., and Goepferich, A. Towards Engineered Adipose Tissue Using Bone Marrow Stromal Cells and Basic Fibroblast Growth Factor. Proc. Int. Symp. Controlled Release Bioact. Mater. [Seoul, Korea]. 2002.

16. Fischbach, C., Seufert, J., Neubauer, M., Lazariotou, M., Göpferich, A., and Blunk, T. Towards a Three-Dimensional in vitro-Model of Adipogenesis. 5th Annual Meeting of GZG/ETCS. 2002.

17. Neubauer, M., Fischbach, C., Lieb, E., Hacker, M., Tessmar, J., Bauer-Kreisel, P., Schulz, M., Göpferich, A., and Blunk, T. Adipogenesis of Rat Marrow Stromal Cells in Two- and Three-Dimensional Cell Culture. 5th Annual Meeting of GZG/ETCS. 2002.

Further presentations:

1. Fischbach, C., Neubauer, M., Blunk, T. and Göpferich, A. Tissue Engineering von Fettgewebe: Adipogenese in einem 3-D Gewebe-Modell und dessen Einsatz im Bereich der Grundlagenforschung. GBF Braunschweig. January 2003.

2. Fischbach, C., Neubauer, M., Blunk, T. and Göpferich, A. Adipose Tissue Engineering: Development of a 3-D in vitro Model of Adipogenesis and its Application in Basic Research. University of Michigan, Ann Arbor. February 2003

Awards:

1. International Tissue Engineering Meeting (ITEM) 2000 Poster Award (see conference abstract 9)

2. Keystone Symposia 2002 "Molecular Control of Adipogenesis and Obesity", David and Lucille Packard Award (see conference abstract 13)

6. Acknowledgements

An dieser Stelle möchte ich mich bei all denen bedanken, die zum Gelingen dieser Arbeit beigetragen haben.

Herrn Prof. Dr. Achim Göpferich danke ich für die Themenstellung, seine vielfältige Unterstützung bei dessen Bearbeitung sowie seinem regen Interesse am Fortgang der Arbeit. Außerdem möchte ich mich für sein Engagement bedanken, den Fortgang der Arbeit vor nationalem und internationalem Forum zu präsentieren.

Mein besonderer Dank gilt Herrn Dr. Torsten Blunk für seine unermüdliche und gewissenhafte Anleitung bei der Durchführung und Niederschrift dieser Arbeit. Sein wissenschaftlicher Enthusiasmus und seine freundschaftliche Unterstützung waren entscheidend am Erfolg dieser Arbeit beteiligt.

Weiterhin möchte ich mich herzlich bedanken bei:

- Herrn Prof. Dr. Georg Löffler und Herrn Dr. Harald Staiger, die ihre umfangreichen Erfahrungen mit 3T3-L1 Präadipozyten bereitwillig zur Verfügung stellten und mich bei der Einarbeitung in das Thema anleiteten.
- Herrn PD Dr. Jochen Seufert und Frau Maria Lazariotou für die Hilfestellung bei der erstmaligen Anwendung von RT-PCR Techniken.
- Herrn Michael Hacker für die eingehende Unterstützung bei den Rasterelektronen-mikroskopischen Untersuchungen.
- Herrn Dr. Thilo Spruß für die Anleitung zur Durchführung der in vivo-Experimente sowie deren anschließender histologischer Auswertung.
- Herrn Wiesenmayer und Herrn Baumann, die an der praktischen Umsetzung der Tierversuche beteiligt waren.
- Frau Thienel für die gewissenhafte Anfertigung der histologischen Paraffin-Schnitte.
- Frau Dr. Edith Schnell für die Durchführung der AFM-Messungen.
- Herrn Dr. Johann Vancea, für die Ausführung der XPS-Analysen.
- Herrn Dr. Thomas Burgemeister, für die Durchführung der ^{1}H-NMR-Messungen.
- Frau Barbara Weiser für die Unterstützung bei immunohistologischen Methoden.

- Frau Dr. Michaela Schulz, Frau Lydia Frommer, Frau Liane Öttl, allen TA´s sowie Herrn Albert Weingart für deren Unterstützung in vielfältigsten Belangen.
- Frau Allison Dennis für ihren unermüdlichen Einsatz bei der sprachlichen Überarbeitung des Manuskripts.
- Frau Dr. Karin Kellner, Frau Dr. Andrea Lucke und Herrn Michael Hacker für nachhaltig in Erinnerung bleibende gemeinsame Erlebnisse.
- Allen hier nicht namentlich genannten Mitarbeitern des Lehrstuhls Pharmazeutische Technologie für deren kollegiale Hilfsbereitschaft, Diskussionsfreudigkeit und freundschaftliche Kritik.

Insbesondere möchte ich mich bei Familie Dr. Jörg Teßmar und Herrn Markus Neubauer für deren mentale, räumliche und sonstige Unterstützung in verschiedensten Lebenslagen bedanken. Ihre aufrichtige Freundschaft wird unvergessen bleiben!

Zum Schluß möchte ich mich natürlich bei meinen Eltern und meinem Bruder Stefan bedanken, die mich in dieser Lebensphase bestärkt und unterstützt haben und mir damit diesen Weg ermöglicht haben.